JSCSEN 75(8)1019–1165(2010)

Journal of the Serbian Chemical Society

Electronic version

VOLUME 75

No 8

BELGRADE 2010

Available on line at

www.shd.org.rs/JSCS/

The full search of JSCS is available through

DOAJ DIRECTORY OF OPEN ACCESS JOURNALS

www.doaj.org

Journal of the Serbian Chemical Society
JSCS-info@shd.org.rs • www.shd.org.rs/JSCS

J. Serb. Chem. Soc. Vol. 75, No. 8 (2010)

CONTENTS

Organic Chemistry

A. S. Alimmari, A. D. Marinković, D. Ž. Mijin, N. V. Valentić, N. Todorović and *G.S. Ušćumlić*: Synthesis, structure and solvatochromic properties of 3-cyano-4,6-diphenyl--5-(3- and 4-substituted phenylazo)-2-pyridones 1019

V. V. Dabholkar and *T. D. Ravi*: Synthesis of Biginelli products of thiobarbituric acids and their antimicrobial activity (Short communication) 1033

Biochemistry and Biotechnology

L. Izrael-Živković, G. Gojgić-Cvijović and *I. Karadžić*: Isolation and partial characterization of protease from *Pseudomonas aeruginosa* ATCC 27853 1041

K. V. Jakovljević, M. R. Spasić, E. J. Mališić, J. D. Dobričić, A. M. Krivokuća and *R. N. Janković*: Comparison of phenol-based and alternative RNA isolation methods for gene expression analyses 1053

Inorganic Chemistry

V. M. Leovac, V. Divjaković, M. D. Joksović, Lj. S. Jovanović, Lj. S. Vojinović-Ješić, V. I. Češljević and *M. Mlinar*: Transition metal complexes with thiosemicarbazide-based ligands. Part 57. Synthesis, spectral and structural characterization of dioxovanadium(V) and dioxomolybdenum(VI) complexes with pyridoxal *S*-methylisothiosemicarbazone 1063

M. Imran, L. Mitu, S. Latif, Z. Mahmood, I. Naimat, S. S. Zaman and *S. Fatima*: Antibacterial Co(II), Ni(II), Cu(II) and Zn(II) complexes with biacetyl-derived Schiff bases 1075

A. Manohar, K. Ramalingam, G. Bocelli and *A. Cantoni*: Synthesis, spectral and single crystal X-ray structural studies on bis(2,2'-bipyridine)sulphidoM(II) (M = Cu or Zn) and diaqua 2,2'-bipyridine zinc(II)sulphate dihydrate 1085

Theoretical Chemistry

D. Vukičević, J. Đurđević and *I. Gutman*: On the number of Kekulé structures of fluoranthene congeners 1093

Physical Chemistry

S. V. Mahamuni, P. P. Wadgaonkar and *M. A. Anuse*: Liquid–liquid extraction and recovery of gallium(III) from acid media with 2-octylaminopyridine in chloroform: analysis of bauxite ore 1099

G. Mitran, I.-C. Marcu, A. Urdă and *I. Săndulescu*: Oxidative dehydrogenation of isobutane over supported V–Mo mixed oxides 1115

Environmental

I. Živadinović, K. Ilijević, I. Gržetić and *A. Popović*: Long-term changes in the eco-chemical status of the Danube River in the region of Serbia 1125

M. Mihailović, M. Petrović, N. Grdović, S. Dinić, A. Uskoković, M. Vidaković, I. *Grigorov, D. Bogojević, S. Ivanović-Matić, V. Martinović, J. Arambašić, D. Joksimović, S. Labus-Blagojević* and *G. Poznanović*: CYP1A and metallothionein expression in the hepatopancreas of *Merluccius merluccius* and *Mullus barbatus* from the Adriatic Sea 1149

Z. P. Višak: Liquid–liquid equilibria in solutions with potential ecological importance (Extended abstract) 1161

Published by the Serbian Chemical Society
Karnegijeva 4/III, 11000 Belgrade, Serbia
Printed by the Faculty of Technology and Metallurgy
Karnegijeva 4, P.O. Box 35-03, 11120 Belgrade, Serbia

Journal of the Serbian Chemical Society
JSCS-info@shd.org.rs • www.shd.org.rs/JSCS
J. Serb. Chem. Soc. 75 (8) 1019–1032 (2010)
JSCS–4027
UDC 667.021+547.821:66.081.2.004.12:
54–145.55:541.621
Original scientific paper

Synthesis, structure and solvatochromic properties of 3-cyano--4,6-diphenyl-5-(3- and 4-substituted phenylazo)-2-pyridones

ADEL S. ALIMMARI[1], ALEKSANDAR D. MARINKOVIĆ[1*#], DUŠAN Ž. MIJIN[1#], NATAŠA V. VALENTIĆ[1#], NINA TODOROVIĆ[2] and GORDANA S. UŠĆUMLIĆ[1#]

[1]*Department of Organic Chemistry, Faculty of Technology and Metallurgy, University of Belgrade, Karnegijeva 4, P.O. Box 3503, 11120 Belgrade and* [2]*Institute for Chemistry, Technology and Metallurgy, Njegoševa 12, 11000 Belgrade, Serbia*

(Received 9 October 2009, revised 10 May 2010)

Abstract: A series of some new pyridone arylazo dyes was synthesized from the corresponding diazonium salts and 3-cyano-4,6-diphenyl-2-pyridone using the classical reaction for the synthesis of the azo compounds. The structures of these dyes were confirmed by UV–Vis, FT-IR and ^{1}H-NMR spectroscopic techniques. The solvatochromism of the dyes was evaluated with respect to visible absorption properties in various solvents. The effects of solvent dipolarity/polarizability and solvent/solute hydrogen bonding interactions were analyzed by means of the linear solvation energy relationship concept proposed by Kamlet and Taft. The 2-pyridone/2-hydroxypiridine tautomeric equilibration was found to depend on the substituents as well as on the solvents.

Keywords: arylazo pyridone dyes; absorption spectra; solvent effect; substituent effect; tautomeric equilibration.

INTRODUCTION

Azo dyes are the most widely used compounds in various fields, such as dyeing of textile fibres, colouring of different materials, in biological–medical studies and advanced applications in organic synthesis.[1–6] The success of azo colorants is due to the simplicity of their synthesis by diazotization and azo coupling, to the almost innumerable possibilities presented by variation on the diazo compounds and coupling components, to the generally high molar extinction coefficient and to the medium to high light and wet fastness properties.[7] Pyridone derivatives are relatively recent heterocyclic intermediates for the preparation of arylazo dyes. The azo pyridone dyes give bright hues and are suitable for the dyeing of polyester fabrics.[8] The physico-chemical properties of arylazo pyri-

* Corresponding author. E-mail: marinko@tmf.bg.ac.rs
# Serbian Chemical Society member.
doi: 10.2298/JSC091009074A

done dyes are closely related to their tautomerism. Determination of azo-hydrazone tautomerism both in the solid state and solution phase is quite interesting both from theoretical and practical standpoints, since the tautomers have different technical properties and dyeing performances. Several investigations on substituted arylazo pyridones have been performed and reviewed.[9–11] It was concluded that the equilibrium between the two tautomers is influenced by the structure of the compounds and the solvent used. In previous publications, the absorption spectra of 3-cyano-6-hydroxy-4-methyl-5-(4-substituted phenylazo)-2-pyridones in different solvents were studied and the results showed that these dyes exist in the hydrazone form in the solid state and in the solvent DMSO-d_6, while equilibrium existed between the hydrazone and the azo form in different solvents.[12] The obtained dyes exhibit their colour hue in the range from orange to red-orange.

Recently, the synthesis of seventeen 3-cyano-4,6-dimethyl-5-(3- and 4-substituted phenylazo)-2-pyridones was reported.[13] The 2-pyridone/2-hydroxy-pyridine tautomeric equilibration was found to depend on the substituents as well as on the solvents. The obtained results showed that the replacement of a hydroxy group in position six in the pyridone ring of 3-cyano-6-hydroxy-4-methyl-5-(3- and 4-substituted phenylazo)-2-pyridones by a methyl group influenced a change of the azo group sensitivity to solvent effects in comparison with 3-cyano-4,6--dimethyl-5-(4-substituted phenylazo)-2-pyridones. The obtained dyes exhibited a light orange to brown-orange colour hue.

In this work, the synthesis of nine new 3-cyano-4,6-diphenyl-5-(3- and 4-substituted phenylazo)-2-pyridones, their UV–Vis absorption spectra (200–800 nm) in fifteen solvents of different polarity and the relationship between colour and constitution of these dyes are reported. The effects of solvent and substituent on the 2-pyridone/2-hydroxypyridine tautomeric equilibrium are also reported.

RESULTS AND DISCUSSION

All of the investigated arylazo pyridone dyes were synthesized from the corresponding diazonium salts and 3-cyano-4,6-diphenyl-2-pyridone using the classical reaction for the synthesis of azo compounds.[14] The chemical structure and the purity of the obtained compounds (which, to the best of our knowledge, have not been registered in the literature) were confirmed by melting points, and ^{1}H--NMR, FT-IR and UV spectral data. The characterization data are given below.

3-Cyano-5-[(4-methoxyphenyl)azo]-4,6-diphenyl-2-pyridone (***1***). Yield: 54 %. Colour: red brown crystals; m.p.: 264–268 °C. IR (KBr, cm^{-1}): 3436 (N–H), 2212 (C–N), 1692 (C=O). ^{1}H-NMR (200 MHz, DMSO-d_6, δ / ppm): 3.35 (3H, *s*, OCH_3), 6.88–6.99 (2H, *d*, ArH), 7.30–7.45 (2H, *m*, ArH), 7.55–7.66 (6H, *m*, ArH), 7.70–7.90 (4H, *m*, ArH), 11.67 (1H, *s*, pyridone–NH).

3-Cyano-5-[(4-methylphenyl)azo]-4,6-diphenyl-2-pyridone (***2***). Yield: 29 %. Colour: dark yellow crystals; m.p.: 243–246 °C. IR (KBr, cm^{-1}): 3376 (N–H),

2212 (C–N), 1681 (C=O). ^{1}H-NMR (200 MHz, DMSO-d_6, δ / ppm): 2.28 (3H, *s*, CH_3), 7.08–7.22 (4H, *d*, ArH), 7.40–7.68 (6H, *m*, ArH), 7.75–8.08 (4H, *m*, ArH), 11.95 (1H, *s*, pyridone–NH).

*3-Cyano-4,6-diphenyl-5-phenylazo-2-pyridone (**3**)*. Yield: 58 %. Colour: orange crystals; m.p.: 241–242 °C. IR (KBr, cm^{-1}): 3371 (N–H), 2212 (C–N), 1666 (C=O). ^{1}H-NMR (200 MHz, DMSO-d_6, δ / ppm): 7.05–7.20 (3H, *m*, ArH), 7.25––7.39 (4H, *m*, ArH), 7.40–7.49 (6H, *m*, ArH), 7.50–7.70 (2H, *m*, ArH), 11.83 (1H, *s*, pyridone–NH).

*3-cyano-5-[(3-methoxyphenyl)azo]-4,6-diphenyl-2-pyridone (**4**)*. Yield: 64 %. Colour: orange crystals; m.p.: 301–303 °C. IR (KBr, cm^{-1}): 3387 (N–H), 2212 (C–N), 1706 (C=O). ^{1}H-NMR (200 MHz, DMSO-d_6, δ / ppm): 3.79 (3H, *s*, OCH_3), 6.67–6.79 (3H, *m*, ArH), 7.20–7.33 (3H, *m*, ArH), 7.45–7.70 (6H, *m*, ArH), 7.90––8.03 (2H, *d*, ArH), 11.83 (1H, *s*, pyridone–NH), 14.04 (1H, *s*, pyridine–OH).

*5-[(4-Chlorophenyl)azo]-3-cyano-4,6-diphenyl-2-pyridone (**5**)*. Yield: 36 %. Colour: brown orange crystals; m.p.: 253–255 °C. IR (KBr, cm^{-1}): 3355 (N–H), 2222 (C–N), 1681 (C=O). ^{1}H-NMR (200 MHz, DMSO-d_6, δ / ppm): 7.20–7.39 (2H, *d*, ArH), 7.40–7.55 (4H, *m*, ArH), 7.60–7.75 (6H, *m*, ArH), 7.90–8.00 (2H, *m*, ArH), 12.27 (1H, *s*, pyridone–NH), 13.75 (1H, *s*, pyridine–OH).

*5-[(4-Bromophenyl)azo)-3-cyano-4,6-diphenyl-2-pyridone (**6**)*. Yield: 69 %. Colour: red brown crystals; m.p.: 292–293 °C. IR (KBr, cm^{-1}): 3351 (N–H), 2220 (C–N), 1681 (C=O). ^{1}H-NMR (200 MHz, DMSO-d_6, δ / ppm): 7.45–7.55 (2H, *d*, ArH), 7.58–7.90 (12H, *m*, ArH), 11.76 (1H, *s*, pyridone–NH), 12.75 (1H, *s*, pyridine–OH).

*3-Cyano-5-[(4-iodophenyl)azo]-4,6-diphenyl-2-pyridone (**7**)*. Yield: 62 %. Colour: dark brown crystals; m.p.: 276–281 °C. IR (KBr, cm^{-1}): 3454 (O–H), 3356 (N–H), 2222 (C–N), 1691 (C=O). ^{1}H-NMR (200 MHz, DMSO-d_6, δ / ppm): 7.05–7.22 (2H, *d*, ArH), 7.25–7.46 (2H, *d*, ArH), 7.52–7.70 (6H, *m*, ArH), 7.74––7.98 (4H, *m*, ArH), 11.75 (1H, *s*, pyridone–NH), 12.57 (1H, *s*, pyridine–OH).

*3-Cyano-5-[(3-nitrophenyl)azo]-4,6-diphenyl-2-pyridone (**8**)*. Yield: 65 %. Colour: dark orange crystals; m.p.: 282–285 °C. IR (KBr, cm^{-1}): 3484 (O–H), 3361 (N–H), 2222 (C–N), 1688 (C=O). ^{1}H-NMR (200 MHz, DMSO-d_6, δ / ppm): 7.40–7.70 (8H, *m*, ArH), 7.76–8.30 (4H, *m*, ArH), 8.32–8.40 (2H, *d*, ArH), 11.80 (1H, *s*, pyridone–NH), 12.15 (1H, *s*, pyridine–OH).

*3-Cyano-5-[(4-nitrophenyl)azo]-4,6-diphenyl-2-pyridone (**9**)*. Yield: 60 %. Colour: dark brown crystals; m.p.: 278–279 °C. IR (KBr, cm^{-1}): 3472 (O–H), 3350 (N–H), 2232 (C–N), 1686 (C=O). ^{1}H-NMR (200 MHz, DMSO-d_6, δ / ppm): 7.60–7.74 (4H, *m*, ArH), 7.76–7.94 (6H, *m*, ArH), 7.96–8.12 (2H, *m*, ArH), 8.15––8.40 (2H, *m*, ArH), 12.08 (1H, *s*, pyridine–OH).

The arylazo pyridone dyes prepared in this work may exist in two tautomeric forms (Fig. 1). The infrared spectra showed an intense carbonyl band in the region 1666–1692 cm^{-1} and an intense N–H band in the region 3376–3495 cm^{-1},

which suggest that these compounds predominantly exist in the 2-pyridone tautomeric form (Fig. 1, **A**) in the solid state. The ^{1}H-NMR spectra of the dyes in DMSO-d_6 exhibit a signal for the –NH proton at the pyridone ring in the range δ 11.67–12.15 ppm. However, for azo dyes with electron-accepting substituents in the phenyl group, the ^{1}H-NMR spectra showed a signal in the range δ 12.08––14.04 ppm, corresponding to the OH proton of enol form (Fig. 1, **B**).

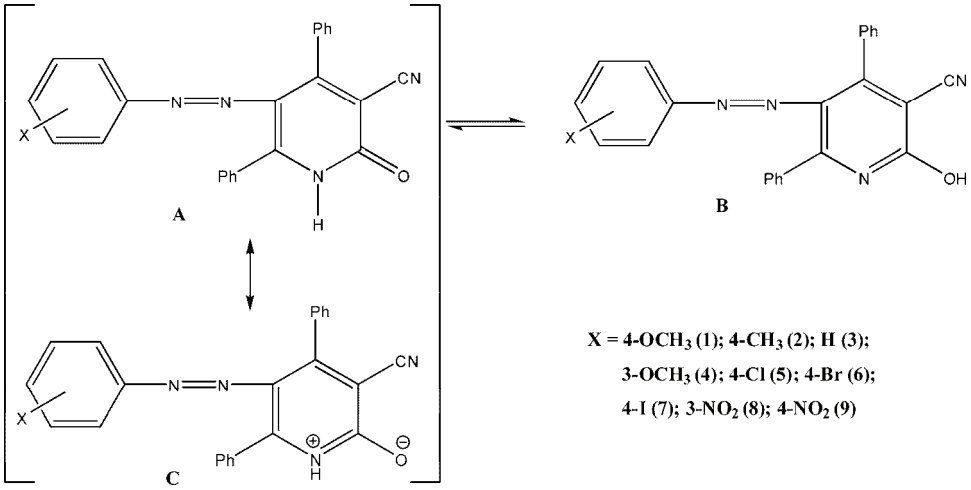

Fig. 1. Structure of dyes **1**–**9** and the equilibrium between 2-pyridone form (**A**) and 2-hydroxypyridine form (**B**) of 3-cyano-4,6-diphenyl-5-(3- and 4-substituted phenylazo)--2-pyridones and the canonical structure (**C**).

Solvent effects on absorption spectra of the dyes

Since the tautomeric equilibria strongly depend on the nature of the media, the behaviour of arylazo pyridone dyes in various protic and aprotic solvents was studied. For this purpose, the absorption spectra of the pyridone dyes (**1**–**9**) were measured in fifteen various solvents at a concentration 10^{-4} mol dm^{-3}, and the ultraviolet absorption maxima of the electronic transitions involving the free non--bonding electrons of the azo group are given in Table I. It was found that the absorption maxima of these dyes are strongly solvent dependent and vary with solvent polarity. The dyes generally showed bathochromic shifts as the polarity of the solvents was increased. The characteristic absorption spectra of investigated azo dyes in ethanol and *N*,*N*-dimethylacetamide are shown in Figs. 2 and 3, respectively.

The equilibrium between the two tautomers is influenced by the structure of the investigated compound and the solvent used. In protic and non-dipolar aprotic solvents (alcohols, dioxane, tetrahydrofuran and acetonitrile) azo pyridone dyes with electron-donating and moderate electron-accepting substituents showed one

absorption band arising from the 2-pyridone tautomeric form. Azo pyridone dyes with strong electron-accepting substituents exhibited two absorption bands in these solvents (Fig. 2). In *N*,*N*-dimethylformamide, *N*,*N*-dimethylacetamide and dimethyl sulphoxide solvents, all the investigated azo pyridone dyes existed as two tautomers, due to the high basicities and high relative permitivities of these solvents (Table I and Fig. 3). The molecular extinction coefficients (ε_{max}) are higher in comparison to the 3-cyano-4,6-dimethyl-5-(4-substituted phenylazo)-2-pyridones reported previously,[13] and vary from 6000 to 38000 $dm^3\ mol^{-1}\ cm^{-1}$ (not listed in Table I). The ratios of the molecular extinction coefficients of the 2-pyridone form **A** and the 2-hydroxypyridine form **B** are listed in Table I for solvents and substituents where tautomeric equilibrium was found.

TABLE I. UV–Vis spectral data (λ_{max} / nm and $\varepsilon_1/\varepsilon_2$) of dyes **1**–**9** in different solvents

No.	Solvent or Substituent	4-OCH_3	4-CH_3	H	3-OCH_3	4-Cl	4-Br	4-I	3-NO_2	4-NO_2
1	Methanol	370	361	375	358	356	355	360, 443	340, 473	372, 551
		–	–	–	–	–	–	2.24	1.15	1.71
2	Ethanol	373	364	374	360	359	356	359, 456	353, 484	371, 562
		–	–	–	–	–	–	1.94	0.69	1.60
3	Propan-1-ol	375	361	374	359	355	354	361, 452	342, 484	373, 565
		–	–	–	–	–	–	1.68	0.79	1.56
4	Propan-2-ol	375	360	371	360	356	356	360, 448	355, 487	371, 572
		–	–	–	–	–	–	2.02	0.63	1.58
5	Butan-1-ol	375	364	373	360	356	346	362, 456	353, 485	374, 566
		–	–	–	–	–	–	1.43	0.74	1.64
6	2-Methyl-2--propanol	372	360	375	360	356	357	357, 439	342, 403	370, 585
		–	–	–	–	–	–	1.93	0.87	3.32
7	Butan-2-ol	373	360	353	361	358	357	360, 448	340, 485	370, 578
		–	–	–	–	–	–	1.79	0.84	1.80
8	Dioxane	368	358	350	353	355	360	360, 429	330, 403	370, 420
		–	–	–	–	–	–	1.08	1.06	2.05
9	Ethyl acetate	364	357	348	350	348	351	355, 431	332, 414	364, 571
		–	–	–	–	–	–	1.25	2.46	2.90
10	Tetrahydrofuran	365	356	352	353	355	354	350, 439	330, 412	375, 602
		–	–	–	–	–	–	0.99	1.18	1.47

TABLE I. Continued

No.	Solvent or Substituent	4-OCH_3	4-CH_3	H	3-OCH_3	4-Cl	4-Br	4-I	3-NO_2	4-NO_2
11	Acetonitrile	368	356	369	352	351	352	341, 467	341, 483	368, 575
		–	–	–	–	–	–	1.20	0.73	0.79
12	Acetone	365, 505	357, 493	350, 439	353, 476	352, 488	354, 479	355, 461	340, 490	375, 588
		21.50	20.02	2.42	9.40	4.55	6.49	1.11	0.71	0.79
13	Dimethyl sulphoxide	376, 495	368, 495	380, 493	364, 493	360, 495	361, 494	364, 495	348, 495	386, 592
		14.58	16.00	10.12	4.11	3.18	2.45	0.98	0.53	0.78
14	*N*,*N*-Dimethyl-formamide	377,510	370, 493	383, 493	362, 488	403, 493	406, 493	372, 497	405, 495	521, 588
		8.69	14.2	8.99	4.47	2.67	1.98	0.42	0.94	1.35
15	*N*,*N*-Dimethyl-acetamide	373, 505	360, 500	370, 502	350, 485	357, 493	355, 492	364, 500	390, 497	526, 595
		10.62	14.40	10.46	5.51	2.65	3.03	0.38	0.51	0.93

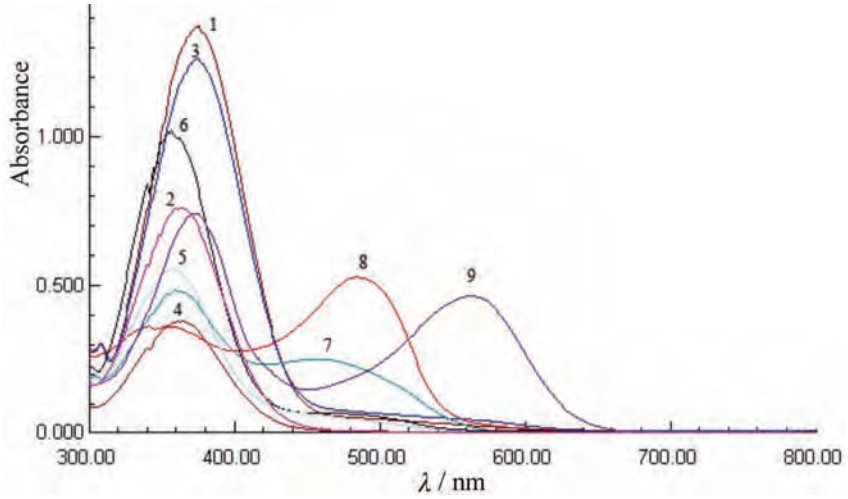

Fig. 2. Absorption spectra of the arylazo pyridone dyes (**1**–**9**) in ethanol.

By considering the equilibrium between the 2-pyridone and 2-hydroxypyridine tautomeric forms[15] in solvents of different polarity, it was found that increasing solvent polarity shifted the equilibrium towards the pyridone form.[16] This form is more dipolar than the hydroxy form due to the contribution of the charge-separated mesomeric form (Fig. 1, **C**). The present results are in agreement with this explanation. Furthermore, the hydrogen-bonding ability of the solvent plays an important role since hydrogen-bond donors tend to stabilize the oxo form (Fig. 1, **A**), whereas hydrogen-bond acceptors stabilize the hydroxy form (Fig. 1, **B**).

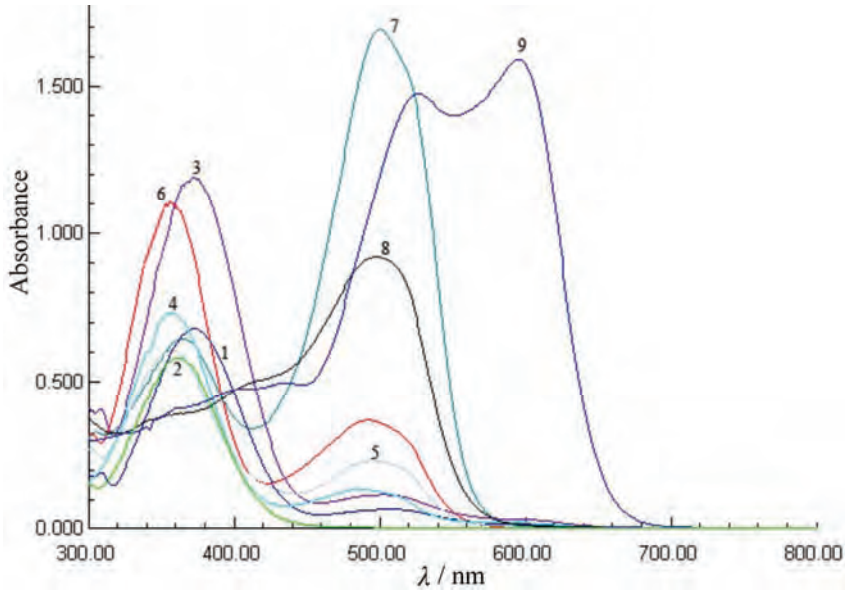

Fig. 3. Absorption spectra of the arylazo pyridone dyes (**1**–**9**) in *N*,*N*-dimethylacetamide.

The effects of solvent dipolarity/polarizability and hydrogen-bonding on the absorption spectra of 3-cyano-4,6-diphenyl-5-(3- and 4-substituted phenylazo)-2--pyridones, and many other compounds,[17,18] can be interpreted by means of the linear solvation energy relationship (LSER) concept using a Kamlet-Taft Equation of the type:[19]

$$v = v_0 + s\pi^* + b\beta + a\alpha \quad (1)$$

where π^* is a measure of the solvent dipolarity/polarizability, β is the scale of the solvent hydrogen-bond acceptor (HBA) basicities, α is the scale of the solvent hydrogen-bond donor (HBD) acidities and v_0 is the regression value of the solute property in the reference solvent cyclohexane. The regression coefficients *s*, *b* and *a* in Eq. (1) measure the relative susceptibilities of the solvent-dependent solute property (absorption frequencies) to the indicated solvent parameters. The solvent parameters[20] are given in Table II. The correlations of the spectroscopic data for 2-pyridone tautomeric form were realised by means of multiple linear regression analysis. It was found that absorption frequencies v_1 for the azo dyes (Table I) in ten selected solvents (Table III) showed satisfactory correlation with the π^*, β and α parameters. The results of the multiple regressions are presented in Tables III and IV, and coefficients v_0, *s*, *b* and *a* (Table III) have confidence intervals at a level of significance of 95 %. The degree of success of Eq. (1) is shown in Fig. 4 by means of a plot of v_{max} calculated *vs.* v_{max} observed in different solvents (the value of v_{max} for 4-NO_2 substituted azo dye in ethyl acetate was excluded from correlation).

TABLE II. Solvent parameters[17]

No.	Solvent	π^*	α	β
1	Methanol	0.60	0.62	0.93
2	Ethanol	0.54	0.77	0.83
3	Propan-1-ol	0.52	0.83	0.78
4	Propan-2-ol	0.48	0.95	0.76
5	Butan-1-ol	0.47	0.88	0.79
6	2-Methyl-2-propanol	0.41	1.01	0.68
7	Butan-2-ol	0.40	0.80	0.69
8	Dioxane	0.55	0.37	0
9	Ethyl acetate	0.55	0.45	0
10	Tetrahydrofuran	0.58	0.55	0
11	Acetonitrile	0.75	0.31	0.19
12	Acetone	0.88	0.76	0
13	Dimethyl sulphoxide	0.71	0.48	0.08
14	*N*,*N*-Dimethylformamide	1.00	0.76	0
15	*N*,*N*-Dimethylacetamide	0.88	0.69	0

TABLE III. Regression fits to the solvatochromic parameters (Eq. (1))

Substituent	$v_0\times10^{-3}$ cm^{-1}	$s\times10^{-3}$ cm^{-1}	$b\times10^{-3}$ cm^{-1}	a$\times10^{-3}$ cm^{-1}	R^a	S^b	F^c	Solvents used in the correlations[d]
4-OCH_3	28.67 (±0.11)	–1.49 (±0.14)	–0.75 (±0.11)	–0.68 (±0.08)	0.990	0.05	102	**2**–**6**, **9**–**11**, **13**, **15**
4-CH_3	29.71 (±0.32)	–1.64 (±0.33)	–1.10 (±0.25)	–0.44 (±0.17)	0.934	0.13	17	**1**–**7**, **10**–**13**
H	31.41 (±0.23)	–3.86 (±0.34)	–1.48 (±0.33)	–1.71 (±0.17)	0.993	0.13	142	**1**–**5**, **8**–**10**, **13**, **15**
3-OCH_3	30.00 (±0.09)	–1.54 (±0.11)	–1.31 (±0.07)	–0.43 (±0.05)	0.995	0.04	204	**1**–**6**, **9**, **11**–**13**
4-Cl	29.84 (±0.10)	–1.36 (±0.11)	–0.87 (±0.07)	–0.40 (±0.06)	0.991	0.04	111	**1**, **3**–**6**, **9**, **11**–**13**, **15**
4-Br	35.92 (±1.00)	–8.65 (±1.14)	–5.03 (±0.75)	0.99 (±0.43)	0.970	0.36	28	**1**–**6**, **9**, **10**, **14**, **15**
4-I	30.85 (±0.60)	–1.22 (±0.67)	–2.89 (±0.53)	–0.29 (±0.34)	0.933	0.25	14	**1**–**3**, **5**, **7**, **10**–**13**, **15**
3-NO_2	37.62 (±0.93)	–8.68 (±1.19)	–6.56 (±0.89)	0.89 (±0.59)	0.979	0.46	46	**1**, **2**, **4**, **5**, **7**–**9**, **11**, **14**, **15**
4-NO_2	41.88 (±0.90)	–19.49 (±1.00)	–7.68 (±0.86)	1.63 (±0.45)	0.996	0.37	235	**1**–**6**, **9**, **10**, **14**, **15**

[a]Correlation coefficient; [b]standard error of the estimate; [c]Fischer's test; [d]solvent numbers are given in Table I

The negative signs of the *s*, *b* and *a* coefficients for all the azo dyes (except the coefficient *a* for 4-Br, 3-NO_2 and 4-NO_2 substituted azo dyes, Table III) indicate a bathochromic shift with increasing solvent dipolarity/polarizability and solvent hydrogen-bond acceptor basicity and hydrogen-bond donor acidity. This suggests stabilization of the electronic excited state relative to the ground state.

The positive sign of the *a* coefficient for the azo dyes with electron-accepting substituents, 4-Br, 3-NO_2 and 4-NO_2, indicates a hypsochromic shift with increasing solvent hydrogen-bond donor acidity. These results show that the solvent effect on UV–Vis absorption spectra of pyridone azo dyes is very complex and strongly dependant on the nature of the groups present on the pyridone nucleus.

TABLE IV. Percentage contribution of the solvatochromic parameters

Substituent	P_{π^*} / %	P_β / %	P_α / %
4-OCH_3	51	26	23
4-CH_3	51	35	14
H	55	21	24
3-OCH_3	47	40	13
4-Cl	52	33	15
4-Br	59	34	7
4-I	28	66	6
3-NO_2	54	41	5
4-NO_2	67	27	6

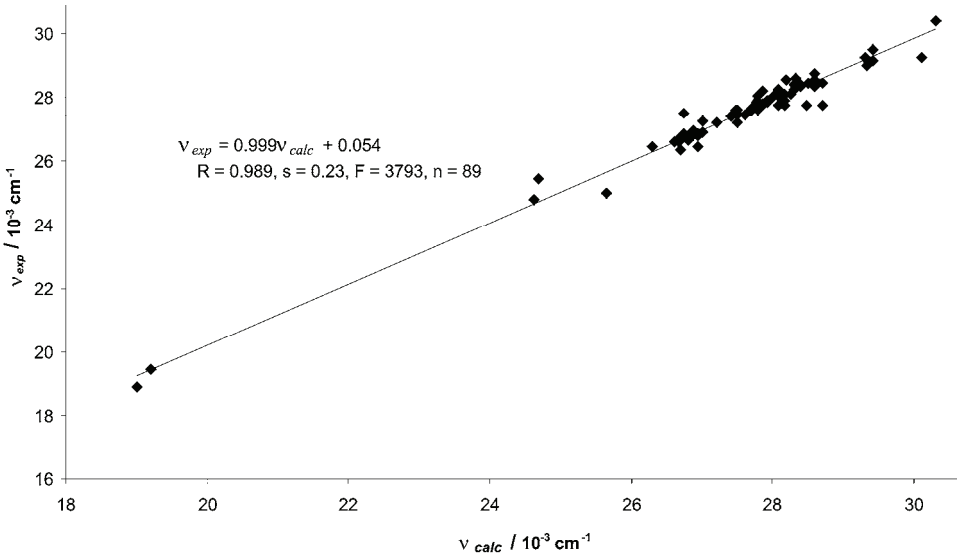

Fig. 4. The plot of ν_{max} observed against ν_{max} calculated from Eq. (1) for the 3-cyano-4,6-diphenyl-5-(3- and 4-substituted phenylazo)-2-pyridones.

Substituent effect on the absorption spectra of the dyes in various solvents

The data from Table I confirm that the positions of the ultraviolet absorption frequencies depend on the nature of the substituents in the phenyl ring of the azo dyes. The percentage contributions of the solvatochromic parameters (Table IV) for the azo dyes with electron-donating and moderate electron-accepting substituents (4-OCH_3, 4-CH_3, H, 3-OCH_3 and 4-Cl) in the phenyl group show that

most of the solvatochromism is due to solvent dipolarity/polarizability and solvent basicity rather than on the solvent acidity. These results are in accordance with the canonical structure of the 2-pyridone form of these dyes (Fig. 1, **C**). The effect of strong electron-accepting substituents (3-NO_2 and 4-NO_2) and 4-Br and 4-I is slightly different and the percentage contributions of the solvatochromic parameters show decreased proton-donating solvent effects. These results can be explained by the positive charge on the azo group in the 2-hydroxypyridine tautomer with electron-accepting substituents in the phenyl group (Fig. 5, **E**), and with a decreasing hydrogen-bond donating solvent effect when the more dipolar tautomeric form NH^+–CO^- transforms into the N=C–OH tautomeric form.

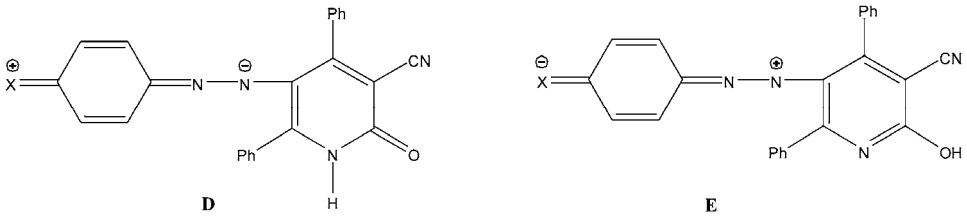

Fig. 5. Resonance effect of electron-donating (structure **D**) and electron-accepting (structure **E**) substituents of the arylazo component of the azo dyes.

In order to explain these results, the absorption frequencies were correlated by the Hammett Equation, Eq. (2), using $\sigma_{m/p}$ or $\sigma^+_{m/p}$ substituent constants:[21]

$$\nu = \nu_0 + \rho\sigma_{m/p} \quad (2)$$

where ρ is the proportionality constant reflecting the sensitivity of the absorption frequencies to the substituent effects. The substituent constants, $\sigma_{m/p}$ and $\sigma^+_{m/p}$, measure the electronic effect of the substituents (in a given position, meta or para).

The plot ν_{max} *vs.* the $\sigma_{m/p}$ substituent constants gave a correlation which showed deviations from the Hammett Equation in all dipolar aprotic solvents (*N*,*N*-dimethylacetamide, excluding the H and 4-NO_2 substituted dyes). However, a linear Hammett correlation was obtained in protic solvents (excluding the H and 4-NO_2 substituted dyes). A better correlation of ν_{max} was obtained with the $\sigma^+_{m/p}$ substituent constants[22] than with the $\sigma_{m/p}$ constants in all solvents (Figs. 6 and 7), which indicates extensive delocalization in the azo group (–N=N–). The existence of the correlation presented in Fig. 6 was interpreted as evidence of the significant role of substituent effects on the 2-pyridone/2-hydroxypyridine tautomerism. Electron-donating and moderate electron-accepting substituents stabilize 2-pyridone tautomeric form, while electron-accepting substituents stabilize the 2-hydroxypyridine tautomeric form. The azo group is an electron-acceptor, hence the azo group is stabilized by the more electron-donating substituents. These results are in accordance with the resonance structure of these dyes as shown in Fig. 5, **D**.

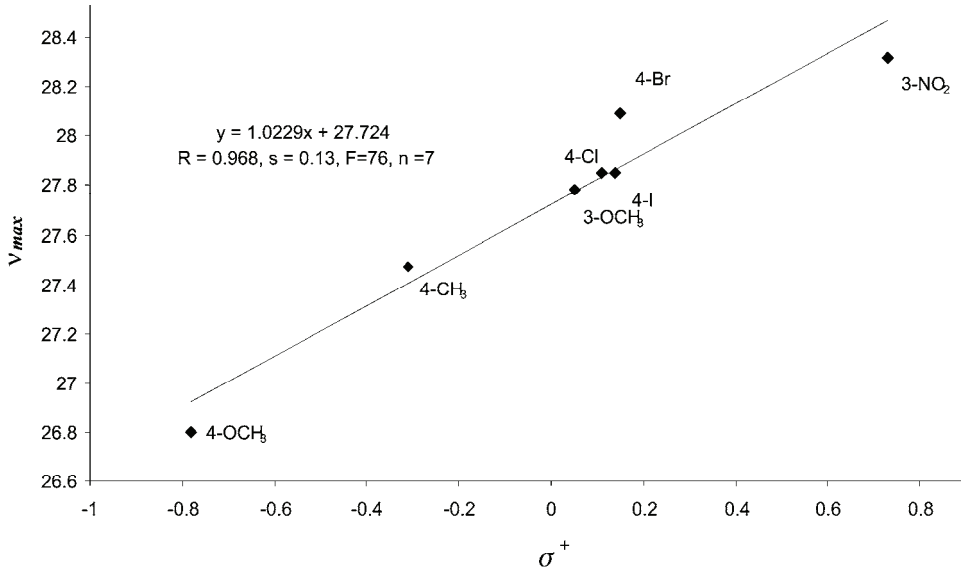

Fig. 6. Hammett correlation of ν_{max} *vs.* $\sigma^{+}_{m/p}$ in ethanol.

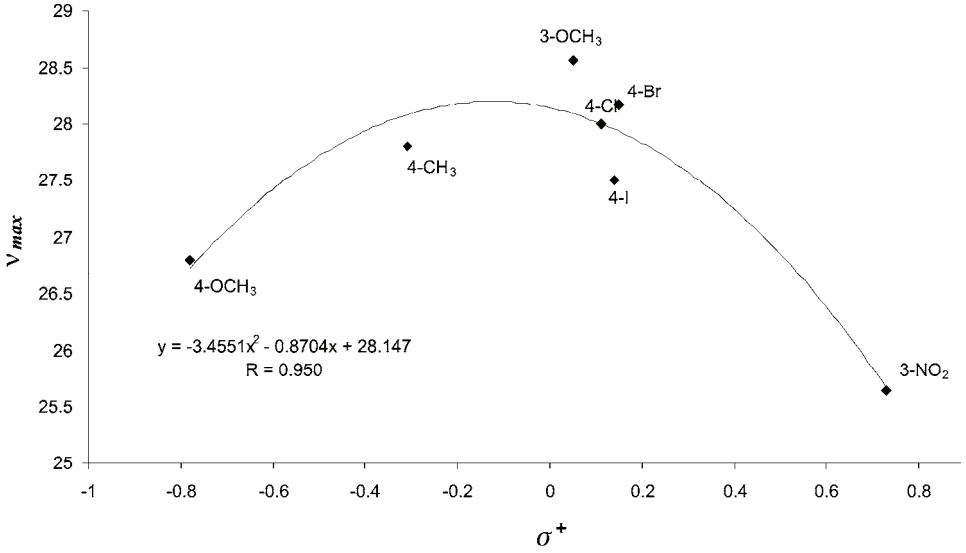

Fig. 7. Hammett correlation of ν_{max} *vs.* $\sigma^{+}_{m/p}$ in *N*,*N*-dimethylacetamide.

These results are contrary to the results published in a previous work for 3-cyano-4,6-dimethyl-5-(4-substituted phenylazo)-2-pyridones.[13] The obtained results show that replacement of methyl groups in the pyridone ring of 3-cyano-4,6-dimethyl-5-(3- and4-substituted phenylazo)-2-pyridones by phenyl groups influences the change of the sensitivity of the azo group to solvent and substituent

effects compared to 3-cyano-4,6-diphenyl-5-(3- and 4-substituted phenylazo)-2--pyridones. Additionally, two phenyl electron rich groups at the 4- and 6-position of the pyridine ring significantly changes the electronic structures of the highest populated molecular orbitals, and influences a different spatial arrangement of the investigated arylazo pyridone dyes in comparison to 3-cyano-4,6-dimethyl-5-(3- and 4-substituted phenylazo)-2-pyridones. Thus, the absorption maxima of 3-cyano-4,6-diphenyl-5-(3- and 4-substituted phenylazo)-2-pyridones showed bathochromic effects in comparison with analogous dyes containing two methyl groups in the pyridone ring. The pyridone azo dyes system, investigated in this work, absorbed at a higher absorption maxima due to the mobility of the electronic densities across the resonating systems (structures **D** and **E**, Fig. 5). The dye system comprising the phenyl moiety absorbed bathochromically compared to the other analogues due to the longer conjugation, which stabilized charge separation in the corresponding stabilized hybrids (Fig. 5). The obtained dyes exhibit their colour hue in the range from dark-yellow to brown.

EXPERIMENTAL

General

The chemicals used in the synthesis of all the dyes were obtained from the Fluka Chemicals Company and were used without further purification. The chemical structure and the purity of the azo pyridone dyes were confirmed by melting points, and by UV–Vis, FT-IR and ^{1}H-NMR spectroscopic techniques. All melting points are uncorrected.

The IR spectra were recorded on a Bomem FTIR spectrophotometer, MB-series, in the form of KBr pellets.

The ^{1}H-NMR spectral measurements were performed on a Varian Gemini 2000 (200 MHz) instrument. The spectra were recorded at room temperature in deuterated dimethyl sulphoxide (DMSO-d_6). The chemical shifts in the ^{1}H-NMR spectra are expressed in ppm values referenced to TMS (δ_H = 0 ppm).

The UV–Vis absorption spectra were recorded in the range 200–800 nm on a Shimadzu 1700 spectrophotometer in spectroquality solvents (Fluka) using a concentration of 10^{-4} mol dm^{-3}.

*Preparation of 3-cyano-4,6-diphenyl-5-(3- and 4-substituted phenylazo)-2-pyridones (**1**–**9**)*

All the investigated azo pyridone dyes were synthesized from the corresponding diazonium salts and 3-cyano-4,6-diphenyl-2-pyridone using the classical reaction for the synthesis of azo compounds.[14]

3-Cyano-4,6-diphenyl-2-pyridone was prepared from dibenzoyl methane and cyanoacetamide using a modified literature procedure.[23] Equimolar amounts of dibenzoyl methane and cyanoacetamide (10 mmol) were heated under reflux in a 50 % water/ethanol mixture (20 cm^3) in the presence of a few drops of piperidine as catalyst for 4 h. The product was purified by crystallization from ethanol (yield: 35 %, m.p.: 310–311 °C; lit.[21] m.p.: 312–313 °C).

The yields of the dyes were in the range 29–69 %. The obtained compounds were purified by crystallization from acetone and then analyzed.

CONCLUSIONS

A series of new pyridone arylazo dyes was synthesized from the corresponding diazonium salts and 3-cyano-4,6-dipenyl-2-pyridone. The solvatochromic behaviours and substituent effects in various solvents were evaluated. The results indicated that these dyes were strongly dependent on solvents and generally showed bathochromic shifts as the polarity of solvents was increased. These dyes exist dominantly in the 2-pyridone tautomeric form in the solid state. The results show that electron-donating and moderate electron-accepting substituents stabilized the 2-pyridone tautomeric form in protic and non-dipolar aprotic solvents, while in dipolar aprotic solvents the existence of two tautomers was observed. Strong electron-accepting substituents stabilized the 2-hydroxypyridine tautomer and existence of two tautomers was determined in all investigated solvents.

The satisfactory correlation of the ultraviolet absorption frequencies of the investigated arylazo pyridone dyes with the general solvatochromic equation indicates that the correct model was selected. It was demonstrated that a solvatochromic equation with three solvatochromic parameters π^*, β and α can be used to evaluate the effects of both types of hydrogen bonding and of the solvent dipolarity/polarizability effect. The obtained results showed that the replacement of the methyl groups in the pyridone ring of 3-cyano-4,6-dimethyl-5-(3- and 4-substituted phenylazo)-2-pyridones by phenyl groups in 3-cyano-4,6-diphenyl-5-(3- and 4-substituted phenylazo)-2-pyridones influenced a change in the sensitivity of the azo group to solvent and substituent effects. The absorption maxima of the 3-cyano-4,6-diphenyl-5-(3- and 4-substituted phenylazo)-2-pyridones showed bathochromic effects in comparison with analogous dyes containing two methyl groups in pyridone ring, and exhibited their colour hue in the range from dark yellow to brown.

Acknowledgements. The authors acknowledge the financial support by the Ministry of Science and Technological Development of the Republic of Serbia (Project Number 142063).

И З В О Д

СИНТЕЗА, СТРУКТУРА И СОЛВАТОХРОМНА СВОЈСТВА 3-ЦИЈАНО-4,6-ДИФЕНИЛ-5-(3- И 4-СУПСТИТУИСАНИХ ФЕНИЛАЗО)-2-ПИРИДОНА

ADEL S. ALIMMARI[1], АЛЕКСАНДАР Д. МАРИНКОВИЋ[1], ДУШАН Ж. МИЈИН[1], НАТАША В. ВАЛЕНТИЋ[1], НИНА ТОДОРОВИЋ[2] и ГОРДАНА С. УШЋУМЛИЋ[1]

[1]Катедра за органску хемију, Технолошко–металуршки факултет, Универзитет у Београду, Карнегијева 4, п. пр. 3503, 11120 Београд и [2]Институт за хемију,технологију и металургију, Његошева 12, 11000 Београд

Серија нових пиридонских арилазо боја је синтетисана реакцијом одговарајућих диазонијум соли и 3-цијано-4,6-дифенил-2-пиридона применом класичне синтезе азо једињења. Структура синтетисаних боја је потврђена на основу података добијених из UV, FT-IR и ^{1}H-NMR спектара. Солватохромна својства боја су процењена у односу на њихову апсорпцију у видљивом делу спектра у различитим растварачима. Ефекти растварача, диполарност/поларизабилност и водоничне интеракције растварач/растворак, су анализиране применом ли-

неарне корелације солватохромних ефеката предложене од стране Kamlet-a и Taft-a. Таутомерна равнотежа 2-пиридон/2-хидроксипиридин зависи како од ефеката супституента тако и од утицаја растварача.

(Примљено 9. октобра 2009, ревидирано 10. маја 2010)

REFERENCES

1. H. Zollinger, *Color Chemistry; synthesis, properties and application of organic dyes and pigments*, 3rd revised ed., VCH, Weinheim, 1987
2. H. S. Bhatti, S. Seshadri, *Color. Technol*. **120** (2004) 151
3. K. Tanaka, K. Matsuo, A. Nakanishi, M. Jo, H. Shiota, M. Yamaguchi, S. Yoshino, K. Kawaguchi, *Chem. Pharm. Bulletin* **32** (1984) 3291
4. G. J. Hallas, *J. Soc. Dyers Colour*. **95** (1979) 285
5. A. D. Towns, *Dyes Pigm.* **42** (1999) 3
6. K. Krishnankutty, M. B. Ummathur, P. Ummer, *J. Serb. Chem. Soc*. **74** (2009) 1273
7. C. C. Chen, I. J. Wang, *Dyes Pigm.* **15** (1991) 69
8. A. Cee, B. Horakova, A. Lyčka, *Dyes Pigm.* **9** (1988) 357
9. P. Y. Wang, I. Y. Wang, *Textile Res. J*. **60** (1990) 519
10. Q. Peng, M. Li, K. Gao, L. Cheng, *Dyes Pigm.* **15** (1991) 236
11. N. Ertan, F. Eyduran, P. Gurkan, *Dyes Pigm.* **27** (1995) 313
12. G. Uščumlić, D. Mijin, N. Valentić, V. Vajs, B. Sušić, *Chem. Phys. Lett*. **397** (2004) 148
13. D. Mijin, G. Uščumlić, N. Perišić-Janjić, N. Valentić, *Chem. Phys. Lett*. **418** (2006) 223
14. *Vogel's Textbook of Practical Organic Chemistry*, 4th ed., Longman, London, 1978, p. 715
15. P. Beak, J. Couvngton, J. M. White, *J. Org. Chem*. **45** (1980) 1347
16. C. Reichardt, *Solvents and Solvent Effects in Organic Chemistry*, Wiley-VCH, Weinheim, 2004, p. 113
17. N. D. Divjak, N. R. Banjac, N. V. Valentić, G. S. Uščumlić, *J. Serb. Chem. Soc*. **74** (2009) 1195
18. S. Ž. Drmanić, A. D. Marinković, B. Ž. Jovanović, *J. Serb. Chem. Soc*. **74** (2009) 1359
19. M. J. Kamlet, J. M. Abboud, R. W. Taft, *Prog. Phys. Org. Chem*. **13** (1981) 485
20. M. J. Kamlet, J. L. M. Abboud, M. H. Abraham, R. W. Taft, *J. Org. Chem*. **48** (1983) 2877
21. L. P. Hammett, *J. Am. Chem. Soc*. **59** (1937) 96
22. H. C. Brown, Y. Okamoto, *J. Am. Chem. Soc*. **80** (1958) 4979
23. J. M. Bobbit, D. A. Skola, *J. Org. Chem*. **25** (1960) 560.

Journal of the Serbian Chemical Society
JSCS-info@shd.org.rs • www.shd.org.rs/JSCS
J. Serb. Chem. Soc. 75 (8) 1033–1040 (2010)
JSCS–4028
UDC 547.853'593+547.854:547.571:615.28–188
Short communication

SHORT COMMUNICATION

Synthesis of Biginelli products of thiobarbituric acids and their antimicrobial activity

VIJAY V. DABHOLKAR* and TRIPATHI DILIP RAVI

Organic Research Laboratory, Department of Chemistry, Mumbai University, K. C. College, Churchgate, Mumbai-400 020, India

(Received 6 January 2009, revised 26 April 2010)

Abstract: A simple and efficient method has been developed for the synthesis of 2,4,7-tri(substituted)phenyl-2,4,8,10-tetraza-3,9-dithioxo-5-oxobicyclo-[4.4.0]dec-1(6)-ene (**4**) and 2,4,7-tri(substituted)phenyl-2,4,8,10-tetraza-3-thioxo-5,9-dioxobicyclo[4.4.0]dec-1(6)-ene (**5**), by a one-pot, three-component cyclocondensation reaction of a 1,3 dicarbonyl compound (thiobarbituric acid), an aromatic aldehyde, and urea/thiourea using catalytic a amount of concentrated HCl in refluxing ethanol. Representative samples were screened for their anti-microbial activity against the Gram-negative bacteria, *Escherichia coli* and *Proteus aeruginosa*, and the Gram-positive bacteria, *Staphyllococcus aureus* and *Corynebacterium diphtheriae* using the disc diffusion method. The structures of the products were confirmed by IR, ^{1}H- and ^{13}C-NMR spectroscopy, as well as by elemental analysis.

Keywords: aromatic aldehydes; dihydropyrimidine; thiobarbituric acid.

INTRODUCTION

The acid-catalyzed Biginelli reaction, which is a three-component reaction between an aldehyde, a β-ketoester and urea/thiourea, is a rapid and facile method for the synthesis of pyrimidones, which are interesting compounds with potential for pharmaceutical applications.

Pyrimidone products have been reported to possess biological activities such as anti-viral, anti-bacterial, anti-hypertensive and anti-tumor.[1] More recently pyrimidones have emerged as integral backbones of several calcium channel blockers.[2] Certain substituted 2-thiobarbituric acids have been used as intravenous anesthetics,[3] anti-convulsants,[4] immunotropic and anti-inflammatory compounds.[5]

Multicomponent reactions (MCRs) are of increasing importance in organic and medicinal chemistry for various reasons.[6] In times when premium is put on

* Corresponding author. E-mail: vijaydabholkar@gmail.com
doi: 10.2298/JSC090106060D

speed, diversity, and efficiency in the drug discovery process,[7] MCR strategies offer significant advantages over conventional linear-type synthesis. MCR condensations involve three or more compounds reacting in a single event, but consecutively to form a new product, which contains the essential parts of all the starting materials. The search and discovery for new MCRs on the one hand,[8] and the full exploitation of already known multicomponent reactions on the other are therefore of considerable current interest. One such MCR that belongs in the latter category is the venerable Biginelli dihydropyrimidine synthesis.

Over the past decade, dihydropyrimidin-2(1*H*)-ones and their derivatives have attracted considerable attention in organic and medicinal chemistry, as the dihydropyrimidine scaffold displays a fascinating array of pharmacological and therapeutic properties. They have emerged as integral backbones of several calcium channel blockers, antihypersentive agents, α-1 antagonists and neuropeptide Y (NPY) antagonists.[9] Moreover, several alkaloids containing the dihydropyrimidine core unit have been isolated from marine sources, which also exhibit interesting biological properties. Most notably, among these are the batzelladine alkaloids, which were found to be potent HIV gp-120-CD4 inhibitors. The scope of this pharmacophore has been further increased by the identification of the 4-(3--hydroxyphenyl)-2-thione derivative (±)-4i, called monastrol,[10] as a novel cell-permeable lead molecule for the development of new anticancer drugs (Fig. 1).

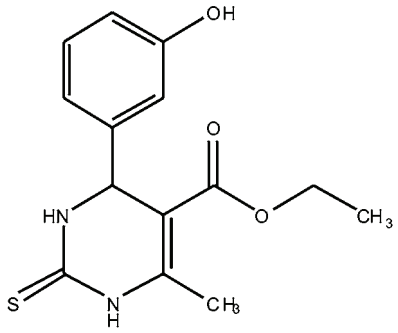

Fig. 1. The structure of monastrol.

In 1893, the Italian chemist Pietro Biginelli reported on the acid-catalyzed cyclocondensation reaction of ethyl acetoacetate, benzaldehyde and urea.[11] The reaction was performed simply by heating a mixture of the three components dissolved in ethanol with a catalytic amount of HCl at reflux temperature. The product of this novel one-pot, three-component synthesis that precipitated on cooling of the reaction mixture was identified correctly by Biginelli as 3,4-dihydropyrimidin-2(1*H*)-one (DHPM).

Thiobarbituric acid derivatives are known to possess antibacterial activity,[12] some are claimed to be sedatives,[13] and herbicides,[14] while some are classified as antiviral agents.[15]

In addition, it was reported[16] that the insertion of an aryl, amino, or a methyl moiety at 5-position of thiobarbituric acid enhances the antidepressant activities of the resulting compounds.

Bearing in mind the high synthetic utility and pharmacological importance, the synthesis of substituted pyrimidones (DHPMs) is reported herein.

Thus, the pharmacophoric activity of pyrimidones and thiobarbituric acid prompted the design and synthesis of 2,4,7-tri(substituted)phenyl-2,4,8,10-tetraza-3,9-dithioxo-5-oxo-bicyclo [4.4.0] dec-1(6)-ene (**4**) and 2,4,7-tri(substituted)phenyl-2,4,8,10-tetraza-3-thioxo-5,9-dioxo-bicyclo [4.4.0] dec-1(6)-ene (**5**) (Scheme I).

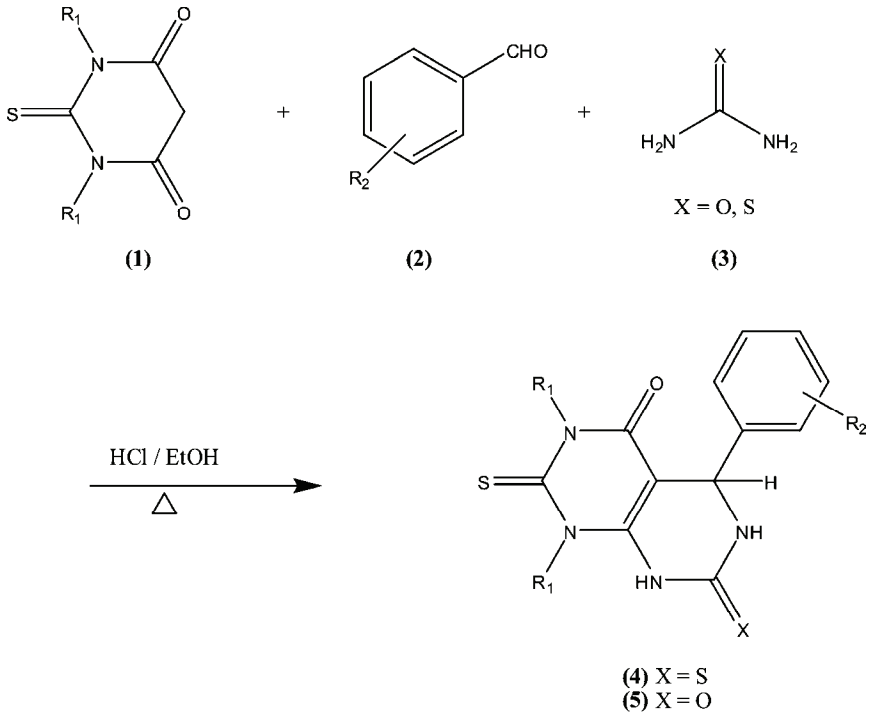

Scheme 1. The synthesis of the compounds **4** and **5**.

RESULTS AND DISCUSSION

The original Biginelli protocol for the preparation of DHPMs consisted of heating a mixture of the three components thiobarbituric acid (β-keto-ester) (**1**), aromatic aldehyde (**2**), and urea/thiourea (**3**) in ethanol containing a catalytic amount of HCl.[17] This procedure leads in one-step one pot to the desired DHMP.

The target molecules, 2,4,7-tri(substituted)phenyl-2,4,8,10-tetraza-3,9-dithioxo-5-oxobicyclo[4.4.0]dec-1(6)-ene **4**(**a**–**d**) and 2,4,7-(substituted)triphenyl--2,4,8,10-tetraza-3-thioxo-5,9-dioxobicyclo[4.4.0]dec-1(6)-ene **5**(**a**–**d**) were syn-

thesized in good yield by the one pot reaction of thiobarbituric acid, aromatic aldehydes, and urea/thiourea in refluxing ethanol using few drops of concentrated HCl as the catalyst. Compound **1** was prepared by the solid phase equimolar addition of thiocarbanilide,[18] malonic acid and acetyl chloride.[19]

The physical characterization data of the derivatives of **4**(**a**–**d**) and **5**(**a**–**d**) are reported in Table I.

TABLE I. Characterization data of compounds **4** (X = S) and **5** (X = O)

Compound	R1	R2	M.p., °C	Yield, %
4a	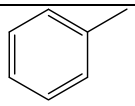	*p*-OCH_3	160	62
4b	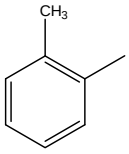	*p*-Cl	88	67
4c	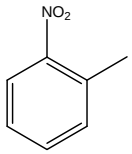	H	77	57
4d	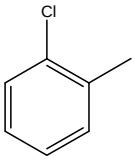	*o*-OH	125	67
5a	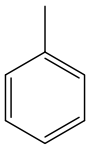	*o*-OH	155	72
5b	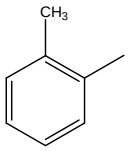	*p*-OCH_3	110	68
5c	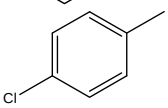	*p*-OCH_3	128	77
5d	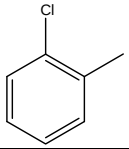	*o*-OH	108	72

*2,4-Diphenyl-7-*p*-methyoxyphenyl-2,4,8,10-tetraza-3,9-dithioxo-5-oxobicyclo[4.4.0]dec-1(6)-ene (**4a**)*. Orange crystals; Anal. Calcd. for $C_{25}H_{20}N_4O_2S_2$: C, 63.56; H, 4.24; N, 11.86 %; Found: C, 63.54; H, 4.23; N, 11.84 %. IR (KBr, cm–1): 1680, 1740, 3310. ^{1}H-NMR (500 MHz, DMSO-d_6, δ / ppm): 3.8 (3H, *s*, OCH_3), 4.4 (1H, *s*, CH), 6.8–7.8 (14H, *m*, Ar–H), 8.6 (1H, *s*, NH), 8.7 (1H, *s*, NH). ^{13}C--NMR (500 MHz, DMSO-d_6, δ / ppm): 52.3 (C–H), 55.1 (OCH_3), 85.2 (C=C), 153.4 (C=C), 172.2 (C=O), 183.4 (C=S), 191.8 (C=S).

*2,4-Di-*o*-methylphenyl-7-*p*-chlorophenyl-2,4,8,10-tetraza-3,9-dithioxo-5-oxobicyclo[4.4.0]dec-1(6)-ene (**4b**)*. Yellow crystals; Anal. Calcd. for $C_{26}H_{21}N_4OS_2Cl$: C, 61.84; H, 4.16; N, 11.10 %; Found: C, 61.82; H, 4.14; N, 11.09 %. IR (KBr, cm^{-1}): 1670, 1730, 3330. ^{1}H-NMR (500 MHz, DMSO-d_6, δ / ppm): 2.1 (3H, *s*, CH_3), 2.2 (3H, *s*, CH_3), 4.5 (1H, *s*, CH), 6.5–7.9 (12H, *m*, Ar–H), 8.8 (1H, *s*, NH), 8.9 (1H, *s*, NH). ^{13}C-NMR (500 MHz, DMSO-d_6, δ / ppm): 31.2 (CH_3), 37.8 (CH_3), 54.3 (C–H), 79.2 (C=C), 152.1 (C=C), 162.3 (C=O), 178.4 (C=S), 201.1 (C=S).

*2,4-Di-*o*-nitrophenyl-7-phenyl-2,4,8,10-tetraza-3,9-dithioxo-5-oxobicyclo[4.4.0]dec-1(6)-ene (**4c**)*. Brick red crystals, Anal. Calcd. for $C_{24}H_{16}N_6O_5S_2$: C, 54.13; H, 3.01; N, 15.79 %; Found: C, 54.11; H, 3.00; N, 15.78 %. IR (KBr, cm^{-1}): 1680, 1780, 3360. ^{1}H-NMR (500 MHz, DMSO-d_6, δ / ppm): 4.5 (1H, *s*, CH), 6.5––7.5 (13H, *m*, Ar–H), 7.9 (1H, *s*, NH), 8.1 (1H, *s*, NH). ^{13}C-NMR (?MHz, DMSO--d_6, δ / ppm): 55.1 (C–H), 83.2 (C=C), 147 (C=C), 159.2 (C=O), 182.6 (C=S), 199.3 (C=S).

*2,4-Di-*o*-chlorophenyl-7-(*o*-hydroxyphenyl)-2,4,8,10-tetraza-3,9-dithioxo-5--oxobicyclo[4.4.0]dec-1(6)-ene (**4d**)*. Light green crystals; Anal. Calcd. for $C_{24}H_{16}Cl_2N_4O_2S_2$: C, 54.65; H, 3.04; N, 10.63 %; Found: C, 54.63; H, 3.02; N, 10.61 %. IR (KBr, cm^{-1}): 1660, 1730, 3290. ^{1}H-NMR (500 MHz, DMSO-d_6, δ / / ppm): 4.3 (1H, *s*, CH), 5.6 (1H, *s*, OH), 6.5–7.8 (12H, *m*, Ar–H), 8.4 (1H, *s*, NH), 8.7 (1H, *s*, NH). ^{13}C-NMR (500 MHz, DMSO-d_6, δ / ppm): 52.4 (C–H), 82.2 (C=C), 154.3 (C=C), 166.4 (C=O), 182.4 (C=S), 200.5 (C=S).

*2,4-Diphenyl-7-(*o*-hydroxyphenyl)-2,4,8,10-tetraza-3-thioxo-5,9-dioxobicyclo-[4.4.0]dec-1(6)-ene (**5a**)*. Red crystals; Anal. Calcd. for $C_{24}H_{18}N_4O_3S$: C, 70.24; H, 4.39; N, 13.66 %; Found: C, 70.23; H, 4.37; N, 13.64 %. IR (KBr, cm^{-1}): 1660, 1750, 3290. ^{1}H-NMR (500 MHz, DMSO-d_6, δ / ppm): 4.4 (1H, *s*, CH), 4.7 (1H, *s*, OH), 6.5–7.7 (14H, *m*, Ar–H), 8.6 (1H, *s*, NH), 8.9 (1H, *s*, NH). ^{13}C-NMR (500 MHz, DMSO-d_6, δ / ppm): 59.6 (C–H), 87.1 (C=C), 155.3 (C=C), 163.2 (C=O), 168.3 (C=O), 179.1 (C=S).

*2,4-Di-*o*-methylphenyl-7-(*p*-methoxyphenyl)-2,4,8,10-tetraza-3-thioxo-5,9-dioxobicyclo[4.4.0]dec-1(6)-ene (**5b**)*. Orange crystals, Anal. Calcd. for $C_{27}H_{24}N_4O_3S$: C, 66.94; H, 4.96; N, 11.57 %; Found: C, 66.92; H, 4.95; N, 11.55 %. IR (KBr, cm^{-1}): 1680, 1770, 3330. ^{1}H-NMR (500 MHz, DMSO-d_6, δ / ppm): 2.1 (3H, *s*, CH_3), 2.4 (3H, *s*, CH_3), 3.9 (1H, *s*, OCH_3), 4.5 (1H, *s*, C–H), 6.5–7.9 (12H, *m*,

Ar–H), 9.2 (1H, *s*, NH), 9.8 (1H, *s*, NH). ^{13}C-NMR (500 MHz, DMSO-d_6, δ / / ppm): 31.2 (CH_3), 33.1 (CH_3) 56.6 (C–H), 58.3 (OCH_3), 87.4 (C=C), 147.4 (C=C), 171.9 (C=O), 187.7 (C=O), 200.8 (C=S).

2,4-Di-p-*chlorophenyl-7-(2'-hydroxy-4'-methoxyphenyl)-2,4,8,10-tetraza-3--thioxo-5,9-dioxobicyclo[4.4.0]dec-1(6)-ene (**5c**)*. Orange crystals, Anal. Calcd. for $C_{25}H_{18}Cl_2N_4O_4S$: C, 55.45; H, 3.33; N, 10.35 %; Found: C, 55.42; H, 3.31; N, 10.33 %. IR (KBr, cm^{-1}): 1650, 1780, 3340. ^{1}H-NMR (500 MHz, DMSO-d_6, δ / ppm): 3.9 (1H, *s*, OCH_3), 4.5 (1H, *s*, C–H), 6.8–7.8 (11H, *m*, Ar–H), 8.3 (1H, *s*, NH), 8.9 (1H, *s*, NH), 9.8 (1H, *s*, OH). ^{13}C-NMR (500 MHz, DMSO-d_6, δ / /ppm): 56.3 (C–H), 62.1 (OCH_3), 63.3 (C=C), 152.2 (C=C), 163.7 (C=O), 167.1 (C=O), 187.3 (C=S).

2,4-di-o-*chlorophenyl-7-(*o-*hydroxyphenyl)-2,4,8,10-tetraza-3-thioxo-5,9-di-oxobicyclo[4.4.0]dec-1(6)-ene (**5d**)*. Purple crystals; Anal. Calcd. for $C_{24}H_{16}Cl_2N_4O_3S$: C, 56.36; H, 3.13; N, 10.96 %; Found: C, 56.35; H, 3.11; N, 10.94 %. IR (KBr, cm^{-1}): 1680, 1730, 3330. ^{1}H-NMR (500 MHz, DMSO-d_6, δ / / ppm): 4.6 (1H, *s*, CH), 6.7–7.9 (12H, *m*, Ar–H), 8.3 (1H, *s*, NH), 8.8 (1H, *s*, NH). ^{13}C-NMR (500 MHz, DMSO-d_6, δ / ppm): 55.5 (C–H), 83.7 (C=C), 157.2 (C=C), 159.2 (C=O), 164.3 (C=O), 191.3 (C=S).

Antimicrobial and antifungal activities

The activities of representative compounds are reported in Table II.

TABLE II. Antibacterial activity of compounds **4** and **5**

Compound	Zone of inhibition, mm			
	Gram-positive		Gram-negative	
	S. aureus	*C. diphtheria*	*P. aeruginosa*	*E. coli*
4a	22	25	22	27
4b	21	26	25	28
4c	19	20	22	23
4d	21	27	28	32
5a	20	22	30	29
5b	15	17	22	23
5c	13	16	25	25
5d	22	23	20	24
Ampiciline trihydrate	26	28	24	21
DMSO	0	0	0	0

EXPERIMENTAL

The melting points of all synthesized compounds were determined in open capillary tubes on an electro thermal apparatus and are uncorrected. The purity of the compounds was monitored by thin layer chromatography on silica gel coated aluminum plates (Merck) as the adsorbent and UV light as the visualizing agent. The ^{1}H-NMR spectra were recorded on Varian 500 MHz NMR spectrophotometer using $CDCl_3$/DMSO-d_6 as solvent and TMS as an internal standard. The C, H, N estimations were recorded on Carlo Erba 1108 (CHN) elemen-

tal analyzer. ^{13}C-NMR was performed on a Varian 500 MHz spectrophotometer using DMSO-d_6 as solvent and IR was performed on PerkinElmer Spectrum 100 FT-IT using a KBr pellet.

Synthesis of 3,4-dihydropyrimidin-2(1H)-ones

Aromatic aldehydes (0.050 mol), substituted thiobarbituric acid (0.050 mol) and urea/ /thiourea (0.050 mol) were dissolved in ethanol and the mixture refluxed on a water bath in the presence of a catalytic amount of concentrated HCl. The progress of the reaction was monitored by TLC. After completion of the reaction, the concentrated reaction mixture was cooled and poured onto ice-cold water. The solid that separated was filtered off, dried, and recrystallized from absolute alcohol to obtain the pure compounds **4** and **5**.

Antimicrobial and antifungal activities

The newly synthesized compounds **4**(**a**–**d**) and **5**(**a**–**d**) were screened for their antibacterial activity against *Staphyllococcus aureus* (ATTC-27853), *Corynebacterium diphtheria* (ATTC-11913), *Proteus aeruginosa* (recultured) and *Escherichia coli* (ATTC-25922) bacterial strains by the disc diffusion method.[20,21] Discs (6 mm) were prepared from Whatman filter paper No. 41 and used after autoclaving at 121 psi for 15 min and drying in a hot air oven. The bacterial inoculums equivalent to the 0.5 McFarland turbidity standard were prepared in normal saline and subsequently diluted. The compounds were dissolved in DMSO and tested at a concentration of 100 μg ml^{-1}. The zone of inhibition after 24 h incubation was measured in mm and the potency was compared with standard drug (ampiciline trihydrate).

Acknowledgements. The authors are thankful to the Principal Ms Manju J Nichani and the Management of K. C. College, Churchgate, Mumbai, India, for the constant encouragement and providing the necessary facilities. The authors are also thankful to the Director, Institute of Science Mumbai for the spectral data.

И З В О Д

СИНТЕЗА BIGINELLI-ЈЕВИХ ПРОИЗВОДА ТИОБАРБИТУРНИХ КИСЕЛИНА И ЊИХОВА АНТИМИКРОБНА АКТИВНОСТ

VIJAY V. DABHOLKAR и TRIPATHI DILIP RAVI

Organic Research Laboratory, Department of Chemistry, Mumbai University, K.C. College, Churchgate, Mumbai-400 020, India

Развијен је једноставан и ефикасан метод за синтхезу 2,4,7-три(супституисаног)фенил--2,4,8,10-тетраза-3,9-дитиоксо-5-оксобицикло[4.4.0]дец-1(6)-ена (**4**) и 2,4,7-три(супституисаног)фенил)-2,4,8,10-тетраза-3-тиоксо-5,9-диоксобицикло[4.4.0]дец-1(6)-ена (**5**), једнофазном трикомпонентном циклоондензационом реакцијом 1,3-дикарбонилног једињења (тиобарбитурне киселине), ароматичног алдехида и урее/тиоурее, користећи каталитичку количину концентроване HCl у рефлуктујућем етанолу. Одабрани узорци тестирани су на анти--микробну активност према грам-негативним бактеријама, *E. coli* и *P. aeruginosa*, и грам-позитивних бактерија, *S, aureus* и *C. diphtheriae*, применом диск-дифузионог поступка. Структуре производа су потврђене помоћу IR, ^{1}H, ^{13}C-NMR и елементалне анализе.

(Примљено 6. јануара 2009, ревидирано 26. априла 2010)

REFERENCES

1. a) D. W. McKinstry, E. H. Reading, *J. Frankin Inst.* **237** (1994) 422; b) T. Matsuda, I. Hirao, *Nippon Kagaku Zasshi* **86** (1965) 1195

2. T. Takatani, H. Takasugi, A. Kuno, Z. Inoue, *Chem. Abstr.* **108** (1988)159930
3. W. J. Doran, in *Medicinal Chemistry*, Vol. 4, F. F. Blicke, R. H. Cox, Eds., Wiley, New York, 1959, p. 5
4. A. Dhasmana, J. P. Barthwal, B. R. Pandey, B. Ali, K. P. Bhargava, S. S. Parmer, *J. Heterocyclic Chem*. **18** (1981) 635
5. T. Zawisza, H. Matczak, S. H. Bronisz, T. Jakobiec, *Pol. Arch. Immunol. Ther. Exp.* **29** (1981) 235
6. Passerini three-component and Ugi four-component condensations are the most popular among many other reactions for their wide scope and synthetic utility. For reviews, see: a) H. Bienayme, C. Hulme, G. Oddon, P. Schmitt, *Chem. Eur. J.* **6** (2000) 3321; b) A. Domling, I. Ugi, *Angew. Chem. Int. Ed.* **39** (2000) 3168
7. a) S. L. Schreiber, *Science* **287 (**2000) 1964; b) R. E. Dolle, K. H. J. Nelson, *Comb. Chem.* **1** (1999) 235; c) D. Obrecht, J. M. Villalgordo, in *Solid-Supported Combinatorial and Parallel Synthesis of Small – Molecular-Weight Compounds Libraries*, J. E. Baldwin, R. M. Williams, Eds., Pergamon Press, New York, 1998
8. L Weber, K. Illgen, M. Almstetter, *Synlett*. **3** (1999) 366
9. a) K. S. Atwal, G. C. Rovnyak, S. D. Kimball, D. M. Floyd, S. Moreland, B. N. Swanson, J. Z. Gougoutas, J. Schwartz, K. M. Smillie, M. F. Malley, *J. Med. Chem.* **33** (1990) 2629; b) G. C. Rovnyak, S. D. Kimball, B. Beyer, G. Cucinotta, J. D. DiMarco, J. Z. Gougoutas, A. Hedberg, M. F. Malley, J. P. Zhang, S. Moreland, *J. Med. Chem.* **38** (1995) 119, and references therein
10. T. U. Mayer, T. M. Kapoor, S. J. Haggarty, R. W. King, S. L. Schreiber, T. J. Mitchison, *Science* **286** (1999) 971
11. P. Biginelli, *Gazz. Chim. Ital.* **23** (1893) 360
12. a) L. K. Akopyan, A. S. Adzhibekyan, G. A. Porkinyan, E. A. Tumasyan, *Bilzh. Arm.* **29** (1976) 80; b) L. K. Akopyan, A. S. Adzhibekyan, G. A. Porkinyan, E. A. Tumasyan *Chem. Abstr*. **85** (1976) 72068
13. a) S. Senda, H. Fugimura, H. Izumi, Japan Patent 193,6824, 1968; S. Senda, H. Fugimura, H. Izumi, *Chem. Abstr*. **70** (1969) 78001
14. a) S. L. Katz, A. W. Gay, U.S. Patent 352,806, 1982; S. L. Katz, A. W. Gay, *Chem. Abstr.* **98** (1983) 215603
15. a) W. G. Brouwer, E. E. Felauerand, A. R. Bell, U.S. Patent 779,982, 1990; W. G. Brouwer, E. E. Felauerand, A. R. Bell, *Chem. Abstr.* **114** (1991) 185539; c) A. Esanu, BE Patent 902,232, 1985; d) A. Esanu *Chem. Abstr.* **104** (1986) 130223
16. V. Singh, R. Khanna, V. K. Srivastava, G. Palit, K. Shanker, *Arzneim–Forsch.* **42** (1992) 277
17. a) C. O. Kappe, *Tetrahedron* **49** (1993) 6937, and references cited therein; b) C. O. Kappe, *Acc. Chem. Res.* **33** (2000) 879
18. A. I. Vogel, *The Text Book of Practical Organic Chemistry*, 4th ed., ELBS/Longmann, Harlow, 1984, p. 735
19. I. N. D. Dass, S. Dutt, Proc. *Indian. Acad. Sci*. **8A** (1938) 145
20. R. Cruickshank, J. P. Duguid, B. P. Marmion, *Medicinal Microbiology*, Vol. 11, 12th ed., Churchill Livingstone, London, 1975
21. B. A. Arthington-Skaggs, M. Motley, C. J. Morrison, *J Clin Microbiol.* **38** (2000) 2254.

Journal of the Serbian Chemical Society
JSCS-info@shd.org.rs • www.shd.org.rs/JSCS
J. Serb. Chem. Soc. *75* (8) 1041–1052 (2010)
JSCS–4029
UDC **Pseudomonas aeruginosa*+54.05:
577.112+612.398
Original scientific paper

Isolation and partial characterization of protease from *Pseudomonas aeruginosa* ATCC 27853

LIDIJA IZRAEL-ŽIVKOVIĆ[1*#], GORDANA GOJGIĆ-CVIJOVIĆ[2#] and IVANKA KARADŽIĆ[1**#]

[1]*School of Medicine, Department of Chemistry, University of Belgrade, Višegradska 26, 11000 Belgrade and* [2]*Institute of Chemistry, Technology and Metallurgy, Department of Chemistry, University of Belgrade, Njegoševa 12, 11000 Belgrade, Serbia*

(Received 25 January, revised 26 April 2010)

Abstract: Enzymatic characteristics of a protease from a medically important, referent strain of *Pseudomonas aeruginosa* ATCC 27853 were determined. According to sodium dodecyl sulfate polyacrylamide gel electrophoresis, SDS-PAGE, and gel filtration, it was estimated that the molecular mass of the purified enzyme was about 15 kDa. Other enzymatic properties were found to be: pH optimum 7.1, pH stability between 6.5 and 10; temperature optimum around 60 °C while the enzyme was stable at 60 °C for 30 min. Inhibition of the enzyme was observed with metal chelators, such as EDTA and 1,10-phenanthroline, suggesting that the protease is a metalloenzyme. Furthermore, the enzyme contains one mole of zinc ion per mole of enzyme. The protease was stable in the presence of different organic solvents, which enables its potential use for the synthesis of peptides.

Keywords: protease; *Pseudomonas aeruginosa*; purification; characterization.

INTRODUCTION

A wide range of investigations on *Pseudomonas aeruginosa* and its exoenzymes were performed: from targeted treatment of infections to decomposition of natural materials and bioremediation.[1–6] Since this strain has the property of forming biofilms (specific communities of cells encased in an extracellular matrix composed of proteins, nucleic acids, and cell debris), *P. aeruginosa* has advantages in the invasion of a host and survival under different environments, in comparison to other strains. The ability to form biofilms and synthesize numerous exoproducts, such as lipase, phospholipase, alkaline phosphatase, exotoxin and proteases, is regulated by cell to cell communication, quorum sensing

Corresponding authors. E-mails: *lidijajob@yahoo.com; **ivankakaradzic@yahoo.com
Serbian Chemical Society member.
doi: 10.2298/JSC100125088I

(QS).[6–9] *P. aeruginosa* produces several extracellular proteases, including LasB elastase, LasA elastase, and alkaline protease.[10] Proteases are assumed to play an important role during acute *P. aeruginosa* infection, however details of their action are sometimes unclear.[11,12]

The prototype strain, *P. aeruginosa* ATCC 27853 has been used as a reference control strain in different kinds of experiments, including: testing of antimicrobial activity of new compounds or combination therapy against *P. aeruginosa*, identification of virulence factors, particularly extracellular enzymes, quailty control testing, drug carrier testing *etc*.[13–16] It has become clear that numerous extracellular enzymes acting as virulence factors, controlled by QS, are important in the development of *P. aeruginosa* biofilms.[17] However, a detailed characterization of extracellular enzymes from microorganisms of medical importance, such as *P. aeruginosa* ATCC 27853, has not yet been reported. In this study, extracellular protease from the prototype strain *P. aeruginosa* ATCC 27853 was isolated and its enzymatic properties were characterized, considering the protease as a potential, new target for the design of antibacterial therapy at the level of exoproduct formation and interaction.[18]

EXPERIMENTAL

Materials

Phenyl-Toyopearl 650 was purchased from Tosoh Bioscience (Montgomeryville, PA, USA). Hammersten casein was purchased from Merck (Darmstadt, Germany). Sephadex G-75 was supplied by Pharmacia (Uppsala, Sweden). Molecular mass standards were supplied by Serva (Heidelberg, Germany). The chemicals used for electrophoresis were purchased from Sigma Chemicals (St. Louis, MO, USA). The equipment employed for chromatography and electrophoresis was purchased from Hoefer Scientific Instruments (San Francisco, CA, USA).

Microorganism

P. aeruginosa ATCC 27853 was provided by American Type Culture Collection (USA).

Culture conditions

P. aeruginosa ATCC 27853 was cultured at 30 °C for 20 h in Luria-Bertani (LB) medium (0.5 % NaCl, 0.5 % yeast extract and 1 % tryptone) agitated at 100 cycles min^{-1} with a horizontal shaker model LT-W (Küchner, Birsfelden, Switzerland). An actively growing culture was dispensed into an Erlenmeyer flask (1 %), and fermentation was realized in LB medium at 30 °C for 120 h. A culture filtrate was then collected after 96 h and used for protease isolation and purification.

Proteolytic activity assays

Proteolytic activity was determined using 0.6 % Hammersten casein solution (50 mM Tris–HCl, pH 7.6) as a substrate. The enzyme solution (1 ml) was mixed with the substrate solution (5 ml) and incubated at 30 °C. After 10 min, 5 ml of trichloroacetic acid (TCA) solution (0.11 mol L^{-1} TCA, 0.22 mol L^{-1} sodium acetate and 0.33 mol L^{-1} acetic acid) was added to the reaction mixture, which was followed by additional 20 min incubation. The precipitate was removed by filtration or centrifugation. The absorbance (A) of the filtrate was measured at 275 nm using a UV–Visible light spectrophotometer (Gilford, Gilford Instruments, Oberlin, OH, USA). One unit of protease activity is defined as the amount of the enzyme that gives an absorbance value equivalent to 1 μg of Tyr per min at 30 °C.[18]

Protease activity inhibition and stability in organic solvents was determined according to Morihara method.[19] In short, the activity was determined by incubating 1 ml of 2 % casein solution (pH 7.6) with 1 ml of enzyme solution at 40 °C for 10 min. The reaction was stopped by the addition of 2 ml of TCA solution followed by 20 min incubation at 40 °C. After filtration, the amount of liberated Tyr was determined spectrophotometrically at 660 nm (Gilford, Gilford Instruments, Oberlin, OH, USA) using Folin-Ciocalteu reagent (dilution 1:4) to develop color. One unit of enzyme activity is defined as the amount of enzyme that results in an ΔA_{660} of one.[18]

Purification of protease

All procedures were performed at 4 °C. The culture filtrate, obtained by centrifugation at 7500 rpm for 15 min (Sorvall, rotor SS-1, New Town, Conn., USA) was lyophilized and resolved in 50 mmol L^{-1} Tris–HCl buffer (pH 7.60), supplemented with 20 % ammonium sulfate, with final concentration of 1 mg ml^{-1} of proteins. This crude sample was purified by hydrophobic chromatography using Phenyl Toyopearl 650 resin previously equilibrated (20 % ammonium sulfate solution in 50 mmol L^{-1} Tris–HCl buffer, pH 7.6). The protease was collected as the flow-through, while all the contaminating proteins were bound to the resin.

Protein concentrations were determined by the Bradford method using crystalline bovine serum albumin (BSA) as the standard.[20] In some cases, the concentration of proteins was determined spectrophotometrically using the equation c (mg mL^{-1}) $=1.55A_{280} - 0.76A_{260}$.

Electrophoresis

Sodium dodecyl sulfate polyacrylamide gel electrophoresis, SDS PAGE, was performed using 12.5 % polyacrylamide gels,[21] under reducing conditions and a standard protein mixture containing: lysozyme (14.4 kDa), trypsin inhibitor (21 kDa), carbonic anhydrase (29 kDa), ovalbumin (45 kDa), bovine serum albumin (BSA) (67 kDa), phosphorylase B (97 kDa), and myosin (220 kDa).

Gel filtration

The molecular mass of the proteolytic enzymes was determined by gel filtration[22] on a Sephadex G-75 column (2.5 cm×75 cm), previously equilibrated with 50 mmol L^{-1} Tris–HCl buffer (pH 7.6) containing 0.5 mol L^{-1} NaCl. The column was calibrated using cytochrome *c* (12.5 kDa), chymotrypsin (25 kDa), ovalbumin (45 kDa), and BSA (67 kDa) as a molecular mass protein standard mix. The molecular masses were determined by plotting the log of molecular masses against the elution volumes.

Optimum pH

The pH optimum was determined using casein as substrate for the protease. 50 mmol L^{-1} buffers of different pH values were used to assay enzymatic activity: sodium citrate buffer (2.79–5.78), Sorensen's phosphate buffer (5.57–7.80), Tris–HCl buffer (7.62–9.39) and borate–NaOH buffer (9.50–11.41). Other conditions were as for the standard assay method.

pH Stability

The buffers used to test pH stability were: sodium citrate buffer (2.79–5.78), Sorensen's phosphate buffer (5.57–7.80), Tris-HCl buffer (7.62–9.39) and borate–NaOH buffer (9.50––11.41). Reaction mixtures (5 mg of enzyme in 1.2 ml buffer solution) were incubated at 30 °C for 3 h. The remaining enzymatic activity was measured under standard test conditions.

Optimum temperature

Using the standard reaction mixture, the proteolytic activity was monitored in 50 mmol L^{-1} Sorensen's phosphate buffer (pH 7.6) at different temperatures (from 25–90 °C) for 10 min.

Thermal stability

The samples in 50 mmol L^{-1} Tris-HCl buffer (pH 7.6) were incubated at different temperatures for various periods of time and then quickly cooled. Standard enzyme assays were then used to determine the enzyme activity.

Effects of inhibitors

The effects of different agents, such as: phenymethylsulfonyl fluoride (PMSF), *p*-chloromercuribenzoic acid (*p*CMB), 1,10-phenanthroline, ethylenediaminetetraacetic acid disodium salt (EDTA), dithiothreitol (DTT), were investigated. Enzyme solution in 50 mmol L^{-1} Tris–-HCl buffer (pH 7.6) was incubated after the addition of 5 mmol L^{-1} of inhibitor at 30 °C for 30 min, and remaining activity was determined by standard methods using casein as described by Morihara.[19]

Proteolytic apoenzyme reactivation

The enzyme activity was completely deactivated by treatment with 1 mmol L^{-1} 1,10-phenanthroline at 30 °C for 15 min. Following deactivation, solutions of different metal ions were added (Cu^{2+}, Mn^{2+}, Zn^{2+}, Ca^{2+} and Mg^{2+}) to a final concentration of 1.2 mmol L^{-1}, and then after incubation at 30 °C for 30 min, the remaining activity was determined under standard conditions.

Metal analysis

Elemental metal analysis (Zn, Cu, Co, Fe and Mn) was performed by means of flame atomic absorption using a Perkin Elmer SAS7500A atomic absorption spectrophotometer (Norwalk, MA, USA).

Substrate specificity

Activities against *N*-hippuryl-L-Lys, *N*-hippuryl-L-Phe, elastin, collagen model, heat-killed *S. aureus*, against synthetic esters, such as *N*-benzoyl-L-Arg-ethyl ester (BAEE), *N*-benzoyl-L-Tyr-ethyl ester (BTEE), and *N*-acetyl-L-Tyr-ethyl ester (ATEE), as well against synthetic oligopeptide-*p*-nitroanilide (*p*-NA) substrates, such as *N*-succinyl-Ala-Ala-Pro-Phe-*p*-NA, *N*-succinyl-Ala-Ala-Pro-Leu-*p*-NA, and *N*-benzoyl-Arg-*p*-NA were determined according to the methods recommended by Biochemica Merck (Darmstadt, Germany).

Organic solvent stability

The effects of various organic solvents (methanol, ethanol, acetone, 1-butanol, 2-propanol, chloroform, *n*-hexane and *N*,*N*-dimethylformamide (DMF)) on the crude protease were investigated. The culture supernatant was incubated in the presence of 30 % (v/v) of organic solvent for a fixed period of time (from 24 to 240 h). The experiments were performed at 30 °C on a rotary shaker at 160 strokes min^{-1}, according to the Ogino method.[18] A crude sample without organic solvent was assayed under the same experimental conditions and was used as a control.

RESULTS AND DISCUSSION

Purification of protease

The fermentation broth was concentrated by lyophilization and the proteolytic enzyme produced by the *P. aeruginosa* ATCC 27853 was purified from the lyophilisate by hydrophobic chromatography and gel filtration chromatography. A summary of the purification procedure is given in Table I. The purification of

protease was accomplished relatively easily, since the protease did not bind to the Phenyl-Toyopearl gel, while almost all the other contaminating proteins from the crude sample were bound to the column. After hydrophobic chromatography, the enzyme had been purified 5-fold with 57.5 % recovery. After gel filtration chromatography, the protease had been purified 30 times with a yield of 25.3 %. This was the final purification step prior to SDS PAGE, which was used to assess the protein homogeneity. The SDS PAGE of the purified protease is shown in Fig. 1.

TABLE I. Purification of the protease from *P. aeruginosa* ATCC 27853

Purification step	Total protein mg	Total activity mU	Specific activity mU mg^{-1}	Yield %	Purification fold
Crude preparation (lyophylisate)	100	1660	16.6	100	1
Phenyl-Toyopearl 650	10.84	954.5	88	57.5	5.3
Sephadex G-75	0.84	420	498	25.3	30

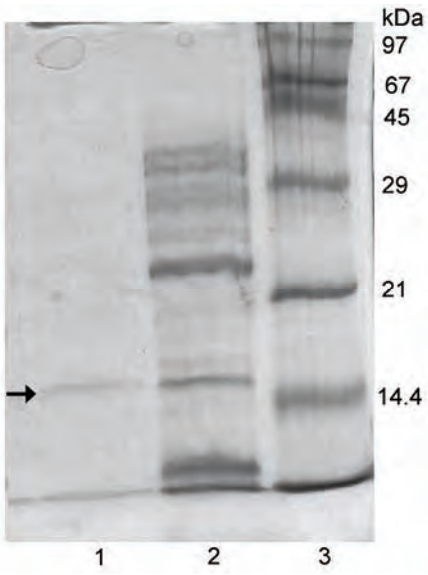

Fig. 1. Molecular mass determination of protease by SDS PAGE (12.5 %) under reducing conditions. Lane 1 – purified protease, lane 2 – crude protease preparation and lane 3 – markers: lysozyme, 14.4 kDa; trypsin inhibitor, 21 kDa; carbonic anhydrase, 29 kDa; ovalbumin, 45 kDa; BSA, 67 kDa; phosphorylase B, 97 kDa (myosin as a 220 kDa protein is too large to migrate under these gel conditions and it remained at the top of the gel lane).

Molecular mass determination of the protease

The molecular mass of the protease from *P. aeruginosa* ATCC 27853 determined by gel filtration on Sephadex G-75 was 14 kDa and by SDS PAGE, 15 kDa (Fig. 1). The group of proteolytic enzymes produced by *P. aeruginosa* strains includes at least four endopeptidases with molecular masses ranging from 20 to 50 kDa.[18] Using the ExPASy UniProt data base, 22 extracellular proteases from *P. aeruginosa* were found. As is given in Table II, among the identified proteases, six belong to the group of alkaline metalloproteinase, with a length of

479 amino acids (50 kDa), and five to the group of elastase LasB, with a length of 498 amino acids (54 kDa). With the exception of putative uncharacterized protease (also known as staphylolytic protease LasA), all the proteases as pre-proenzymes have a length of more than 400 amino acids (45 kDa), and according to available data, all of them have molecular mass ranging from 20 to 50 kDa, when they are in the form of mature extracellular protease. Molecular mass determination of proteases is difficult because of the presence of a protease-related processing intermediary protein, from which the mature enzyme is formed.[28] The molecular mass of the protease from *P. aeruginosa* ATCC 27853, obtained by SDS PAGE, suggests it is a small protease, different from any other hitherto characterized protease from *P. aeruginosa*. *P. aeruginosa* ATCC 27853 was declared as a strain producing elastase and alkaline protease, both having a molecular mass of about 30 kDa.[29]

TABLE II. *P. aeruginosa* proteases (search was performed using the network service of ExPASy)

Protein name (EC 3.4.24.-)	Accession number	Length of pre-proenzyme (AA)/calculated mass of pre-proenzyme (kDa)	Mass of extracellular protein, kDa
Putative uncharac-terized protein	P72166	263/28	20[18]
Protease lasA	P14789	418/46	20[23]
Alkaline proteinase	Q6SQM7	459/50	–
Alkaline proteinase	P72120	476/50	–
Alkaline metallo-proteinase	Q03023, Q4Z8K9, Q02J90, B7UWT0, A3LKRI7, A6V8W2	479/50	–
Organic solvent tolerant protease	Q6UL02	479/50	33[24]
Pseudolysin	P14756	498/54	33[25]
PseA protease	Q3Y6H8		
Elastase LasB	A3KXZ5, A3LEH5, A6V146, B7UZP0, Q02RJ6		35[26]
Elastase	A9QUN1		34[27]
Organic solvent tolerant elastase	A7LI11		33[24]

Effects of pH on the activity and stability of the protease

The effect of pH on the protease activity toward casein was examined at various pH values at 30 °C. The enzyme from ATCC strain was the most active in the pH range 7–8, as shown in Fig. 2. This pH optimum is similar to that of the protease isolated from *P. aeruginosa* ME4[30] and lower than those of san-ai protease and aeruginolysin protease (pH 9).[18,19]

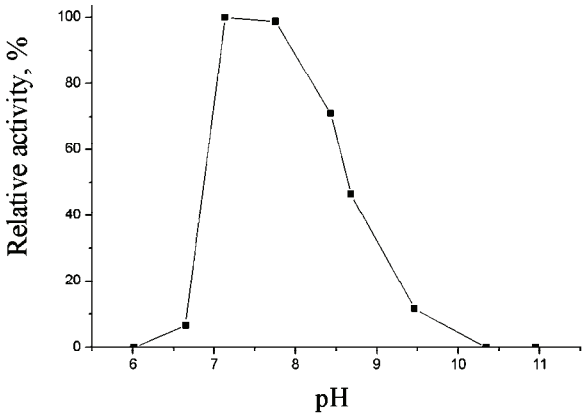

Fig. 2. Effect of pH on protease activity. The pH optimum was determined using casein as the substrate for protease in 50 mmol L^{-1} buffers of various pH values.

The stability of the ATCC enzyme was examined under various pH conditions. The enzyme was stable between pH 6.5 and pH 10, when the incubation was performed at 30 °C for 3 h, as shown in Fig. 3. This is similar to the pH stability of the protease from *P. aeruginosa* ME4.[30] On the other hand, the protease from the *P. aeruginosa* san ai strain and the alkaline protease aeruginolysin have different pH stability ranges (pH 5.5–11.5 and pH 5–9, respectively).[18,19]

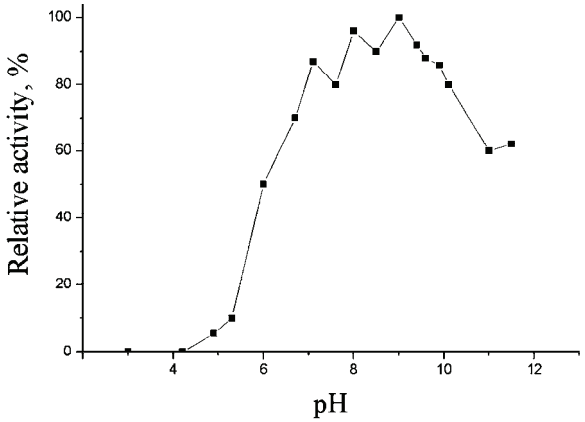

Fig. 3. The pH stability of the protease. Reaction mixtures (enzyme in buffer solutions) were incubated at 30 °C for 3 h. The remaining activity was measured under standard enzyme test conditions.

Effects of temperature on the activity and stability of the protease

The effect of temperature on the protease activity towards casein was examined at various temperatures for 10 min at pH 7.6 (50 mmol L^{-1} Sorensen's phosphate buffer). The optimum temperature of the ATCC protease was found to be around 60 °C, as shown in Fig. 4. This temperature optimum is the same as those reported for the proteases from the san ai strain and aeruginolysin,[18,19] and higher than that of protease from *P. aeruginosa* ME4, which is 50 °C.[30]

The thermostability of the enzyme was examined by measuring the residual activity after incubation at various temperatures for different periods of time. As shown in Fig. 5, the residual activity of the ATCC enzyme at pH 7.6 (50 mmol L^{-1} Tris–HCl buffer) was more than 50 % after incubation for 30 min at 60 °C, and about 43 % after incubation for 15 min at 70 °C. Thus, the ATCC protease is more stable than aeruginolysin (10 min at 60 °C), but less stable than the san-ai protease (90 min at 60 °C).[18,19]

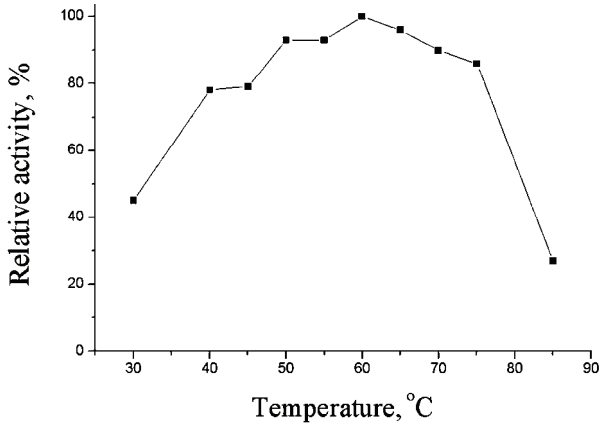

Fig. 4. Effect of temperature on protease activity. Using the standard reaction mixture, the proteolytic activity was monitored in 50 mmol L^{-1} Sorensen's phosphate buffer (pH 7.6) at different temperatures (from 25–90 °C) for 10 min.

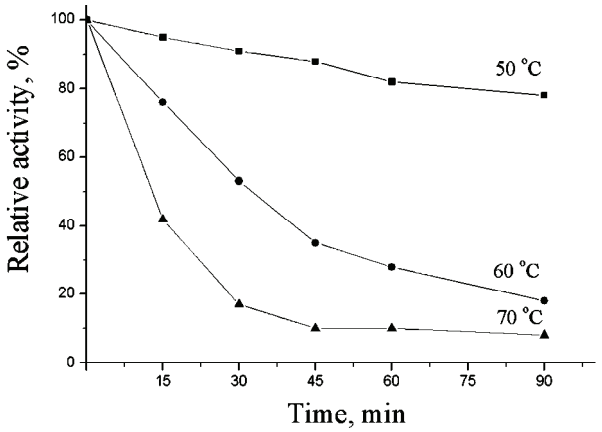

Fig. 5. Thermal stability of the enzyme. The enzyme solutions in 50 mmol L^{-1} Tris–HCl buffer (pH 7.6) were incubated at different temperatures for various periods and then quickly cooled. Standard enzyme assays were then used to determine the enzyme activity.

Effect of inhibitors

The protease activity was inhibited by EDTA and 1,10-phenanthroline, 96 % and 100 % respectively. The inhibition observed with the metal chelators EDTA and 1,10-phenanthroline suggests that the protease is a metalloenzyme. Additionally, the protease activity was significantly inhibited by DTT (54 %). This signifies that the enzyme contains a disulfide bond as part of its monomeric structure and that the activity of the enzyme is disulfide bond-dependent. This

effect is consistent with its aforementioned thermal stability, which was shown to be primarily the result of disulfide bond formation.[18,31] The serine protease inhibitor PMSF had no significant effect on the enzyme activity (inhibition of 5 %). *p*CMB had no effect on the protease activity, which suggests that the enzyme activity does not depend on sulfhydryl groups. Inhibition by metal chelators such as EDTA and 1,10-phenanthroline is a common property of almost all *P. aeruginosa* endopeptidases,[18,23,25,30] suggesting that the protease from *P. aeruginosa* ATCC 27853 is similar to other *P. aeruginosa* proteases, with the exception of serine protease Ps-1, which is not a metalloendopeptidase.[32] However, it should be noted that, with the exception of LasA,[33] *P. aeruginosa* metalloendopeptidases are not inhibited by reducing agents such as DTT or mercaptoethanol, suggesting that the activity of the enzyme is not disulfide bonds dependent. A similar inhibition pattern was reported for san ai and ME4 proteases.[18,30]

Enzyme reactivation

To determine the metal ion in *P. aeruginosa* ATCC 27853 metalloenzyme, the enzyme was treated with 1,10-phenanthroline and the obtained apoenzyme was reactivated by addition of different metal ions: Cu^{2+}, Mn^{2+}, Zn^{2+}, Fe^{2+}, Co^{2+}, Ca^{2+} and Mg^{2+}. Only Zn^{2+} efficiently restored the activity of the apoenzyme to 73 % of its original level, indicating that Zn^{2+} is essential for the protease. Reactivation of protease with the other ions was less than 50 % (Mn^{2+} restored the activity to 45 %; the other ions restored less than 10 % of the activity). This result was verified by atomic absorption spectrometry, which demonstrated one mol of Zn^{2+} per mol of enzyme. It was reported previously that Zn^{2+} is also present in other *P. aeruginosa* proteases, including aeruginolysin,[19] elastase,[34] LasA,[33] san ai[18] and ME4 protease.[30]

Substrate specificity

The protease acts on the protein substrate casein but not on elastin–orcein or on heat-killed *Staphylococcus aureus*. Thus, the enzyme is not an elastase and has no staphylolytic activity. No activity was found against chromogenic oligopeptide-*p*-NA substrates, *i.e.*, *N*-succinyl-Ala-Ala-Pro-Phe-*p*-NA, *N*-succinyl-Ala-Ala-Pro-Leu-
-*p*-NA and *N*-benzoyl-Arg-*p*-NA, the dipeptides hippuryl-L-Lys and hippuryl-L-
-Phe, and the pentapeptide $(Gly\text{-}Pro)_5$. Activity against synthetic substrates, such as ethyl esters: *N*-benzoyl-L-Arg-ethyl ester (BAEE) and *N*-benzoyl-L-Tyr-ethyl ester (BTEE), was very low but detectable, including activity against *N*-acetyl-L-
-Tyr-ethyl ester (ATEE). The enzyme was not active against Leu-*p*-NA.

Although the rules governing the substrate specificity of the protease from *P. aeruginosa* ATCC 27853 remain unclear, it should be emphasized that aeruginolysin[35] isolated from various strains of *P. aeruginosa* (IFO 3080, IFO 3455,

and T 30; stock cultures at the Institute of Fermentation of Osaka) and serralysin proteases have quite similar substrate specificity with a preference for small- to medium-sized substrates with hydrophobic residues at their P1' positions.[18,35]

Organic solvent stability

The effects of various organic solvents (such as methanol, ethanol, acetone, 1-butanol, 2-propanol, chloroform, *n*-hexane and *N*,*N*-dimethylformamide (DMF)) on the crude extracellular enzyme were investigated. The stability of the protease in organic solvents is shown in Fig. 6. The enzyme was stable in selected organic solvents, concentration 30 %, for 24 h, with the exception of 2-propanol, chloroform and ethanol. The protease activity remained unaltered in *n*-hexane, acetone, 1-butanol and methanol, even after a 240-h long exposure to these organic solvents. The stability of the protease in organic solvents may allow its employment in organic solvents for the synthesis of peptides.

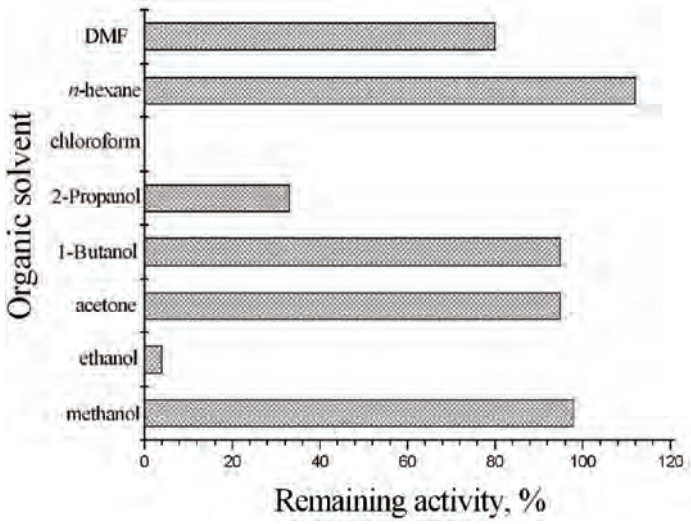

Fig. 6. Organic solvent stability of the enzyme. The effects of various organic solvents (30 % (v/v) of organic solvent) on the crude protease were investigated. A crude preparation without organic solvent was assayed under the same experimental conditions and was used as a control with 100 % activity.

CONCLUSIONS

Extracellular protease from the referent *P. aeruginosa* ATCC 27853 strain was purified, characterized, and its stability in water and different organic solvents determined. The protease molecular mass, pH optimum and substrate specificity indicate that a new protease has been identified. Enzymatic characterization of the protease yielded important information about its optimal catalytic conditions and organic solvent stability.

Acknowledgements. This research was supported by Ministry of Science and Technological Development of the Republic of Serbia, Grant No. 142018 B.

ИЗВОД

ИЗОЛОВАЊЕ И ДЕЛИМИЧНО КАРАКТЕРИСАЊЕ ПРОТЕАЗЕ ИЗ *Pseudomonas aeruginosa* ATCC 27853

ЛИДИЈА ИЗРАЕЛ-ЖИВКОВИЋ[1], ГОРДАНА ГОЈГИЋ-ЦВИЈОВИЋ[2] и ИВАНКА КАРАЦИЋ[1]

[1]*Медицински факултет, катедра за хемију, Универзитет у Београду, Вишеградска 26, 11000 Београд и* [2]*Институт за хемију, технологију и металургију, Центар за хемију, Универзитет у Београду, Његошева 12, 11000 Београд*

У овом раду је окарактерисана екстрацелуларна протеаза медицински значајног, референтног соја *Pseudomonas aeruginosa* ATCC 27853. Молекулска маса пречишћеног ензима одређена SDS PAGE и гел филтрацијом износи око 15 kDa. Одређени су следећи ензимски параметри: pH оптимум 7,1; pH стабилност у опсегу 6,5–10; температурни оптимум 60 °C, а ензим је стабилан на 60 °C 30 min. На основу инхибиције ензима помоћу EDTA и 1,10-фенантролина, утврђено је да протеаза представља металоензим. Показано да протеаза садржи 1 мол јона цинка по молу ензима. Протеаза је стабилна у присуству различитих органских растварача, што омогућава употребу за синтезу пептида.

(Примљено 25. јануара, ревидирано 26. априла 2010)

REFERENCES

1. E. Oldak, E. A. Trafny, *Antimicrob. Agents Chemother*. **49** (2005) 3281
2. J. L. Malloy, R. A. W. Veldhuizen, B. A. Thibodeaux, R. J. O'Callaghan, J. R. Wright, *Am. J. Physiol. Lung Cell Mol. Physiol.* **288** (2005) 409
3. M. H. Fulekar, M. Geetha, J. Sharma, *Biol. Med.* **1** (2009) 1
4. K. Jellouli, A. Bayoudh, L. Manni, R. Agrebi, M. Nasri, *Appl. Microbiol. Biotechnol.* **79** (2008) 989
5. S. Wilhelm, A. Gdynia, P. Tielen, F. Rosenau, K.-E. Jaeger, *J. Bacteriol*. **189 (**2007) 6695
6. V. E. Wagner, B. H. Iglewski, *Clin. Rev. Allergy Immunol.* **35** (2008) 124
7. A. Glessner, R. S. Smith, B. H. Iglewski, J. B. Robinson, *J. Bacteriol*. **181** (1999) 1623
8. D. L. Erickson, R. Endersby, A. Kirkham, K. Stuber, D. D. Vollman, H. R. Rabin, I. Mitchell, D. G. Storey, *Infect. Immun*. **70** (2002) 1783
9. M. C. Chifiriuc, L. M. Ditu, O. Banu, C. Bleotu, O. Drăcea, M. Bucur, C. Larion, A. M. Israil, V. Lazăr, *Roum. Arch. Microbiol. Immunol.* **68** (2009) 27
10. L. Passador, B. H. Iglewski, *Virulence mechanisms of bacterial pathogens*, J. A. Roth, Ed., ASM Press, Washington DC, 1995. p. 65
11. D. R. Galloway, *Mol. Microbiol*. **5 (**1991) 2315
12. K. A. Kernacki, J. A. Hobden, L. D. Hazlett, R. Fridman, R. S. Berk, *Invest. Ophthalmol. Vis. Sci.* **36** (1995) 1371
13. E. Lattmann, S. Dunn, S. Niamsanit, N. Sattayasa, *Bioorg. Med. Chem. Lett.* **15** (2005) 919
14. R. K. Tiwari, D. Singh, J. Singh, A. K. Chhillar, R. Chandra, A. K. Verma, *Eur. J. Med. Chem*. **41 (**2006) 40
15. W. H. Tong, R. Wang, D. Chai, Z. X. Li, F. Pei, *Int. J. Antimicrob. Agents* **28** (2006) 454
16. G. Ginalska, D. Kowalczuk, M. Osińska, *Int. J. Pharm*. **339** (2007) 39

17. D. G. Davies, M. R. Parsek, J. P. Pearson, B. H. Iglewski, J. W. Costerton, E. P. Greenberg, *Science* **280 (**1998) 295
18. I. Karadžić, A. Masui, N. Fujiwara, *J. Biosci. Bioeng.* **98** (2004) 145
19. K. Morihara, *Biochim. Biophys. Acta* **73** (1963) 113
20. M. M. Bradford, *Anal. Biochem*. **72** (1976) 248
21. U. K. Laemmli, *Nature* **227** (1970) 680
22. P. Andrews, *Biochem. J.* **96** (1965) 595
23. E. Kessler, M. Safrin, J. C. Olson, D. E. Ohman, *J. Biol. Chem.* **268** (1993) 7503
24. A. Gupta, S. Ray, S. Kapoor, S. K. Khare, *J. Mol. Microbiol. Biotechnol.* **15** (2008) 234
25. E. Kessler, D. E. Ohman**,** *Handbook of Proteolytic Enzymes (CD-ROM)*, A. J. Barret, N. D. Rawlings, J. F Woessner, Eds., Academic Press, London, 1998
26. A. Gupta, I. Roy, S. K. Khare, M. N. Gupta, *J Chromatogr. A* **1069** (2005) 155
27. X. Lin, W. Xu, K. Huang, X. Mei, Z. Liang, Z. Li, J Guo Y.B. Luo, *Protein Express. Purif.* **63** (2009) 69
28. J. K. Gustin, E. Kessler, D. E. Ohman, *J. Bacteriol.* **178** (1996) 6608
29. R. J. O'Callaghan, L. S. Engel, J. A. Hobden, M. C. Callegan, L. C. Green, J. M. Hill, *Invest. Ophthalmol. Vis. Sci.* **37** (1996) 534
30. M. Cheng, S. Takenaka, S. Aoki, S. Murakami, K. Aoki, *J. Biosci. Bioeng.* **107** (2009) 373
31. J. W. Jang, H. J. Ko, E. K. Kim, W. H. Jang, J. H. Kang, O. J. Yoo, *Biotechnol. Appl. Biochem.* **34** (2001) 81
32. B. W. Elliot Jr., C. Cohen, *J. Biol. Chem.* **261** (1986) 11259
33. M. W. Pantoliano, L. C. Ladner, P. N. Bryan, M. L. Rollence, J. F. Wood, T. L. Poulos, *Biochemistry* **26** (1987) 2077
34. S. Fukuchi, K. Nishikawa, *J. Mol. Biol*. **309** (2001) 835
35. H. Maeda, K. Morihara, *Methods Enzymol*. **248** (1995) 395.

Journal of the Serbian Chemical Society
JSCS-info@shd.org.rs • www.shd.org.rs/JSCS
J. Serb. Chem. Soc. 75 (8) 1053–1061 (2010)
JSCS–4030
UDC 547.963.32+547.455.5+57.088:
612.12:575.113
Original scientific paper

Comparison of phenol-based and alternative RNA isolation methods for gene expression analyses

KSENIJA V. JAKOVLJEVIĆ*, MILENA R. SPASIĆ, EMINA J. MALIŠIĆ, JELENA D. DOBRIČIĆ, ANA M. KRIVOKUĆA and RADMILA N. JANKOVIĆ

Department of Experimental Oncology, Institute of Oncology and Radiology of Serbia, Pasterova 14, 11000 Belgrade

(Received 23 December 2009, revised 5 February 2010)

Abstract: The widespread use of gene expression analyses has been limited by the lack of critical evaluations of the methods used to extract nucleic acids from human tissues. For evaluating gene expression patterns in whole blood or leukocytes, the method of RNA isolation needs to be considered as a critical variable in the design of the experiments. Quantitative real-time PCR (qPCR) is widely used for the quantification of gene expression in today's clinical practice. Blood samples as a preferred RNA source for qPCR should be carefully handled and prepared in order not to inhibit gene expression analyses. The present study was designed to compare the frequently employed guanidine thiocyanate–phenol–chloroform-based method (TRI Reagent®) with two alternative RNA isolation methods (6100 PrepStation and QIAamp®) from whole blood or leukocytes for the purpose of gene expression analysis in chronic myeloid leukemia (CML) patients. Based on the results of this study, for the best combination of yield and RNA extraction purity, taking into account the necessary amount of the clinical sample and performance time, the protocol using phenol-based TRI Reagent® for RNA extraction from leukocytes is suggested as the most suitable protocol for this specific gene expression analysis.

Keywords: RNA isolation; blood; leukocytes; TRI Reagent®; PCR.

INTRODUCTION

The development of molecular medicine, particularly in the last decade, undoubtedly put new molecular diagnostic tests into the focus. Most of these tests employ some kind of gene expression analysis. The widespread use of gene expression analyses has been limited by the lack of critical evaluation of the methods used to extract nucleic acids from human tissues. Quantitative real-time PCR (qPCR) is widely used for the quantification of gene expression in today's

* Corresponding author. E-mail: ksenija.jakovljevic@ncrc.ac.rs
doi: 10.2298/JSC091223084J

clinical practice.[1] Blood is an easy to obtain tissue and reflects the relevant information about the body, which makes it the preferred source of RNA for diagnostic tests. Blood samples for qPCR should be carefully handled and prepared so as not to inhibit gene expression analysis.[2] The absence of widely accepted protocols for blood sampling and further RNA extraction among laboratories is evident. Each laboratory has to establish the optimal procedure for the specific clinical application.

For evaluating gene expression patterns in whole blood or leukocytes, the method of RNA isolation needs to be considered as a critical variable in the design of the experiments.[3] Low quality and quantity of RNA often make all downstream applications impossible to conduct. Inadequate sampling, shipping and handling could easily cause degradation of RNA.[4] It is crucial to decrease the sampling time to a minimum and preferably store samples in RNA later.[5] Clinical samples of limited quantity are specially challenging, since unsuccessful RNA isolation means that the opportunity to analyze that particular sample is irretrievably lost.

Phenol-based methods are most commonly used for RNA isolation. When dealing with small clinical samples, a single extraction reagent (such as phenol--based TRI Reagent®) is crucial in order to obtain sufficient material for subsequent analyses.[6] Due to the high activity of RNAses in tissues, it is necessary to include a strong chaotropic (biologically disruptive) agent into the isolation reagent mixture. Guanidinium salts, together with phenol and chloroform (added to improve the deproteinization efficacy of phenol) denature and precipitate proteins without altering the solubility of RNA.[7]

In our laboratory, monitoring of the minimal residual disease in patients diagnosed with chronic myeloid leukemia (CML) is performed by detection of the bcr-abl fusion-gene (specific for chromosomal translocation t (9:22)) by qPCR.[8] The present study was designed to compare the mentioned guanidine thiocyanate–phenol–chloroform-based method with two alternative methods for RNA isolation from whole blood or leukocytes in order to establish the most adequate one for this specific downstream qPCR. To validate the quality of isolation process, both the yield and the purity of RNA were assessed and also the quality control of cDNA synthesis was performed by PCR amplification of reference genes. As a result of this evaluation, subsequent qPCR analysis was successfully conducted (the results are not included in this manuscript).

EXPERIMENTAL

Patient and control samples

The current study included five control (healthy) subjects and fourteen patients with CML. The patients were under medical treatment for CML and had been under constant observation for detection of minimal residual disease in our laboratory for several months. From each control and patient, 20 mL EDTA blood were drawn by venipuncture and further pro-

cessed within a few hours. According to the RNA isolation protocols from whole blood, specified amounts of blood, just from control samples, were transferred immediately into separate tubes and processed the same day. The rest of the blood was used for leukocyte isolation by centrifugation, according to the established procedure used in our laboratory. The isolated cells were counted and pellets were stored at –70 °C until RNA isolation.

RNA isolation

Three methods for extraction of total cellular RNA from blood and leukocytes were evaluated. The isolations were performed following the manufacturers' instructions with minor modifications.

Whole blood RNA isolation

Total RNA samples were isolated from whole blood only from the controls using TRI Reagent® BD kit (Sigma) (the TRI Reagent®), Applied Biosystems Total RNA Isolation Chemistry kit for Abi Prism™ 6100 Nucleic Acid PrepStation (the 6100 PrepStation) and QIAamp® RNA Blood Mini kit (Qiagen) (the QIAamp®). Briefly, 200 µL of the blood samples were lysed in TRI Reagent® BD supplemented with 5 M acetic acid, and the lysate was separated into aqueous and organic phases *via* chloroform addition and centrifugation. The RNA sample was then precipitated from the aqueous phase by 2-propanol and solubilized with 40 µL RNAase-free water. For the standard RNA isolation protocol on the 6100 PrepStation, 200 µL of the blood samples were lysed and purified using Applied Biosystems Total RNA isolation chemistry. For the QIAamp® method, the protocol for human whole blood was realized without any modification using 1 mL of blood as the starting material. The extracted RNA was eluted in 40 µL RNAase-free water.

Leukocyte RNA isolation

Total RNA samples were isolated from leukocytes from four controls (the fifth had to be discarded) and from all CML patients using the same methods, performing the protocols for whole blood according to the manufacturers' recommendations with minor modifications. The only difference in the phenol-based method was the first step, in which the cells (5×10^6 cells from controls; 10^7 cells from patients) were lysed with TRI Reagent® (Sigma) (TRI Reagent®). Aliquots of 2.1×10^6 and 1.3×10^6 cells from controls and patients, respectively, were taken for the standard RNA isolation protocol on the 6100 PrepStation. Finally, aliquots of 5×10^6 cell pellets from controls and patients were dissolved in 1 mL of normal saline solution and further processed according to the QIAamp® protocol for whole blood. This additional step was performed in order to selectively lyse the remaining erythrocytes in the pellets.

RNA quantization and visualization

The total RNA of each sample was quantified using a spectrophotometer (Eppendorf BioPhotometer) by the ultraviolet light absorbance at 260 nm. The ratio A_{260}/A_{280} was used to assess the purity of the isolated RNA. The RNA concentration was calculated in µg μL^{-1}. To analyze the RNA banding pattern, gel electrophoresis (Pharmacia Biotech) in 2 % agarose gels with ethidium bromide was performed. The RNA samples (6 µL) mixed with xylene cyanol color (3 µL; 0.25 % xylene cyanol in 30 % glycerol in water) and 0.5-µL portion (1.0 µg μL^{-1}) of molecular weight marker 1 kb DNA Ladder (Invitrogen) were run in 0.5xTBE buffer for 50 min at 25 mA. The RNA bands were visualized on a UV transilluminator (Hoefer) and photographed using a Nikon D70s camera.

cDNA Synthesis and PCR

cDNA synthesis (RT-PCR) from total RNA and following PCR reactions with Abl and p53 primers were performed only for the control (n = 4) and patient (n = 14) samples isolated from leukocytes by the TRI Reagent® method.

To perform RT-PCR with random primers, 2 μg of total RNA were used as template for MultiScribe™ Reverse Transcriptase (50 U μL^{-1}) in a High-Capacity cDNA Reverse Transcription kit (Applied Biosystems) according to manufacturer's instructions. The reaction mixtures (20 μL) were incubated in a Mastercycler gradient (Eppendorf). cDNAs were analyzed by 2 % agarose gel electrophoresis and visualized on a UV transilluminator.

The PCR step was performed in a volume of 25 μL, including 2 μl 100 ng μL^{-1} of cDNA, 12.5 μL of AmpliTaq Gold PCR Master Mix (Applied Biosystems), 1 μL 10 pmol μL^{-1} each of the two Abl primers (Applied Biosystems) and 0.8 μL 10 pmol μL^{-1} each of the two p53 primers (Applied Biosystems). A tube with water instead of cDNA was used as the negative control (NTC – non-template control) in both PCR reactions. The sequence of the forward PCR primer for Abl was TGGAGATAACACTCTAAGCAT, whereas the sequence of the reverse PCR primer for Abl was GATGTAGTTGCTTGGGACCCA. The sequences of the forward and reverse PCR primers for p53 were ACTGGCCTCATCTTGGGCCT and TGTGCAGGGTGGCAAGTGGC, respectively. PCR for Abl was performed in a Mastercycler gradient for 30 s denaturation at 95 °C followed by 35 cycles consisting of 30 s at 94 °C, 1 min at 65 °C, 1 min at 72 °C and a hold at 16 °C. For the p53 PCR, the reaction mixtures were heated at 95 °C for 5 min and then subjected to 35 cycles at 95 °C for 1 min and at 60 °C for 1 min, followed by a hold at 4 °C in the same thermal cycler. A 6-μL portion of PCR products and 3-μL portion of ready-to-use molecular weight marker O'Gene Ruler 100 bp DNA Ladder (Fermentas) were analyzed by 40 min agarose electrophoresis. The PCR product bands were visualized on a UV transilluminator and photographed. A sample was considered positive for Abl when it generated a PCR product of the expected size of 123 bp in the Abl PCR reaction, whereas the generated product of 171 bp in p53 PCR reaction indicated a sample positive for p53.

RESULTS AND DISCUSSION

The RNA concentrations and A_{260}/A_{280} ratios of each control and patient sample obtained using the TRI Reagent®, 6100 PrepStation and QIAamp® method are given in Table I. In all tested samples, the highest concentration was achieved with the TRI Reagent® (between 0.888 and 6.338 μg μL^{-1}), while with QIAamp®, it was much lower (between 0 and 0.197 μg μL^{-1}). The 6100 PrepStation system showed a poor performance (between 0 and only 0.012 μg μL^{-1}). The average RNA concentrations for each method are shown in Fig. 1. There is a clear difference in mean RNA concentrations between the TRI Reagent® method and the other two methods (those obtained using the TRI Reagent® were noticeably higher). The results also show the difference between concentrations of the RNA samples isolated from blood and those from leukocytes (the blood RNA concentrations were lower).

One of possible explanations for the highest yield of RNA obtained with TRI Reagent® could be the amount of the starting material, as well as the different biochemical mechanism of cell lysis. In the cases of QIAamp® and the 6100

PrepStation, we were limited at the beginning by the maximum amount of starting material, recommended by manufacturer.

TABLE I. Concentrations and purity of the RNA samples

Material	Samples	c / μg μL^{-1} (A_{260}/A_{280} ratio)		
		RNA isolation methods		
		TRI Reagent®	6100 PrepStation	QIAamp®
		Blood		
Controls (n = 5)	C1	1.293 (1.43)	0.004 (NA)[a]	0.076 (1.38)
	C2	2.176 (1.75)	0.004 (NA)	0.163 (1.27)
	C3	2.711 (1.53)	0.000 (NA)	0.061 (1.92)
	C4	2.422 (1.55)	0.000 (NA)	0.062 (1.74)
	C5	2.007 (1.52)	0.000 (NA)	0.082 (1.71)
		Leukocytes		
Controls (n = 4)	C1	2.096 (1.50)	0.000 (NA)	0.012 (NA)
	C2	3.211 (1.57)	0.012 (NA)	0.197 (1.38)
	C3	3.611 (1.59)	0.000 (NA)	0.092 (1.54)
	C5	3.397 (1.54)	0.000 (NA)	0.072 (1.59)
Patients (n = 14)	1	4.100 (1.48)	0.008 (0.29)	0.016 (NA)
	2	2.014 (1.57)	0.000 (NA)	0.000 (NA)
	3	4.189 (1.55)	0.000 (NA)	0.000 (NA)
	4	3.333 (1.49)	0.000 (NA)	0.000 (NA)
	5	3.801 (1.47)	0.004 (NA)	0.008 (NA)
	6	6.338 (1.57)	0.000 (NA)	0.050 (1.80)
	7	3.458 (1.47)	0.000 (NA)	0.008 (NA)
	8	3.538 (1.46)	0.000 (NA)	0.036 (NA)
	9	0.888 (1.37)	0.000 (NA)	0.032 (NA)
	10	1.818 (1.43)	0.000 (NA)	0.000 (NA)
	11	3.039 (1.50)	0.000 (NA)	0.000 (NA)
	12	2.263 (1.41)	0.000 (NA)	0.024 (3.03)
	13	4.574 (1.50)	0.000 (NA)	0.016 (NA)
	14	3.517 (1.51)	0.000 (NA)	0.000 (NA)

[a]Not available, A_{280} = 0

The A_{260}/A_{280} ratios (Table I) had values lower than 2.0 (the expected value for a pure RNA sample) for most of the samples (just one sample had an A_{260}/A_{280} ratio 3.0). The QIAamp® method resulted in the highest values, ranging from 1.3 to 3.0, but many of the samples even had no available value (NA) because A_{280} was zero. For the TRI Reagent® method, these values ranged from 1.4 to 1.8 and practically all values for 6100 PrepStation, except one (0.3), were NA. The highest purity of RNA obtained by the QIAamp® method was expected due to high selective binding properties of the silica-based membrane, but the yield of RNA, regardless of its purity, was not sufficient for further cDNA synthesis and expression analysis by qPCR. During the isolation procedure with TRI Reagent®, one ethanol washing of the RNA pellet was omitted in an effort to ma-

ximize the yield, which may be the reason of the lower purity RNA. The 6100 PrepStation employs selective precipitation of RNA and its physical capture on a membrane, giving the possibility of isolating very pure RNA but, except in a few cases, measurable values of the RNA concentration were not obtained.

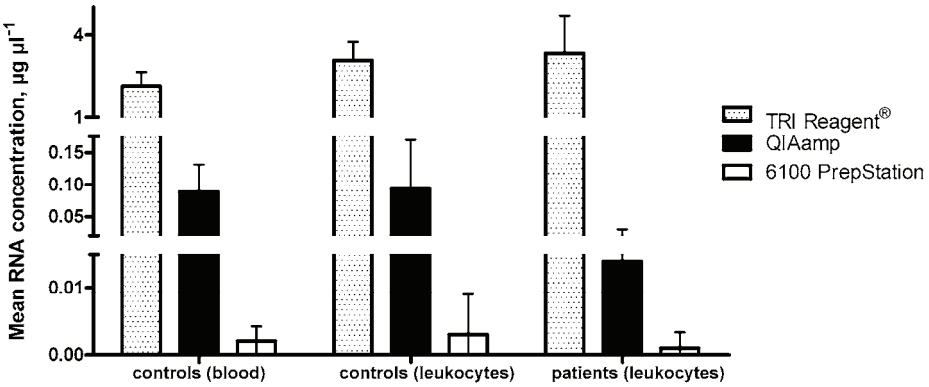

Fig. 1. Obtained RNA concentrations, the resulting bars shown are the average, and the standard deviation, from values obtained for each extraction method.

In order to verify the integrity, all RNA samples for each of the extraction methods were analyzed using 2 % agarose gel electrophoresis. High quality RNA was indicated by visible bands on the agarose gels only for certain methods. Agarose gel electrophoresis of isolated control RNA samples is shown in Fig. 2.

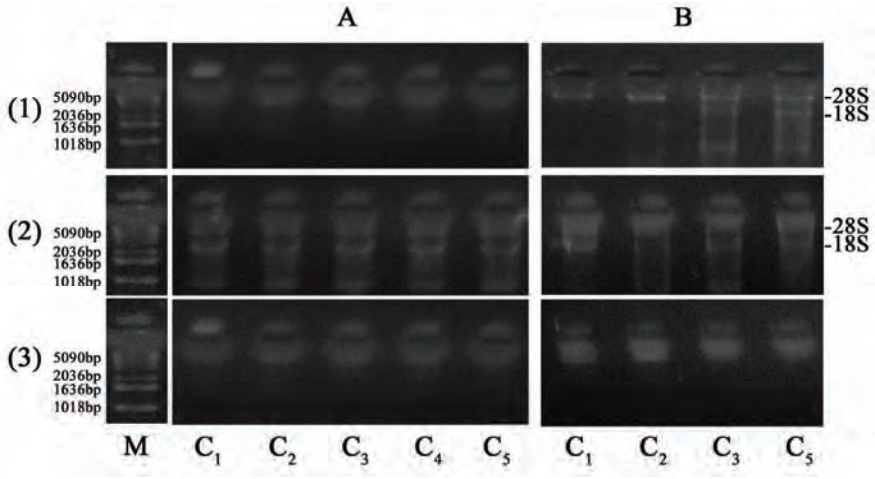

Fig. 2. Agarose gel electrophoresis of isolated control RNA samples. A) Whole blood; B) leukocytes. 1) TRI Reagent®, 2) QIAamp® and 3) 6100 PrepStation. C1–C5: control subjects, M: molecular weight marker.

From whole blood control samples, RNA bands are visible only for the QIAamp® method, while from leukocytes control samples, they are also visible for the QIAamp® and TRI Reagent® methods. Clearly, the RNA obtained from leukocytes showed more defined and visible bands, indicating a low level of degradation. Therefore, it was decided to use leukocytes as the RNA source. The RNA band patterns for patient samples isolated from leukocytes by the TRI Reagent® and QIAamp® methods are shown in Fig. 3 (the agarose gel for the 6100 Prep-Station method is not shown because there were no visible RNA bands). The RNA bands obtained by QIAamp® are more defined than those obtained by TRI Reagent®, due the higher purity of the former, but the problem of the amount remains. Since the next step of the analysis is RT-PCR, which requires in this specific case 2 μg of RNA (in order to obtain the minimal amount of cDNA for qPCR), it is evident that the QIAamp® method would not provide enough RNA from all samples. Although some control and patient samples may have sufficient RNA concentrations when obtained by the QIAamp® method, it is crucial that the method of choice always provides the necessary amounts of RNA. On the other hand, the TRI Reagent® method consistently provided sufficient amounts of RNA for all the analyzed samples and was therefore chosen as the most adequate protocol for this specific purpose.

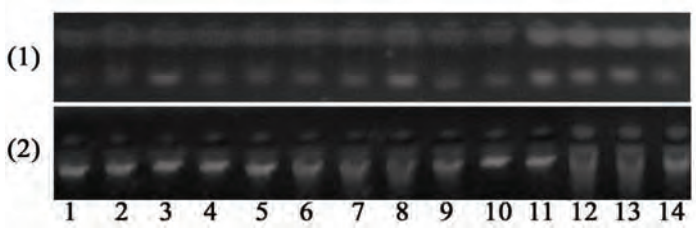

Fig. 3. Agarose gel electrophoresis of patients' RNA samples isolated from leukocytes. 1) TRI Reagent® and 2) QIAamp®. 1–14: Patients.

Following electrophoresis, RNA obtained with TRI Reagent® from leukocytes from each control and patient subject were assayed in RT-PCR, as described in the Experimental (results not shown). The synthesized cDNAs were further amplified with Abl and p53 primers in separate PCR reactions according to the protocol described in the Experimental. Agarose gels with PCR product bands and DNA molecular weight marker are represented in Fig. 4. PCR products of 123 bp in the Abl PCR reaction and of 171 bp in the p53 PCR reaction were obtained in practically all tested samples. The fact that visible bands of PCR products for both genes were obtained indicates that there are no inhibitors in template RNA preparations and that obtained cDNA was of satisfactory quality for further analysis. The subsequent gene expression analysis by qPCR for the detection of the bcr–abl fusion transcript was successfully performed on all patient

cDNA samples (the results are not shown). This diagnostic procedure is a part of everyday clinical routine in our laboratory.

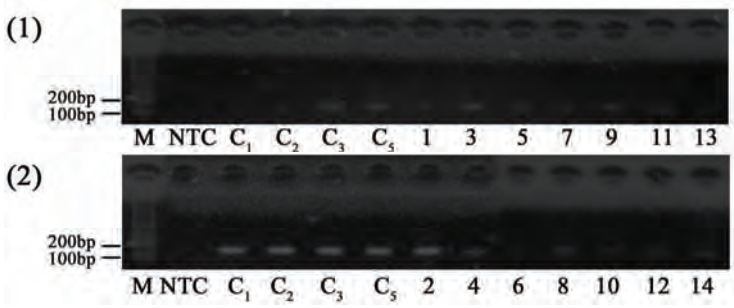

Fig. 4. Agarose gel electrophoresis of PCR products; 1) Abl gene primers and 2) p53 gene primers. M: Molecular weight marker; NTC: non-template control. C1, C2, C3, C5: Control subjects; 1–14: patients.

CONCLUSIONS

In light of the obtained results for the best combination of yield and RNA extraction purity, taking into account the required amount of the clinical sample and the performance time, the protocol using the phenol-based TRI Reagent® for RNA extraction from leukocytes is suggested as the most suitable protocol for this specific gene expression analysis.

Acknowledgements. The authors wish to thank Filip Stojanović and Gordana Kukić for their excellent technical assistance.

ИЗВОД

ПОРЕЂЕЊЕ ФЕНОЛСКЕ СА АЛТЕРНАТИВНИМ МЕТОДАМА ИЗОЛАЦИЈЕ РНК У СВРХУ АНАЛИЗЕ ГЕНСКЕ ЕКСПРЕСИЈЕ

КСЕНИЈА В. ЈАКОВЉЕВИЋ, МИЛЕНА Р. СПАСИЋ, ЕМИНА Ј. МАЛИШИЋ, ЈЕЛЕНА Д. ДОБРИЧИЋ, АНА М. КРИВОКУЋА и РАДМИЛА Н. ЈАНКОВИЋ

Одељење за експерименталну онкологију, Институт за онкологију и радиологију Србије, Пастерова 14, 11000 Београд

Недостатак критичне процене ефикасности метода за изолацију нуклеинских киселина из ткива ограничава шире коришћење анализа генске експресије. Изолација РНК представља критичну променљиву при одређивању генске експресије из узорака крви или леукоцита. Квантитативни „real-time“ PCR (qPCR) се у савременој клиничкој пракси често користи за квантификацију генске експресије. Узорци крви, као најчешћи извор РНК, морају бити пажљиво припремљени да не би дошло до инхибиције анализе генске експресије у току qPCR-а. Ова студија је спроведена у циљу упоређивања често коришћене гванидин-тиоцијанат–фенол–хлороформске методе изолације (TRI Reagent®) са друге две алтернативне методе за изолацију РНК (6100 PrepStation и QIAamp®) из пуне крви или леукоцита у сврху анализе генске експресије код пацијената са хроничном мијелоидном леукемијом. Имајући у виду количину клиничког узорка и време потребно за анализу, фенолска метода (TRI Reagent®) је

дала најбољу комбинацију приноса РНК и њене чистоће, те се стога ова метода предлаже за изолацију РНК из леукоцита у сврху ове специфичне клиничке анализе.

(Примљено 23. децембра 2009, ревидирано 5. фебруара 2010)

REFERENCES

1. S. A. Bustin, V. Benes, T. Nolan, M. W. Pfaffl, *J. Mol. Endocrinol.* **34** (2005) 597
2. L. Rainen, U. Oelmueller, S. Jurgensen, R. Wyrich, C. Ballas, J. Schram, C. Herdman, D. Bankaitis-Davis, N. Nicholls, D. Trollinger, V. Tryon, *Clin. Chem.* **48** (2002) 1883
3. R. J. Feezor, H. V. Baker, M. Mindrinos, D. Hayden, C. L. Tannahill, B. H. Brownstein, A. Fay, S. MacMillan, J. Laramie, W. Xiao, L. L. Moldawer, J. Perren Cobb, K. Laudanski, C. L. Miller-Graziano, R. V. Maier, D. Schoenfeld, R. W. Davis, R. G. Tompkins, *Physiol. Genomics* **19** (2004) 247
4. C. A. Perez-Novo, C. Claeys, F. Speleman, P. V. Cauwenberge, C. Bachert, J. Vandesompele, *Biotechniques* **39** (2005) 52
5. S. Fleige, M. Pfaffl, *Mol. Aspects Med.* **27** (2006) 126
6. A. Hummon, S. Lim, M. Difilippantonio, T. Ried, *BioTechniques* **42** (2007) 467
7. S. Mitra, *Sample Preparation Techniques in Analytical Chemistry*, Wiley, Hoboken, NJ, 2003, p. 306
8. T. Hughes, M. Deininger, A. Hochhaus, S. Branford, J. Radich, J. Kaeda, M. Baccarani, J. Cortes, N. C. P. Cross, B. J. Druker, J. Gabert, D. Grimwade, R. Hehlmann, S. Kamel-Reid, J. H. Lipton, J. Longtine, G. Martinelli, G. Saglio, S. Soverini, W. Stock, J. M. Goldman, *Blood* **108** (2006) 28.

Journal of the Serbian Chemical Society
JSCS-info@shd.org.rs • www.shd.org.rs/JSCS
J. Serb. Chem. Soc. 75 (8) 1063–1074 (2010)
JSCS–4031
UDC 546.881–31+546.77–31+
547.82:548.7:543.422.25
Original scientific paper

Transition metal complexes with thiosemicarbazide-based ligands. Part 57. Synthesis, spectral and structural characterization of dioxovanadium(V) and dioxomolybdenum(VI) complexes with pyridoxal *S*-methylisothiosemicarbazone

VUKADIN M. LEOVAC[1*#], VLADIMIR DIVJAKOVIĆ[1], MILAN D. JOKSOVIĆ[2], LJILJANA S. JOVANOVIĆ[1#], LJILJANA S. VOJINOVIĆ-JEŠIĆ[1#], VALERIJA I. ČEŠLJEVIĆ[1#] and MILENA MLINAR[1]

[1]*Faculty of Sciences, University of Novi Sad, Trg D. Obradovića 3, 21000 Novi Sad and* [2]*Faculty of Sciences, University of Kragujevac, R. Domanovića 12, 34000 Kragujevac, Serbia*

(Received 13 January, revised 2 February 2010)

Abstract: This work is concerned with the synthesis of neutral dioxovanadium(V) and dioxomolybdenum(VI) complexes with tridentate ONN pyridoxal *S*-methylisothiosemicarbazone (PLITSC) of the respective formulas $[VO_2(PLITSC–H)]\cdot 2H_2O$ and $[MoO_2(PLITSC–2H)]$. Structural X-ray analysis of the vanadium complex showed that it has an almost ideal square-pyramidal structure, while the molybdenum complex is supposed to have a polymeric octahedral structure. In addition to elemental analysis, both complexes were characterized by conductometric and magnetometric measurements, as well as by IR, UV–Vis, ^{1}H- and ^{13}C-NMR spectra.

Keywords: dioxovanadium(V); dioxomolybdenum(VI); complexes; pyridoxal *S*-methylisothiosemicarbazone; crystal structure; spectra.

INTRODUCTION

Due to their interesting physicochemical, structural, and biological properties, tridentate ONS Schiff-bases derivatives of pyridoxal (one of the forms of vitamin B_6), along with the unsubstituted and substituted thiosemicarbazide (PLTSC), as well as their complexes, have constantly attracted research interest during the last 20 years. As a result, a number of complexes have been prepared and studied with different metals,[1–4] including the most recently synthesized complexes of V(V)[5] and Mo(VI,V)[6] with these ligands. In contrast to the numerous metal complexes with PLTSC, interest in tridentate ONN pyridoxal isothiosemicarbazone is of a more recent date, so that only a limited number of complexes, namely with

* Corresponding author. E-mail: vukadin.leovac@dh.uns.ac.rs
# Serbian Chemical Society member.
doi: 10.2298/JSC100113045L

Cu(II), Fe(III) and Co(III),[1] have been prepared and characterized. In view of the biological importance of not only molybdenum,[7,8] but also of vanadium,[9,10] together with the more recently reported biological activity of some isothiosemicarbazones,[11,12] it is not surprising that the synthesis of complexes of these metals with the mentioned ligands aroused also a notable interest. Hence, the objective of this work was to study the syntheses, as well as the spectral and structural characteristics of the neutral complexes of dioxovanadium(V) and dioxomolybdenum(VI) with pyridoxal *S*-methylisothiosemicarbazone (PLITSC) of the formula $[VO_2(PLITSC–H)]\cdot 2H_2O$ and $[MoO_2(PLITSC–2H)]$.

EXPERIMENTAL

Reagents

All the employed chemicals were commercially available products of analytical reagent grade, except for the ligand pyridoxal *S*-methylisothiosemicarbazone and $MoO_2(acac)_2$, which were prepared according to known procedures.[13,14]

Synthesis of the complexes

$[VO_2(PLITSC–H)]\cdot 2H_2O$. Over a mixture of NH_4VO_3 (0.070 g, 0.60 mmol) and $PLITSC\cdot H_2O$ (0.160 g, 0.60 mmol) was poured 3 cm^3 $ccNH_3$ (aq.) and 3 cm^3 MeOH and the mixture was refluxed for about 1.5 h. After 50 h standing at room temperature, orange crystals formed which were filtered and washed with MeOH. Yield: 0.14 g (64 %).

$[MoO_2(PLITSC–2H)]$. Over a mixture of 0.27 g (1.0 mmol) of $PLITSC\cdot H_2O$ and 0.33 g (1.0 mmol) $MoO_2(acac)_2$ was poured 15 cm^3 EtOH and the mixture was refluxed for 1 h. The readily soluble reactants formed a red solution from which, while still warm, a microcrystalline orange complex precipitated. After warm filtration, the precipitate was washed with EtOH. Yield: 0.20 g (74 %).

Analytical methods

Elemental analyses (C, H, N, S) of the air-dried complexes were realized by standard micromethods in the Centre for Instrumental Analyses of the ICTM in Belgrade.

The molar conductivities of freshly prepared DMF solutions (c = 1.0×10^{-3} mol/dm^3) were measured on a Jenway 4010 conductivity meter.

The magnetic susceptibilities were measured on an MSB-MKI magnetic balance (Sherwood Scientific Ltd., Cambridge, England).

The IR spectra were recorded using KBr pellets on a Thermo Nicolet (NEXUS 670 FT-IR) spectrophotometer in the range of 4000–400 cm^{-1}.

The electronic UV–Vis spectra in DMF solutions were recorded on a T80+UV/Vis spectrometer, PG Instruments Ltd., in the spectral range of 260–1000 nm.

The ^{1}H- and ^{13}C-NMR spectra were collected on a Varian Gemini 200 instrument operating at 200 MHz in DMSO-d_6 solution, with TMS as the internal standard.

Single crystal X-ray experiment of $[VO_2(PLITSC–H)]\cdot 2H_2O$

A single crystal was selected and glued on glass threads. Diffraction data were collected at 150 K on a Bruker Platform three-circle goniometer equipped with SMART 1K CCD detector. The crystal to detector distance was 30 mm. Graphite monochromated MoKα X-radiation (λ = 0.71073 Å) was employed. A frame width of 0.3° in ω, with 10 s exposure per frame was used to acquire each frame. The data were reduced using the Bruker program Saint

(Siemens, 1995). A semi-empirical absorption-correction based upon the intensities of equivalent reflections was applied (program SADABS, Siemens, 1996), and the data were corrected for Lorentz, polarization, and background effects. Scattering curves for neutral atoms, together with anomalous-dispersion corrections, were taken from International Tables for X--ray Crystallography.[15] The structure was solved by SIR92 – a program for automatic solution of crystal structures by direct methods,[16] and the figures were drawn using Mercury CSD 2.0 – new features for the visualization and investigation of crystal structures.[17] Refinements were based on F^2 values and realized by full-matrix least-squares (SHELXL-97)[18] with all non-H atoms anisotropic. The positions of all non-H atoms were located by direct methods. Although all H atoms were possible to find in the ΔF maps, with the exception of the H atoms belonging to the water molecules, all others were positioned geometrically and refined using a riding model. The crystal data and refinement parameters for $[VO_2(PLITSC–H)]\cdot 2H_2O$ are listed in Table I.

TABLE I. Crystal data and refinement parameters for $[VO_2(PLITSC–H)]\cdot 2H_2O$

Empirical formula	$C_{10}H_{17}N_4O_6SV$
Formula weight	372.28
Temperature, K	150
Wavelength, Å	0.71073
Crystal system	Triclinic
Space group	P-1
Unit cell dimensions, Å	a = 9.1713(2), α = 113.6716(8)°
	b = 9.2715(2), β = 93.1788(8)°
	c = 10.3170(2), γ = 107.6116(8)°
Volume, Å^3	749.91(3)
Mosaicity, °	0.398(2)
Z	2
D_c / g cm^{-3}	1.649
D_0 / g cm^{-3}	1.59
Absorption coefficient, mm^{-1}	0.84
F(000)	384
Crystal size, mm	0.25 x 0.13 x 0.08
Color/shape	orange/prism
Theta range	2.55-27.48°
Index ranges $–h + h$; –k + k; –l +l	–11 +11; –12 +12; –13 +12
Reflections collected	6514
Unique reflections	3402 (R_{int} = 0.0167)
Refinement methods	Full matrix L.S. on F^2
Data/restraints/parameters	3402/0/267
Goodness-of-fit on F^2	1.049
Final R indices ($F_0 > 4\text{sig}F_0$)	$R1$ = 0.0260
R indices (all data)	$R1$ = 0.0298, $wR2$ = 0.0778
Extinction coefficient	No
Larg. diff. peak and hole, e Å^{-3}	0.41 and –0.30

RESULTS AND DISCUSSION

Synthesis

The dioxo complexes of vanadium(V) and molybdenum(VI) were obtained by the reaction of a warm ammonia–methanolic solution of NH_4VO_3, or an ethanolic solution of $MoO_2(acac)_2$, with pyridoxal *S*-methylisothiosemicarbazone (PLITSC) in a mole ratio 1:1 (Scheme 1).

$$NH_4VO_3 + PLITSC \xrightarrow{NH_3(aq)-MeOH,\ reflux} [VO_2(PLITSC-H)]\cdot 2H_2O$$

$$MoO_2(acac)_2 + PLITSC \xrightarrow{EtOH,\ reflux} [MoO_2(PLITSC-2H)]$$

Scheme 1. Formation of the dioxovanadium(V) and dioxomolybdenum(VI) complexes.

As was to be expected, the obtained complexes were diamagnetic, which means that no change occurred in the metal oxidation state during the reaction.

Both complexes were stable in air. The mass loss after isothermal heating at 110 °C of the vanadium complex was 9.58 %, which corresponds to the departure of two water molecules (9.67 %).

The complexes were sparingly soluble in H_2O, MeOH and EtOH, and better in DMF.

The low values of the molar conductivities of DMF solutions of the complexes are in accordance with their coordination formulas. As is evident from the formulas, the vanadium complex contained a monoanionic, and molybdenum complex a dianionic form of the tridentate ONN ligand PLITSC. The monoanionic form of the ligand, as well as in its complexes with some other metals,[1] is formed by deprotonation of the isothiosemicarbazide, while the dianionic form by additional deprotonation of the pyridoxal moiety, which results in the formation of neutral complexes in both cases.

The deprotonation of the pyridinium moiety of PLITSC in the molybdenum complex is facilitated by the good proton-acceptor properties of both substituted acetylacetonato anions.

Analytic and spectral characteristics

PLITSC·H_2O ligand. FTIR (KBr, cm^{-1}): 3368, 3094, 2850, 1662, 1491, 1254, 1152, 1020. ^{1}H-NMR (200 MHz, DMSO-d_6, δ / ppm): 12.12, 11.72 (1H, *s*, phenolic OH), 8.69, 8.58 (1H, *s*, azomethine), 7.89 (1H, *s*, pyridine C-6); 7.23, 7.21 (2H, *s*, NH_2), 5.31, 5.28, (1H, *t*, J = 5.22 Hz, OH, hydroxymethyl), 4.60, 4.58 (2H, *d*, J = 5.22 Hz, CH_2), 2.47, 2.41 (3H, *s*, CH_3–S); 2.39, 2.38 (3H, *s*, CH_3–Py). ^{13}C-NMR (50 MHz, DMSO-d_6, δ / ppm): 167.36, 162.83 (N=C(N)–S), 152.26, 151.04 (CH=N), 148.37 (C-3, Py), 146.95 (C-2, Py), 138.88, 138.71 (C-6, Py), 132.45, 132.14 (C-5, Py), 121.06 (C-4, Py), 58.95 (CH_2), 19.07 (CH_3–Py),

12.81 (CH_3–S). UV–Vis (DMF; λ_{max}/ nm (log (ε / mol^{-1} dm^3 cm^{-1})): 325 (4.45), 352 (4.43), 365 (4.38).

[VO_2(PLITSC–H)]·2H_2O. Yield: 0.14 g (64 %), Anal. Calcd. for $C_{10}H_{17}N_4O_6SV$ (FW = 372.28): C, 32.26; H, 4.50; N, 15.05; S, 8.61 %. Found: C, 32.48; H, 4.31; N, 14.83; S, 8.40 %. FTIR (KBr, cm^{-1}): 3401, 3265, 2852, 2730, 2070, 1650, 1613, 1455, 1375, 920, 907. ^{1}H-NMR (200 MHz, DMSO-d_6, δ / / ppm): 8.83 (1H, *s*, azomethine), 7.96 (1H, *bs*, NH), 7.88 (1H, *s*, pyridine C-6), 5.72 (2H, very *bs*, hydroxymethyl OH and pyridinium H), 4.76 (2H, *s*, CH_2), 2.51 (3H, *s*, CH_3–S), 2.48 (3H, *s*, CH_3–Py). ^{13}C-NMR (50 MHz, DMSO-d_6, δ / / ppm): 172.90 (N=C(N)–S), 157.65 (CH=N), 146.46 (C-3, Py), 142.13 (C-2, Py), 135.73 (C-6, Py), 128.00 (C-5, Py), 127.26 (C-4, Py), 58.76 (CH_2), 16.82 (CH_3–Py), 13.73 (CH_3–S). UV–Vis (DMF; λ_{max} / nm (log (ε / mol^{-1} dm^3 cm^{-1})): 273 (4.22), 356 (3.92), 418 (4.02). Λ_M (DMF) = 3.2 S cm^2 mol^{-1}.

[MoO_2(PLITSC–2H)]. Yield: 0.20 g (74 %); Anal. Calcd. for $C_{10}H_{12}MoN_4O_4S$ (FW = 380.43): C, 31.57; H, 3.18, N; 14.73; S, 8.43 %. Found: C, 31.69; H, 3.27; N, 14.70; S, 8.44 %. FTIR (KBr, cm^{-1}): 3294, 1638, 1450, 1344, 1160, 945, 926, 908. ^{1}H-NMR (200 MHz, DMSO-d_6, δ / ppm): 9.41 (1H, *s*, NH), 8.68 (1H, *s*, azomethine), 7.91 (1H, *s*, pyridine C-6), 5.54, (1H, *t*, J = 5.22 Hz, OH, hydroxymethyl), 4.62 (2H, *d*, J = 5.22 Hz, CH_2), 2.48 (3H, *s*, CH_3–S), 2.33 (3H, *s*, CH_3–Py). ^{13}C-NMR (50 MHz, DMSO-d_6, δ / ppm): 172.58 (N=C(N)–S), 153.56 (CH=N), 148.68 (C-3, Py), 146.49 (C-2, Py), 139.71 (C-6, Py), 134.12 (C-5, Py), 123.50 (C-4, Py), 59.31 (CH_2), 19.92 (CH_3–Py), 14.51 (CH_3–S). UV–Vis (DMF; λ_{max} / / nm (log (ε / mol^{-1} dm^3 cm^{-1})): 308 (4.22), 364 *sh* (3.81), 441 (3.50). Λ_M(DMF) = = 7.5 S cm^2 mol^{-1}.

IR Spectra

The X-ray analysis of the square-pyramidal vanadium complex (*vide infra*) showed that the PLITSC was coordinated in the usual way,[1] *i.e.*, *via* the oxygen of the phenolic group, the azomethine nitrogen and the nitrogen atom of the deprotonated amino group of the isothioamide fragment (Figs. 1 and 2). In addition, the analysis showed that the pyridoxal moiety occurred in a zwitterionic form, with the protonated pyridine nitrogen and deprotonated aromatic phenolic group. The occurrence of a protonated pyridine nitrogen atom, apart from the X-ray analysis, is also suggested by the appearance of a broader $\nu(NH^+)$ band in the IR spectrum in the range 2730–2850 cm^{-1},[1,4] which was missing from the spectrum of the molybdenum complex, in which this ligand is coordinated as a dianion.

In the IR spectra of both complexes, the characteristic bands of the *cis*-MO_2^{n+} group, recognizable by their strong intensity, can easily be identified Thus, the $\nu_{sym/asym}(VO_2^+)$ bands were observed at 920 and 907 cm^{-1}, respectively, *i.e.*, in the range characteristic for the *cis*-VO_2 moiety.[19,20] As X-ray structural analysis of the MoO_2^{2+} complex was not possible in that study[19,20], which was the case in

the present work, the number and position of the ν(MoO_2^{2+}) bands may indicate the role of the MoO_2 group (terminal, bridging) and, thus, also the structure (monomer, dimer, polymer) of the complex. Namely, it is known from the literature[6,8] that the great majority of these complexes have an octahedral structure. In the case of the very frequent neutral monomeric complexes of MoO_2^{2+} with tridentate dianionic ligands, the tendency of MoO_2 to enter the hexacoordination was so pronounced that the sixth coordination site, apart from the typical neutral monodentate donors (Py, DMSO, DMF, PPh_3, H_2O), could also be occupied by some more weakly coordinated ligands, such as EtOH, MeOH, acetaldehyde.[14] The spectra of such complexes have, as a rule, two very strong bands in the region of 950–880 cm^{-1}, of which the one at the higher energy corresponds to the symmetric and the other to asymmetric stretching vibrations of the *cis*-MoO_2 group.[21] In some cases, these bands are split due to the crystal packing effect.[22] In the absence of a monodentate donor, the hexacoordination of molybdenum is most often realized *via* the intermolecular molybdenum···oxygen interaction, with the formation of a double oxygen bridge Mo_2O_2 (μ-O)$_2$[6,23,24] or the Mo=O···Mo interaction in polymeric complexes,[6,14,25,26] which results in the appearance of very strong bands in the 850–800 cm^{-1} region of the IR spectra.[27–29] In view of the composition of the present tridentate complex and absence of a band in the region of 850–800 cm^{-1}, together with the presence of three bands that correspond to the terminal (bridging) *cis*-MoO_2 group (945, 926 and 908 cm^{-1}), the isolated complex can be thought of as having either a pentacoordinated structure,[6,30] very rare for MoO_2^{2+}, or the usual dimer/polymer octahedral structure, but without the participation of the Mo=O···Mo bridge. This means that the dimer/polymer octahedral structure of the present complex in the coordination of PLITSC may be realized, apart from the oxygen atom of the phenoxy group, *via*

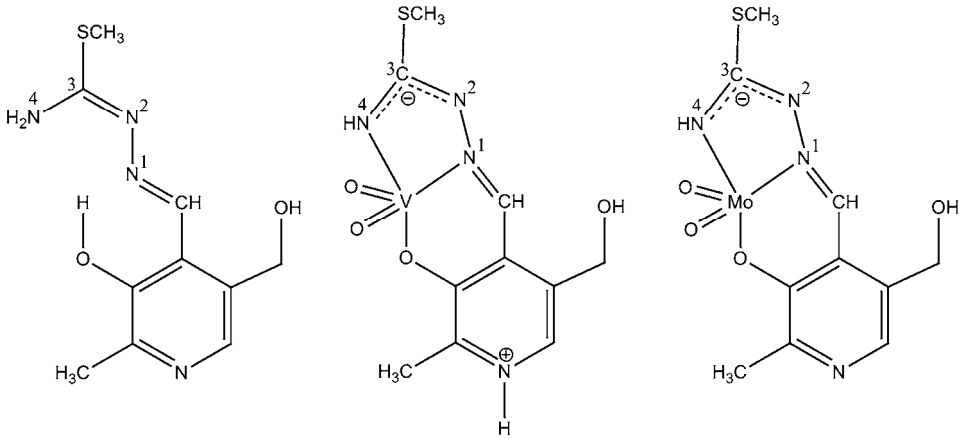

Fig. 1. Chemical structures of the ligand, and the [VO_2(PLITSC–H)]·2H_2O and [MoO_2(PLITSC–2H)] complexes.

two nitrogen atoms of the isothiosemicarbazide fragment and the bridging coordination of the oxygen atom of the hydroxymethyl group. The latter coordination mode of the pyridoxal moiety was also assumed in a similar MoO_2^{2+} complex with pyridoxal 4-phenylthiosemicarbazone,[6] and unambiguously found in the structures of some complexes of Cu(II)[2] and Ni(II)[31] with pyridoxal thiosemi- and semicarbazone.

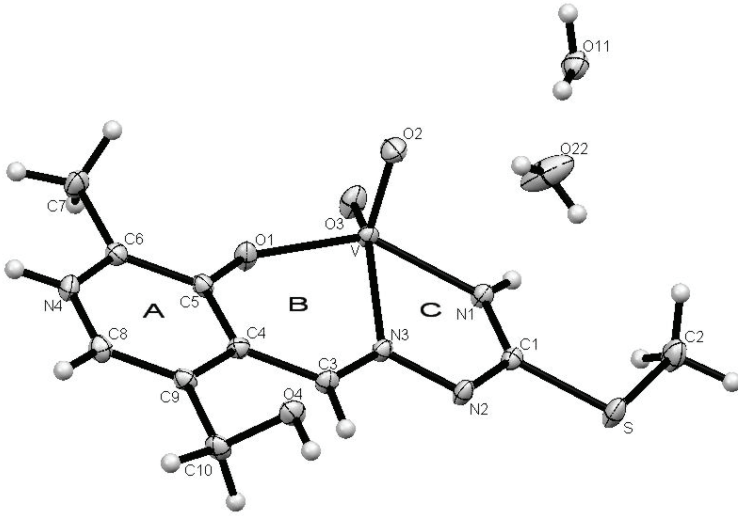

Fig. 2. MERCURY view of $[VO_2(PLITSC–H)]\cdot 2H_2O$ shown with 50 % probability level of the thermal ellipsoids.

NMR Spectra

The ^{1}H-NMR spectrum of the ligand in DMSO-d_6 solution was recorded with a systematic pattern of isomer peaks of all protons, with the exception of the pyridine one at the C-6 position, which was poorly resolved and appeared as a singlet. The *syn*/*anti* isomerism results from the double bond in the azomethine group (CH=N1) (Fig. 1).[32] In the ^{1}H-NMR spectrum of the ligand, the *syn* and *anti* isomers were defined by the dual peak system with a 23:77 integral ratio, respectively. The *cis*/*trans* isomerism occurred with respect to the N2=C3 double bond of the amide group. The chemical shifts of the two isomeric phenolic protons were at 12.12 and 11.72 ppm, with a *cis*/*trans* integral ratio 82:18. The absence of a resonance of both these signals for OH in the spectrum of the vanadium complex is in accordance with the coordination of the phenolate oxygen to vanadium. The spectrum of the complex contains no isomer peaks for CH=N1, indicating the fixed geometry after coordination and existence of the complex in only one isomeric form (Fig. 1). The significant downfield shift of the azomethine proton in the complex (Δ^* = 0.14 ppm), with respect to the corresponding free ligand, confirms the coordination of the azomethine nitrogen. A similar down-

field shift was observed for the carbon atom of the azomethine group in its ^{13}C--NMR spectrum.

A comparison of the ^{1}H-NMR spectra of the ligand and its dioxomolybdenum complex revealed that the ligand behaved as a tridentate binegative ONN donor. The disappearance of the signals at 12.12 and 11.72 ppm was ascribed to the fact that the ligand also underwent deprotonation of the phenolic group during complexation. Similarly, the appearance of a new signal at 9.41 ppm with integral intensity of 1.0 suggests that the complexation was followed by deprotonation of the terminal amino group. Finally, the absence of two isomeric peaks of the azomethine group of the free ligand indicates coordination to molybdenum with a fixed geometry, without the possibility for any isomerism.

Electronic spectra

In the available spectral range in DMF, the complexes displayed spectra with three bands of high and medium intensities. The two bands at shorter λ values (below 400 nm) can be ascribed to intraligand $\pi \rightarrow \pi^*$ and $n \rightarrow \pi^*$ transitions.[5,13,33] The third one (above 400 nm) belongs to an LMCT, *i.e.*, charge transfer from the highest occupied ligand orbital to an empty d-orbital of the metal atom.[34] As expected for MoO_2^{2+} and VO_2^{+}, (d^0), no d–d transitions were observed in the visible spectral range.

Crystal structure of [VO_2(PLITSC–H)]·2H_2O

The asymmetric unit consists of a tridentate ONN monodeprotonated ligand chelating the VO_2^{+} and two water molecules. The well-separated complex units of [VO_2(PLITSC–H)] and H_2O are connected by hydrogen bonds. The vanadium atom is pentacoordinated in an almost ideal square-pyramidal environment (τ = = 0.042) (Fig. 2), with the apical O2 atom at a distance V–O2 = 1.641(1) Å and the equatorial O3 at a distance V–O3 = 1.630(1) Å (Table II). The VO_2 group is in the *cis*-configuration with an O–V–O angle of 108.03(6)° (Table II). A very similar square-pyramidal arrangement around the vanadium(V) ion was also found in the crystal structure of ammonium(2,4-dihydroxybenzaldehyde *S*-methylthiosemicarbazonato)dioxovanadate(V).[35] The chelate ligand donors–vanadium bond distances V–O1, V–N1 and V–N3 are 1.917(1), 2.006(1) and 2.200(1) Å, respectively. Thus, as with some other tridentate ONN isothiosemicarbazones,[36] the V–N3 bond is longer than the V–N1 bond. However, while these differences for non-oxo metal complexes are significantly smaller (≈0.05 Å),[36] the difference in the case of this complex is much more pronounced, amounting to even 0.195 Å. The significant elongation of the V–N3 bond is a consequence of the stronger *trans* effect of the basal oxo O3 ligand bound to vanadium by a double bond, compared to the *trans* effect of the (also basal) oxygen atom O1 bonded to vanadium by a single bond.

TABLE II. Selected bond distances and bond angles for $[VO_2(PLITSC–H)]\cdot 2H_2O$

Bond	Bond distances, Å	Bond	Bond angles, °
V–O1	1.917(1)	O1–V–O2	103.65(5)
V–O2	1.641(1)	O1–V–O3	96.83(5)
V–O3	1.630(1)	O1–V–N1	143.96(5)
V–N1	2.006(1)	O1–V–N3	80.89(5)
V–N3	2.200(1)	O2–V–O3	108.03(6)
O1–C5	1.315(2)	O2–V–N1	106.22(5)
N1–C1	1.317(2)	O2–V–N3	105.07(5)
N2–N3	1.381(2)	O3–V–N1	92.71(5)
N2–C1	1.337(2)	O3–V–N3	146.37(6)
		N1–V–N3	72.27(5)
		C6–N4–C8	123.8(1)

The whole ligand molecule, which possesses an extended system of conjugated double bonds and, hence, should be planar, is on the contrary significantly distorted. The dihedral angle between the mean planes of the pyridoxal moiety (A) and the six-membered chelate ring (B) is 7.8°, the dihedral angles between the average plane of five-membered chelate ring (C) and the A and B rings are 8.7 and 12.0°, respectively. The basal plane (O1, N1, O3, N3) of the coordination polyhedron is slightly tetrahedrally deformed, with the distances from the least squares plane being between 0.0137(1) and 0.0159(1) Å. The vanadium atom is displaced towards the apical O2 atom by 0.5146(1) Å. The pyridoxal ring adopts the role of a zwitterion.[1] The bond distances and angles in the pyridoxal ring are in agreement with those found in some other compounds containing the same moiety when a zwitterion was adopted. The C6–N4–C8 angle of the pyridine ring (123.8(1)°) is significantly increased with respect to the C–N–C angle of about 120°, which could be expected for a non-protonated pyridyl-N.[1,3] This is also in agreement with the N4···O11 distance (2.677(2) Å), corresponding fairly well to a strong hydrogen bond (Table III) and with the O1–C5 distance (1.317(2) Å), which is intermediate between a single (1.43 Å) and a double C=N bond (1.23 Å). All the other bond distances and bond angles in the PLITSC chelate ligand are in agreement with the corresponding bonds found in the related pyridoxal isothiosemicarbazone ligand.[1] The packing of the structural units is determined by an extended 3D network of hydrogen bonds, listed in Table III.

Two of them: O4–H···N2 (2.762(2) Å) and N1–H···O3 (2.969(2)) bind the complex molecules along the *x* and *y* directions, respectively (Fig. 3), forming layers parallel to the ab plane at the levels $c = 0$ and $c = 1$ (C-layers). As can be seen from Fig. 4, between these layers, at the $c/2$ level, there is a layer composed of the crystalline water molecules H_2O11 and H_2O22, mutually connected by the hydrogen bond O11–H11···O22 (2.723(3)), along the (110) direction. The water layers (W-layers) and layers of the complex (C-layers) alternate along the *z*-direction and are interconnected by the relatively strong pairs: O11–H12···O4

(2.735(2) Å) and N4–H···O11 (2.674(2) Å), as well as by O22–H21···O2 (2.799(2) Å) and O22–H22···O2' (2.991(2) Å).

TABLE III. Hydrogen-bonding geometry (Å, °)

D–H	D···A	H···A	D–H···A	Equivalent position[a]
O11–H11	O11···O22	H16···O22	O11–H16···O22	(0)
0.78(4)	2.723(3)	1.96(4)	167(4)	
O4–H4	04···N2	H8···N2	O4–H8···N2	(1)
0.84(4)	2.762(2)	1.93(4)	172(3)	
N1–H1	N1···O3	H9···O3	N1–H9···O3	(2)
0.88(3)	2.969(2)	2.11(3)	167(3)	
N4–H4A	N4···O11	H10···O11	N4–H10···O11	(3)
0.88(2)	2.674(2)	1.80(2)	172(3)	
O11–H12	O11···O4	H15···O4	O11–H15···O4	(4)
0.81(3)	2.735(2)	1.93(4)	171(3)	
O22–H21	O22···O2	H14···O2	O22–H14···O2	(4)
0.86(3)	2.799(2)	1.94(3)	177(3)	
O22–H22	O22···O2	H17···O2	O22–H17···O2	(5)
0.77(4)	2.991(2)	2.24(3)	167(4)	

[a](0): *x*, *y*, *z*; (1): –*x*+1, –*y*+2, –*z*; (2): –*x*+2, –*y*+1, –*z*; (3): *x*+1, +*y*+1, +*z*; (4): –*x*+1, –*y*+2, –*z*+1; (5): *x*–1, +*y*, +*z*

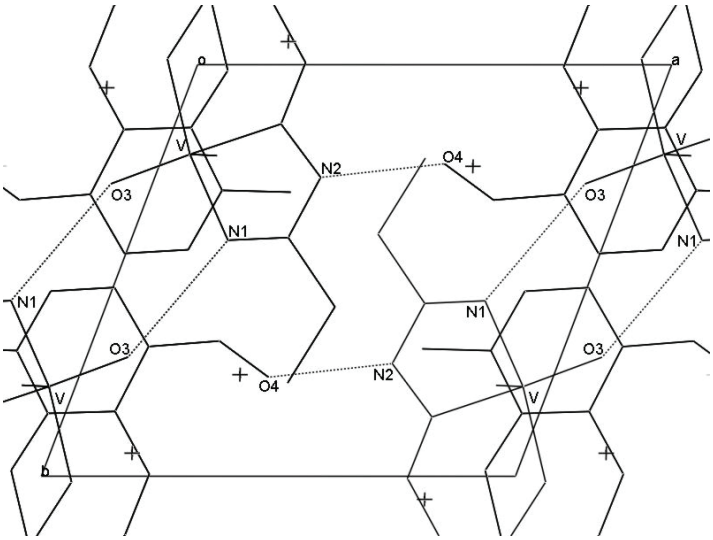

Fig. 3. Projection of the structure parallel to the (001) direction. Water oxygens are marked with +.

Crystallographic data reported for the complex $[VO_2(PLITSC–H)]\cdot 2H_2O$ have been deposited with CCDC, No. CCDC-641145. Copies of the data can be obtained free of charge *via* www.ccdc.cam.ac.uk (or from the Cambridge Crystallographic Data Centre, 12, Union Road, Cambridge, CB2 1EZ, UK; fax: +44 1223 336033; or deposit@ccdc.cam.ac.uk).

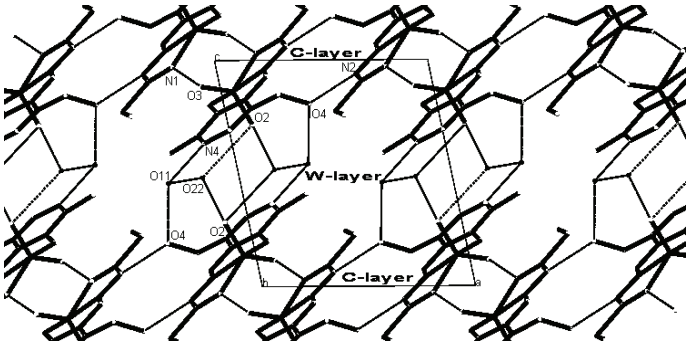

Fig. 4. Projection of the structure parallel to the (010) direction.
H-atoms are omitted for the sake of clarity.

Acknowledgements. This work was supported by the Ministry of Science and Technological Development of the Republic of Serbia (Grant No. 142028) and the Provincial Secretariat for Science and Technological Development of Vojvodina. The authors would like to thank Dr Andrej Pevec (Faculty of Chemistry and Chemical Technology, University of Ljubljana, Slovenia) for measuring the crystal data of $[VO_2(PLITSC–H)]\cdot 2H_2O$.

И З В О Д

КОМПЛЕКСИ ПРЕЛАЗНИХ МЕТАЛА СА ЛИГАНДИМА НА БАЗИ ТИОСЕМИКАРБАЗИДА. ДЕО 57. СИНТЕЗА, СПЕКТРАЛНА И СТРУКТУРНА КАРАКТЕРИЗАЦИЈА КОМПЛЕКСА ДИОКСОВАНАДИЈУМА(V) И ДИОКСОМОЛИБДЕНА(VI) СА *S*-МЕТИЛИЗОТИОСЕМИКАРБАЗОНОМ ПИРИДОКСАЛА

ВУКАДИН М. ЛЕОВАЦ[1], ВЛАДИМИР ДИВЈАКОВИЋ[1], МИЛАН Д. ЈОКСОВИЋ[2], ЉИЉАНА С. ЈОВАНОВИЋ[1], ЉИЉАНА С. ВОЈИНОВИЋ-ЈЕШИЋ[1], ВАЛЕРИЈА И. ЧЕШЉЕВИЋ[1] и МИЛЕНА МЛИНАР[1]

[1]*Природно-математички факултет, Универзитет у Новом Саду, Трг Д. Обрадовића 3, 21000 Нови Сад и* [2]*Природно-математички факултет, Универзитет у Крагујевцу, Р. Домановића 12, 34000 Крагујевац*

Описана је синтеза неутралних комплекса диоксованадијума(V) и диоксомолибдена(VI) са тридентатним ONN *S*-метилизотиосемикарбазоном пиридоксала (PLITSC), формула $[VO_2(PLITSC–H)]\cdot 2H_2O$ и $[MoO_2(PLITSC–2H)]$. Структурна анализа комплекса ванадијума је показала да исти има скоро идеалну квадратно-пирамидалну структуру, а за комплекс молибдена је претпостављена полимерна октаедарска структура. Оба комплекса су, осим елементалном анализом, окарактерисана кондуктометријским и магнетометријским мерењима, те IR-, UV–Vis и ^{1}H- и ^{13}C-NMR спектрима.

(Примљено 13. јануара, ревидирано 2. фебруара 2010)

REFERENCES

1. V. M. Leovac, V. S. Jevtović, L. S. Jovanović, G. A. Bogdanović, *J. Serb. Chem. Soc.* **70** (2005) 393, and references therein
2. M. Belicchi-Ferrari, F. Bisceglie, C. Casoli, S. Durot, I. Morgenster-Badaran, G. Pelosi, E. Pilotti, S. Pinelli, P. Tarasconi, *J. Med. Chem*. **48** (2005) 1671
3. E. W. Yemeli Tido, E. J. M. Vertelman, A. Meetsma, P. J. van Koningsbruggen, *Inorg. Chim. Acta* **360** (2007) 3896

4. S. Floquet, M. C. Muños, R. Guillot, E. Rivière, G. Blain, J.-Antonio Real, M.-L. Boillot, *Inorg. Chim. Acta* **362** (2009) 56
5. M. R. Maurya, A. Kumar, M. Abid, A. Azam, *Inorg. Chim. Acta* **359** (2006) 2439
6. V. Vrdoljak, J. Pisk, B. Prugovečki, D. Matković-Čalogović, *Inorg. Chim. Acta* **362** (2009) 4059
7. *Molybdenum and Molybdenum-Containing Enzymes*, M. Coughlan, Ed., Pergamon Press, New York, 1980
8. E. I. Stiefel, *Prog. Inorg. Chem.* **22** (1977) 8
9. M. R. Maurya, *Coord. Chem. Rev.* **237** (2003) 163
10. *Vanadium Compounds: Chemistry, Biochemistry and Therapeutic Applications*, Ch. 12, V. L. Pecoraro, C. Slebodnick, B. Hamstra, D. C. Crans, A. S. Tracy, Eds., ACS Symposium Series, 1998
11. K. Waisser, L. Heinisch, M. Šlosárek, J. Janota, *Folia Microbiol.* **50** (2005) 479
12. A. De Logu, M. Saddi, V. Onnis, C. Sanna, C. Congiu, R. Borgna, M. T. Cocco, *Int. J. Antimicrob. Agents* **26** (2005) 28
13. V. S. Jevtović, L. S. Jovanović, V. M. Leovac, L. J. Bjelica, *J. Serb. Chem. Soc.* **68** (2003) 929
14. O. A. Rajan, A. Chakravorty, *Inorg. Chem.* **20** (1981) 660
15. J. A. Ibers, W. C. Hamilton, *International Tables for X-ray Crystallography*, Vol. IV, The Kynoch Press, Birmingham, 974
16. A. Altomare, G. Cascarano, C. Giacovazzo, A. Guagliardi, M. C. Burla, G. Polidori, M. Camalli, SIR92, *J. Appl. Crystallogr.* **27** (1994) 435
17. C. F. Macrae, I. J. Bruno, J. A. Chisholm, P. R. Edgington, P. McCabe, E. Pidcock, L. Rodriguez-Monge, R. Taylor, J. van de Streek, P. A. Wood, Mercury 2.3, *J. Appl. Crystallogr.* **41** (2008) 466
18. G. M. Sheldrick, SHELX 97 – *Programs for Crystal Structure Analysis*, Göttingen, 1998
19. X. Wang, X. M. Zhang, H. X Liu, *Inorg. Chim. Acta* **223** (1994) 193
20. I. C. Mendes, L. M. Botion, A. V. M. Ferreira, E. E. Castellano, H. Beraldo, *Inorg. Chim. Acta* **362** (2009) 414
21. V. M. Leovac, I. Ivanović, K. Anđelković, S. Mitrovski, *J. Serb. Chem. Soc.* **60** (1995) 1
22. A. Syamal, D. Kumar, *Transition Met. Chem.* **7** (1982) 118
23. J. M. Sobcak, T. Glowiak, J. J. Ziólkowski, *Transition Met. Chem.* **15** (1990) 208
24. M. Cindrić, G. Galin, D. Matković-Čalogović, P. Novak, T. Hrener, I. Ljubić, T. K. Novak, *Polyhedron* **28** (2009) 562
25. A. Nakajima, K. Yokoyma, T. Kano, M. Kojima, *Inorg. Chim. Acta* **282** (1998) 209
26. J. M. Berg, R. Holm, *Inorg. Chem.* **22** (1983) 1768
27. M. Cindrić, V. Vrdoljak, N. Strukan, B. Kamenar, *Polyhedron* **24** (2005) 369
28. R. A. Lal, A. Cumar, J. Chakravorty, S. Bhaumik, *Transition Met. Chem.* **26** (2001) 557
29. V. Vrdoljak, M. Cindrić, D. Matković-Čalogović, B. Prugovečki, P. Novak, B. Kamenar, *Z. Anorg. Allg. Chem.* **631** (2005) 928
30. J. M. Berg, R. H. Holm, *J. Am. Chem. Soc.* **107** (1985) 925
31. V. M. Leovac, S. Marković, V. Divjaković, K. Mészáros Szécsényi, M. Joksović, I. Leban, *Acta Chim. Slov.* **55** (2008) 850
32. C. Yamazaki, *Can. J. Chem.* **53** (1975) 610
33. A. Syamal, M. R. Maurya, *Transition Met. Chem.* **11** (1986) 255
34. E. B. Seena, M. R. P. Kurup, *Polyhedron* **26** (2007) 3595
35. V. M. Leovac, A. F. Petrović, *Transition Met. Chem.* **8** (1983) 337
36. V. M. Leovac, V. I. Češljević, *Coordination Chemistry of Isothiosemicarbazide and Its Derivatives*, Faculty of Science, Novi Sad, 2002 (in Serbian).

Journal of the Serbian Chemical Society
JSCS-info@shd.org.rs • www.shd.org.rs/JSCS
J. Serb. Chem. Soc. 75 (8) 1075–1084 (2010)
JSCS–4032
UDC 542.9+547.571+547.551+547.442.2+546.732'742'472:615.281–188
Original scientific paper

Antibacterial Co(II), Ni(II), Cu(II) and Zn(II) complexes with biacetyl-derived Schiff bases

MUHAMMAD IMRAN[1], LIVIU MITU[2]*, SHOOMAILA LATIF[1], ZAID MAHMOOD[1], IMTIAZ NAIMAT[1], SANA S. ZAMAN[1] and SURRYA FATIMA[1]

[1]*Institute of Chemistry, University of the Punjab, Lahore-Pakistan and* [2]*Department of Physics and Chemistry, Faculty of Science, University of Pitesti, Pitesti, 110040, Romania*

(Received 26 October 2009, revised 1 March 2010)

Abstract: The condensation reactions of biacetyl with *ortho*-hydroxyaniline and 2-aminobenzoic acid to form bidendate NO donor Schiff bases were studied. The prepared Schiff base ligands were further utilized for the formation of metal chelates having the general formula $[ML_2(H_2O)_2]$ where M = Co(II), Ni(II), Cu(II) and Zn(II) and L = HL^1 and HL^2. These new compounds were characterized by conductance measurements, magnetic susceptibility measurements, elemental analysis, and IR, ^{1}H-NMR, ^{13}C-NMR and electronic spectroscopy. Both Schiff base ligands were found to have a mono-anionic bidentate nature and octahedral geometry was assigned to all metal complexes. All the complexes contained coordinated water which was lost at 141–160 °C. These compounds were also screened for their *in vitro* antibacterial activity against four bacterial species, namely: *Escherichia coli*, *Staphylococcus aureus*, *Salmonella typhi* and *Bacillus subtilis*. The metal complexes were found to have greater antibacterial activity than the uncomplexed Schiff base ligands.

Keywords: Schiff base; biacetyl; metal ion; antibacterial activity.

INTRODUCTION

The promising bacterial resistance to the currently available antibiotics has forced the exploration for new prokaryotic targets as well as novel molecules to inhibit their activity. Among such novel derivatives, metal complexes of biologically active ligands may represent an attractive approach for designing new antimicrobial compounds, due to the dual possibility of both ligands and metal ions interacting with different steps in the life cycle of pathogens.[1–3] Much work has been realized by bioinorganic as well as medicinal chemists to launch the relationship between the metal ions and their complexes as antitumor and antibacterial agents.[4–8] It is however noteworthy that some biologically active com-

* Corresponding author. E-mail: ktm7ro@yahoo.com
doi: 10.2298/JSC091026098I

pounds may become more carcinostatic and bacteriostatic upon chelation.[9] Ketones and amines are versatile reactive organic compounds due to presence of C=O and NH_2 groups, respectively. The nucleophilic addition reactions of these compounds result in an important class of compounds known as Schiff bases, which are considered to be the best candidates for coordination with metal ions. A number of studies have reported the ligational aspects and biological role of Schiff bases and their metal complexes.[10–23] A comprehensive search through the literature revealed that no work has been realized on the preparation and characterization of metal complexes of Schiff bases derived from biacetyl, *ortho*--hydroxyaniline and 2-aminobenzoic acid. Consequently, an attempt has been made to synthesize and characterize some novel metal complexes of these Schiff base ligands. The prepared ligands as well as their metal complexes were also investigated for their *in vitro* activity against some bacterial species. The purpose of the work was to understand the coordination as well as the biological chemistry of these novel synthesized compounds.

EXPERIMENTAL

Analytical reagent grade ethanol was used after distillation. All other chemicals and solvents were of reagent grade and procured from Sigma Aldrich or Merck. Metal chlorides were used as the metal(II) salts for synthetic purposes. The IR spectra were recorded on Philips Analytical PU 9800 FT-IR spectrometer. The UV/Vis spectra were obtained on a Specord-200 spectrometer using Software Acuta710, while the ^{1}H-NMR spectra were recorded on a Bruker 250 MHz NMR spectrometer in DMSO-d_6. The conductance of the metal complexes was determined in DMF on a Hitachi YSI-32 model conductometer. The magnetic measurements were realized on solid complexes using the Gouy method. Melting points were determined using a Gallenkamp apparatus.

Preparation of the Schiff bases

An ethanolic solution of biacetyl (0.010 mol, 20 ml) was mixed with an ethanolic solution of 2-aminobenzoic acid (0.010 mol, 20 ml) and *o*-hydroxyaniline (0.010 mol, 20 ml) separately, then 2–3 drops of glacial acetic acid were added and the mixture was refluxed for four hours. The resulting solution was concentrated and cooled. The obtained colored products were filtered off, washed with ethanol and dried. Recrystallization with warm ethanol gave the desired products HL^1 and HL^2 (Scheme 1).

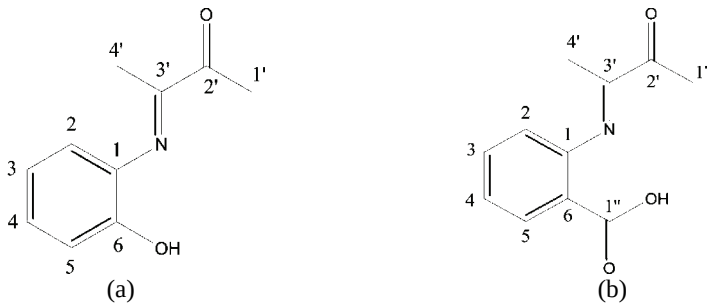

Scheme 1. Numbering of the C atoms in the a) HL^1 and b) HL^2 ligands.

Preparation of metal complexes

Metal chloride (0.0010 mol) was dissolved in distilled water (30 ml) and the resulting solution was stirred magnetically. To this magnetically stirred solution was added 0.0020 mol of each Schiff base ligand in an ethanolic solution (25 ml). The mixture was refluxed for 2–3 h and cooled to room temperature. After cooling, the formed precipitates were filtered, washed with water, ethanol and dried.

Antibacterial studies

All the synthesized metal complexes were tested for their *in vitro* antibacterial activity against some bacterial strains using the spot on Mueller–Hinton agar by following the reported method.[24] Four test pathogenic bacterial strains, *viz*. *Staphylococcus aureus* (MTCC 1144), *Bacillus subtilis* (MTCC 2423), *Salmonella typhi* (MTCC 733) and *Escherichia coli* (MTCC 739), were considered for the determination of the minimum inhibitory concentration (*MIC*). The minimum inhibitory concentrations were determined by the microbroth dilution technique using Mueller–Hinton broth. Serial two-fold dilutions ranging from 5000 to 4.8 μg ml^{-1} were prepared in Mueller–Hinton broth. The inoculum was prepared with a 4–6 h broth culture of each strain adjusted to a turbidity equivalent to 0.5 McFarland standard, diluted in Mueller–Hinton broth to give a concentration of 50 CFU L^{-1} in the test tray. The trays were covered and placed in plastic bags to prevent drying; incubation was at 37 °C for 18–20 h. The MIC was defined as the lowest concentration of a compound giving complete inhibition of visible growth.

RESULTS AND DISCUSSION

The physico-analytical data for the Schiff base ligands HL^1 and HL^2 are given in Table I. These Schiff bases were prepared by refluxing an appropriate amount of *o*-hydroxyaniline and 2-aminobenzoic acid with biacetyl in absolute ethanol. The prepared Schiff base ligands were further reacted with Co(II), Ni(II), Cu(II) and Zn(II) ions to form the respective metal complexes. These metal complexes were soluble in polar organic solvents, such as MeOH, $CHCl_3$, DMF and EtOH, but less soluble in non-polar solvents, such as 1-hexane, 1-heptane and toluene. These air-stable complexes were obtained in excellent yields (Table I).

TABLE I. Physico-analytical data of the ligands and their metal complexes

S. No.	Compound[a]	Color	M.p. °C	μ_{eff} / μ_B	Λ_m[b] Ω^{-1} cm^2 mol^{-1}	Yield %
1	HL^1	Yellowish brown	180	–	–	75
2	HL^2	Pale Yellow	176	–	–	67
3	$[Cu(L^1)_2(H_2O)_2]$	Sky blue	≈290	1.86	11	70
4	$[Cu(L^2)_2(H_2O)_2]$	Light blue	≈291	1.78	13	56
5	$[Co(L^1)_2(H_2O)_2]$	Tea pink	≈285	4.18	8	62
6	$[Co(L^2)_2(H_2O)_2]$	Brown	≈267	4.21	14	43
7	$[Ni(L^1)_2(H_2O)_2]$	Greenish blue	≈218	3.42	12	55
8	$[Ni(L^2)_2(H_2O)_2]$	Dirt green	≈212	3.26	18	44
9	$[Zn(L^1)_2(H_2O)_2]$	Colorless	≈255	Diamagnetic	17	65
10	$[Zn(L^2)_2(H_2O)_2]$	Colorless	≈243	Diamagnetic	15	54

[a]HL^1, HL^2 = Schiff base ligands; [b]10^{-3} M solution in DMF

All the metal complexes **3**–**10** (Table I) of these Schiff bases were prepared at a mole ratio of the appropriate metal to ligand of 1:2. The low values of the molar conductivity (8–18 Ω^{-1} cm^2 mol^{-1}) of the resulting complexes in DMF showed that they were non-electrolytic in nature.[25] The elemental analysis data (Table II) support the proposed structures of the synthesized compounds (Figs. 1 and 2).

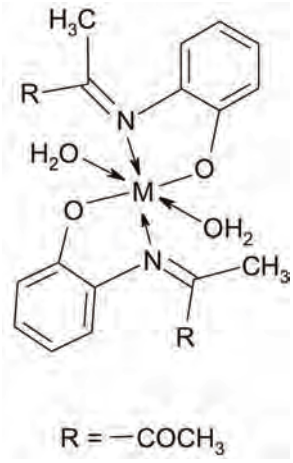

Fig. 1. Proposed structures of metal complexes with HL^1; M = Co(II), Ni(II), Cu(II) and Zn(II).

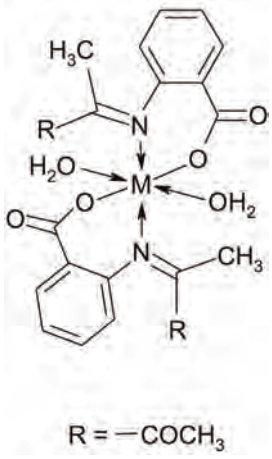

Fig. 2. Proposed structures of metal complexes with HL^2; M = Co(II), Ni(II), Cu(II) and Zn(II).

TABLE II. Elemental analysis data (Calcd. (Found) %) of the ligands and their metal complexes

S. No.	Compound	C	H	N	M
1	HL^1	64.12 (64.39)	5.02 (5.37)	6.55 (6.82)	–
2	HL^2	67.22 (67.42)	6.26 (6.74)	7.68 (7.87)	–
3	$[Cu(L^1)_2(H_2O)_2]$	51.78 (52.02)	4.60 (4.73)	5.50 (5.52)	12.12 (12.52)
4	$[Cu(L^2)_2(H_2O)_2]$	52.90 (53.15)	5.12 (5.32)	6.02 (6.20)	13.79 (14.07)
5	$[Co(L^1)_2(H_2O)_2]$	52.17 (52.49)	4.12 (4.77)	5.43 (5.56)	11.45 (11.72)
6	$[Co(L^2)_2(H_2O)_2]$	53.55 (53.70)	5.13 (5.37)	6.12 (6.27)	13.01 (13.19)
7	$[Ni(L^1)_2(H_2O)_2]$	52.09 (52.52)	4.56 (4.76)	5.23 (5.58)	11.55 (11.66)
8	$[Ni(L^2)_2(H_2O)_2]$	53.56 (53.74)	5.10 (5.37)	6.12 (6.30)	13.01 (13.13)
9	$[Zn(L^1)_2(H_2O)_2]$	51.59 (51.82)	4.44 (4.71)	5.34 (5.50)	12.65 (12.84)
10	$[Zn(L^2)_2(H_2O)_2]$	52.78 (52.93)	5.15 (5.29)	6.11 (6.18)	14.09 (14.43)

IR Spectroscopy

The assignment of the characteristic IR frequencies for the Schiff base ligands and their resulting complexes are tabulated in Table III and can be discussed as follows. The IR spectra of the Schiff base ligands do not show any band in the region 3400–3150 cm^{-1} which could be assigned to –NH_2 vibrations; instead, new bands at 1638 and 1631 cm^{-1} appeared that can be assigned to (>C=N) lin-

TABLE III. Selected IR data (cm^{-1}) of the ligands and their metal complexes

S. No.	Compound	COO^- ν_{C-O}	COO^- $\nu_{C=O}$	ν_{OH}	ν_{H_2O}	ν_{aCOO^-}	ν_{sCOO^-}	$\Delta\nu^a$	$\nu_{C=N}$	ν_{M-O}	ν_{M-N}
1	HL^1	–	–	3415	–	–	–	–	1638	–	–
2	HL^2	1242	1724	–	–	–	–	–	1631	–	–
3	$[Cu(L^1)_2(H_2O)_2]$	–	–	–	3456	1607	1388	219	1619	438	349
4	$[Cu(L^2)_2(H_2O)_2]$	–	–	–	3478	1594	1377	217	1607	453	363
5	$[Co(L^1)_2(H_2O)_2]$	–	–	–	3488	1591	1367	224	1622	459	370
6	$[Co(L^2)_2(H_2O)_2]$	–	–	–	3508	1582	1375	207	1609	434	378
7	$[Ni(L^1)_2(H_2O)_2]$	–	–	–	3567	1588	1379	209	1634	456	359
8	$[Ni(L^2)_2(H_2O)_2]$	–	–	–	3477	1590	1389	201	1623	450	377
9	$[Zn(L^1)_2(H_2O)_2]$	–	–	–	3456	1567	1295	272	1610	427	345
10	$[Zn(L^2)_2(H_2O)_2]$	–	–	–	3523	1578	1344	234	1608	478	367

[a] $\Delta\nu = \nu_{aCOO^-} - \nu_{sCOO^-}$

kages.[26] In addition to this characteristic (>C=N) absorption, the Schiff base ligand HL^1 also exhibited bands at 3415 cm^{-1}, which can be assigned to phenolic (O–H) group vibrations, while Schiff base ligand HL^2 showed two characterristic bands at 1724 and 1242 cm^{-1}, assigned to asymmetric and symmetric vibrations of the carboxylic acid group.[26] A comparison of the IR spectra of Schiff base ligands with their metal complexes reveals that they are coordinated mainly in two ways with the metal ions, thus representing their bidentate nature. Both the Schiff base ligands showed a lower shift (1634–1607 cm^{-1}) in the >C=N stretching frequency (Table III), indicating their coordination with metal ions through the nitrogen atom. In the metal complexes of the Schiff base ligand HL^1, the bands at 3415 cm^{-1} assigned to (O–H) vibrations are absent, thus indicating chelating of oxygen to the metal atoms after deprotonation. Similarly, in HL^2 complexes, the absence of bands at 1724 and 1242 cm^{-1} showed that the –COOH group was deprotonated on complexation. It is well recognized by some authors[27] that ionic carboxylato groups do not have any peak around 1700 cm^{-1} due to the C=O group but show two peaks in the region 1610–1550 cm^{-1} and 1400–1280 cm^{-1}, assigned to asymmetric and symmetric vibrations of the COO^- group, respectively. It is also well recognized in the literature[28,29] that this group can act as monodentate, bidentate or as a bridging ligand and differentiation of these binding states can be made from the frequency separation ($\Delta\nu = \nu_a(COO) - \nu_s(COO)$) between the symmetric and the asymmetric stretching of this group. By probing the symmetric and the asymmetric stretching vibrations of large number of carboxylato complexes with known crystal structure, a criteria was established by Deacon and Phillips[29] that can be used to discriminate between these three binding states of carboxylate complexes. These criteria are: a) monodentate carboxylato complexes display $\Delta\nu$ values which are much larger than those of the ionic salts ($\Delta\nu > 200$ cm^{-1}), b) bidentate carboxylato complexes demonstrate $\Delta\nu$ values significantly smaller than the ionic values ($\Delta\nu < 100$ cm^{-1}) and c) brid-

ging complexes demonstrate $\Delta\nu$ values comparable to the ionic values ($\Delta\nu \approx 150$ cm^{-1}). The $\Delta\nu$ values for the prepared complexes (**3**–**10**) were in the range 201––272 cm^{-1}, which suggests that the carboxylato group is acting as monodentate. Furthermore, the presence of peak at 1702 cm^{-1} in the IR spectra of the ligands with no change in the spectra of complexes rejects the possibility for coordination of the second, uncondensed carbonyl group. In all metal complexes some new low frequency bands in the region 478–427, 378–345 and > 3450 and 893––878 cm^{-1} were also observed and can be assigned to ν(M–O), ν(M–N) and coordinated water modes, respectively.[26]

^{1}H- and ^{13}C-NMR spectroscopy

The assignments of the ^{1}H- and ^{13}C-NMR chemical shifts are tabulated in Table IV. In the ^{1}H-NMR spectrum of the Zn-complex of HL^{2}, a signal assignnable to carboxylic group proton was absent, indicating that deprotonation of carboxylic group occurred and that coordination through this group took place.

TABLE IV. NMR data (δ / ppm) of ligands and their Zn complexes

S. No.	Compound	^{1}H-NMR	^{13}C-NMR
1	HL^{1}	10.9 (1H, *s*, OH), 6.7–7.1 (4H, *m*, H^{2}-H^{5}), 2.20 (3H, *s*, H-1'), 1.90 (3H, *s*, H-4')	197.5 (C-2'), 164 (C-3'),137 (C-1), 122.7 (C-3), 117.2 (C-5), 128.7 (C-4), 123.7 (C-2), 151.5 (C-6), 24.1 (C-1'), 10.1 (C-4')
2	HL^{2}	11.1 (1H, *s*, OH), 7.5–8.1 (4H, *m*, H^{2}-H^{5}), 2.30 (3H, *s*, H-1'), 1.92 (3H, *s*, H-4')	197.5 (C-2'), 164 (C-3'),149 (C-1), 135.3 (C-3), 131.6 (C-5), 127.2 (C-4), 122.2 (C-2), 116.4 (C-6), 24.1 (C-1'), 10.1 (C-4'), 169.4 (C-1'')
9	Zn-complex (HL^{1})	6.6–7.4 (4H, *m*, H^{2}-H^{5}), 2.22 (3H, *s*, H-1'), 1.91 (3H, *s*, H-4')	197.5 (C-2'),164 (C-3'),137.9(C-1), 122.7 (C-3), 118.5 (C-5), 128.7 (C-4), 123.7 (C-2), 152.3 (C-6), 24.1 (C-1'), 10.1 (C-4')
10	Zn-complex (HL^{2})	7.4–8.0 (4H, m, H^{2}-H^{5}), 2.32 (3H, *s*, H-1'), 1.92 (3H, *s*, H-4')	197.5 (C-2'), 164 (C-3'), 150 (C-1), 135.3 (C-3), 132.2 (C-5), 127.2 (C-4), 122.2 (C-2), 117.7 (C-6), 24.1 (C-1'), 10.1 (C-4'), 173.2 (C-1'')

The Zn-complex of this ligand was also characterized by means of ^{13}C--NMR spectroscopy. The higher values of the chemical shift of C-1", C-1, C-6 and C-5 atom signals in the Zn-complex in comparison with those of the signals in the respective non-coordinated ligand[30] strongly suggest that coordination through the carboxylate groups had occurred. On the other hand, the absence of a change of the chemical shift of the uncondensed carbonyl moiety C-2' indicates that this group did not participate in the coordination. A similar pattern of the change in the chemical shift was found with ligand HL^{1}. Thus, both the ^{1}H- and

^{13}C-NMR spectroscopic data support the proposed structures of the ligands and their coordination behavior as well.

Electronic absorption spectra

In the electronic spectra, the Co(II) complexes exhibited two low energy peaks at 7275, 7260 cm^{-1}; 17234, 17224 cm^{-1} and a strong high energy peak at 20482, 20172 cm^{-1}, which can be assigned[31] to the transitions $^4T_{1g}(F) \rightarrow$ $\rightarrow$ $^4T_{2g}(F)$, $^4T_{1g}(F) \rightarrow {}^4A_{2g}(F)$ and $^4T_{1g}$ (F) $\rightarrow {}^4T_{2g}$ (P) for a high spin octahedral geometry, respectively. The final high intensity band at 27145, 27123 cm^{-1} is assigned to charge transfer (Table V). The electronic spectra of the Ni(II) complexes showed d–d transition at 10213, 10110; 15597, 15654 and 26360, 26197 cm^{-1}. These are assigned[31] to $^3A_{2g}(F) \rightarrow {}^3T_{2g}(F)$, $^3A_{2g}(F) \rightarrow {}^3T_{1g}(F)$ and $^3A_{2g}$ (F) $\rightarrow {}^3T_{2g}(P)$ transitions, respectively. These are consistent with a well-defined octahedral geometry. The Zn(II) complexes exhibited only a high intensity band at 28251, 28231 cm^{-1}, which is assigned to ligand–metal charge transfer. In case of the Cu(II) complexes, a broad band at 16644, 16612 cm^{-1} was observed that is assigned to the $^2E_g \rightarrow {}^2T_{2g}$ transition, which confirms its octahedral geometry.

TABLE V. Electronic spectroscopic data of the metal complexes

S. No.	Complex	λ_{max} / cm^{-1}	Assignments
3	$[Cu(L^1)(H_2O)_2]$	16644	$^2E_g \rightarrow {}^2T_{2g}$
4	$[Cu(L^2)_2(H_2O)_2]$	16612	$^2E_g \rightarrow {}^2T_{2g}$
5	$[Co(L^1)_2(H_2O)_2]$	7260	$^4T_{1g}(F) \rightarrow {}^4T_{2g}(F)$
		17234	$^4T_{1g}(F) \rightarrow {}^4A_{2g}(F)$
		20482	$^4T_{1g}(F) \rightarrow {}^4T_{2g}(P)$
		27123	Charge transfer
6	$[Co(L^2)_2(H_2O)_2]$	7275	$^4T_{1g}(F) \rightarrow {}^4T_{2g}(F)$
		17224	$^4T_{1g}(F) \rightarrow {}^4A_{2g}(F)$
		20172	$^4T_{1g}(F) \rightarrow {}^4T_{2g}(P)$
		27145	Charge transfer
7	$[Ni(L^1)_2(H_2O)_2]$	10213	$^3A_{2g}(F) \rightarrow {}^3T_{2g}(F)$
		15654	$^3A_{2g}(F) \rightarrow {}^3T_{1g}(F)$
		26360	$^3A_{2g}(F) \rightarrow {}^3T_{2g}(P)$
8	$[Ni(L^2)_2(H_2O)_2]$	10110	$^3A_{2g}(F) \rightarrow {}^3T_{2g}(F)$
		15597	$^3A_{2g}(F) \rightarrow {}^3T_{1g}(F)$
		26197	$^3A_{2g}(F) \rightarrow {}^3T_{2g}(P)$
9	$[Zn(L^1)_2(H_2O)_2]$	28251	Charge transfer
10	$[Zn(L^2)_2(H_2O)_2]$	28231	Charge transfer

Magnetic susceptibility measurement

The magnetic moment value 4.18; 4.21 μ_B (Table I) for the solid Co(II) complexes suggests[32] an octahedral environment, indicating three unpaired electrons. The magnetic moment value of the Cu(II) complexes 1.86; 1.78 μ_B suggests dis-

torted octahedral geometry.[33] The magnetic moment value of the Ni(II) complexes 3.42; 3.26 μ_B, showing two unpaired electrons, suggests[33] an octahedral geometry for the Ni(II) complexes. The Zn(II) complexes were found to be diamagnetic, as expected for d^{10} configuration.

Antibacterial activity

The antimicrobial activity (*MIC*, μg ml^{-1}) of the metal complexes/ligands are given in Table VI, from which it can be seen that the complexes had variable antimicrobial activities. The Cu(II)L^1 complex showed an *MIC* of 4 μg ml^{-1} against the bacterial strain *B. subtilis* which is equal to the *MIC* shown by the standard antibiotic cefaclor against the same bacterial strain. The Cu(II)L^2 complex exhibited an *MIC* of 9 μg ml^{-1} against the bacterial strain *S. aureus* which is the same as the *MIC* shown by standard antibiotic cefaclor against the same bacterial strain. Furthermore, complexes of Co(II)L^1 and Co(II)L^2 showed a minimum inhibitory concentration of 5 μg ml^{-1} against the bacterial strain *B. subtilis*, which is the same as the *MIC* shown by the standard antibiotic linezolid against the same bacterial strain. The *MIC* of the complex Ni(II)L^2 against *S. typhi* was found to be 18 μg ml^{-1}, which is equal to the *MIC* shown by the standard antibiotic linezolid against the same bacterial strain. Similarly, the complex Zn(II)L^2 registered an *MIC* of 5 μg ml^{-1} against the bacterial strain *B. subtilis*, which is the same as the *MIC* shown by the standard antibiotic linezolid against the same bacterial strain.

TABLE VI. Minimum inhibitory concentration (*MIC*) exhibited by the ligands and their metal complexes against test bacteria

S. No.	Compound	*MIC* / μg ml^{-1}			
		S. aureus	*B. subtilis*	*S. typhi*	*E. coli*
–	Cefaclor	9	4	7	15
–	Linezolid	6	5	18	12
1	HL^1	–	–	110	118
2	HL^2	–	–	–	149
3	$[Cu(L^1)_2(H_2O)_2]$	18	4	15	10
4	$[Cu(L^2)_2(H_2O)_2]$	9	9	7	14
5	$[Co(L^1)_2(H_2O)_2]$	23	5	11	15
6	$[Co(L^2)_2(H_2O)_2]$	11	5	16	12
7	$[Ni(L^1)_2(H_2O)_2]$	15	24	22	13
8	$[Ni(L^2)_2(H_2O)_2]$	56	33	18	19
9	$[Zn(L^1)_2(H_2O)_2]$	11	7	22	12
10	$[Zn(L^2)_2(H_2O)_2]$	13	5	7	16

Among the series under test for the determination of the *MIC*, complexes **1** and **3** were found to be the most potent as compared to the other complexes. This effect can be logically explained by the fact that the Schiff base derivatives must be activated by the metal ions in some way. This enhancement in antibacterial activity of these metal complexes can be explained based on the chelation theory.[34]

When a metal ion is chelated with a ligand, its polarity will be reduced to a greater extent due to the overlap of ligand orbital and the partial sharing of the positive charge of the metal ion with donor groups. Furthermore, the chelation process increases the delocalization of the π-electrons over the whole chelate ring, which results in an increase in the lipophilicity of the metal complexes. Consequently, the metal complexes can easily penetrate into the lipid membranes and block the metal binding sites of enzymes of the microorganisms. These metal complexes also affect the respiration process of the cell and thus block the synthesis of proteins, which restrict further growth of the organism.

CONCLUSIONS

The complexes of Co(II), Ni(II), Cu(II) and Zn(II) with biacetyl-derived Schiff bases have been described. They were characterized by their physico–analytical and spectral data. The Schiff base ligands were found to have mono-anionic bidentate nature and octahedral geometry was assigned to all the metal complexes. All the metal complexes were found to have appreciable antimicrobial activity against some bacterial strains.

ИЗВОД

АНТИБАКЕТРИЈСКА АКТИВНОСТ КОМПЛЕКСА Co(II), Ni(II), Cu(II) И Zn(II) КОЈИ КАО ЛИГАНДЕ САДРЖЕ ДЕРИВАТЕ ШИФОВИХ БАЗА

MUHAMMAD IMRAN[1], LIVIU MITU[2], SHOOMAILA LATIF[1], ZAID MAHMOOD[1], IMTIAZ NAIMAT[1], SANA S. ZAMAN[1] и SURRYA FATIMA[1]

[1]*Institute of Chemistry, University of the Punjab, Lahore-Pakistan и* [2]*Department of Physics and Chemistry, Faculty of Science, University of Pitesti, Pitesti, 110040, Romania*

Испитивана је кондензациона реакција биацетила са *o*-хидроксианилином и 2-аминобензоевом киселином, у којој настају бидентатни лиганди типа Шифових база које као доноре садрже атоме азота и кисеоника. Ови лиганди су употребљени за грађење хелатних комплекса опште формуле $[ML_2(H_2O)_2]$ (M = Co(II), Ni(II), Cu(II) и Zn(II); L = HL^1, HL^2). За карактеризацију комплекса употребљена су кондуктометријска и магнетна мерења, као и резултати елементарне микроанализе, IR, ^{1}H-NMR, ^{13}C-NMR и електронске спектроскопије. На основу ових мерења нађено је да ови лиганди граде моноанјонске комплексе октаедарске геометрије. Добијени комплекси садрже координовани молекул воде, који се губи из координационе сфере при температури од 140–160 °C. Испитивана је *in vitro* антибактеријска активност изолованих комплекса на следећим врстама бактерија: *Escherichia coli*, *Staphylococcus aureus*, *Salmonella typhi* и *Bacillus subtilis*. Добивени резултати ових испитивања су показали да је активност комплекса метала већа од активности некоординованих лиганада.

(Примљено 26. октобра 2009, ревидирано 1. марта 2010)

REFERENCES

1. A. Scozzafava, C. T. Supuran, *J. Med. Chem*. **43** (2000) 3677
2. D. H. Brown, W. E. Smith, J. W. Teape, A. J. Lewis, *J. Med. Chem*. **23** (1980) 729

3. A. Scozzafava, L. Menabuoni, F. Mincione, G. Mincione, C. T. Supuran, *Bioorg. Med. Chem. Lett.* **11** (2001) 575
4. R. J. P. William, *Quart. Rev.* **24** (1970) 331
5. B. Rosenberg, L. Van Camp, *Cancer. Res.* **30** (1970) 1799
6. M. J. Clare, J. D. Heeschele, *Bioinorg. Chem.* **2** (1973) 187
7. V. L. Narayanan, M. Nasr, K. O. Paull, *Tin Based Antitumour Drugs*, NATO ASI Series, Springer, Berlin, 1990, p. 200
8. A. J. Crowe, *Metal-Based Antitumor Drugs*, Vol. 1, Freund, London, 1989, p. 103
9. R. S. Srivastava, *Indian J. Chem.* **29 A** (1990) 1024
10. S. Kiran, S. B. Manjeet, T. Parikshit, *Eur. J. Med. Chem.* **41** (2006) 147
11. P. Mishra, H. Rajak, A. Mehta, *J. Gen. Appl. Microbiol.* (2005) 133
12. S. Gandhe, M. D. Gautam, *Asian J. Chem.* **16** (2004) 261
13. M. Sonmez, A. Levent, M. Sekerci, *Russ. J. Coord. Chem.* **30** (2004) 655
14. X. Tai, X. Yin, Q. Chen, M. Tan, *Molecules* **8** (2003) 439
15. W. T. Gao, Z. Zheng, *Molecules* **8** (2003) 788
16. Z. H. Chohan, M. F. Jaffery, C. T. Supuran, *Metal Based Drugs* **8** (2001) 95
17. Z. H. Chohan, A. Munawar, C. T. Supuran, *Metal Based Drugs* **8** (2001) 137
18. V. K. Sharma, S. Srivastava, A. Srivastava, *Pol. J. Chem.* **80** (2006) 387
19. R. V. Singh, N. Fahmi, M. K. Biyala, *J. Iran. Chem. Soc.* **2** (2005) 40
20. M. Tümer, C. Celik, H. Köksal, S. Serin, *Transition Met. Chem.* **24** (1999) 525
21. J. A. Gutierrez, J. A. Lopez-Jimenez, R. Gavino, H. Noth, *Monatsh. Chem.* **126** (1995) 505
22. Z. H. Chohan, H. Pervez, A. Rauf, C. T. Supuran, *Metal Based Drugs* **8** (2002) 263
23. F. A. Adam, M. T. El-Haty, A. A. Ibrahem, *J. Chin. Chem. Soc.* **31** (1984) 345
24. D. P. Singh, V. Malik, R. Kumar, *Res. Lett. Inorg. Chem.* (2009) 1
25. D. J. Finney, *Probit analysis*, Cambridge University Press, Cambridge, 1971
26. J. Iqbal, M. Imran, S. Iqbal, S. Latif, *J. Chem. Soc. Pak.* **29** (2007) 151
27. F. Gao, P. Yang, J. Xie, H. Wang, *J. Inorg. Biochem.* **60** (1995) 61
28. K. Nakamoto, *Infrared and Raman Spectra of Inorganic and Coordination Compounds*, Wiley, New York, 1986
29. G. B. Deacon, R. J. Phillips, *Coord. Chem. Rev.* **33** (1980) 227
30. H-Y. Zhang, D-L. Chen, P-K.Chen, D-J. Che, G-X.Cheng,H-Q. Zhang, *Polyhedron* **11** (1992) 2313
31. L. J. Bellamy, *The Infrared Spectra of Complex Molecules*, Methuen, London, 1966, p. 13
32. M. U. Hassan, Z. H. Chohan, C. T. Supuran, *Main Group Metal Chem.* **25** (2002) 291
33. C. J. Balhausen, *An Introduction to Ligand Field Theory*, McGraw-Hill, New York, 1962, p. 134
34. L. Mishra, V. K. Singh, *Indian J. Chem.* **32 A** (1997) 446.

Journal of the Serbian Chemical Society
JSCS-info@shd.org.rs • www.shd.org.rs/JSCS
J. Serb. Chem. Soc. *75* (8) 1085–1092 (2010)
JSCS–4033
UDC 547.496.2+547.821:
546.562'472:548.7:54–77
Original scientific paper

Synthesis, spectral and single crystal X-ray structural studies on bis(2,2'-bipyridine)sulphidoM(II) (M = Cu or Zn) and diaqua 2,2'-bipyridine zinc(II)sulphate dihydrate

ARUMUGAM MANOHAR[1]*, KUPPUKANNU RAMALINGAM[2], GABRIELE BOCELLI[3] and ANDREA CANTONI[3]

[1]*Department of Chemistry, Kalasalingam University, Krishnankoil - 626 190,* [2]*Department of Chemistry, Annamalai Unviversity, Annamalainagar - 608 002, India and* [3]*Centro di studio per la strutturistica, Diffractometrica del CNR, Parma, Italy*

(Received 19 October, revised 8 December 2009)

Abstract: Reaction of bis(diethanoldithiocarbamato)copper(II), [Cu(deadtc)$_2$] and bis(di-*n*-propyldithiocarbamato)zinc(II), [Zn(dnpdtc)$_2$] complexes with 2,2'-bipyridine (2,2'-bipy) (1:1 ratio) in ethanol was investigated. Simple mixing of the reactants in 1:1 ratio resulted in five-coordinated [Cu(2,2'-bipy)$_2$S]·$CH_3CH_2OSO_3H$ (**1**) and [Zn(2,2'-bipy)$_2$S]·$CH_3CH_2OSO_3H$·2H_2O (**2**). Refluxing the reactants and cooling the contents result in the formation of [Zn(2,2'-bipy)(H_2O)$_2$]SO_4 (**3**) and [Cu(2,2'-bipy)(H_2O)$_2$]SO_4 (**4**). Complexes **1** and **2** are monomeric with trigonal bipyramidal geometry. A distorted octahedral environment was observed in complexes **3** and **4**. The crystal structure of **4** has already been reported in the literature. Crystal structures of **1**, **2** and **3** are reported in this paper. The M–S distances in **1** and **2** are 2.318(1) Å and 2.323 Å, respectively. The N–M–S angles are larger than the N–M–N angles due to the steric requirements.

Keywords: dithiocarbamates; 2,2'-bipyridine; tbp geometry; single crystal X-ray.

INTRODUCTION

Bisdithiocarbamate complexes have been investigated extensively.[1,2] The interaction of metal dithiocarbamates with Lewis bases leads to the formation of the corresponding base adducts.[3–7] Bis(dialkyldithiocarbamato)nickel(II) complexes, [Ni(dtc)$_2$] show interesting variations in their reactions with Lewis bases.[8–12] Bis(diethyldithiocarbamato)nickel(II) was shown to form an adduct with pyridine only at liquid nitrogen temperature, whereas similar complexes with electron withdrawing substituents on the dithiocarbamate moiety formed an adduct with ease at ambient temperature.[13] Other than the adduct formation reac-

* Corresponding author. E-mail: navmanohar@yahoo.co.in
doi: 10.2298/JSC091019097M

tion, similar complexes were shown to also promote redox reactions of the ligands under basic conditions. A copperthiol complex $[Cu(RSH)_2Cl]$ in pyridine was shown to oxidize thioamides, thiols, sulphide ion and sulphur to sulphate ion.[14] Transition metal ions, such as copper(II), iron(II) and nickel(II), are known to promote oxidation of sulphur compounds under basic conditions.[15] One such instance is the oxidation of sulphides, thioamides and sulphur to SO_4^{2-} by the copper(II)/pyridine system. A new mononuclear copper(II) complex, $[CuCl(2,2'\text{-bipy})_2]BF_4{\cdot}CH_2Cl_2$, was reported and its X-ray analysis revealed a slightly distorted trigonal-bipyramidal coordination geometry of copper(II).[16] The crystal structure of $[Zn(5,5'\text{-}Me_2\text{-}2,2'\text{-bipy})(H_2O)_4]SO_4$ was reported recently.[17] The Zn(II) complex cation, with approximate twofold symmetry, displayed a slightly distorted octahedral geometry around the Zn(II) atom, which was coordinated by two N atoms from the 5,5'-dimethyl-2,2'-bipyridine ligand and by the O atoms of four water molecules. Reaction of bis(diethanoldithiocarbamato)nickel(II) with ethylenediamine produced $[Ni(en)_3]S_2O_3$.[18] Oxidation of dithiocarbamate to thiosulphate in basic medium was established. In continuation of our interest in such reactivity studies, bis(diethanoldithiocarbamato)copper(II), $[Cu(deadtc)_2]$ and bis(di-*n*-propyl dithiocarbamato)zinc(II), $[Zn(dnpdtc)_2]$ complexes were allowed to react with 2,2'-bpy (1:2 ratio) in ethanol. The products were analysed and structurally investigated and the results are reported herein.

EXPERIMENTAL

Materials

Diethanolamine (99 %), di-*n*-propylamine (97 %), CS_2 (95 %), copper(II) chloride dihydrate (95 %), zinc(II) sulphate heptahydrate (97 %) and 2,2'-bipyridine (97 %) were obtained from Merck. Ethanol was of HPLC grade.

Preparation

The parent $Cu(deadtc)_2$ and $Zn(dnpdtc)_2$ complexes were prepared by literature methods.[1,2]

i) Ethanolic solutions of $Cu(deadtc)_2$ (10 mmol, 423 mg, 25 cm^3 ethanol) and 2,2'-bipyridine (20 mmol, 312 mg, 25 cm^3 ethanol) were thoroughly mixed and then left undisturbed. The solutions turned bluish green overnight and light blue crystals separated from the solution after about seven days. The crystals analysed to the formula $[Cu(2,2'\text{-bipy})_2S]CH_3CH_2OSO_3H$ (**1**). Yield: 80 %; Anal. Calcd. for $C_{22}H_{22}N_4O_4S_2Cu$: C, 49.4; H, 4.1; N, 10.5 %. Found: C, 49.3; H, 4.0; N, 10.3 %; UV-Vis (ethanol) (λ_{max} / nm (ε / L mol^{-1} cm^{-1})): 750 (100), 365 (14400).

ii) A similar procedure as described above was followed with $Zn(dnpdtc)_2$ in ethanol. Pale yellow crystals separated from the solution. The crystals analysed to the formula $[Zn(2,2'\text{-bipy})_2S]CH_3CH_2OSO_3H{\cdot}2H_2O$ (**2**). Yield: 80 %; Anal. Calcd. for $C_{22}H_{26}N_4O_6S_2Zn$: C. 46.1; H, 4.6; N, 9.8 %. Found: C, 46.0; H, 4.5; N, 9.6 %; UV–Vis (ethanol) (λ_{max} / nm (ε / L mol^{-1} cm^{-1})): 320 (15700).

iii) Ethanolic solution 2,2'-bipyridine (20 mmol, 312 mg, 25cm^3 ethanol) and $Zn(dnpdtc)_2$ (10 mmol, 417 mg, 25 cm^3 ethanol) were thoroughly mixed with continuous stirring and the resulting solution was refluxed for one hour and then allowed to cool. Dirty colourless crystals

were obtained which analysed to [Zn(2,2'-bipy)$(H_2O)_2$]SO_4 (**3**). Yield: 75%. Anal. Calcd. for $C_{10}H_{12}N_2O_6SZn$: C, 33.9; H, 3.4; N, 7.9 %. Found: C, 33.8; H, 3.2; N, 7.8 %. UV–Vis (ethanol) (λ_{max} / nm (ε / L mol^{-1} cm^{-1})): 325(15200).

iv) A similar procedure as described for compound **3** was followed with Cu(deadtc)$_2$ of ethanol. Pale blue crystals were obtained which analysed to [Cu(2,2'-bipy)$(H_2O)_2$]SO_4 (**4**). Yield: 75%. Anal. Calcd. for $C_{10}H_{12}N_2O_6SCu$: C, 34.2; H, 3.4; N, 7.9 %. Found: C, 34.1; H, 3.2; N, 7.7 %. UV–Vis (ethanol) (λ_{max} / nm (ε / L mol^{-1} cm^{-1})): 745(100), 360(14200).

Analytical and physical measurements

UV-Visible spectra were recorded on a Jasco Uvdec-650 spectrometer and the IR spectra were recorded as KBr pellets using a Jasco IR-100 spectrometer. Elemental analyses (C, H, N) were realised with a Heraeus Carlo Erba 1108 instrument.

X-Ray crystallography

Details of crystal data, data collection and refinement parameters for complexes **1**–**4** are summarized in Table I. Selected bond distances and angles are given in Table II. The intensity data were collected at room temperature (298 K) on a Philips PW100 single crystal diffractometer using Mo-Kα radiation (0.71060 Å) for compound **1**. A Siemens AED and an Enraf Nonius CAD4 diffractometer were used for compounds **2** and **3,** respectively, employing Cu--Kα radiation (1.541780 Å) for data collection. For compound **1**, the structure was solved by the Shelxl 92 program and refined by Shelx 93.[19] Structures **2** and **3** were solved by using the SIR92[20] program and refined using Shelx 93.[19] All the non-hydrogen atoms were refined anisotropically and the hydrogen atoms were refined isotropically.

RESULTS AND DISCUSSION

Electronic spectra and IR spectra

The electronic spectra of both copper complexes showed a prominent band around 750 nm. Another band around 365 nm observed for compound **1** was more intense indicating a charge transfer transition. However, the zinc complexes showed only a strong charge transfer band around 320 nm. The IR spectra of all four complexes showed strong absorptions due to ν(O–H), other than ring ν(C–N) vibrations in the range 1590 cm^{-1}, as observed before.[21]

X-Ray structures

Molecular diagrams of complexes are given in Figs. 1–3. Complexes **1** and **2**, and **3** and **4** are isostructural. Although the crystal structure of complex **4** has already been reported in the literature,[22] the compound was prepared by a direct procedure involving the reactants. In this investigation, complex **4** was obtained from reactivity studies. Therefore, only the crystal structures of three complexes, *viz.*, **1**–**3**, are reported in this paper.

Complex **1** displays a distorted trigonal bipyramidal geometry around the Cu(II) atom, which is coordinated by four N atoms from a 2,2'-bipyridine ligand and by the S atom. Two sets of Cu–N distances were observed. The axial distances are short compared to the equatorial ones. The axial Cu–N distances are 1.988(2) and 1.991(2) Å and the equatorial distances are 2.105(2) and 2.109(2) Å.

TABLE I. Crystal data, data collection and refinement parameters for the complexes **1**–**4**

Parameter	**1**	**2**	**3**	**4**
Empirical formula	$C_{22}H_{22}N_4O_4S_2Cu$	$C_{22}H_{26}N_4O_6S_2Zn$	$C_{10}H_{12}N_2O_6SZn$	$C_{10}H_{12}N_2O_6SCu$
FW	535.1	573.0	353.7	351.7
Crystal system	Monoclinic	Monoclinic	Monoclinic	Monoclinic
Space group	C2/c	C2/c	I2/a	I2/a
a / Å	27.130(3)	27.104(2)	6.990(3)	7.010(3)
b / Å	7.782(3)	7.787(3)	12.466(3)	12.488(3)
c / Å	23.697(2)	23.650(3)	14.867(3)	14.883(2)
α / °	90	90	90	90
β / °	97.99(4)	97.97(3)	101.11(3)	101.12(4)
γ / °	90	90	90	90
U / Å^3	4954.48(2)	4943.33(2)	1272.83	1278.4
Z	8	8	4	4
Dc / g cm^{-3}	1.4346	1.5396	1.504	1.8070
μ / cm^{-1}	10.879	33.345	30.474	18.929
F(000)	2352	2360	2512	2392
λ / Å	Mo-Kα (0.71069)	Cu-Kα (1.54178)	Cu-Kα (1.54178)	Mo-Kα (0.71069)
θ range, ° (scan type ω-2θ)	3–30	3–70	3–70	3–30
Index ranges	$-38 \le h \le 37$, $0 \le k \le 10$, $0 \le l \le 33$	$-32 \le h \le 32$, $0 \le k \le 9$, $0 \le l \le 28$	$-7 \le h \le 8$, $0 \le k \le 15$, $0 \le l \le 18$	$-4 \le h \le 8$, $-14 \le k \le 15$, $-19 \le l \le 18$
Reflections collected	7199	10344	2661	1395
Observed reflections	4516	4329	1201	937
Weighting scheme	$w = 1/(\sigma^2(Fo)^2 +$ $+ (0.0356P)^2 + 0.0000P)$	$w = 1/(\sigma^2(Fo)^2 +$ $+ (0.1709P)^2 + 2.27P)$	$w = 1/(\sigma^2(Fo)^2 +$ $+ (0.0606P)^2 + 6.91P)$	$w = 1/(\sigma^2(Fo)^2 + (0.0645P)^2$ $+ 0.000P)$
$P = \max(Fo^2 + 2Fc^2)/3$				
Number of parameters refined	417	417	409	109
Final *R*, R_w (obs, data)	0.0469, 0.0842	0.0522, 0.1941	0.0515, 0.1497	0.0377, 0.0917
GOOF	0.998	1.037	1.392	0.927

TABLE II. Selected bond distances and angles

Compound **1**		Compound **2**		Compound **3**	
Distances, Å					
Cu–S2	2.318(1)	Zn–S2	2.323(1)	Zn–O4	2.451 (3)
Cu–N3	1.991(2)	Zn–N3	2.101(2)	Zn–N6	1.992(2)
Cu–N14	2.109(2)	Zn–N14	1.980(2)	S2–O4	1.462(2)
Cu–N15	2.105(2)	Zn–N26	2.111(3)	S2–O5	1.489(2)
Cu–N26	1.988(2)	N3–C4	1.334(4)	N6–C7	1.339(5)
N3–C4	1.343(4)	N3–C8	1.355(3)	N6–C11	1.355(4)
N3–C8	1.344(3)	C4–C5	1.396(5)	Zn–O3	2.033(2)
C4–C5	1.376	C9–N14	1.346(4)	C7–C8	1.350(7)
C9–N14	1.353(3)	C13–N14	1.344(4)	C8–C9	1.368(6)
C13–N14	1.337(4)	N15–C16	1.333(4)	C10–C11	1.392(5)
N15–C16	1.341(4)	Zn–N15	1.980(2)		
Angles, °					
N15–Cu–N26	79.9(1)	N15–Zn–N26	79.8(1)	C8–C9–C10	119.71(2)
N14–Cu–N26	96.5(1)	N14–Zn–N26	96.6(1)	C9–C10–C11	117.81(2)
N14–Cu–N15	113.5(1)	N14–Zn–N15	174.5(1)	N6–C11–C10	121.71(2)
N3–Cu–N26	174.5(1)	N3–Zn–N26	113.5(1)	N6–C7–C8	123.5(4)
N3–Cu–N15	97.9(0)	N3–Zn–N15	97.8(0)	O4–S2–O5	108.4(2)
N3–Cu–N14	79.6(1)	N3–Zn–N14	79.7(1)	Zn–O4–S2	133.1(2)
S2–Cu–N26	92.8(0)	S2–Zn–N26	120.7(0)	C7–N6–C11	118.1(3)
S2–Cu–N15	125.9(0)	S2–Zn–N15	92.4(0)	C7–C8–C9	119.2(4)
S2–Cu–N14	120.5(0)	S2–Zn–N14	93.0(0)		
S2–Cu–N3	92.5(0)	S2–Zn–N3	126.0(0)		

Interestingly, the Cu–S distance is 2.318(1) Å. This is in keeping with the distances observed in similar Cu(2,2'-bpy)$_2$X complexes, where X = $S_2O_3^{2-}$ and $S_4O_6^{2-}$ and the corresponding distances are 2.367 and 2.672 Å, respectively.[23,24] The heteroatom lies in the equatorial plane in all the cases, as observed in the present case also. The heteroatom because of its bulkiness shows a distortion and hence the N–Cu–N angle is 113.5(1)° whereas the N–Cu–S angles are 120.5(0)° and 125.9(0)°.

Complex **2** is also monomeric with a trigonal bipyramidal geometry. The heteroatom 'S' is in the equatorial plane with a Zn–S distance of 2.323(1) Å. Two sets of Zn–N distances, as in **1**, were observed, with those in equatorial position, *viz*., 2.101(3) and 2.111(3) Å, being longer than those in axial positions, *viz*., 1.980(2) and 1.980(2) Å. In addition, the N–Zn–N angle is smaller (113.3(1)°) than the larger two, *viz*., 120.7(0) and 126.0(0)°. The observed angles are close to those reported for [Zn(2,2'-bpy)$_2$(ONO)]NO_3.[25] Both structures **1** and **2** are similar and a molecule of $CH_3CH_2OSO_3H$ co-crystallized with them. The bond parameters associated with the bipyridine rings are normal.

Complex **3** has a ZnN_2O_4 coordination environment with SO_4^{2-} acting as bridging ligand between two zinc ions, as observed in the case of the already reported copper analogue.[22] The largest Zn–O distance with sulphate ion is 2.451(3)

Å. The Zn–N distances are 1.992(2) Å and 1.993(2) Å. A distorted octahedral environment around zinc was observed.

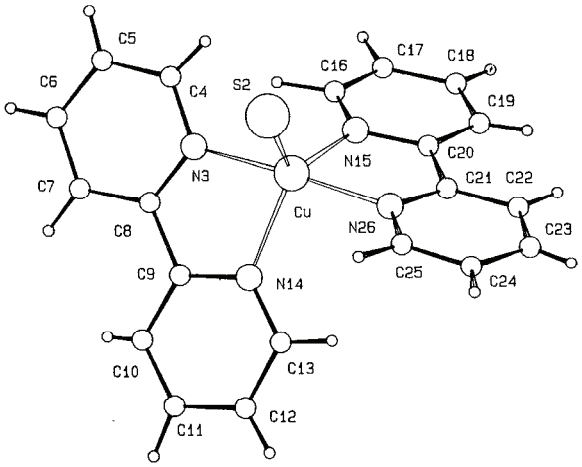

Fig. 1. Molecular structure of $[Cu(2,2'\text{-bpy})_2S]\cdot CH_3CH_2OSO_3H$; ($CH_3CH_2OSO_3H$ is omitted from the diagram).

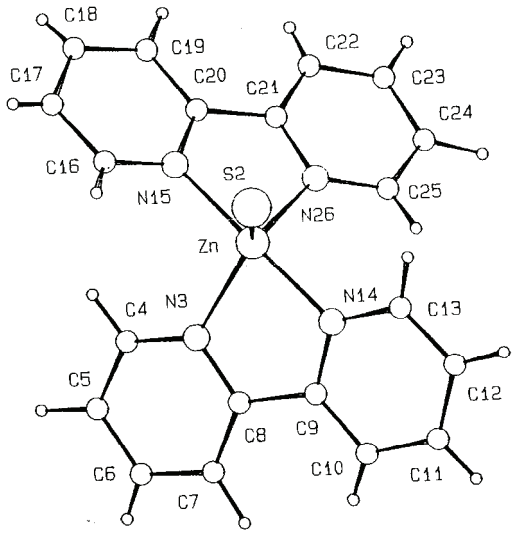

Fig. 2. Molecular structure of $[Zn(2,2'\text{-bpy})_2S]\cdot CH_3CH_2OSO_3H\cdot 2H_2O$; ($CH_3CH_2OSO_3H\cdot 2H_2O$ is omitted from the diagram).

The crystallographic data for the structures are deposited at the Cambridge Crystallographic Data Centre, under deposition numbers: CCDC 163525, CCDC 163526, CCDC 163527. Copies of the data can be obtained free of charge on application to the Director, CCDC, 12 Union Road, Cambridge CB2 1EZ, UK (fax: intcode+(1223)336 033; e-mail: teched@chemcrys.cam.ac.uk).

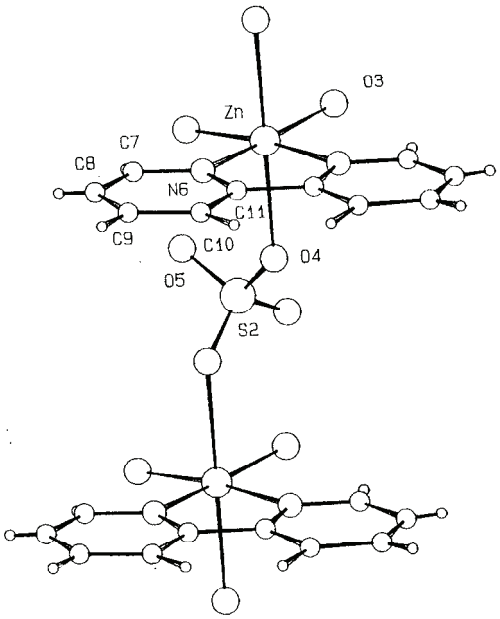

Fig. 3. Molecular structure of $[Zn(2,2'\text{-bpy})(H_2O)_2]SO_4$.

CONCLUSIONS

Reaction of $[Cu(deadtc)_2]$ and $[Zn(dnpdtc)_2]$ with 2,2'-bipyridine produced the complexes **1**–**4** at room temperature and under refluxing conditions, respectively. The crystal structures of the complexes **1**–**3** are reported in this paper. Complexes **1** and **2** have trigonal bipyramidal geometry, while a distorted octahedral environment was observed in complexes **3** and **4**. This paper reports the oxidation of the dithiocarbamate ligand to a sulphate anion. Conversion to $CH_3CH_2OSO_3H$ was observed at room temperature. However, under refluxing conditions, complete conversion to SO_4^{2-} was observed. Sulphide ion coordination was observed on rare occasions leading to the formation of the five-coordinated MN_4S (M = Cu or Zn) chromophore. Although, a similar conversion of dithiocarbamate to $S_2O_3^{2-}$ in ethylenediamine was reported, this paper reports the first instance of oxidation of dithiocarbamate to SO_4^{2-}.

ИЗВОД

СИНТЕЗА, СПЕКТРАЛНА И РЕНДГЕНСКА СТРУКТУРНА ПРОУЧАВАЊА НА МОНОКРИСТАЛУ БИС(2,2'-БИПИРИДИН)СУЛФИДО-М(II) (М = Cu ИЛИ Zn) И ДИАКВА-2,2'-БИПИРИДИН-ЦИНК(II)-СУЛФАТА ДИХИДРАТА

ARUMUGAM MANOHAR[1], KUPPUKANNU RAMALINGAM[2], GABRIELE BOCELLI[3] и ANDREA CANTONI[3]

[1]Department of Chemistry, Kalasalingam University, Krishnankoil – 626 190, [2]Department of Chemistry, Annamalai Unviversity, Annamalainagar – 608 002, India и [3]Centro di studio per la strutturistica, Diffractometrica del CNR, Parma, Italy

Изучавана је реакција комплекса бис(диетанолдитиокарбамато)бакра(II), $[Cu(deadtc)_2]$ и бис(ди-*n*-пропилдитиокарбамато)цинка(II), $[Zn(dnpdtc)_2]$ са 2,2'-бипиридином (2,2'-bipy) (у

односу 1:1) у етанолу. Једноставним мешањем реактаната у односу 1:1 даје петокоординатне $[Cu(2,2'\text{-bipy})_2S]\cdot CH_3CH_2OSO_3H$ (**1**), $[Zn(2,2'\text{-bipy})_2S]\cdot CH_3CH_2OSO_3H.2H_2O$ (**2**). Рефлуктовањем реактаната и хлађењем садржаја добијају се $[Zn(2,2'\text{-bipy})(H_2O)_2]SO_4$ (**3**) и $[Cu(2,2'\text{-bipy})(H_2O)_2]SO_4$ (**4**). Комплекси **1** и **2** су мономерни са тригонално-бипирамидалном геометријом. Дисторгована октаедарска околина је примећена у комплексима **3** и **4**. Кристална структура **4** је већ објављена у литератури. кристалне структуре **1**, **2** и **3** су објављене у овом раду. M–S растојања у **1** и **2** су 2.318(1) Å односно 2.323 Å. N–M–S углови су већи од углова N–M–N из стерних разлога.

(Примљено 19. октобра, ревидирано 18. децембра 2009)

REFERENCES

1. D. Coucouvanis, *Prog. Inorg. Chem.* **11** (1979) 233
2. G. Hogarth, *Prog. Inorg. Chem.* **53** (2003) 71
3. A. Manohar, V. Venkatachalam, S. Thirumaran, K. Ramalingam, G. Bocelli, A. Cantoni, *J. Chem. Crystallogr.* **28** (1998) 861
4. N. Srinivasan, S. Thirumaran, S. Ciattini, *J. Mol. Struct.* **921** (2009) 63
5. A. Manohar, K. Ramalingam, G. Bocelli, L. Righi, *Inorg. Chim. Acta* **314** (2001) 177
6. S. Thirumaran, K. Ramalingam, G. Bocelli, A. Cantoni, *Polyhedron* **28** (2009) 263
7. N. Srinivasan, S. Thirumaran, S. Ciattini, *J. Mol. Struct.* **936** (2009) 234
8. A. Manohar, V. Venkatachalam, K. Ramalingam, U. Casellato, R. Graziani, *Polyhedron* **16** (1997) 1971
9. A. Manohar, K. Ramalingam, R. Thiruneelakandan, G. Bocelli, L. Righi, *Z. Anorg. Allg. Chem.* **627**(2001**)** 1103
10. R. Thiruneelakandan, A. Manohar, K. Ramalingam, G. Bocelli, L. Righi, *Z. Anorg. Allg. Chem.* **628** (2002) 685
11. A. Manohar, K. Ramalingam, R. Thiruneelakandan, G. Bocelli, L. Righi, *Z. Anorg. Allg. Chem.* **632** (2006) 461
12. Z. Travnicek, R. Pastorek, V. Slovak, *Polyhedron* **27** (2008) 411
13. R. Dingle, *Inorg. Chem.* **10** (1971) 1141
14. E. W. Ainscough, A. G. Bingham, A. M. Brodie, *Inorg. Chim. Acta* **96** (1985) L47
15. T. J. Wallace, *J. Org. Chem.* **31** (1966) 1217
16. L. Jia, W. Fu, Q. Yin, M. Yu, J. Zhang, Z. Li, *Acta Crystallogr., Sect E* **61** (2005) m1039
17. Q. L. Zhao, H. F. Bai, *Acta Crystallogr., Sect E* **65** (2009) m866
18. K. Ramalingam, G. Aravamudan, V. Venkatachalam, *Bull Chem. Soc. Jpn.* **66** (1993) 1555
19. G. M. Sheldrick, *Shelx 93, Program for crystal structure refinement*, Univ. of Göttingen, Germany, 1993
20. A. Altomare, M. C. Burla, M. Camali, G. Cascarano, C. Giacovazzo, A. Guagliardi, G. Polidori, *J. Appl. Crystallogr.* **27** (1994) 435
21. S. Thirumaram, K. Ramalingam, G. Bocelli, A. Cantoni, *Polyhedron* **18** (1999) 925
22. J. C. Tedenac, E. Philippot, *J. Inorg. Nucl. Chem.* **37** (1975) 846
23. W. D. Harrison, B. J. Hathaway, *Acta Crystallogr., Sect. B* **36** (1980) 1069
24. W. D. Harrison, B. J. Hathaway, *Acta Crystallogr., Sect. B* **34** (1978) 2843
25. A. Walsh, B. Walsh, B. Murphy, B. Hathaway, *Acta Crystallogr., Sect. B* **37** (1981) 1512.

Journal of the Serbian Chemical Society
JSCS-info@shd.org.rs • www.shd.org.rs/JSCS
J. Serb. Chem. Soc. *75* (8) 1093–1098 (2010)
JSCS–4034
UDC 547.53:547.686:54.02
Original scientific paper

On the number of Kekulé structures of fluoranthene congeners

DAMIR VUKIČEVIĆ[1], JELENA ĐURĐEVIĆ[2] and IVAN GUTMAN[2*#]

[1]*Faculty of Natural Sciences and Mathematics, University of Split, Nikole Tesle 12, HR-21000 Split, Croatia and* [2]*Faculty of Science, University of Kragujevac, P. O. Box 60, 34000 Kragujevac, Serbia*

(Received 7 December 2009)

Abstract: The Kekulé structure count K of fluoranthene congeners is studied. It is shown that for such polycyclic conjugated π-electron systems, either $K = 0$ or $K \geq 3$. Moreover, for every $t \geq 3$, there are infinitely many fluoranthene congeners having exactly t Kekulé structures. Three classes of Kekuléan fluoranthenes are distinguished: *i*) Φ_0 – fluoranthene congeners in which neither the male nor the female benzenoid fragment has Kekulé structures, *ii*) Φ_m – fluoranthene congeners in which the male benzenoid fragment has Kekulé structures, but the female does not, and *iii*) Φ_{fm} – fluoranthene congeners in which both the male and female benzenoid fragments have Kekulé structures. Necessary and sufficient conditions are established for each class, $\Phi = \Phi_0$, Φ_m, Φ_{fm}, such that for a given positive integer t, there exist fluoranthene congeners in Φ with the property $K = t$.

Keywords: fluoranthenes; Kekulé structure; polycyclic aromatic hydrocarbons.

INTRODUCTION

Continuing our studies of the π-electron properties of polycyclic conjugated molecules of the fluoranthene-type,[1–8] in this work, attention was focused on their Kekulé structures. As explained in detail elsewhere,[1,6] the systems considered consist of two benzenoid fragments, joined so as to form an additional five-membered ring (*cf*. Fig. 1). Thus, fluoranthene congeners are, from a structural point of view, closely similar to benzenoid systems.[9–13] The Kekulé structures and various Kekulé-structure-based properties of benzenoid molecules have been extensively studied in the past; for details see the books,[13–16] review[17] and recent papers.[18–21] Analogous properties of the fluoranthene-type systems were, so far, analyzed only to a limited extent.[8] In this paper, we are concerned with the possible number of Kekulé structures (Kekulé structure count, K) of fluoranthene congeners. If $K > 0$, the respective molecule is said to be Kekuléan.[13,16]

* Corresponding author. E-mail: gutman@kg.ac.rs
# Serbian Chemical Society member.
doi: 10.2298/JSC091207077V

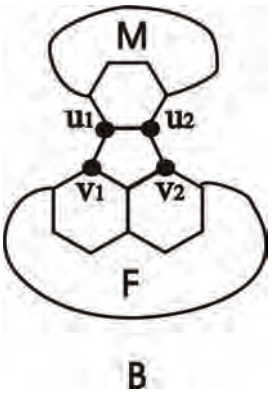

Fig. 1. The general form of a fluoranthene congener B; it is obtained by joining two benzenoid fragments (M and F) so as to form a five-membered ring. The fragments M and F are referred to as male and female, respectively. For details see text.

Following the terminology of an earlier work,[6] the benzenoid fragments of a fluoranthene-type system are called "male" and "female", so that the male fragment (M in Fig. 1) is connected to the female fragment (F in Fig. 1) by two adjacent vertices (u_1 and u_2 in Fig. 1), whereas the female fragment is connected to the male fragment *via* two vertices at distance 2 (v_1 and v_2 in Fig. 1). In other words, three vertices of the five-membered ring belong to the female fragment and two vertices to the male fragment.

Bearing in mind the notation specified in Fig. 1, if *B* is a fluoranthene congener, then be deleting from B the edges u_1v_1 and u_2v_2, a subgraph is obtained consisting of two disconnected benzenoids, referred to as male $M = M_B$ and female $F = F_B$. Denote *i*) by Φ_0 the class of Kekuléan fluoranthenes in which neither the female nor the male benzenoid fragment have Kekulé structures, *ii*) by Φ_m the class of Kekuléan fluoranthenes in which the male fragment has Kekulé structures, but the female does not, and *iii*) by Φ_{fm} the class of fluoranthenes in which both the male and female fragments have Kekulé structures.

The main results obtained are the following:

i) there exist fluoranthenes of the type Φ_0 with *K* Kekulé structures if and only if *K* is the product of two integers both greater than 2;

ii) a fluoranthene of type Φ_m can have *K* Kekulé structures if and only if $K \geq 3$;

iii) a fluoranthene of the type Φ_{fm} can have *K* Kekulé structures if and only if $K \geq 6$, and *K* is not a prime number, *i.e.*, $K \neq 7, 11, 13, 17, 19, 23, \ldots$

NOTATION AND PRELIMINARIES

Let B be the molecular graph[22] of a benzenoid or fluoranthene system, and let κ be a Kekulé structure of B. Denote by $d_1 = d_1(B) = d_1(B,\kappa)$ the number of double bonds of κ belonging to only one ring and by $d_2 = d_2(B) = d_2(B,\kappa)$ the number of double bonds that are shared by two rings. Let R be a ring of B and $D(R) = D(R,\kappa)$ the number of double bonds belonging to *R*. Then,

$$\sum_{\mathrm{R}} D(\mathrm{R}) = d_1 + 2d_2$$

where the summation goes over all rings of B.

Denote by $n = n(\mathrm{B})$ the number of vertices of B, by $n_\mathrm{i} = n_\mathrm{i}(\mathrm{B})$ the number of internal vertices of B and by $h = h(\mathrm{B})$ number of hexagons of B. The number of Kekulé structures of B is $K = K(\mathrm{B})$.

Let B' be a subgraph of B and let κ be a Kekulé structure of B. Then, κ(B') denotes the set of double bonds of κ that belong to B'.

In the proof of the main results, the following theorems were used.

Theorem A.[1,16] If B is a benzenoid system, then $n = 4h + 2 - n_\mathrm{i}$. If B is a fluoranthene-like system, then $n = 4h + 5 - n_\mathrm{i}$.

Theorem B.[8] *i*) Let $\mathrm{B} \in \Phi_0$. Then $K(\mathrm{B}) = K(F_\mathrm{B} - v_i) \cdot K(M_\mathrm{B} - u_i)$ for either $i = 1$ or $i = 2$. Moreover, for $i \neq j$, $K(F_\mathrm{B} - v_j) = K(M_\mathrm{B} - u_j) = 0$; *ii*) let $\mathrm{B} \in \Phi_\mathrm{m}$. Then $K(\mathrm{B}) = K(F_\mathrm{B} - v_1 - v_2)K(M_\mathrm{B})$. Moreover, if κ is a Kekulé structure of B, then $\kappa(F_\mathrm{B} - v_1 - v_2)$ is a Kekulé structure of $F_\mathrm{B} - v_1 - v_2$; *iii*) let $\mathrm{B} \in \Phi_\mathrm{fm}$. Then $K(\mathrm{B}) = K(F_\mathrm{B})K(M_\mathrm{B})$.

MAIN RESULTS

The main results obtained are stated in the following three theorems.

Theorem 1. Let $B \in \Phi_0$. Then $K(\mathrm{B})$ is equal to the product of two numbers, each greater than 2. Moreover, for every number t that is a product of two numbers greater than 2, there are infinitely many fluoranthenes $\mathrm{B} \in \Phi_0$ for which $K(\mathrm{B}) = t$.

Theorem 2. Let $\mathrm{B} \in \Phi_\mathrm{m}$. Then $K(\mathrm{B}) \geq 3$. Moreover, for every $t \geq 3$, there are infinitely many fluoranthenes $\mathrm{B} \in \Phi_\mathrm{m}$ for which $K(\mathrm{B}) = t$.

Theorem 3. Let $B \in \Phi_\mathrm{fm}$. Then, $K(\mathrm{B}) \geq 6$ and $K(\mathrm{B})$ is not a prime number. For every $t \geq 6$ which is not a prime number, there is at least one $\mathrm{B} \in \Phi_\mathrm{fm}$, such that $K(\mathrm{B}) = t$. Moreover, for every positive integer t there are infinitely many fluoranthenes with t Kekulé structures in Φ_fm if and only if $t = t_1 t_2 t_3$, such that $t_1 \geq 3$, $t_2 \geq 3$ and $t_3 \geq 2$.

Proof of Theorem 1. Let $B \in \Phi_0$ and κ be a Kekulé structure of B. It will be shown that $K(\mathrm{B})$ is the product of two numbers, each of which being greater than 2.

From Theorem B for *i*), it follows that $\mathrm{K(B)} = K(M_\mathrm{B} - u_i)K(F_\mathrm{B} - v_i)$. Therefore, it is sufficient to prove that $K(M_\mathrm{B} - u_i) \geq 3$ and $K(F_\mathrm{B} - v_i) \geq 3$. Both proofs are completely analogous and, therefore, only the validity of $K(F_\mathrm{B} - v_i) \geq 3$ will be demonstrated. Note that $\kappa(F_\mathrm{B} - v_i)$ is a Kekulé structure of $F_\mathrm{B} - v_i$. Furthermore, $n(F_\mathrm{B} - v_i) = n(F_\mathrm{B}) - 1$. Then by Theorem A:

$$d_1(F_\mathrm{B}) + d_2(F_\mathrm{B}) = \frac{\left(4h(F_\mathrm{B}) + 2 - n_i(F_\mathrm{B})\right) - 1}{2} = 2h(F_\mathrm{B}) - \frac{n_i(F_\mathrm{B})}{2} + \frac{1}{2}$$

As, evidently, $d_2(F_\mathrm{B}) \geq \frac{1}{2} n_i(F_\mathrm{B})$, one obtains:

$$\sum_{\mathrm{R}} D(\mathrm{R},\kappa) = d_1(F_\mathrm{B}) + 2d_2(F_\mathrm{B}) \geq 2h(F_\mathrm{B}) + \frac{1}{2}$$

with the left-hand side summation going over all rings of F_B. Since this sum is an integer, it follows that:

$$\sum_{\mathrm{R}} D(\mathrm{R},\kappa) \geq 2h(F_\mathrm{B}) + 1$$

Hence, at least one hexagon of F_B contains three double bonds of the Kekulé structure κ.

It is necessary to distinguish between two cases:

Case 1. In F_B, the relation $D(\mathrm{R}_1,\kappa) = D(\mathrm{R}_2,\kappa) = 3$ holds for (at least) two six--membered rings, R_1 and R_2.

Let κ_1 and κ_2 be the Kekulé structures obtained by rotation of the double bonds of $\kappa(F_\mathrm{B} - v_i)$ in the rings R_1 and R_2, respectively. Then, κ_1, κ_2 and $\kappa(F_\mathrm{B} - v_i)$ are three distinct Kekulé structures on $F_\mathrm{B} - v_i$, which means that $K(F_\mathrm{B} - v_i) \geq 3$.

Case 2. In F_B, the relation $D(\mathrm{R},\kappa) = 3$ holds for only one six-membered ring R.

Then, $D(\mathrm{R}') = 2$ for all other six-membered rings R'. Let κ' be the Kekulé structure obtained by rotating the double bonds in *R*. Then:

$$\sum_{\mathrm{R}} D\left(R,\kappa'\right) \geq 2h(F_\mathrm{B}) + 1$$

Hence, either κ' has at least two hexagons R_1 and R_2 for which $D(\mathrm{R}_1,\kappa') = D(\mathrm{R}_2,\kappa') = 3$ or $D(\mathrm{R},\kappa') = 3$ and $D(\mathrm{R}',\kappa') = 2$ for all other hexagons R'. In the latter case, $D(\mathrm{R}',\kappa(F_\mathrm{B}))$ and $D(\mathrm{R}',\kappa')$ would coincide for all hexagons R'. However, these two terms differ in the hexagon(s) adjacent to R, which is a contradiction. Therefore, it must be $D(\mathrm{R}_1,\kappa') = D(\mathrm{R}_2,\kappa') = 3$.

Let κ_1 and κ_2 be the Kekulé structures obtained by rotation of the double bonds of κ' in the rings R_1 and R_2, respectively. Then, κ_1, κ_2 and κ' are three Kekulé structures of $F_\mathrm{B} - v_i$, which means that also in this case $K(F_\mathrm{B} - v_i) \geq 3$.

This proves that $K(\mathrm{B})$ is a product of two numbers, each of which is greater than 2. The example depicted in Fig. 2 shows that it is possible to design arbitrarily many fluoranthenes of class Φ_0 for which $K = t_1 t_2$, $t_1 \geq 3$, $t_2 \geq 3$.

This concludes the proof of the Theorem.

Proofs of Theorems 2 and 3 are analogous, except that instead of Theorem B (i), it is necessary to use Theorem B (ii) and (iii), respectively.

By combining Theorems 1–3, one obtains:

Corollary 4. Let B be a Kekuléan fluoranthene. Then $K(\mathrm{B}) \geq 3$. Moreover, for every number $t \geq 3$, there are infinitely many fluoranthenes B such that $K(\mathrm{B}) = t$.

According to Theorems 1–3, the minimal Kekulé structure count of a fluoranthene in class Φ_0, Φ_m and Φ_fm is 9, 3 and 6, respectively. The smallest such minimal-*K* fluoranthenes are depicted in Fig. 3.

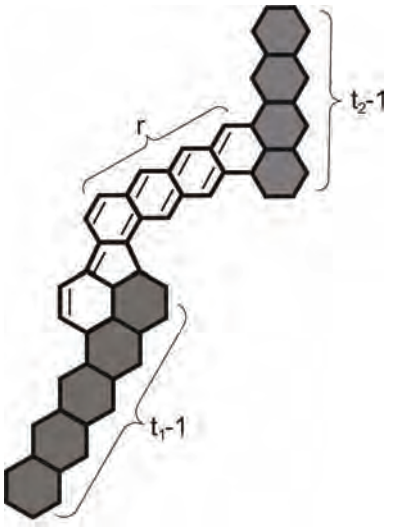

Fig. 2. Fluoranthenes belonging to the class Φ_0, having t_1t_2 Kekulé structures, $t_1 \geq 3$ and $t_2 \geq 3$, irrespective of the value of the parameter r, $r = 1, 2, 3,\ldots$ The fixed double bonds are indicated, whereas the shaded areas are domains in which the π–electrons are delocalized. In this example the shaded areas pertain to polyacenes with $t_1 - 1$ and $t_2 - 1$ hexagons; recall that a polyacene with h hexagons has $h + 1$ Kekulé structures.

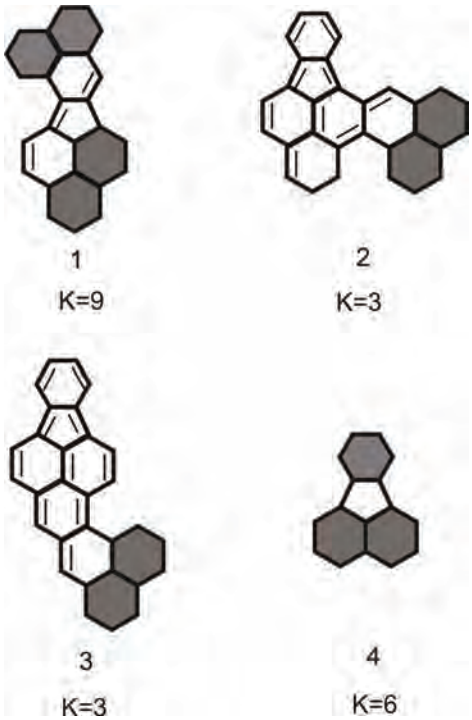

Fig. 3. Fluoranthenes **1**, **2** **3** and **4** are the smallest members of the classes Φ_0, Φ_m and Φ_{fm}, respectively, having the smallest possible number of Kekulé structures (K). In these formulas the fixed double bonds are indicated, whereas the shaded areas are domains in which the π–electrons are delocalized.

Acknowledgements. The partial support of Croatian Ministry of Science, Education and Sport (Grant Nos. 177-0000000-0884 and 037-0000000-2779) is gratefully acknowledged. The authors also thank the Ministry of Science and Technological Development of the Republic of Serbia for partial support of this work through Grant No. 144015G.

ИЗВОД

О БРОЈУ KEKULÉ СТРУКТУРА У ЈЕДИЊЕЊИМА ФЛУОРАНТЕНСКОГ ТИПА

DAMIR VUKIČEVIĆ[1], ЈЕЛЕНА ЂУРЂЕВИЋ[2] и ИВАН ГУТМАН[2]

[1]*Faculty of Natural Sciences and Mathematics, University of Split, Nikole Tesle 12, HR-21000 Split, Croatia* и [2]*Природно-математички факултет Универзитета у Крагујевцу*

Проучаван је број Kekulé структура K у једињењима флуорантенског типа. Показано је да је код ових полицикличних конјугованих π-електронских система $K = 0$ или $K \geq 3$. Осим тога, за свако $K \geq 3$ постоји бесконачно много флуорантена са тачно K Kekulé структура. Разликују се три класе Kekulé флуорантена: *i*) Φ_0 – флуорантене код који ни мушки ни женски бензеноидни фрагмент немају Kekulé структуре, *ii*) Φ_m – флуорантене код којих мушки бензеноидни фрагмент има Kekulé структуре, а женски нема, и *iii*) Φ_{fm} – флуорантене код којих и мушки и женски бензеноидни фрагмент имају Kekulé структуре. Одређени су неопходни и довољни услови за сваку класу $\Phi = \Phi_0, \Phi_m, \Phi_{fm}$, да за задани позитивни цео број m, постоји једињење флуорантенског типа у Φ са особином $K = m$.

(Примљено 7. децембра 2009)

REFERENCES

1. I. Gutman, J. Đurđević, *MATCH Commun. Math. Comput. Chem*. **60** (2008) 659
2. J. Đurđević, S. Radenković, I. Gutman, *J. Serb. Chem. Soc.* **73** (2008) 989
3. I. Gutman, J. Đurđević, A. T. Balaban, *Polyc. Arom. Comp.* **29** (2009) 3
4. J. Đurđević, I. Gutman, J. Terzić, A. T. Balaban, *Polyc. Arom. Comp.* **29** (2009) 90
5. A. T. Balaban, J. Đurđević, I. Gutman, *Polyc. Arom. Comp.* **29** (2009) 185
6. I. Gutman, J. Đurđević, *J. Serb. Chem. Soc.* **74** (2009) 765
7. I. Gutman, J. Đurđević, S. Radenković, A. Burmudžija, *Indian J. Chem*. **37A** (2009) 194
8. I. Gutman, *Z. Naturforsch.* **65a** (2010) 473
9. N. Trinajstić, *J. Math. Chem.* **5** (1990) 171
10. N. Trinajstić, *J. Math. Chem.* **9** (1992) 373
11. G. Brinkmann, B. Coppens, *MATCH Commun. Math. Comput. Chem.* **62** (2009) 209
12. A. Vesel, *MATCH Commun. Math. Comput. Chem*. **62** (2009) 221
13. I. Gutman, S. J. Cyvin, *Introduction to the Theory of Benzenoid Hydrocarbons*, Springer-Verlag, Berlin, 1989
14. L. Pauling, *The Nature of the Chemical Bond*, Cornell Univ. Press, Ithaca, 1960
15. E. Clar, *The Aromatic Sextet*, Wiley, London, 1972
16. S. J. Cyvin, I. Gutman, *Kekulé Structures in Benzenoid Hydrocarbons*, Springer-Verlag, Berlin, 1988
17. M. Randić, *Chem. Rev*. **103** (2003) 3449
18. I. Gutman, S. Radenković, *J. Serb. Chem. Soc.* **71** (2006) 1039
19. S. Gojak, I. Gutman, S. Radenković, A. Vodopivec, *J. Serb. Chem. Soc.* **72** (2007) 673
20. J. Đurđević, S. Radenković, I. Gutman, *J. Serb. Chem. Soc.* **73** (2008) 989
21. S. Radenković, I. Gutman, *J. Serb. Chem. Soc.* **74** (2009) 155
22. I. Gutman, O. E. Polansky, *Mathematical Concepts in Organic Chemistry*, Springer-Verlag, Berlin, 1986.

Journal of the Serbian Chemical Society
JSCS-info@shd.org.rs • www.shd.org.rs/JSCS
J. Serb. Chem. Soc. 75 (8) 1099–1113 (2010)
JSCS–4035
UDC 546.681.3:622.349.2:66.061.247:543
Original scientific paper

Liquid–liquid extraction and recovery of gallium(III) from acid media with 2-octylaminopyridine in chloroform: analysis of bauxite ore

SANDIP V. MAHAMUNI[1], PRAKASH P. WADGAONKAR[2] and MANSING A. ANUSE[1]*

[1]*Analytical Chemistry Laboratory, Department of Chemistry, Shivaji University, Kolhapur – 416 004 and* [2]*Polymer Science and Engineering Division, National Chemical Laboratory, Dr. Homi Bhabha Road, Pune – 411 008, India*

(Received 30 June 2009, revised 26 April 2010)

Abstract: The liquid–liquid extraction of gallium(III) from hydrochloric acid solution using 2-octylaminopyridine (2-OAP) in chloroform was investigated. The extraction of gallium(III) from 6.0–9.0 mol dm^{-3} hydrochloric acid was found to be quantitative using 0.033 mol dm^{-3} 2-OAP in chloroform. The effect of the reagent concentration and other parameters on the extraction of gallium(III) was also studied. The stoichiometry of the extracted species of gallium(III) was determined based on the slope analysis method. The extraction reaction proceeded *via* the anion exchange mechanism from hydrochloric acid and the extracted species was $[RR'NH_2^+GaCl_4^-]_{org}$. The extraction of gallium(III) was performed in the presence of various ions to ascertain the tolerance limit to individual ions. The temperature dependence of the extraction equilibrium constants was examined to estimate the apparent thermodynamic functions (ΔH, ΔS and ΔG) for the extraction reaction. Gallium(III) was successfully separated from commonly associated metal ions, such as Zn(II), Pb(II), Cd(II), Hg(II), Bi(III), Al(III), Se(IV), Sb(III), Sn(IV), In(III), Tl(I) and Tl(III). However, gallium(III) was separated from Fe(III) from weak organic acid media. The procedure was also extended to the determination of gallium(III) in bauxite ore by the standard addition method.

Keywords: liquid–liquid extraction; gallium(III); 2-OAP; recovery of gallium from bauxite.

INTRODUCTION

Gallium is widely spread in nature, although minerals rich in gallium are rare. Owing to this, gallium is usually obtained as a by-product of the processing of other minerals (bauxite, sphalerite). The most important commercial source of gallium is bauxite and sodium aluminate from the Bayer process, its main raw

* Corresponding author. E-mail: mansinganuse@yahoo.co.in
doi: 10.2298/JSC090630072M

material.[1–3] Hence, the separation of gallium from aluminium is of practical importance.

The earliest applications of solvent extraction of gallium were in analytical procedures established before a significant commercial demand for this metal existed. Gallium is used primarily in electronic devices because of the specific band structure of its crystalline compounds (mostly gallium arsenide). Such a structure provides for efficient optical transitions as well as high electron mobilities. Interest in the development of recovery processes of gallium increased in the late 1970s due to the potential of much faster computer chips made of gallium arsenide in place of silicon. In the following years, however, the manufacture of GaAs-based integrated circuits (IC) on a large scale and at low cost proved to be more difficult than initially thought, which led to the role of GaAs in the computer industry being redefined. Today, the sale of GaAs-IC is rising fast.[4] Other than digital circuits, GaAs is finding increasing application in optoelectronics: for light emitting diodes (LED), semiconductor lasers, solar cells and optical computing in analogue microware devices.[5]

Gallium is present in very small amounts compared to common or similar metals. Thus, its recovery is a difficult task in which solvent extraction plays a significant role. Organophosphorus acid reagents are known to be generally suitable for gallium(III) extraction from either mineral acid media or weak organic acid media. Di-2-ethylhexylphosphoric acid (D2EHPA),[6] divinylbenzene homopolymeric microcapsules containing di-2-ethylhexylphosphoric acid, 2-ethylhexylphosphonic acid mono-2-ethylhexyl ester,[7] cyanex-921,[8] cyanex-923,[9] cyanex-301,[10] cyanex-272,[11] and 2-ethylhexylphosphonic acid mono-2-ethylhexyl ester (PC-88A)[12] are reported as effective extractants for gallium(III). However, Fe(III), Ru(III), Os(VIII), Pt(IV), Au(I) interfere in the extraction.[8]

Oxygen-containing extractants play important role in the extraction of gallium(III). 8-Quinolinol and its derivatives, under the trade name kelex-100, are the most famous reagents used for the extraction of metal ions. Using 1-octanol/octane mixed solvent systems, the extraction of gallium(III) with 8-quinolinol was realized at 25 °C. The shaking time required for gallium(III) extraction was 2 h.[13] Gallium(III) was extracted from aqueous solution with 5-amylthio-8-quinolinol into the organic phase,[14] however, a 3-hour equilibrium time was needed. Alkylsubstituted-8-hydroxyquinoline (LIX-26) chelating reagents in *n*-decanol are good extractants for gallium(III) in the higher pH range.[15] They extract gallium(III) in 30 min at pH 9.2 and the reactions were exothermic. The extraction kinetics of gallium(III) with 5-chloro-8-quinolinol diluted in toluene was examined and clarified by Kondo and *et al.*[16,17] The extraction of gallium(III) was found to be 80 % after 3 h equilibration. The fundamental extraction kinetics with the pure kerosene/kelex 100 system and a method of selective re-extraction boosted by possible chloro-complex formation in HCl media was proposed by

Kekesi.[18] The steric effect of 3,5-bis(trifluoro)methyl phenol (BTMP) as a hydrogen-bond donor on the outer-sphere complexation in the synergistic extraction of gallium(III) with 2,4-pentanedione was investigated.[19] The chelate extraction behaviour of gallium(III) with the tripod quadridentate phenolic ligand, tris(2--hydroxy-3,5-dimethylbenzyl)amine (H_3tdmba) was studied by Hirayama *et. al.*[20]

Extraction behaviour and mechanism of gallium(III) with naphthenic acid (NA), *sec*-octylphenoxyacetic acid (CA-12) and *sec*-nonylphenoxyacetic acid (CA-100) dissolved in kerosene from hydrochloric acid solution was investigated.[21,22] A study was conducted on the solvent extraction of gallium(III) from hydrochloric acid media with 3-chlorinated organic solvents containing a non--ionic surfactant, polyoxyethylene nonyl phenyl ether (PONPE) as the extractant.[23] Gallium(III) could be separated from flue dust residues from aluminium production plants using a poly-ether type polyurethane foam from 3 mol dm^{-3} sulphuric acid and 3 mol dm^{-3} sodium chloride solutions with at least 92 % efficiency of the total recovery. The interference of iron was minimized by its reduction.[24]

Katiyar *et al.*,[25] and Vibhute and Khopkar,[26] determined the amount of gallium(III) in bauxite ore by neutron activation analysis and solvent extraction methods, respectively.

High molecular weight amines (HMWAs) have emerged as powerful extractants for many elements. The distribution equilibria of 0.01 mol dm^{-3} gallium(III) from 1–2 mol dm^{-3} hydrochloric acid media were studied using a commercial trialkyl amine, ADOGEN 364, dissolved in kerosene as the extractant.[27] Trioctyl amine (TOA) in benzene was investigated as an extractant for trivalent gallium from aqueous solutions containing hydrochloric acid and/or lithium chloride.[28] Recently *n*-octylaniline was used for quantitative extraction of gallium(III) from succinate media.[29] 2-Octylaminopyridine[30] was superior to *n*-octylaniline for the following reasons: *i*) *n*-octylaniline is commercially available but it is more expensive; *ii*) the synthesis of *n*-octylaniline by the Pohlandt method[31] in laboratory is tedious and time consuming; *iii*) 2-octylaminopyridine is a sensitive extractant as a lower concentration is required for the extraction of gallium(III) (0.033 mol dm^{-3}) as compared with *n*-octylaniline (0.29 mol dm^{-3}); *iv*) difficulties in phase separation arise when toluene is used as the diluent for *n*-octylaniline and *v*) *n*-octylaniline is effective only when it is freshly synthesized and used after distillation, otherwise the immediate formation of a solid phase occurs during the extraction.

In the present study, the extraction of gallium(III) from mineral acid media and weak organic acid media using a solution of 2-octylaminopyridine (2-OAP) in chloroform was investigated. The method permits the separation of gallium(III) from commonly associated metals and was used to separate and determine gallium(III) in bauxite ores.

EXPERIMENTAL

Apparatus

An Elico digital spectrophotometer model SL–171 with 1 cm quartz cells was used for the absorbance measurements. The pH measurements were realised using an Elico digital pH meter model LI–120. A constant temperature (±0.1 °C) water bath MIC-66 A (Modern Scientific Instrument Company, Mumbai, India) was used for the temperature controlled studies.

Reagents

Gallium(III) solution. A standard stock solution of gallium(III) was prepared by dissolving 0.898 g of gallium trichloride in 6.0 mol dm^{-3} hydrochloric acid and diluted to 250 mL with distilled water and standardized complexometrically.[32] The solution contains 1.42 mg mL^{-1}, of gallium(III). The working solution was prepared by appropriate dilution of the stock solution with distilled water.

Thorium (IV) nitrate solution. A standard water solution of thorium nitrate (0.010 mol dm^{-3}) was prepared by dissolving 5.881 g thorium nitrate (AR) and diluted to 1 L with distilled water and standardized against a standard zinc(II) solution.[33]

EDTA solution. A standard solution of EDTA disodium salt (0.010 mol dm^{-3}) was prepared by dissolving 3.722 g disodium salt of EDTA in 1 L of distilled water.

2-Octylaminopyridine (2-OAP) solution. A 0.033 mol dm^{-3} solution of 2-octylaminopyridine[30] was prepared by dissolving in chloroform.

All the chemicals used were of analytical grade. Double distilled water was used throughout the experiments.

General extraction and determination procedure for gallium(III)

An aliquot of solution containing 0.500 mg of gallium(III) was mixed with a sufficient quantity of hydrochloric acid to make its concentration 7.0 mol dm^{-3} in a total volume of 25 mL of solution. The solution was then transferred to a 125 mL separation funnel, 10 mL of 0.033 mol dm^{-3} 2-OAP in chloroform was added, which was then shaken gently for about 2 min. The layers were allowed to separate and the aqueous layer was carefully withdrawn. Gallium(III) from the organic phase was stripped with 1.0 mol dm^{-3} hydrochloric acid (2×10 mL). The back extracts were evaporated almost to dryness and the residue was extracted with distilled water with warming.

The aqueous solution was then transferred into a 125 mL conical flask, followed by addition of 10 mL 1.0 mol m^{-3} EDTA solution. The excess of EDTA solution was titrated against a standard 1.0 mol m^{-3} solution of thorium nitrate using xylenol orange as the indicator. The end point was the yellow to pink red colour transition.[32] The percentage extraction, E, was calculated using Expression (1):

$$\%E = (\text{metal extracted/metal taken}) \times 100 \quad (1)$$

and the distribution ratio, D, was calculated using Expression (2):

$$D = (\%E / (100 - \%E)) \times \text{Volume aqueous phase/Volume organic phase} \quad (2)$$

RESULTS AND DISCUSSION

Effect of acidity

The extraction of 0.500 mg of gallium(III) from different acid media was performed with 0.033 mol dm^{-3} 2-OAP in chloroform at a constant aqueous:or-

ganic volume ratio of 2.5:1.0. The extraction was found to be quantitative from hydrochloric acid (Table I), while there is no extraction from sulphuric, nitric, perchloric and hydrobromic acid media. The extraction of gallium(III) starts at 4.0 mol dm^{-3} hydrochloric acid and becomes quantitative in the range of 6.0–9.0 mol dm^{-3} hydrochloric acid, after which there is decrease of extraction. This may be due to the formation of the stable hydrochloride of 2-OAP. Thus, hydrochloric acid concentration of 7.0 mol dm^{-3} was used for the further extraction experiments.

TABLE I. Extraction behaviour of gallium(III) as a function of hydrochloric acid concentration. Gallium(III) = 0.500 mg, 2-OAP = 10 mL of 0.033 mol dm^{-3} in chloroform, aqueous:organic ratio = 2.5:1, equilibrium time = 2 min, strippant = 1.0 mol dm^{-3} hydrochloric acid (2×10 mL)

HCl Concentration, mol dm^{-3}	Amount of Ga(III) extracted, %	*D*
1.0	0.0	–
2.0	0.0	–
3.0	0.0	–
4.0	14.9	0.43
5.0	50.0	2.50
5.5	98.6	176.07
6.0	100.0	∞
6.5	100.0	∞
7.0[a]	100.0	∞
8.0	100.0	∞
9.0	100.0	∞
10.0	85.1	14.27

[a]Recommended for general extraction procedure

Extraction as a function of 2-octylaminopyridine concentration

The concentration of 2-OAP in chloroform was varied from 0.0004 to 1.0 mol dm^{-3} in 7.0 mol dm^{-3} hydrochloric acid. It was found that 10 mL 0.029 mol dm^{-3} 2–OAP in chloroform was required for quantitative recovery of gallium(III). However, 0.033 mol dm^{-3} 2-OAP was used for the further studies in order to ensure complete extraction. There was no adverse effect if an excess of 2-OAP was used.

Extraction with various diluents

Extractions of gallium(III) were performed from 7.0 mol dm^{-3} hydrochloric acid medium using 10 mL of 0.033 mol dm^{-3} 2-OAP in various solvents as diluents. The extraction of gallium(III) was quantitative with chloroform, xylene and amyl acetate because the ion-pair complex had a high distribution ratio in these solvents. The extraction was incomplete in benzene, toluene, methyl isobutyl ketone (MIBK), amyl alcohol, 1,2-dichloroethane and kerosene (Table II).

There was no extraction in carbon tetrachloride. Hence, chloroform was used for the further extractions.

TABLE II. Extraction behaviour of gallium(III) as a function of the diluent. Gallium(III) = = 0.500 mg, hydrochloric acid = 7.0 mol dm^{-3}, 2-OAP = 10 mL 0.033 mol dm^{-3}, aqueous:organic ratio = 2.5:1, equilibrium time = 2 min, strippant = 1.0 mol dm^{-3} hydrochloric acid (2×10 mL)

Diluent	Relative permittivity, ε_r	Amount of Ga(III) extracted, %	*D*
Benzene	2.28	11.5	0.32
Xylene	2.30	100.0	∞
Toluene	2.38	1.3	0.03
Chloroform[a]	4.40	100.0	∞
Carbon tetrachloride	2.24	0.0	–
MIBK	13.10	41.0	1.73
Amyl alcohol	13.90	14.1	0.41
Amyl acetate	4.80	100.0	∞
1,2-Dichloroethane	10.50	85.8	15.10
Kerosene	1.80	71.7	6.33

[a]Recommended for general extraction procedure

Nature of the extracted species

Attempts were made to ascertain the nature of the extracted complex species using log *D*–log *c* plots. A graph of log $D_{[Ga(III)]}$ *versus* log $c_{[2\text{-OAP}]}$ at 4.5 and 5.0 mol dm^{-3} hydrochloric acid concentration gave slopes of 1.21 and 1.22, respectively (Fig. 1). The possible mechanism of the extraction appears to be protonation of 2-OAP, which forms cationic species, such as $[RR'NH_2^+Cl^-]_{(org)}$, while the chloride ions combines with gallium(III) to form anionic species such as $[GaCl_4^-]_{(aq.)}$, both of which associate to form an ion-pair of the type $[RR'NH_2^+GaCl_4^-]_{(org)}$, which being neutral, constitutes the extractable species. The mechanism of formation of the ion-pair complex is:

$$[RR'NH]_{(org)} + HCl_{(aq)} \leftrightarrows [RR'NH_2^+Cl^-]_{(org)} \quad (3)$$

$$GaCl_{3(aq)} + Cl^-_{(aq)} \leftrightarrows [GaCl_4^-]_{(aq)} \quad (4)$$

$$[RR'NH_2^+Cl^-]_{(org)} + [GaCl_4^-]_{(aq.)} \leftrightarrows [RR'NH_2^+GaCl_4^-]_{(org)} + Cl^-_{(aq)} \quad (5)$$

where R = $-C_5H_4N$ and R' = $-CH_2(CH_2)_6CH_3$.

The influence of equilibrium time

Variation of the shaking time from 10 s to 20 min showed that a 1-min equilibrium time was adequate for the quantitative extraction of gallium(III) from chloride media. However, for the general procedure a 2-min equilibrium time is recommended in order to ensure the complete extraction of the metal ion. Nevertheless, prolonged shaking up to 20 min had no adverse effect on the extraction.

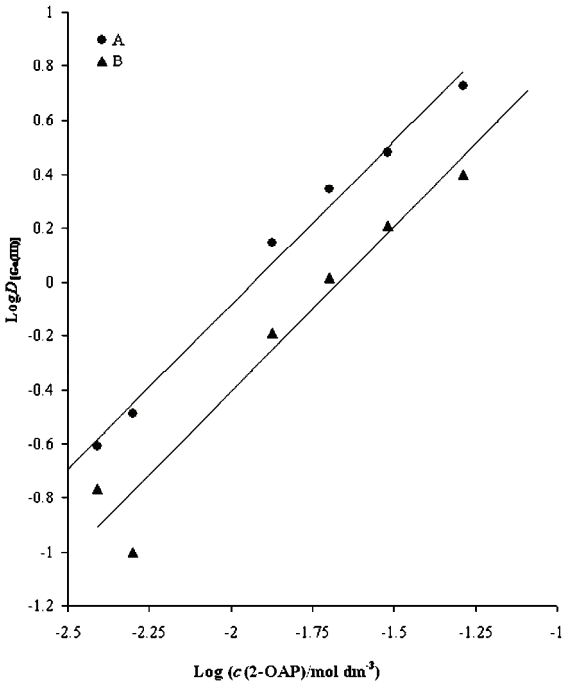

Fig. 1. Log–log plot of the distribution ratio, $D_{[Ga(III)]}$, *vs.* $c_{[2\text{-OAP}]}$ at 4.5 mol dm^{-3} (A, slope = 1.21) and at 5.0 mol dm^{-3} hydrochloric acid (B, slope = 1.22).

Loading capacity of 2-OAP

The loading capacity of the extractant was determined by repeated contact of the organic phase with a fresh feed solution of the metal at the same concentration. For 10 mL of a 0.033 mol dm^{-3} solution of 2–OAP in chloroform at 7.0 mol dm^{-3} concentration of hydrochloric acid, the maximum loading capacity for gallium(III) was found to be 2.0 mg at 300 K.

Effect of aqueous to organic volume ratio

The results of contacting different volume ratios of aqueous to organic phase were investigated. The study indicated that the preferred aqueous to organic phase ratio is 5:1 or less. This is evident from the sharp increase in the separation efficiency as well as the distribution ratio of gallium(III) when phase ratio was changed from 20:1 to 5:1. This may simply due to the non-availability of the reagent for metal extraction, so that a crowding effect occurred at low phase ratios. However, in the recommended procedure the phase ratio was maintained at 2.5:1 in order to avoid a large consumption of hydrochloric acid.

Effect of stripping agents

Stripping is the reverse of extraction. Various stripping agents (2×10 mL), such as hydrochloric acid, sulphuric acid, perchloric acid, nitric acid, ammonia, potassium hydroxide, sodium hydroxide, ammonia buffer solution (pH 10.0),

acetate buffer solution (pH 4.63) and water, were used for the recovery of gallium(III) from the organic phase. It was found that of all the stripping solutions examined, only hydrochloric acid (0.5–2.0 mol dm^{-3}) was effective in stripping gallium(III) from the organic phase. In the actual practice, two 10 mL portions of 1.0 mol dm^{-3} hydrochloric acid were used (Table III).

TABLE III. Extraction behaviour of gallium(III) as a function of the strippant. Gallium(III) = = 0.500 mg, hydrochloric acid = 7.0 mol dm^{-3}, 2-OAP = 10 mL 0.033 mol dm^{-3} in chloroform, aqueous:organic ratio = 2.5:1, equilibrium time = 2 min

c	Recovery, %						
mol dm^{-3}	HCl[b]	H_2SO_4[a]	$HClO_4$	HNO_3	KOH	NaOH	NH_3
0.1	98.1	98.4	98.5	94.5	26.1	19.1	60.7
0.5	100.0	95.5	97.0	63.9	16.4	0.0	60.7
1.0[b]	100.0	95.5	97.0	42.2	0.0	0.0	60.7
2.0	100.0	95.5	97.0	13.8	0.0	0.0	60.7
2.5	96.7	95.5	96.0	0.0	0.0	0.0	60.7
3.0	96.6	95.5	96.0	0.0	0.0	0.0	60.7
4.0	77.6	95.5	96.0	0.0	0.0	0.0	60.7
5.0	77.6	95.5	96.0	0.0	0.0	0.0	60.7

Strippant	Recovery, %
Ammonia buffer (pH 10)	21.8
Acetate buffer (pH 4.63)	75.2
Water	29.2

[a]Concentrations in normal; [b]recommended for general extraction procedure

Effect of temperature on the extraction of gallium(III)

The extraction of gallium(III) from 5.0 mol dm^{-3} hydrochloric acid using 0.033 mol dm^{-3} 2-OAP in chloroform at varying temperatures from 298 to 310 K gave the results presented in Table IV. It was found that in the extraction of gallium(III) by 2-OAP in chloroform, the distribution coefficient increased with increasing temperature.

TABLE IV. Effect of temperature on the extraction of gallium(III) with 2-OAP in chloroform. Gallium(III) = 0.500 mg, hydrochloric acid = 5.0 mol dm^{-3}, 2–OAP = 10 mL 0.033 mol dm^{-3}, aqueous:organic ratio = 2.5: 1, equilibrium time = 2 min, strippant =1.0 mol dm^{-3} HCl (2×10 mL)

T / K	Log K_{ex}	ΔG / kJ mol^{-1}	ΔS / J K mol^{-1}	ΔH / kJ mol^{-1}
298	0.2829	–10.9	237.2	59.73
301	0.3979	–14.4	246.3	
304	0.4436	–16.1	249.5	
307	0.5637	–21.5	264.6	
310	0.7075	–30.3	290.3	

The change in the extraction equilibrium constant, K_{ex}, with temperature is expressed by the van't Hoff Equation:

$$d(\log K_{ex})/d(1/T) = -\Delta H/2.303R \quad (6)$$

The plot of log K_{ex} *vs.* $1/T$ was linear with a slope of –3.12 (Fig. 3) and the enthalpy change of the extraction realized at a hydrochloric acid concentration 5.0 mol dm^{-3} was evaluated as ΔH = 59.7 kJ mol^{-1}, which means that the extraction was an endothermic process. The change in Gibbs energy ΔG and entropy ΔS were calculated from Eqs. (7) and (8):

$$\Delta G = -2.303RT \log K_{ex} \quad (7)$$

$$\Delta S = \Delta H - \Delta G/T \quad (8)$$

The negative value of the Gibbs energy change implies that the reaction was spontaneous. The positive value of the enthalpy change indicates that the extraction of gallium(III) with 2-OAP in chloroform was more favourable with increasing temperature.

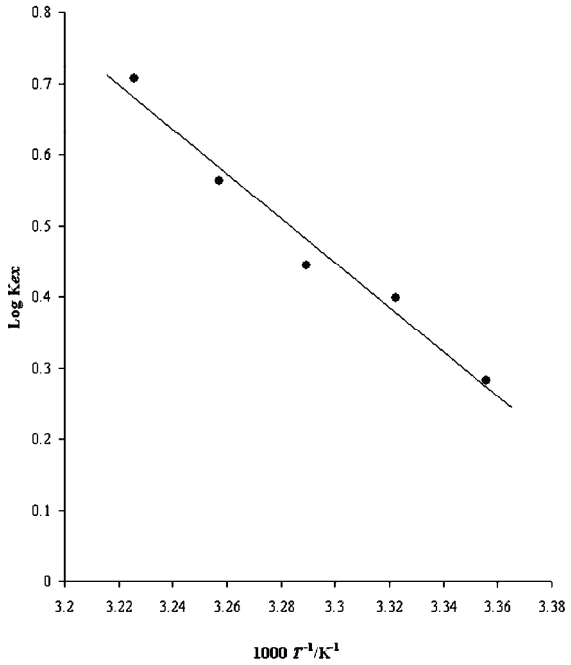

Fig. 2. Plot of log K_{ex} *vs.* T^{-1} at constant pH 4.0 (slope = –3.12) with 2-OAP in chloroform.

Effect of various foreign ions on percentage extraction of gallium(III)

The effect of large number of foreign ions on the extraction of 0.500 mg of gallium(III) by the proposed reagent was investigated following the recommended procedure. Initially the foreign ions were added to the gallium(III) solution in large excess, 100 mg for the tested anions and 25 mg for the tested cations. When interference was found to be intensive, the tests were repeated with successively smaller amounts of foreign ion. The tolerance was set at the amount of the fo-

reign ion that could be present to give an error less than ±2 % in the recovery of gallium(III) (Table V). It was observed that the method was free from interference from a large number of cations and anions. However, interference due to Bi(III) and Tl(III) had to be eliminated by masking with 100 mg tartrate each. In addition, to mask Sn(II), Co(II) and Ge(IV), 10 mg citrate, 100 mg thiocyanate and 5 mg oxalate were used respectively for each metal. The method suffered from strong interference due to Fe(III), V(V) and Ni(II). Under the optimum extraction conditions for gallium(III), these metals were found to be co-extracted.

TABLE V. Effect of various foreign ions on percentage extraction of gallium(III). Gallium(III) = 0.500 mg, hydrochloric acid = 7.0 mol dm^{-3}, 2-OAP = 10 mL of 0.033 mol dm^{-3} in chloroform, aqueous: organic ratio = 2.5:1, equilibrium time = 2 min, strippant =1.0 mol dm^{-3} hydrochloric acid (2×10 mL)

Tolerance limit, mg	Foreign ion added
100	Bromide, iodide, acetate, thiourea, thiocyanate, salicylate, ascorbate, nitrate, nitrite, succinate, malonate, tartrate, phosphate
50	Fluoride
25	Cd(II), Ba(II), Cr(VI), Sr(II), Mn(VII), Mn(II)
15	Mo(VI)
10	Citrate, Pb(II), Al(III), Ca(II), W(VI), Sn(IV), Sn(II)[a], Se(IV), Sb(III)
5	Oxalate, Hg(II), Cu(II), Tl(I), Bi(III)[b]
2	Zn(II), Te(IV), Tl(III)[b]
1	Co(II)[c]
0.5	In(III), Ge(IV)[d]
0	Fe(III), V(V), Ni(II)

Masked with: [a]10 mg citrate, [b]100 mg tartrate; [c]100 mg thiocyanate and [d]5 mg oxalate

APPLICATIONS

Separation and determination of gallium(III) from binary mixtures

The suitability of the above-developed method was examined by applying it to the separation and determination of gallium(III) in a variety of binary mixtures, which are frequently in association (Table VI).

It was found that Zn(II), Pb(II), Cd(II), Hg(II), Al(III), Se(IV), Sb(III), Sn(IV), In(III) and Tl(I) remained unextracted under the optimum extraction conditions for gallium(III) using 7.0 mol dm^{-3} hydrochloric acid with 10 mL 0.033 mol dm^{-3} 2–OAP in chloroform. The loaded organic phase was stripped with 1.0 mol dm^{-3} hydrochloric acid (2×10 mL) and determined complexometrically, as recommended in the procedure. The raffinate containing the added metal ion was estimated by standard procedures.[32–34]

The proposed method was also extended to the separation of gallium(III) from Bi(III) and Tl(III) by masking with 100 mg tartrate. The masked metals remained quantitatively in the aqueous phase under the optimum extraction condi-

tions of gallium(III). Gallium(III) was stripped with 1.0 mol dm^{-3} hydrochloric acid (2×10 mL) and estimated as in the recommended procedure.

TABLE VI. Separation of gallium(III) from binary mixtures in mineral acid media

Metal ions	Amount taken, mg	Average recovery[a], %	Method of estimation
Ga(III)	0.500	100.0	–
Zn(II)	0.500	100.0	EDTA[33]
Ga(III)	0.500	99.5	–
Pb(II)	0.500	100.0	EDTA[33]
Ga(III)	0.500	99.5	–
Cd(II)	0.500	100.0	EDTA[33]
Ga(III)	0.500	100.0	–
Hg(II)	1.0	99.5	EDTA[33]
Ga(III)	0.500	99.4	–
Bi(III)[b]	1.0	100.0	EDTA[32]
Ga(III)	0.500	99.4	–
Al(III)	1.0	100.0	EDTA[32]
Ga(III)	0.500	100.0	–
Se(IV)	0.500	100.0	Selenium sol[34]
Ga(III)	0.500	100.0	–
Sb(III)	0.500	100.0	Potassium iodide[34]
Ga(III)	0.500	99.8	–
Sn(IV)	0.05	100.0	Pyrocatechol violet[34]
Ga(III)	0.500	100.0	–
In(III)	0.500	100.0	EDTA[32]
Ga(III)	0.500	99.2	–
Tl(I)	0.500	99.1	EDTA[32]
Ga(III)	0.500	100.0	–
Tl(III)	0.500	100.0	EDTA[32]
Ga(III)[c]	0.500	100.0	–
Fe(III)[b]	0.500	99.3	Thiocyanate[34]

[a]Average of six determinations; [b]masked by 100 mg tartrate; [c]separation from sodium succinate media

It was found that there is co-extraction of iron(III) with gallium(III) from hydrochloric acid media. This is due to formation of ion-pair complex of both the metal ions according to Eq. (4). However, the separation can be achieved from weak organic acid media, such as sodium succinate. Gallium(III) was extracted at pH 4.0 from 5.0 mol m^{-3} sodium succinate solution into the organic phase. It was back extracted into 0.010 mol dm^{-3} EDTA (2×5 mL) or 1.0 mol dm^{-3} hydrochloric acid solution (2×10 mL). The back extracts were estimated using xylenol orange as the indicator and thorium(IV) nitrate as the titrant. Microlevels of gallium(III) can be estimated spectrophotometrically by the PAR method.[35]

An aqueous solution containing a mixture of 0.500 mg, each of gallium(III) and iron(III) in 5.0 mol m^{-3} sodium succinate at pH 4.0 was equilibrated for 2 min with 0.033 mol dm^{-3} 2-OAP in chloroform, whereby iron(III) was masked

with 100 mg tartrate. It was found that only gallium(III) was extracted into organic phase while iron(III) remained unextracted in the aqueous phase. Gallium(III) from the organic phase was back extracted into 0.010 mol dm^{-3} EDTA (2×5 mL) or 1.0 mol dm^{-3} hydrochloric acid solution (2×10 mL). The back extracts were estimated using xylenol orange as the indicator and thorium(IV) nitrate as the titrant. The iron(III) from the aqueous phase was demasked with concentrated hydrochloric acid and estimated spectrophotometrically by the thiocyanate method.[34]

Determination of gallium(III) in a synthetic mixture

The proposed method was applied for the analysis of gallium(III) from a multi-component mixture (Table VII).

TABLE VII. Separation of gallium(III) in synthetic mixtures

Composition of multicomponent mixture, mg	Ga(III) found, mg	Recovery[a], %
Ga(III) 0.500,Tl(III) 0.500, Al(III) 0.500	0.499	99.8
Ga(III) 0.500, In(III) 0.500, Tl(III) 0.500	0.500	100.0
Ga(III) 0.500, Al(III)0.500, In(III) 0.500	0.500	100.0
Ga(III) 0.500, Pb(II) 0.500, Bi(III)[b] 0.500	0.496	99.3
Ga(III)[c] 0.500, Fe(III)[b] 0.500, Al(III) 0.500	0.496	99.3
Ga(III)[c] 0.500, Fe(III)[b] 0.500, Mn(VII) 0.500	0.500	100.0
Ga(III)[c] 0.500, Fe(III)[b] 0.500, Cu(II) 0.500	0.500	100.0

[a]Average of six determination; [b]masked by 100 mg tartrate; [c]separation from sodium succinate media

A solution containing 0.500 mg of gallium(III) was taken and known amounts of other metals were added. The extraction of gallium(III) was performed using the method developed herein. The results obtained were in good agreement with the amount added. The selectivity of the extraction of gallium(III) can be achieved by the use of suitable masking agent for the added metal ions.

Analysis of bauxite ore for its gallium(III) content by standard addition method

Owing to the trace amounts of gallium(III) present in bauxite ores, the standard addition method was followed for the analysis.

Bauxite ore or red mud sample (1 g) was fused with four times its weight of sodium hydroxide (4 g), which dissolves most of the alumina and gallia. The residue was leached with 0.50 mol dm^{-3} sodium hydroxide. The solution was diluted with a little distilled water and filtered by suction on a 7 cm Buchner funnel.[36] The residue left was again washed with 0.50 mol dm^{-3} sodium hydroxide. The obtained alkaline solution containing gallia was nearly neutralized and then made 7.0 mol dm^{-3} in concentrated hydrochloric acid. To this, 0.500 mg of standard gallium(III) solution was added and the solution was made up to 100 mL with 7.0 mol dm^{-3} hydrochloric acid. An aliquot of the solution was taken for

extraction of gallium(III) and estimated spectrophotometrically using the PAR method (Table VIII).[33]

TABLE VIII. Analysis of gallium(III) in bauxite ore. Initial pH: 4.0, aqueous phase = 0.005 mol dm^{-3} sodium succinate, aqueous: organic ratio = 2.5:1, 2-OAP = 10 mL of 0.033 mol dm^{-3} in chloroform, equilibrium time = 2 min, strippant = 0.010 mol dm^{-3} EDTA (2×5 mL) or 1.0 mol dm^{-3} hydrochloric acid (2×10 mL)

Bauxite ore sample	Amount of gallium(III) found by AAS, μg/g	Amount[a] of gallium(III) found by proposed method, μg/g
1	90.5	90.0
2	93.0	92.0
3	91.2	91.0

[a]Average of six determinations

CONCLUSIONS

The important features of the method described herein are:

– it is very simple, selective, reproducible and rapid;

– it permits the selective separation of gallium(III) from other metals which are generally associated with it in real samples;

– gallium(III) is separated from iron(III) by use of a weak organic acid medium (sodium succinate) at pH 4.0 using 2-OAP;

– a very low reagent concentration (0.033 mol dm^{-3} 2-OAP) is required for the quantitative recovery of gallium(III);

– gallium(III) can be extracted both in mineral acid as well as weak organic acid media;

– the equilibrium constant and thermodynamic parameters ΔH, ΔS and ΔG in the extraction of gallium(III) with 2-OAP were evaluated. The extraction is an endothermic process. The extraction of gallium(III) increases with increasing temperature;

– the method is free from interference from a large number of foreign ions which are often associated with naturally occurring gallium(III);

– the time required for the extraction separation is very short. The very short extraction time indicates a high distribution ratio of the ion pair complex involved in the quantitative recovery of gallium(III);

– the developed method involves a one-stage extraction step;

– gallium(III) occurs in trace amount in bauxite ores; hence, the proposed method can be applied for the estimation of gallium(III) in bauxite ore.

Acknowledgements. The financial support of the work by the University Grants Commission (UGC), New Delhi, India, is gratefully acknowledged. One of the authors (SVM) is thankful to UGC for the award of a fellowship.

ИЗВОД

ТЕЧНО–ТЕЧНО ЕКСТРАКЦИЈА ГАЛИЈУМА(III) ИЗ КИСЕЛЕ СРЕДИНЕ ПОМОЋУ 2-ОКТИЛАМИНОПИРИДИНА У ХЛОРОФОРМУ: АНАЛИЗА РУДЕ БОКСИТА

SANDIP V. MAHAMUNI[1], PRAKASH P. WADGAONKAR[2] и MANSING A. ANUSE[1]

[1]*Analytical Chemistry Laboratory, Department of Chemistry, Shivaji University, Kolhapur – 416 004 и*
[2]*Polymer Science and Engineering Division, National Chemical Laboratory, Dr. Homi Bhabha Road, Pune – 411 008, India*

Испитиван је утицај концентрације реактаната и други параметри течно–течно екстракције галијума(III) из хлороводоничне киселине (6,0–9,0 mol dm^{-3}) коришћењем 0,033 mol dm^{-3} раствора 2-октиламинопиридина (2-OAP) у хлороформу и нађено је да је у овим условима екстракција квантитативна. Стехиометријски састав узорака галијума(III) одређен је методом анализе нагиба. Екстракција се одиграва по механизму измене анјона хлороводоничне киселине, а екстраховани узорак је $[RR'NH_2^+GaCl_4^-]_{org}$. Ради утврђивања границе толеранције екстракција галијума(III) рађена је уз присуство различитих јона. Испитана је температурна зависност равнотежне константе екстракције да би се одредиле привидне термодинамичке функције екстракције (ΔH, ΔS и ΔG). Галијум(III) је успешно одвојен од обично присутних металних јона као што су Zn(II), Pb(II), Cd(II), Hg(II), Bi(III), Al(III), Se(IV), Sb(III), Sn(IV), In(III), Tl(I) и Tl(III). Галијум(III) је, међутим, одвојен од Fe(III) из слабо киселе органске средине. Поступак је такође проширен на одређивање галијума(III) у руди боксита стандардном методом додавања.

(Примљено 30. јуна 2009, ревидирано 26. априла 2010)

REFERENCES

1. D. A. Kramer, *U.S. Bureau of Mines Information Circular* **1** (1988) 9208
2. I. R Grant, *Trans. Inst. Min. Metall. Sect. C* **97** (1988) C129
3. B. Petkof, Bureau of Mines, Preprint from Bulletin1, 675, , 1985
4. G. M. Phatak, K. Gangadharan, in *Proceedings of 10th ISAS National Symposium on Strategic and Hi-Tech Metals Extraction and Process Characterization*, Udaipur, India, 1994, p. 4
5. S. Mahajan, *Trans. IIM* **41** (1988) 205
6. M. S. Lee, J. G. Ahn, E. C. Lee, *Hydrometallurgy* **63** (2002) 269
7. E. Kamio, M. Matsumoto, K. Kondo, *J. Chem. Eng. Jpn.* **35** (2002) 178
8. B. Y. Mishra, M. D. Rokade, P. M. Dhadke, *Indian J. Chem.* **39A** (2000) 1114
9. S. D. Pawar, P. M. Dhadake, *J. Serb. Chem. Soc.* **68** (2003) 581
10. B. Gupta, N. Mudhar, S. N. Tandon, *Ind. Eng. Chem. Res.* **44** (2005)192
11. B. Gupta, N. Mudhar, I. Singh, *Sepr. Purif. Technol.* **57** (2007) 294
12. J. Jayachandran, P. Dhadke, *Hydrometallurgy* **50** (1998) 117
13. H. Yamada, H. Hayashi, T. Yasui, *Anal. Sci.* **22** (2006) 371
14. A. N. Turanov, N. K. Evseeva, B. G. Karepov, *Russ. J. App. Chem.* **74** (2001) 1305
15. B. D. Bhattacharya, K. Mandal, S. Mukherjee, *Sep. Sci. Technol.* **38** (2003) 1417
16. K. Kondo, T. Okubo, M. Matsumoto, *J. Chem. Eng. Jpn.* **37** (2004) 465
17. K. Kondo, M. Matsamuto, *J. Chem. Eng. Jpn.* **39** (2006) 292
18. T. Kekesi, *Hydrometallurgy* **88** (2007) 170
19. H. Imura, T. Namai, K. I. Ishimori, S. Hayashi, A. Ohashi, K. Ohashi, *Bull. Chem. Soc. Jpn.* **78** (2005) 2146

20. N. Hirayama, Y. Horita, S. Oshima, K. Kubono, H. Kokusen, T. Honjo, *Talanta* **53** (2001) 857
21. X. Zhang, G. Yin, Z. Hu, *Talanta* **59** (2003) 905
22. X. Zhang, X. Lou, G. Yin, Y. Zhang, *Rare Metals* **23** (2004) 6
23. T. Kinoshita, S. Akita, S. Nii, F. Kawaizumi, K. Takahashi, *Sepr. Purif. Technol.* **37** (2004) 127
24. M. S. Carvalho, K. C. M. Neto, A. W. Nobrega, J. A. Medeiros, *Sep. Sci. Technol.* **35** (2000) 57
25. G. S. Katiyar, M. R. Patil, B. C. Haldar, *Indian J. Technol.* **19** (1981) 380
26. R. G. Vibhute, S. M. Khopkar, *Mikrochim. Acta* **106** (1992) 261
27. E. Rodríguez De San Migue, J. C. Aguilar, M. T. J. Rodríguez, J. De Gyves, *Hydrometallurgy* **57** (2000) 151
28. T. Sato, K. Sato, Y. Noguchi, I. Ishikawa, *Shigen to Sozai* **113** (1997) 185
29. T. N. Shilmkar, S. S. Kolekar, M. A. Anuse, *J. Serb. Chem. Soc.* **70** (2005) 853
30. N. A. Borshch, O. M. Petrukhin, *Zh. Anal. Khim.* **33** (1978) 1805
31. C. Pohlandt, *Talanta* **26** (1979) 199
32. F. J. Welcher, *The Analytical Uses of Ethylenediamine Tetraacetic Acid*, D. Van Nostrand Company, Inc., New York, London, 1958, pp. 176, 178, 182
33. A. I. Vogel, *A Textbook of Quantitative Inorganic Analysis*, ELBS, London, 1961, pp. 432, 442, 444
34. Z. Marckzenko, *Spectrophotometric Determination of Elements*, Ellis Horwood Ltd., Chichester, 1976, pp. 125, 307, 475, 522, 549
35. H. A. Flashka, A. J. Barnard, *Chelates in Analytical Chemistry*, Marcell Dekker Inc., New York, 1972, pp. 136, 137
36. W. R. Schoeller, A. R. Powell, *The Analysis of Minerals and Ores of the Rarer Elements*, Charles Griffin Co. Ltd., London, 1955, p. 81.

Journal of the Serbian Chemical Society
JSCS-info@shd.org.rs • www.shd.org.rs/JSCS
J. Serb. Chem. Soc. 75 (8) 1115–1124 (2010)
JSCS–4036
UDC 547.214+546.881'77–31+
544.478:66.094.258.094.3
Original scientific paper

Oxidative dehydrogenation of isobutane over supported V–Mo mixed oxides

GHEORGHIȚA MITRAN*, IOAN-CEZAR MARCU, ADRIANA URDĂ and IOAN SĂNDULESCU

Department of Technological Chemistry and Catalysis, Faculty of Chemistry, University of Bucharest, 4-12, Blv. Regina Elisabeta, 030018, Bucharest, Romania

(Received 4 December 2009)

Abstract: Vanadium–molybdenum oxides supported on Al_2O_3, CeO_2 and TiO_2 were prepared by a "wet" impregnation method, characterized using XRD, N_2 adsorption, UV–Vis spectroscopy, electrical conductivity measurements and tested in the oxidative dehydrogenation of isobutane. The catalytic performance in the oxidative dehydrogenation of isobutane at 400–550 °C depended on the nature of support and on the content of VMoO species on the support. The catalysts supported on alumina were more active and selective than those supported on ceria and titania.

Keywords: vanadia–molybdena catalysts; isobutene; oxidative dehydrogenation.

INTRODUCTION

Oxidative dehydrogenation of alkanes provides a thermodynamically accessible route to the synthesis of alkenes from alkanes.[1–9] Most catalysts for selective oxidations possess vanadium as a key element. Mixed-metal oxide catalysts are efficient for the oxidation alkanes to olefins, oxygenates and nitriles. Supported vanadium–molybdenum oxides catalyze the oxygenation of alkanes but unselective combustion pathways limit alkene selectivities.[5]

The advantages of supported metal oxides include higher mechanical strength, better thermal stability and larger surface area. However, the catalytic behavior of supported vanadium-molybdenum oxides is modified by the nature of the metal oxide support and the vanadium–molybdenum loading.

The local coordination and symmetry of Mo^{6+} and V^{5+} centers in bulk and supported catalysts have frequently been implicated in the observed effects of the support, as well as of the VO_x–MoO_x concentration and pretreatment procedures on catalytic behavior. Many of these structure–function relations remain incomp-

* Corresponding author. E-mails: mitran.gheorghita@unibuc.ro; geta_mitran@yahoo.com
doi: 10.2298/JSC091204099M

lete because of difficult structural characterization, undetected transport restrictions, and kinetic analyses, complicated by parallel and sequential combustion pathways.

The extent of dispersion and the local and extended structure of supported VO_x–MoO_x species depend on the chemical identity and the surface area of the support.[10,11] It was shown that basic metal oxides (*e.g.*, MgO and Bi_2O_3) as supports lead to supported VO_x–MoO_x species with higher alkene selectivities than when acidic oxides are used as the support.[8] Several authors have proposed that acidic VO_x–MoO_x species interact weakly with acidic supports, leading to poorly dispersed MoO_3 and V_2O_5 crystallites.

The structure of selective VO_x–MoO_x species and the reaction pathways in oxidative dehydrogenation of alkanes remain subjects of active discussion.

In this study, the effect of the support (Al_2O_3, TiO_2 and CeO_2) on the catalytic behavior of VO_x–MoO_x species in the oxidative dehydrogenation of isobutane was examined over two ranges of VO_x–MoO_x surface loadings. X-Ray diffraction, electrical conductivity measurements and UV–Visible spectroscopy were used to examine the structure and electronic properties of the catalysts.

EXPERIMENTAL

Catalysts preparation and characterization

The TiO_2 and CeO_2 supports were obtained from commercial sources. Al_2O_3 was prepared from $Al(NO_3)_3{\cdot}9H_2O$ by co-precipitation at a controlled pH. V_2O_5–MoO_3 was introduced at two concentration levels, 5 % and 10 %, *via* incipient wet impregnation of the supports with aqueous NH_4VO_3 and $(NH_4)_6MoO_{24}{\cdot}4H_2O$ solutions. The ratio between the V-containing and Mo-containing reactants was set so that the supported component had the composition 10 % V_2O_5–90 % MoO_3. After impregnation, the samples were dried in air at 100 °C and then calcined at 600 °C for 4 h.

Powder X-ray diffraction (XRD) patterns were obtained using a Bruker D5005 diffractometer and CuKα radiation. They were recorded with 0.02° (2θ) steps over 3–70° angular range with a 1s counting time per step.

The surface areas of the catalysts were measured from N_2 adsorption isotherms at 77 K by the BET method using an ASAP 2000 sorptometer.

Diffuse reflectance UV–Visible spectra were obtained using MgO as the reference on a Varian-Cary 4 spectrophotometer equipped with a Harrick diffuse-reflectance attachment. The reflectance data were converted to absorption spectra using Kubelka–Munk functions. The sample cell was equipped with a heater unit, a water-cooling system, a thermocouple and a gas flow system for *in situ* measurements.

The electrical conductivity of the different samples was investigated using a cell specially designed to study the electronic interactions between the samples and various gaseous atmospheres. A pastille of catalyst was placed between two platinum electrodes. The temperature of each electrode was given by a thermocouple the wires of which were also used as connections for the electrical measurements. Hence, semi-quantitative comparisons between solids could be made and the electrical conductivity measurements provided an estimate of the variations in the concentration of the main charge carriers as a function of physical para-

meters, such as temperature and the nature of the gas, under conditions as close as possible to those of the catalytic reaction.

Catalytic activity tests

The oxidative dehydrogenation of isobutane was realized in a fixed bed quartz tube down-flow reactor (i. d. 15 mm) operated at atmospheric pressure. Quartz chips were placed above and below the catalyst bed to reduce the reactor void volume and to avoid homogeneous reactions in the free space. The temperature of the catalyst bed was monitored by a thermocouple in a coaxial thermo-well in its center. The gas mixture consisting of isobutane and air was fed into the reactor at a volume hourly space velocity (*VHSV*) in the range of 1000–2500 h^{-1}. The reaction temperature was varied between 400 and 550 °C, the isobutane/O_2 molar ratio, between 0.5 and 2, while the catalyst bed volume was always kept to 2 cm^3.

In all studies, the reactor effluent was passed through a condenser to remove water and liquid oxygenated products. Gas-phase reactants and products were analyzed with a Thermo Finnigan gas chromatograph equipped with a flame ionization detector and a thermal conductivity detector. Chromatograph separation was accomplished with an alumina column and a CTRI column. The condensate was analyzed with a Thermo Finnigan chromatograph using a DB-5 column and a flame ionization detector. Isobutene, CO and CO_2 were the major products formed under the employed reaction conditions. Minor amounts of the liquid oxygenated products, acetic acid, methacrolein and unknowns, were detected. Conversion of isobutane and olefin selectivity is expressed as mol % on a carbon atom basis. The carbon balance was in all runs greater than 95 %.

RESULTS AND DISCUSSION

Catalysts characterization

The surface areas of the catalysts are given in Table I. The surface areas of the catalysts supported on Al_2O_3 were much higher than those of the catalysts supported on CeO_2 and TiO_2. It can also be observed that an increase of the support coverage led to a sharp drop in the surface area for the alumina-supported vanadia–molibdena catalysts. This was not the case for the ceria- and titania-supported catalysts.

TABLE I. V_2O_5–MoO_3 content, surface area and activation energy of conduction in air for the studied supported vanadium-molybdenum oxide catalysts

Support	Catalyst	V_2O_5–MoO_3 content mass %	BET Surface area m^2/g	Activation energy of conduction in air kJ mol^{-1}
Al_2O_3	5VMoO/Al_2O_3	5	298	–
	10VMoO/Al_2O_3	10	195	–
TiO_2	5VMoO/TiO_2	5	5.6	88.5
	10VMoO/TiO_2	10	6.5	73.3
CeO_2	5VMoO/CeO_2	5	3.3	62.8
	10VMoO/CeO_2	10	3.4	53.4

The X-ray diffraction measurements (Fig. 1) showed that the MoO_x–VO_x species were dispersed on the support but that they did not influence the

crystallinity of the rutile TiO_2 and ceria CeO_2 structure. Bulk V_2O_5 and MoO_3 crystallites were not detected at any MoO_x–VO_x loading on alumina and also not on titania- and ceria-supported samples with the lower MoO_x–VO_x loading. The higher loading on TiO_2 led to the appearance of orthorhombic Mo_4O_{11} crystallites and on Al_2O_3 led to the appearance of triclinic aluminum vanadium oxide – $AlVO_4$, tetragonal vanadyl molybdenum oxide – $VOMoO_4$, and monoclinic molybdenum vanadium oxide – $Mo_{0.67}V_{0.33}O_2$.

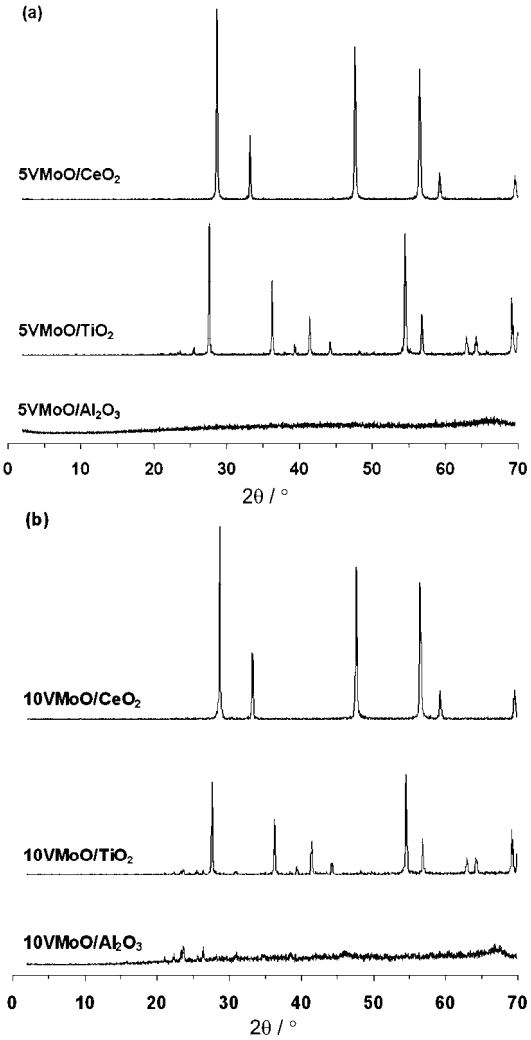

Fig. 1. X-Ray diffraction patterns for $VMoO/Al_2O_3$, $VMoO/TiO_2$ and $VMoO/CeO_2$; a) 5VMoO/support, b) 10VMoO/support.

The UV–Vis spectra of the catalysts are comparatively shown in Fig. 2. The absorption bands detected in the range 250–450 nm are mainly related to the presence of Mo^{6+} and V^{5+} in an octahedral environment.[12,13] The band observed at

340 nm is attributed to Mo6+ in octahedral coordination with tetragonal distortion. The spectrum shows a band at 350–400 nm, typical of charge transfer of V^{5+} species in octahedral symmetry.[14,15] This band, which is large and asymmetric, can be interpreted by charge transfer of O^{2-} to V^{5+} in the V=O bond or by the presence of polymeric chains of distorted VO_6 as a monolayer on the support. The 320–330 nm bands indicate a local interaction between molybdenum and vanadium. This is evidence for the high mobility of these species at the surface of the support.

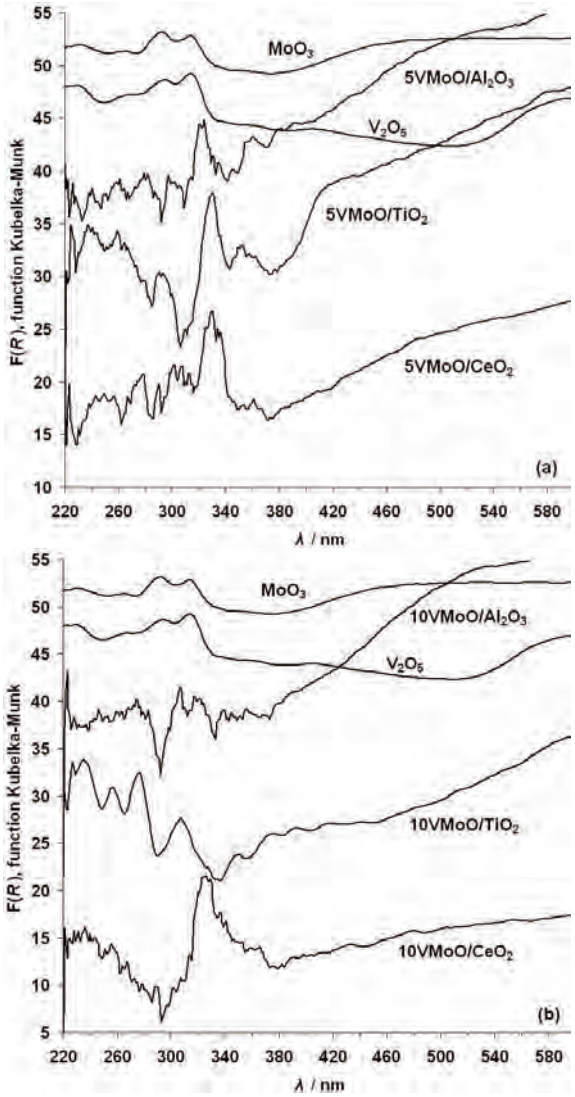

Fig. 2. UV–Visible spectra of the supported V–Mo–O catalysts;
a) 5VMoO/support,
b) 10VMoO/support.

The electrical conductivities of the titania and ceria-supported catalysts were measured as a function of temperature under air, nitrogen and isobutane at atmospheric pressure. Applying the Heckelsberg criterion,[16] the nature of the semiconductor type of a solid can be determined. To ensure the reversibility of the experiments, the measurements were performed with increasing and decreasing temperature. The obtained semi-log plots (log $\sigma = f(1/T)$) are given in Fig. 3.

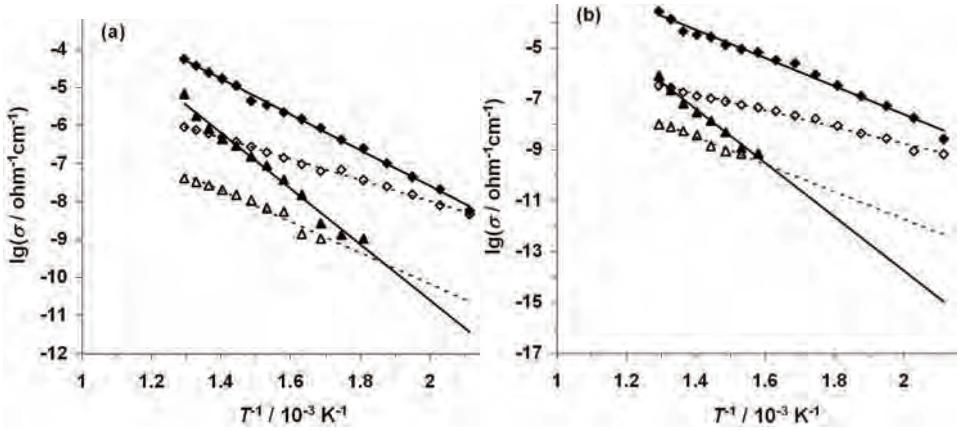

Fig. 3. Arrhenius plots of the electrical conductivity for the a) 5VMoO/support and b) 10VMoO/support catalyst; air (◊, Δ) and isobutane (♦,▲) ♦ – CeO_2, ▲ – TiO_2.

Variations in conductivity for mixed or for supported oxides are generally attributed to a doping effect.[17] This phenomenon results from the dissolution of heterovalent ions in the lattice of the host oxide, which creates free charge carriers (electrons or holes) according to the valence induction law. This dissolution is favored by calcination at high temperature of the support impregnated with the precursor of the deposited oxide. For *n*-type semiconductors, such as TiO_2 and CeO_2, an increase in σ results from the dissolution of a heterocation with a valence higher than 4. The deposition of MoO_x–VO_x species by impregnation and calcination is probably accompanied by a partial dissolution of V^{5+} and Mo^{6+} in the surface sub-layers of TiO_2 and CeO_2. The substitution of a Ti^{4+} by a V^{5+} or a Mo^{6+} induces free conduction electrons. If pentavalent V^{5+} or hexavalent Mo^{6+} are inserted into tetravalent sites, they can only share four valence electrons with four neighboring O^{2-}. The fifth and the sixth electron cannot be shared and are delocalized around the V^{5+} and the Mo^{6+} positive centers. Only a small amount of thermal energy is required for the delocalization of these electrons and their promotion into the conduction band.

For catalysts supported on CeO_2, the electrical conductivity is higher than for catalysts supported on TiO_2. As expected, the electrical conductivity of the catalytic materials increased with increasing amount of deposited VO_x–MoO_x. Since these materials are predominantly *n*-type semiconductors, the dependence

of the conductivity on the VO_x–MoO_x loading is attributed to an increase in the concentration of free electrons in the conduction band. On replacing air by isobutane, the total conductivity of the supported VO_x–MoO_x material increased. When the VO_x–MoO_x/TiO_2 and VO_x–MoO_x/CeO_2 materials were exposed to a reducing atmosphere, the electrical conductivity increased by several orders of magnitude, due to the reduction of the catalytic material and the formation of anion vacancies with two electrons (Eq. 1). These electrons can be readily promoted into the conduction band:

$$(O^{2-})^0 + \text{i-}C_4H_{10} \rightarrow \text{i-}C_4H_8 + H_2O + (V_O)^0 \quad (1)$$

where $(O^{2-})^0$ represents an oxygen anion of the solid. The zero-charge superscript indicates that it is a neutral entity with respect to the solid. $(V_O)^0$ represents a filled anionic vacancy with the two electrons of the former anion trapped.

Catalytic testing

The catalytic data obtained in the oxidative dehydrogenation of isobutane are presented in Table II. It can be observed that the alumina-supported catalysts were the most active, followed by the ceria- and titania-supported ones. Simultaneously, the isobutene selectivity decreased in the same order: V–Mo/Al_2O_3 > > V–Mo/CeO_2 > V–Mo/TiO_2. One likely advantage of using high surface area alumina is the possibility of a better dispersion of the active sites on the surface of the support. On the other hand, it seems that the acidic character of alumina did not negatively influence the catalytic behavior of the catalysts. The catalytic activity increased with increasing vanadia–molibdena loading for all supports, which was accompanied by a decrease of the isobutene selectivity. It should be emphasized that the catalytic activities of the supported oxides were higher than that of the respective unsupported oxide.[18]

In agreement with the redox mechanism of the oxidative dehydrogenation, a higher concentration of free electrons implies a higher rate of incorporation of gas-phase oxygen into lattice oxygen (the active oxygen species, which influences the rate of isobutane activation).

It should be noted that, for ceria- and titania-supported catalysts, the catalytic performances were better for the solids with a higher conductivity. 5VMoO/TiO_2 that exhibited the poorest catalytic properties is also the least conductive solid. Its activation energy of conduction (Table I), which is directly connected to the heat of formation of anionic vacancies, is the highest. This indicates that the endothermic reduction of 5VMoO/TiO_2 requires more energy.

The conversion of isobutane and the selectivity to isobutene for the supported MoO_x–VO_x catalysts as a function of the reaction temperature are shown in Fig. 4. The conversion of isobutane increased with increasing reaction temperature for all catalysts. The selectivity to isobutene passed through a maximum at temperatures between 450 and 500 °C.

In the UV–Vis spectra, the band corresponding to the Mo–V interaction (330 nm) had the smallest intensity for the 10VMoO/Al_2O_3 catalyst compared to the other supports. It can be also observed that the intensity of these bands decreased with increasing amount of active component. It is considered that the interaction between Mo and V is responsible for the catalytic activity since a correlation was observed between the intensity of these bands and the activity of the catalyst.

TABLE II. Catalytic performance of the supported vanadium–molybdenum oxide catalysts in the oxidative dehydrogenation of isobutane (*VHSV* = 1500 h^{-1}, molar ratio isobutane to O_2: 2:1)

Catalyst	*t* / °C	Conversion, %	Selectivity, %		
			i-C_4H_8	Cracking products	CO_x
5VMoO/Al_2O_3	450	15.0	73.5	8.5	18.0
	500	22.2	72.3	9.4	18.3
5VMoO/CeO_2	450	12.9	58.3	8.1	33.6
	500	17.3	59.9	9.8	20.3
5VMoO/TiO_2	450	10.7	48.0	4.2	47.8
	500	16.8	50.7	8.8	40.5
10VMoO/Al_2O_3	450	20.0	69.0	8.4	25.1
	500	25.5	70.5	7.8	19.2
10VMoO/CeO_2	450	15.2	53.7	7.6	38.7
	500	20.7	55.0	8.1	24.8
10VMoO/TiO_2	450	12.3	44.0	7.1	48,9
	500	18.5	48.1	11.3	40.6

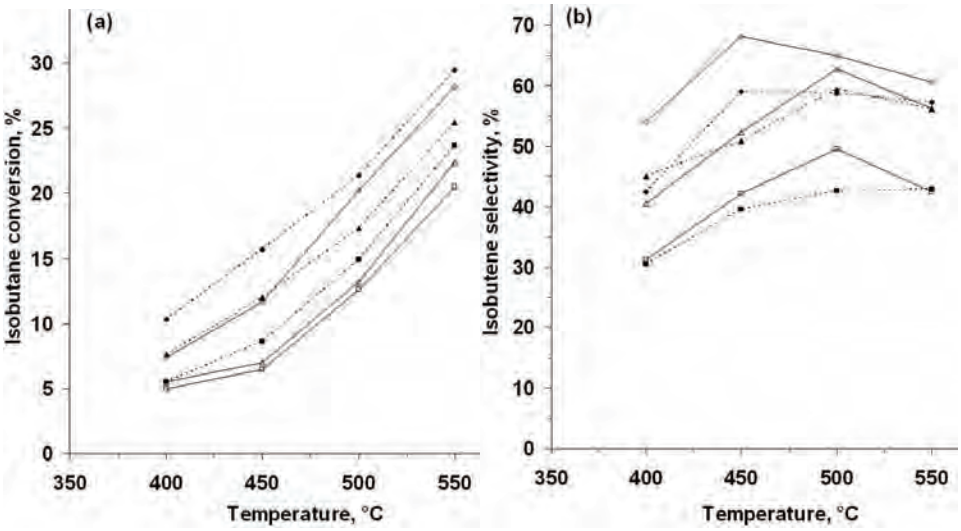

Fig. 4. Variation of the isobutane conversion (a) and isobutene selectivity (b) with the reaction temperature over supported V–Mo–O catalysts (*VHSV* = 2000 h^{-1}, *i*-C_4H_{10}:O_2 molar ratio: 1); ♦ – VMoO/Al_2O_3, ■ – VMoO/TiO_2, ▲ – VMoO/CeO_2 (—, 5 %; ····,10 %).

CONCLUSIONS

Promising catalytic results were obtained for the dehydrogenation of isobutane in presence of oxygen using Mo–V–O/supported catalysts. The use of alumina as the support with a high surface area led to an increase of both the catalytic activity and the selectivity to isobutene.

The electrical conductivity measurements clearly indicated that the ceria- and titania-supported systems are *n*-type semiconductors, and it was shown that the catalytic performances were better on catalysts with a higher conductivity.

Increasing the amount of active component led to a higher catalytic activity, but a diminished selectivity to isobutene.

ИЗВОД

ОКСИДАЦИОНА ДЕХИДРОГЕНИЗАЦИЈА ИЗОБУТАНА ПРЕКО V–Mo МЕШОВИТИХ ОКСИДА НАНЕТИХ НА ПОДЛОГУ

GHEORGHIŢA MITRAN, IOAN-CEZAR MARCU, ADRIANA URDĂ и IOAN SĂNDULESCU

Department of Technological Chemistry and Catalysis, Faculty of Chemistry, University of Bucharest, 4-12, Blv. Regina Elisabeta, 030018, Bucharest, Romania

Ванадијум–молибден оксиди нанети на подлоге од Al_2O_3, CeO_2 и TiO_2 мокрим поступком карактерисани су применом рентгенске дифракционе анализе, адсорпцијом азота, UV–Vis спектроскопијом, мерењем електричне проводљивости и тестирањем активности у реакцији оксидативне дехидрогенизације изобутана. Каталитичке особине особине оксидативне дехидрогенизације изобутана у температурном интервалу 400–550 °C зависе од природе носача и садржаја VMoO врста на носачу. Катализатори нанети на алуминијум-оксид су много активнији од катализатора који су нанети на титаноксид или церијум-оксид.

(Примљено 4. децембра 2009)

REFERENCES

1. P. Botella, J. M. López Nieto, B. Solsona, A. Mifsud, F. Márquez, *J. Catal.* **209** (2002) 445
2. P. Botella, J. M. López Nieto, A. Dejos, M. I. Vásquez, A. Martínez-Arias, *Catal. Today* **78** (2003) 507
3. H. Jiang, W. Lu, H. Wan, *J. Mol. Catal. A* **208** (2004) 213
4. K. Oshihara, T. Hisano, W. Ueda, *Top. Catal.* **15** (2001) 153
5. M. Banares, S. Khatib, *Catal. Today* **96** (2004) 251
6. Y. Takita, X. Qing, A. Takami, H. Nishiguchi, K. Nagaoka, *Appl. Catal. A* **296** (2005) 63
7. S. N. Koc, G. Gurdag, S. Geissler, M. Guraya, M. Orbay, M. Muhler, *J. Mol. Catal.* **225** (2005) 197
8. B. Solsona, A. Dejoz, T. Garcia, P. Concepción, J. M. Lopez Nieto, M. I. Vázquez, M. T. Navarro, *Catal. Today* **117** (2006) 228
9. T. V. Malleswara Rao, E. Vico-Ruiz, M. A. Bańares, G. Deoa, *J. Catal.* **258** (2008) 324
10. S. Albonetti, F. Cavani, F. Trifiro, *Catal. Rev. Sci. Eng.* **38** (1996) 413
11. G. Centi, *Appl. Catal. A* **147** (1996) 267
12. H. Aritani, T. Tanaka, T. Funabiki, S. Yoshida, K. Eda, N. Sotani, M. Kudo, S. Hasegawa, *J. Phys. Chem.* **100** (1996) 19495

13. E. García-Gonzáles, J. M. López Nieto, P. Botella, J. M. González-Calbet, *Chem. Mater*. **14** (2002) 4416
14. G. Centi, S. Perathoner, F. Trifirò,, A. Aboukais, C. F. Aisi, M. Guelton, *J. Phys. Chem*. **96** (1992) 2617
15. M. Scraml-Marth, A. Wokaun, A. Baiker, *J. Catal*. **124** (1990) 86
16. L. F. Heckelsberg, A. Clark, G. C. Bailey, *J. Phys. Chem*. **60** (1956) 559
17. J. M. Herrmann, J. Disdier, G. Deo, I. Wachs, *J. Chem. Soc. Faraday Trans*. **93** (1997) 1655
18. G. Mitran, I. C. Marcu, A. Urda, I. Sandulescu, *Revue Roumaine de Chimie* **53** (2008) 383.

Journal of the Serbian Chemical Society
JSCS-info@shd.org.rs • www.shd.org.rs/JSCS
J. Serb. Chem. Soc. 75 (8) 1125–1148 (2010)
JSCS–4037
UDC 504.45+502.37(282.243.7)(497.11)
Original scientific paper

Long-term changes in the eco-chemical status of the Danube River in the region of Serbia

IVAN ŽIVADINOVIĆ[1], KONSTANTIN ILIJEVIĆ[2#], IVAN GRŽETIĆ[2*#] and ALEKSANDAR POPOVIĆ[2#]

[1]*Srbijavode, Bulevar umetnosti 2, 11070 Belgrade and* [2]*Faculty of Chemistry, University of Belgrade, Studentski trg 12–16, 11000 Belgrade, Serbia*

(Received 2 November, revised 8 December 2009)

Abstract: The Danube River is an international river, one part of which flows through Serbia. The eco-chemical status of the Danube River is a constant topic of interest both at the local level, in each country through which the Danube flows, and at the international level. General interest to ensure the sustainable and equitable use of waters and freshwater resources in the Danube River Basin led to the development of a system for monitoring the river, which has produced data sets of its eco-chemical status. These have been collected over many years in Serbia; however, the present interest was focused only on the period from 1992 until 2006, *i.e.*, a 15-year period. The process of defining trends of selected eco-chemical parameters, using linear regression analysis with a defined level of significance, and their separation from natural variability is of the highest importance for defining the changes in the water parameters. Through them, the fate and behavior of the eco-chemical parameters of the Danube in Serbia can be recognized and the prediction of their trends in the near future can be attempted. The obtained results revealed a constant improvement and acceptable trends of the eco-chemical status of the Danube River, as well as, substantial differences in the quality of the inflowing and out flowing water.

Keywords: Danube River; long-term spatial and temporal trends; self-purification; linear regression.

INTRODUCTION

The Danube River is 2783 km long and has a basin of 817000 km^2. Around 10 % of its length belongs to the territory of Serbia, through which the Danube runs 587.4 km. It enters into Serbia from the north, from Hungary (1425.5 km away from the sea), and outflows to the east, right on the border between Serbia,

* Corresponding author. E-mail: grzetic@chem.bg.ac.rs
# Serbian Chemical Society member.
doi: 10.2298/JSC091102075Z

Romania and Bulgaria (825 km away from the sea). The Serbian part of Danube belongs to the middle section of the river, from the Devín Gate (at the border of Slovakia and Austria) to the Iron Gate (at the border of Serbia and Romania), where the riverbed widens and the average bottom gradient is 0.6×10^{-4} %.[1] The average water volume of the Danube on entering Serbia is 2400 m^3 s^{-1} and 5500 m^3 s^{-1} on leaving the country.[1]

The Serbian Danube can be divided into an upper and a lower section (Fig. 1). The upper section, covering the stretch from the Hungarian border to Belgrade, belongs to the Pannonian Basin. The lower section, from Belgrade to the Bulgarian border, is strongly influenced by the Iron Gates I and II dam complex (943 km and 863.4 km, respectively), which are located in the border area of Romania and Serbia. The dams cause slowdown of the flow velocity which can be observed at the confluence of the Nera River (Romania) or at the end of Danube––Tisza–Danube (DTD) canal near Banatska Palanka (Serbia) during high water level. During low water level, the slowdown of flow velocity becomes observable at the village Surduk (Serbia) 37 km upstream of Belgrade, but the confluences of the big Danube tributaries (Tisza, Tamis, Sava and Velika Morava) can also be affected.[2]

The biggest Danube tributaries with confluences in the territory of Serbia are the Tisza, the Tamiš and the DTD canal on the left side, and Drava, Sava and Velika Morava on the right side.

Two large cities, Belgrade (1.7 million inhabitants) and Novi Sad (300,000 inhabitants) lie on the Danube River, as well as many smaller towns (Apatin, Bačka Palanka, Pančevo, Smederevo, Donji Milanovac and Kladovo) and villages (small settlements with less than 10,000 inhabitants contribute 48 % to the Serbian population). None of them have a system for treating municipal waste waters.[3]

The eco-chemical status of the Danube River is a topic of constant interest both on the local level, in each country thought which the Danube flows, and on the international level through organizations such as the International Commission for the Protection of the Danube River (ICPDR).[1] Their main interest is to ensure sustainable and equitable use of the waters and freshwater resources in the Danube River Basin. Protection of the River is strongly supported by data of its eco-chemical status that have been collected over many years in Serbia. After validation of the available records, it was decided to process data sets for the period from 1992 until 2006 (a period of 15 years).

There is a range of factors that can influence the eco-chemical dynamics of a river. They are useful only over a range of time scales; therefore eco-chemical dynamics may only be fully investigated when long-term time-series data are available.

The goal of this work was to investigate long-term changes of the eco-chemical status of the Danube River in relation to pollution changes during previous

years and to identify seasonal fluctuations, averaged during the investigation period, which could reveal some regularities of the Danube pollution over time. Particular attention was paid to determine the average trends over time with the aim to forecast the behavior of pollutants under different conditions or in the near future.

The Danube River is constantly the focus of various environmental studies. The most considered topics were pollution with: metals in the water[4–7] and sediments, [8–11] nutrients,[12–17] radioisotopes,[18–20] oil,[21] *etc*. There are many studies dealing with the general pollution status of the river, hence covering more than one group of pollutants[22–25] and also from a regulatory point of view.[26]

EXPERIMENTAL

Materials and methods

The main sampling material for the measurement was the river water sampled and analyzed according to APHA (1976–1992)[27] and US EPA standard methods (1983).[28] The measured parameters (the corresponding methods are given in brackets) important for the determination of the eco-chemical status of the Danube River were:

– suspended matter (13.060.30 JUS H.Z1. 160);[29]
– nitrates (NO_3-N) (APHA AWWA WEF 4500-NO3);[30]
– total nitrogen (N) (JUS ISO 5663);[31]
– total phosphorus (P) (APHA AWWA WEF 4500-P);[32]
– Biological oxygen demand for 5 days (BOD-5) (EPA 360.2);[33]
– Chemical oxygen demand (COD) (JUS ISO 8467, ISO 8467).[34]

Analysis of blanks and duplicates were the main instruments of quality assurance/quality control (QA/QC) during measurement throughout the years.

Regular monthly measurements were performed every year for a period of 15 years (1992–2006).

Surface water samples were taken as they were assumed representative for the entire water stream, while the water was always well mixed. Sampling was performed 40 cm below the water surface from the water-front area, in order to prevent contamination of the sample with mud from the bottom or floating particles from the water surface. The samples were collected in 5-L plastic jerry cans.

The temperatures and pH of the water samples were determined on site. Samples for the determination of dissolved oxygen concentrations were collected and treated separately. All samples were stored at 4 °C and normally analyzed within one day. The maximum storage time was less than 2 days after sampling.

Sampling locations

Seventeen sampling stations are located on the Serbian part of the Danube River (Fig. 1), of which four were excluded from consideration because the data they provided was insufficient for the present investigations, due to a too short an operation time (just a few years). Data from remaining stations were analyzed for the selected period, although some parameters were not monitored for all the years and during every month. In other cases, sampling was performed one to two times per month.

List of the sampling stations:

1. Bezdan – Hungarian border (inflow of the Danube River into Serbia),

2. Apatin – downstream from the town,
3. Bogojevo (excluded from the considerations),
4. Bačka Palanka (excluded from the considerations),
5. Novi Sad – before the confluence of the DTD canal,
6. Slankamen – upstream from the confluence of the Tisza River,
7. Čenta (excluded from the considerations),
8. Zemun – before the confluence of the Sava River,
9. Pančevo – downstream from Visnjica, at the confluence of the Tamiš River,
10. Vinča (excluded from the considerations),
11. Smederevo – above the steel factory, before the confluence of the Grand Morava River,
12. Banatska Palanka – at the confluence of the Vršac canal, upstream from the confluence of the Nera River
13. Veliko Gradište – at the water meter,
14. Dobra – in the town,
15. Tekija – in the town, before the Iron Gate I dam,
16. Brza Palanka – at the water meter, between the Iron Gate I and II dams and
17. Radujevac – after the Iron Gate II dam (outflow of the Danube River from Serbia).

Fig. 1. Location of the sampling stations on the Serbian part of the Danube River.

RESULTS

The process of defining trends and their extrication from natural variability is of highest importance for defining how environmental parameters change and thereby recognizing the fate and behavior of the environment in the near future.

Regression analysis was employed for determining whether a trend over time was, on average, linear. Based upon these results, it was possible to describe the direction of a trend (a negative or positive slope), while the quality of linear regression lines of the trend could be described by the Pearson's coefficient of determination (R^2). This is useful because it gives the proportion of the variance of one variable that is predictable from the others.[35,36]

Selected parameters for the present investigations were, in principle, sum/ /collective parameters which covered several inorganic or organic species. These sum/collective parameters were divided into four groups:

1. Suspended matter and dissolved species (dry matter, residue after ignition and conductivity). These parameters describe, in general, how much the river water is burdened with inorganic and organic matter together, while the conductivity describes the amount of ionic species present in the water;
2. UV Absorption at 254 nm, COD and BOD. These parameters generally cover dissolved organic matter and the biological activity in the river water;
3. Oxygen concentration and oxygen saturation. The oxygen parameters are essential to all aquatic life, which maintains a healthy river water environment;
4. The pH, total P, total N, NO_3, and N/P ratio. Nutrients, such as nitrogen and phosphorus, occur naturally in water but very often they are the main causes of pollution of rivers when their concentration levels are elevated.

In addition to these group parameters, there are numerous single parameters that were, however, not the subject of this work since each of them could be a separate topic of investigation.

The eco-chemical status of the Danube River, as an international river, is best described through discussions of the available results from two different aspects:

– trends of the measured parameters during time – investigation of long term changes for the 1992–2006 period and

– trends of the measured parameters in space – investigation of long term changes from place to place from the inflow to outflow points in Serbia.

Trends of the measured parameters in time and in space

Numerous studies in which the spatial and temporal trends of the water quality parameters of the Danube River were analyzed, have been performed in recent years,[13,37] many of them with the goal of predicting their values in future,[38,39] or improving the theoretical models for their understanding.[40–42]

However, the present study is specific as it deals with the largest quantity of data covering the broadest range of water quality parameters for the Danube that has ever been accumulated. It applies median values for data reduction instead of arithmetic or geometric means, which enables the use well-known parametric tests

for trend detection. Therefore, one more aspect of investigations of the Danube River is herewith revealed.

The source data sets each contain hundreds of measurements and some of them have non-normal distributions, therefore median, minimum and maximum values are the only remaining statistical parameters that give meaningful averaged data appropriate for the present investigation. Hence, each number used in this work corresponds to a yearly median value. Medians were assumed to be sufficient and very useful for the purposes of this study as they are values that do not reflect individual outliers which are sometimes present in large data sets.[35,36]

To estimate the quality of the regression/fitness of the curves, the square of the Pearson's correlation coefficient, R^2, was used. However, the value of R^2 gives no information as to whether a correlation is significant or not. Thus, for this purpose, a parametric method for calculating t values was used. The t value was calculated using the formula:

$$t = \frac{R\sqrt{n-2}}{\sqrt{1-R^2}} \tag{1}$$

where R is the correlation coefficient and n is number of observations.

The t value was calculated using a two-sided t-test and then compared with the tabulated value[43] at the desired level of significance and (n–2) degrees of freedom. The null hypothesis that there is no significant correlation between the x and y coordinates in the charts (and therefore no significant trend) was rejected if the calculated t value was greater than the tabulated value at the desired significance level. A 95 % significance level ($\alpha = 0.05$) was used. The coefficients R, and therefore t, are influenced by the slope of the regression line and by the size of the residuals, because the more the points are scattered from the regression line, the worse the correlation coefficient is.[35,37,44]

Long term changes in the Danube River parameters were recognized in time and space. These changes can be well-presented in 3D (3 dimensions) surface charts with continuous curves, which are very convenient for quick visual estimation of trends, in addition to statistical analysis. The horizontal x and y axes present time (years from 1992 until 2006) and space (sampling locations from Bezdan to Radujevac). The vertical z axis shows the yearly median values.

To determine whether there was a temporal trend, the change between median yearly values at each single location was observed for the period from 1992 until 2006.

To determine whether there was a spatial trend, the change of median yearly values between sampling locations was observed for every year from 1992 until 2006.

First group of parameters (Fig. 2)

Suspended matter (Fig. 2a). Temporal trends for change of median yearly values between 1992 and 2006 observed for each sampling station (from Bezdan to Radujevac) had positive slope for 8 locations and negative ones for 5; the average slope was positive but significant trends were observed only at Slankamen, Radujevac (negative trends) and Smederevo (positive trend). Therefore, no clear tendency for changes in the amount of suspended matter over the years could be estimated.

Spatial trends for the change of median yearly values between sampling locations observed for each year from 1992 until 2006 had negative slope for every year and all of them were statistically significant, except for years 1993 and 2005 (which also had negative slope but their *t*-value vas less than the critical value). A decreasing tendency of the amount of suspended matter from Bezdan toward Radujevac was evident.

Dry matter (Fig. 2b). The temporal trends for the change of the median yearly values for the period from year 1992 until 2004 observed for each sampling station (from Bezdan to Radujevac) had positive slopes for only 2 locations (but not statistically significant) and negative for 11. The average slope was negative, but statistically significant negative trends were observed only for 2 locations (Smederevo and Dobra), and 2 more had *t*-values close to the critical value. On the other hand, 11 of 13 locations showed negative trends which statistically had a very low probability ($P < 0.05$); therefore, a negative trend for dry matter over the years was observed.

The dry matter concentrations are well correlated with conductivity and ignition residual. The correlation coefficients for dry matter/ conductivity correlation were positive for all 13 sampling locations and statistically significant for 5 of them (average $R = 0.42$) and for dry matter/ignited residual correlation, the coefficients were positive at 11 and statistically significant at 6 sampling locations (average $R = 0.37$). It is interesting that the dry matter and ignition residual were much better correlated at the first 5 sampling locations (from Bezdan to Zemun with the average R being 0.76) than at other sampling locations downstream from Zemun.

The spatial trends for the change of median yearly values from place to place observed for each year from 1992 until 2004 (without 1993) had negative values in 10 years out of 12; the average slope was also negative. The slope was significant for 4 negative trends (years 1994, 2002, 2003 and 2004) while two positive slopes (for years 1992 and 2000) had *t*-values less then critical. It can be concluded that the dry matter content decreases from Bezdan toward Radujevac.

Conductivity (Fig. 2c). The temporal trends for the change of median yearly values for the period 1992 until 2006 were observed for each sampling station (from Bezdan to Radujevac). The slope was negative for 12 locations

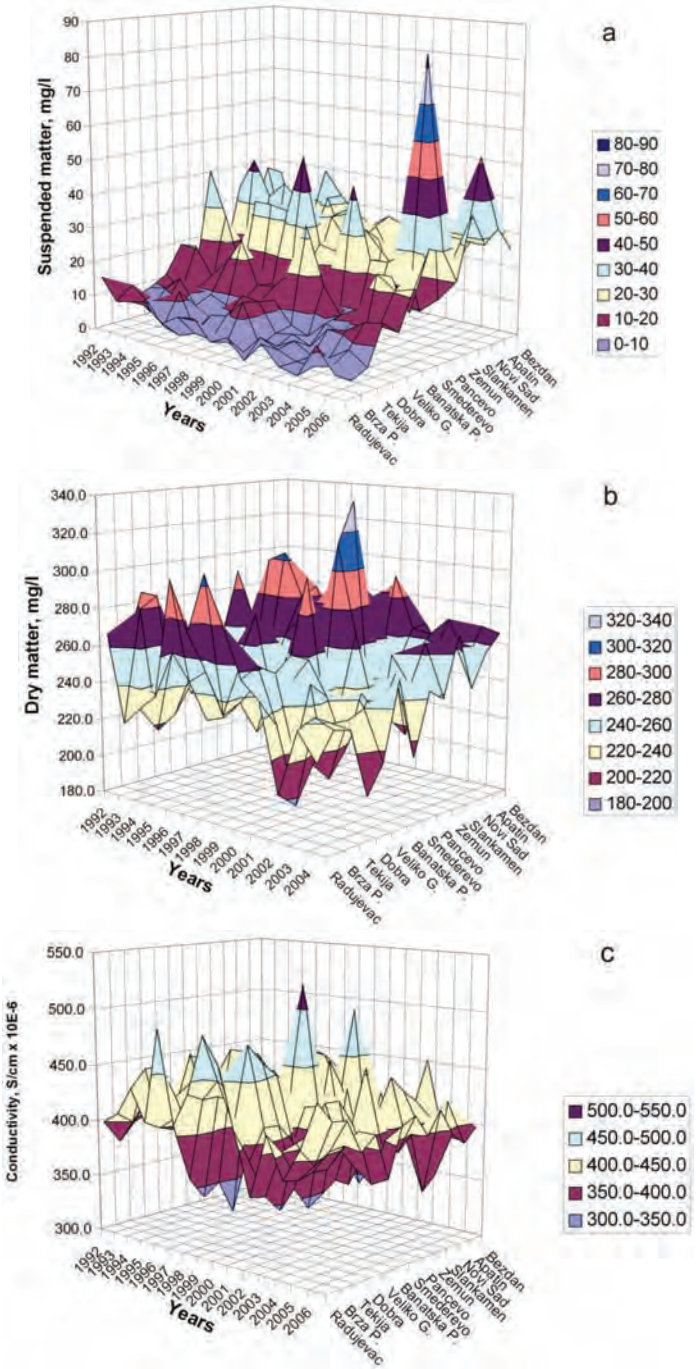

Fig. 2. Temporal and spatial trends of the amount of a) suspended matter, b) dry matter and c) conductivity.

and positive just for one; the average slope was negative but a significant trend was observed only at Zemun. Although a statistically significant negative trend was observed at only one place, a decreasing trend through the years was evident, based on the fact that the slope was negative at 12 out of 13 locations, which is statistically highly unexpected.

The spatial trends for the change of the median yearly values from place to place observed for each year from 1992 until 2006 had negative slopes for 6 years (3 of them statistically significant, 1997, 2002, 2003) and positive slopes for 9 years (4 of them statistically significant 1994, 1998, 2000, 2006). The average slope was slightly positive, but based on an even distribution of statistically significant trends, an unambiguous conclusion about increasing or decreasing of conductivity from Bezdan to Radujevac cannot be drawn.

Generally speaking, suspended mater, dry mater and conductivity are very much dependant on hydrological conditions, such as flow rate and water level, or current seasonal conditions, such as rainy or dry periods.[45] The decrease in the flow rate that is present in the Danube River in Serbia, particularly in the region of the artificial lake before Iron Gate,[8,46] favors a tendency of decreasing suspended matter in the river water from Bezdan toward Radujevac.

Second group of parameters

The surrogate parameters characteristic for organic matter, COD, BOD and UV absorption at 254 nm, are very well correlated. COD and BOD showed negative trends with time (from 1992 until 2006) and in space (from Bezdan to Radujevac) (Fig. 3). The absorbance at 254 nm has long been an acknowledged parameter for the description of organic carbon compounds (aromatics, phenolics, hydrocarbons, and most chromophores) in water analysis (DIN38404). However, the choice of this wavelength was made, above all, for historical rather than analytical reasons. In most cases, organic matter generates the strongest signal at other wavelengths.

As for the first group, the second group of parameters was also investigated through time and space. The same principles for trend analysis were applied.

COD. The temporal trends for the change of median yearly values for the period from 1992 until 2006 observed for all sampling stations (from Bezdan to Radujevac) had negative slope for 12 out of 13 locations; the average slope was also negative and statistically significant trends were observed at Bezdan, Slankamen and Banatska Palanka. Only one positive (and simultaneously statistically significant) trend was observed at the Zemun sampling location. Therefore, it can be concluded that the summary trend for COD decreased over the years.

The COD values were well correlated with the BOD-5 values. The correlation coefficients for the COD/BOD-5 correlation were positive for 12 of the 13 sampling locations and statistically significant for 4 of them (average $R = 0.39$).

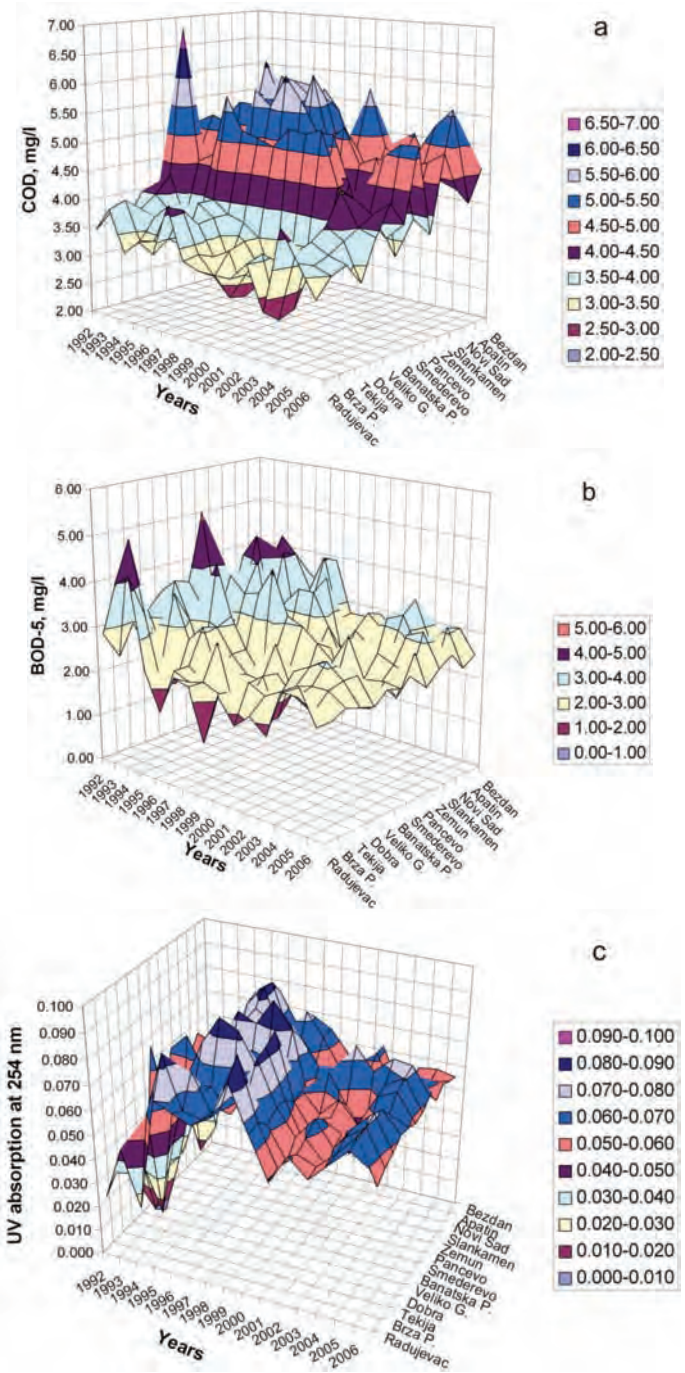

Fig. 3. Temporal and spatial trends of the a) COD values, b) BOD-5 values and c) UV absorption.

The spatial trends for the change of the median yearly values from location to location observed for each year from 1992 until 2006 had negative slopes for every year and all of them were significant, except for the years 1993 and 2004 (which also had a negative slope but their *t* value vas smaller than the critical value). A decreasing tendency of COD from Bezdan toward Radujevac was evident.

BOD-5. The temporal trends for the change of the median yearly values for the period from 1992 until 2006 observed for each sampling station (from Bezdan to Radujevac) had negative slopes for 12 out of 13 locations; the average slope was also negative and statistically significant trends were observed at Bezdan, Apatin, Slankamen Pancevo, Banatska Palanka and Veliko Gradište. The only positive (but not statistically significant) trend was observed at Tekija sampling location. Therefore, it can be concluded that the BOD-5 value decreased through the investigated years.

The spatial trends for the change of the median yearly values from location to location observed for every year from 1992 until 2006 had negative slopes for all year (except in 1993 which was not statistically significant). Four years (1995, 1997, 1999 and 2000) were statistically significant while for another four years (1992, 1996, 2001 and 2003), the *t* values were close to the critical level. A decreasing tendency of BOD-5 from Bezdan toward Radujevac was evident, but a change of the rate of decrease was observed and it became less negative from 1995 to 2006. If the slope coefficients are plotted against time, a regression line with a positive slope was obtained, with an R^2 value of 0.706, a *t* value of 4.897 and a *P* value of 0.000625, indicating that soon after 2006 there will be no further decrease of the BOD-5 value in the Serbian part of the Danube.

UV Absorption at 254 nm. The temporal trends for the change of the median yearly values for the period 1992 until 2006 observed for every sampling station (from Bezdan to Radujevac) were evenly distributed (6 negative and 7 positive). The negative slopes possessed no statistical significance and among the positive slopes, 4 were statistically significant (Zemun, Smederevo, Veliko Gradište, Dobra). The average slope was also positive but, nevertheless, it cannot be unambiguously stated that the UV absorption increased over the years. However, it is interesting that at first 4 (of the 13 in total) sampling locations (Bezdan to Slankamen), the regression slopes were all negative and at last five sampling locations (Veliko Gradište. to Radujevac), the regression slopes were all positive. After closer data inspection, it was noticed that the UV absorption rapidly increased until 1995 or 1996, after which it slowly decreased or stagnated. The rate of decrease after 1996 was larger in upper than in lower section of the River, resulting in negative overall temporal trends in the upper and positive overall temporal trends in the lower section.

The UV absorbance values are well correlated with the pH values. The correlation coefficients for the UV absorption/pH correlation were positive for 10 out of the 13 sampling locations and statistically significant for 5 of them (average $R = 0.32$).

Spatial trends for change of median yearly values from place to place observed for each year from 1992 until 2006 had negative slope for first 7 years (1992–1998) and 3 of them were statistically significant (1992, 1994 and 1996). In 1999 and afterwards, the regression slope became positive (except in 2001 and 2002) but it was statistically significant only for the years 1999, 2000 and 2005. Therefore, an increasing or decreasing tendency of UV absorption from Bezdan toward Radujevac cannot be declared.

Third group parameters

Oxygen parameters are quite significant. They are very well correlated, they show practically negative trends in time (from 1992 until 2006) and in space (from Bezdan to Radujevac) but they are statistically insignificant (Fig. 4).

Dissolved oxygen. The temporal trends for the change of the median yearly values for 1992 until 2006 was observed for every sampling station (from Bezdan to Radujevac) and they had negative slopes for 11 out of the 13 locations; the average slope was also negative but a statistically significant trend was observed only at Banatska Palanka. Positive, but statistically insignificant, trends, were observed only at the Pancevo and Smederevo sampling locations. A decreasing trend through the years can be postulated based on the fact that the slope was negative at 11 out of 13 locations, which statistically would have a very low probability.

A negative correlation was observed between the amount of dissolved oxygen and temperature at 11 out of 13 locations (3 out of the 11 were statistically significant) with an average R value of –0.32. Oxygen saturation was positively correlated with dissolved oxygen at all 13 locations (7 of them with statistical significance). The average R value was 0.59.

The spatial trends for the change of the median yearly values from location to location observed for each year from 1992 until 2006 had a negative slope for every year (except in 1998 which was not statistically significant). Three of them (2002, 2003 and 2006) were statistically significant. The average slope was also negative. Therefore it can be inferred that dissolved oxygen decreased from Bezdan toward Radujevac.

Oxygen saturation. The temporal trends for the change of the median yearly values for the period from 1992 until 2006 observed for all sampling stations (from Bezdan to Radujevac) varied between 6 negative and 7 positive values none of them statistically significant. The average slope was slightly negative. No trend through the years could be identified.

The spatial trends for the change of the median yearly values from location to location observed for all years from 1992 until 2006 were equally distributed among positive and negative values. The average slope was only slightly negative and there was only one statistically significant trend (negative in 2005). No decrease in the oxygen saturation from Bezdan toward Radujevac could be proven.

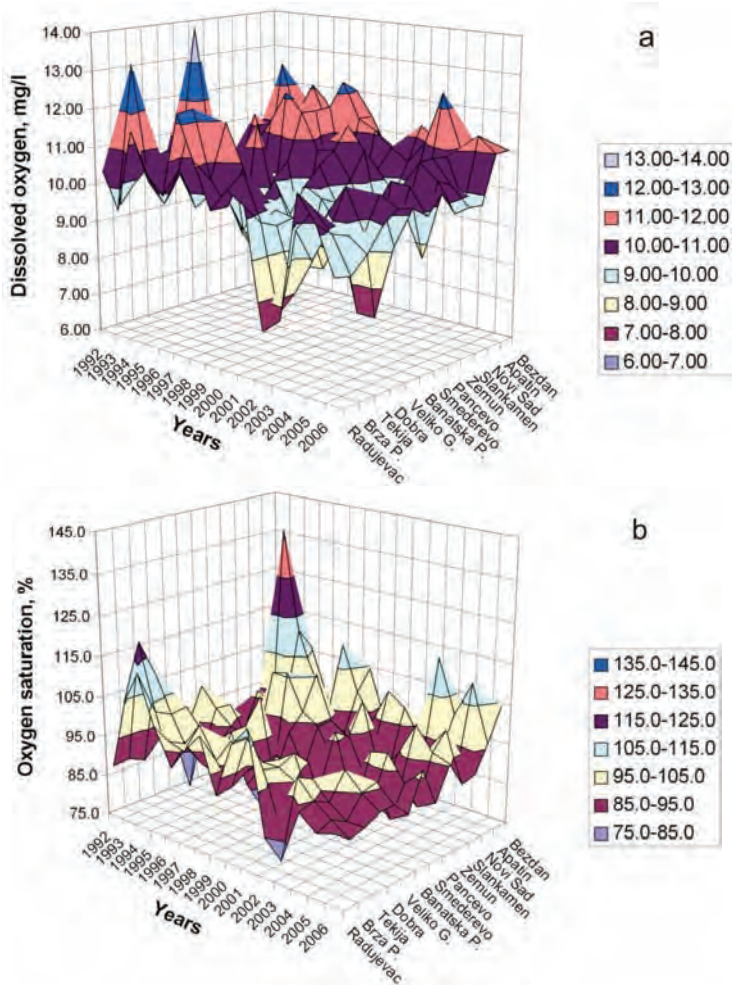

Fig. 4. Temporal and spatial trends of a) the amount of dissolved oxygen and b) the oxygen saturation values.

Fourth group of parameters

Among these parameters (Fig. 5), the pH value is a special parameter. Levels of pH greater than 8.5 usually indicate the presence of algal blooms because intense photosynthesis by algae removes CO_2 from the water, which increases

the pH value. Increased algal activities are closely related to the nutrient content (N and P) and oxygen saturation. The greater is the content of nutrients, the greater is the algal activity and, consequently, the production of oxygen increases resulting in increased oxygen saturation.

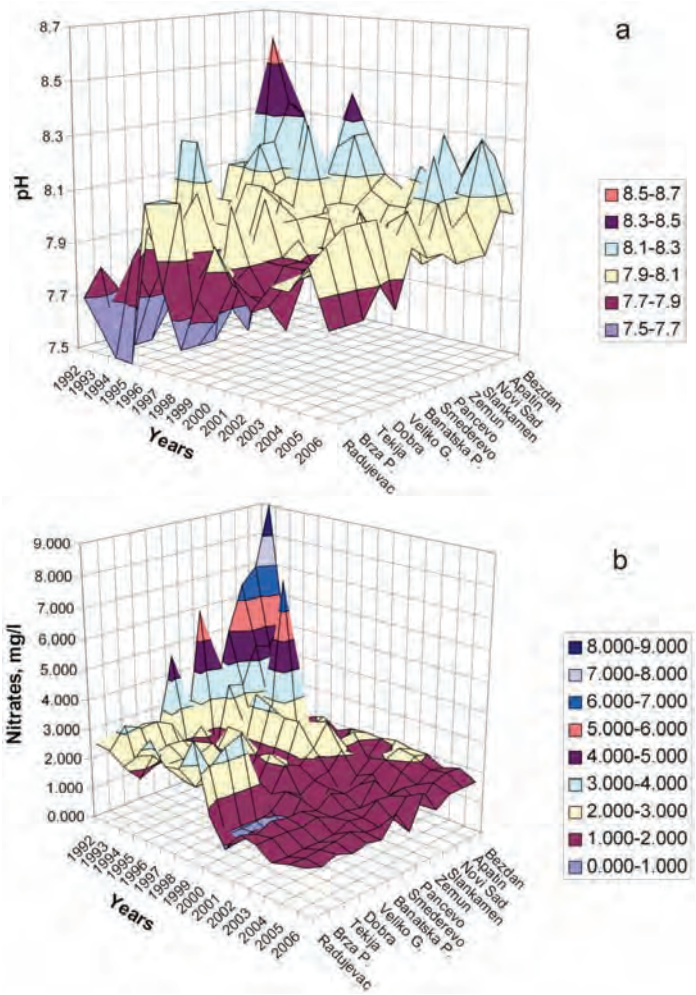

Fig. 5. Temporal and spatial trends of a) the pH values and b) concentration of nitrates.

pH Value. The temporal trends for the change of the median yearly values for the period from 1992 until 2006, observed for all sampling station (from Bezdan to Radujevac) had a negative slope for 6 out of 13 locations, while the other 7 were positive. Among the 4 statistically significant slopes, one was negative and other 3 were positive. The average slope was slightly positive. Interesting, before Smederevo, almost all the slopes were negative and thereafter positive.

The spatial trends for the change of the median yearly values from location to location observed from 1992 until 2006 had negative slope for every year and 9 of the 15 were statistically significant. A tendency of decreasing pH value from Bezdan toward Radujevac is evident.

Concentration of nitrates. The temporal trends for the change of the median yearly values for the period 1992 until 2006 observed at all sampling station (from Bezdan to Radujevac) had negative slopes, and 8 of them were statistically significant. Therefore, it can be concluded that the concentration of nitrates decreased over the years.

A slight negative correlation was established between the nitrate concentrations and the pH values at 10 of 13 locations, with an average R value of –0.17. The nitrate concentrations were positively correlated with the total P concentrations at all 13 locations (8 of them with statistical significance). The average R value was 0.65.

The spatial trends for the change of the median yearly values from location to location observed for every year from 1992 until 2006 had negative slopes for 9 years (6 had statistically significant slopes) while for the other 5, the trends were positive but only one was statistically significant. The average slope was negative; hence, a decreasing tendency of the nitrate concentration from Bezdan toward Radujevac was evident.

In general, the total P and total N showed negative trends in time (from 1992 until 2006) and in space (from Bezdan to Radujevac) (Fig. 6). Nutrients are usually the limiting factors in algal growth.

Concentration of total P. The temporal trends for the change of the median yearly values for period 1992 until 2006 observed for every sampling station (from Bezdan to Radujevac) had negative slopes for all locations, 2 of them (Bezdan, Slankamen) were statistically significant, but another four had t values close to critical value. Therefore, it can be concluded that the total P decreased over the years.

The spatial trends for the change of the median yearly values from location to location observed every year from 1992 until 2006 had negative slopes for 14 out of the 15 years (8 were statistically significant), and just one was positive but not statistically significant. The average slope was negative. Hence, total P concentration showed a decreasing tendency from Bezdan toward Radujevac.

Concentration of total N. Unfortunately, the data for the assessment of trend in the total N concentration was insufficient due to a lack of measurements prior to 2002 (with exception of the year 1995 for some sampling locations). For this reason, it is very hard to detect statistically significant trends within the small data sets because they have very high critical t values for comparison with test statistics. These limited data, however, indicated that the concentration of total N decreased over the years, which is consistent with the negative trend of nitrate concentrations (nitrates participate to a significant extent to the total N load).

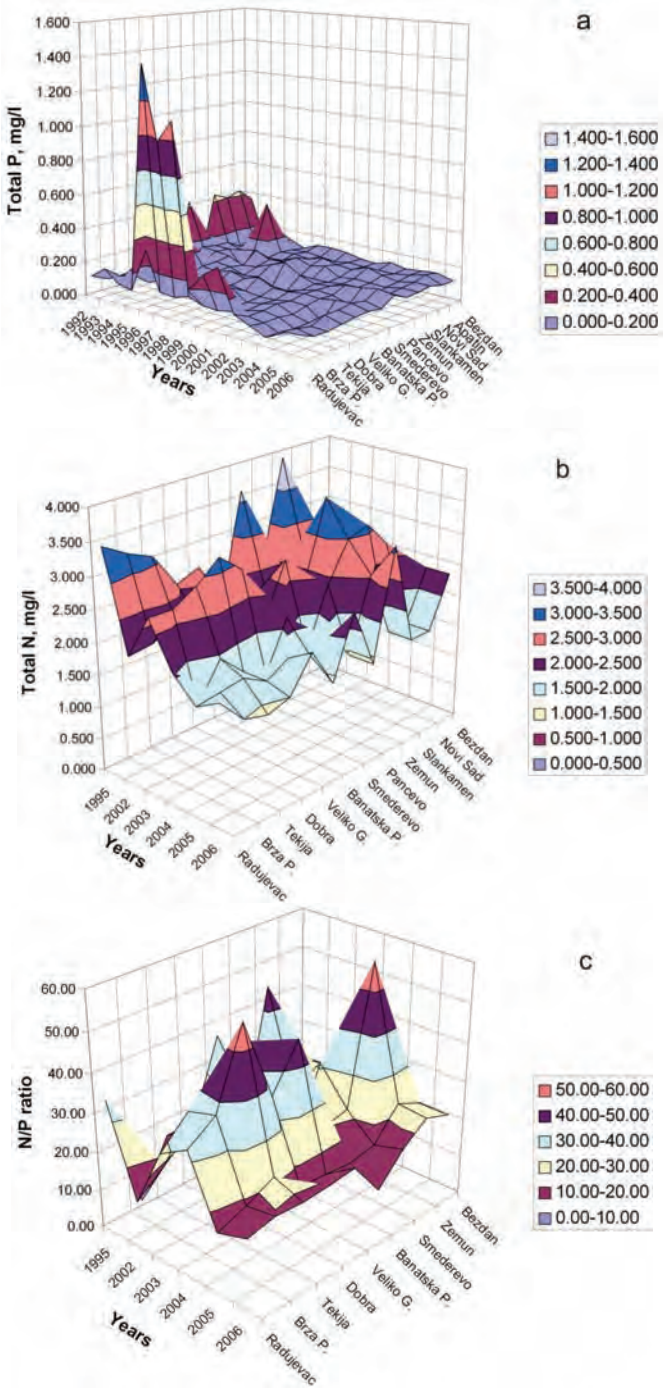

Fig. 6. Temporal and spatial trends of the amount of a) total P, b) total N and c) the N/P ratio.

The total N concentration correlated very well with the nitrate concentrations. The correlation with the pH values was similar to the correlation with the nitrate concentrations and exhibited a negative average value.

If the change in the total N concentration is followed downstream from Zemun to Radujevac (with exception of Bezdan, there is not sufficient data for the sampling locations before Zemun), a few statistically significant negative trends can be observed (in years 2002 and 2004). The average trend was also negative but the limited monitoring time of the trend prevents a serious conclusion to be derived, although indications of a decrease in the total N concentrations from Bezdan toward Radujevac do exist.

Total nitrogen to total phosphorus ratio (TN/TP). The TN/TP ratio is used to compare the availability of these nutrients. Ratios smaller than 10 indicate that nitrogen is limiting. Ratios greater than 16 indicate that phosphorus is limiting,[47] whereas ratios greater than 10 but smaller than 16 indicate that there are enough of both nutrients for excessive algal growth. Throughout all the years, the TN/TP ratio was over 16, which indicates that phosphorous could be the limiting factor for algal growth in the Danube River, but since data for total N is limited (as mentioned above) serious trend analysis can not be performed.

DISCUSSION

In this discussion, all the particular conclusions drawn on the basis of linear regression analysis with a defined significance level of 95 % concerning time and space trends are summarized (Tables I and II).

First group parameters

Suspended matter. With time (1992–2006) no clear tendency for the suspended matter change could be estimated, but in space (from the inflow to outflow point), a tendency of the suspended matter to decrease from Bezdan toward Radujevac was evident.

Dry matter. With time, a decreasing (improving) trend for the dry matter could be observed and in space, it could be concluded that the dry matter content decreased from Bezdan toward Radujevac.

Conductivity. With time, a decreasing trend was found but in space, no trend of the conductivity from Bezdan to Radujevac could be clearly evidenced.

Second group parameters

COD. With time, a decreasing trend for COD was found and in space, a tendency of the COD to decrease from Bezdan toward Radujevac was evident.

BOD-5. In time, the BOD-5 exhibited a decreasing trend and in space, a tendency of BOD-5 to decrease from Bezdan toward Radujevac was evident. A change in the rates of decrease was observed as they become less negative between 1995 and 2006. This indicates that soon after 2006, the BOD-5 will not be a spatially decreasing parameter in the Serbian part of the Danube.

TABLE I. Temporal trends of the median yearly value changes for the period 1992–2006 observed for all sampling station

Parameter	No. of positive trends	Average Pearson's correlation coefficient square	No. of statistically significant positive trends	Average Pearson's correlation coefficient square	No. of negative trends	Average Pearson's correlation coefficient square	No. of statistically significant positive trends	Average Pearson's correlation coefficient square	Overall trend estimation and comments
Dry matter	2	0.046	0	0.000	11	0.193	2	0.433	Negative trend
Suspended matter	8	0.063	1	0.273	5	0.182	2	0.340	Inconclusive
Conductivity	1	0.000	0	0.000	12	0.072	1	0.323	Negative trend
COD	1	0.495	1	0.495	12	0.168	3	0.368	Negative trend
BOD-5	1	0.001	0	0.000	12	0.275	6	0.398	Negative trend
UV absorption (254 nm)	7	0.306	4	0.388	6	0.051	0	0.000	Negative to positive switch[a]
Dissolved oxygen	2	0.021	0	0.000	11	0.122	1	0.434	Negative trend
Oxygen saturation	7	0.025	0	0.000	6	0.099	0	0.000	Inconclusive
pH	7	0.292	3	0.426	6	0.173	1	0.314	Negative to positive switch[b]
Nitrates	0	0.000	0	0.000	13	0.342	8	0.472	Negative trend
Total P	0	0.000	0	0.000	13	0.171	2	0.273	Negative trend
Total N	1	0.001	0	0.000	7	0.470	0	0.000	Negative trend

[a]The UV absorption at 254 nm increased rapidly until the years 1995 or 1996, after which it slowly decreased or stagnated. The rate of decrease after 1996 was larger in upper than in lower section of the River, resulting in negative overall temporal trends in the upper and positive overall temporal trends in the lower section;
[b]in the upper section of the River, the pH tends to have negative temporal trend while in the lower section, the temporal trend is positive

TABLE II. Spatial trends of the median yearly values changes from location to location observed for every year from 1992 to 2006

Parameter	No. of positive trends	Average Pearson's correlation coefficient square	No. of statistically significant positive trends	Average Pearson's correlation coefficient square	No. of negative trends	Average Pearson's correlation coefficient square	No. of statistically significant positive trends	Average Pearson's correlation coefficient square	Overall trend estimation and comments
Dry matter	2	0.079	0	0.000	10	0.261	4	0.525	Negative trend
Suspended matter	0	0.000	0	0.000	15	0.503	13	0.541	Negative trend
Conductivity	9	0.215	4	0.436	6	0.330	3	0.421	Inconclusive
COD	0	0.000	0	0.000	15	0.468	13	0.505	Negative trend
BOD-5	1	0.008	0	0.000	14	0.227	4	0.416	Negative trend
UV absorption (254 nm)	6	0.343	3	0.603	9	0.167	3	0.385	Negative to positive switch[a]
Dissolved oxygen	1	0.000	0	0.000	14	0.174	3	0.575	Negative trend
Oxygen saturation	7	0.068	0	0.000	8	0.167	1	0.322	Inconclusive
pH	0	0.000	0	0.000	13	0.456	9	0.597	Negative trend
Nitrates	5	0.165	1	0.321	9	0.433	6	0.580	Negative trend
Total P	1	0.005	0	0.000	14	0.330	8	0.484	Negative trend
Total N	1	0.000	0	0.000	6	0.391	2	0.609	Negative trend

[a]UV absorption at 254 nm had a negative spatial trend until the year 1998. In the later years, the spatial trend became positive

UV Absorption at 254 nm. In time, it cannot be unambiguously stated that the UV absorption was increasing and in space, no changing tendency of the UV absorption from Bezdan toward Radujevac was evidenced.

Third group parameters

Dissolved oxygen. In time, the decreasing trend had a very low probability and in space, it could only be suspected that a decrease in dissolved oxygen content from Bezdan toward Radujevac existed.

Oxygen saturation. In time, no trend through the years could be identified but in space, a decrease in oxygen saturation from Bezdan toward Radujevac could be proven.

Fourth group parameters

pH Value. In time, trends for the change of the median yearly values for period from 1992 until 2006 could not be identified, while in space, a tendency of pH value to decrease from Bezdan toward Radujevac was evident.

Concentration of nitrates. In time, it could be concluded that the concentration of nitrates exhibited a decreasing trend and in space, a tendency of the nitrate concentration to decrease from Bezdan toward Radujevac was evident.

Concentration of total P. In time, it could be concluded that the concentration of total P had a decreasing trend and in space, a tendency of the total P concentration to decrease from Bezdan toward Radujevac was evident.

Concentration of total N. The limited data indicated that the concentration of total N had a decreasing trend in time and in space, the total N concentration decreased from Bezdan toward Radujevac.

TN/TP ratio. Throughout all the years, the TN/TP ratio was over 16, which indicates that phosphorous could be the limiting factor for algal growth in the Danube River, but since the data for total N was limited (as mentioned above), a serious trend analysis could not be realized.

The strong positive correlation of nitrates with total P and total N indicates that these nutrients have same source, probably fertilizers used in agriculture.

The analysis of the trends of the investigated parameters strongly indicates that the eco-chemical status of the Danube River is improving with time. None of the parameters have reached their natural minimum, such as dry matter, conductivity, COD, BOD-5, pH, nitrates, total P and possibly total N, therefore further improvements in the eco-chemical status of the Danube River are to be expected. However, some of the parameters, such as suspended matter, UV absorption at 254 nm, oxygen saturation and pH did not show decreasing trends. For the later group of parameters, there are no indications that they are going to improve in the near future.

The trends related to space, which are particularly important for Serbia, are very indicative; the eco-chemical parameters are improving from the inflow to the outflow point for all parameters except for conductivity, oxygen saturation and UV absorption at 254 nm. Several reasons are responsible for this, such as a decrease in the flow rate, self-purification of the river, contribution of tributaries, but the most important fact is the existence of the Đerdap Dam (Iron Gate I) at the outflow point of Serbia that strongly influences the process of self-purification,[48] which is characteristic for the entire region of Serbia being constantly present for the whole period covered by this article.

Only dissolved oxygen showed undesired but statistically insignificant trends (decreasing) in time and space that are most probably the result of a gradual temperature increase from Bezdan to Radujevac.

CONCLUSIONS

The general concluding remark is that the eco-chemical status of the Danube River is constantly improving. The total river load is much higher at the entrance of the Danube River into Serbia (Bezdan) in comparison to the outflow point (Radujevac). The improvement of the eco-chemical status is twofold: with time (from 1992 until 2006) and in space (from Bezdan to Radujevac).

The results of the present study showed that the slopes of the decreasing trend lines are not significantly affected either by tributaries (Sava, Tisa, Tamiš or Velika Morava) or bigger pollutant sources, such as cities and industrial centers (Novi Sad, Belgrade, Pančevo or Smederevo).

The time improvement is most probably related to several factors:

– the decrease in industrial activities in Serbia during the last decade of the 20th century;

– the coordinated activates of countries located in the Danube Basin – ICPDR;

– the constrained use of fertilizers in the agricultural sector of Serbia.

Space improvements are related to following factors:

– the contribution of tributary rivers, especially the Sava River, to the total discharge (Q) of the Danube River;

– the decrease in the flow rate, particularly in the lower section of the Danube, closely related to the Iron Gate, favors self-purification of some river water quality parameters;

– transition of the river surroundings affected by high agricultural activity and dense population in the upper stream of the River to the Djerdap National Park in the lower part of the River.

It is suspected that a part of the river load is transferred into river sediments due to self-purification and precipitation, but thorough investigations are yet to be performed.

Acknowledgements. This project was partly financed by the Ministry of Science and Technological Development of the Republic of Serbia (Project No. 146008) and partly by a "Srbijavode" grant, which are gratefully acknowledged.

И З В О Д

ДУГОРОЧНЕ ПРОМЕНЕ ЕКОХЕМИЈСКОГ СТАТУСА ДУНАВА НА ТЕРИТОРИЈИ СРБИЈЕ

ИВАН ЖИВАДИНОВИЋ[1], КОНСТАНТИН ИЛИЈЕВИЋ[2], ИВАН ГРЖЕТИЋ[2] и АЛЕКСАНДАР ПОПОВИЋ[2]

[1]Србијаводе, Булевар уметности 2, 11070 Београд и [2]Хемијски факултет, Универзитет у Београду, Студентски трг 12–16, 11000 Београд

Дунав је међународна река која једним делом пролази и кроз Србију. Екохемијски статус Дунава је тема која је константно у жижи интересовања како на локалном (унутар држава кроз које Дунав протиче), тако и на међународном нивоу. Услед генералног интереса да се обезбеди и одржива равномерна употреба воде и слатководних ресурса у басену реке Дунав, развијен је речни мониторинг систем који је групе података о екохемијском статусу Дунава на простору Србије прикупљао током више година. Овај рад је фокусиран на петнаестогодишњи период, од 1992. до 2006. године. Утврђивање постојања трендова коришћењем линеарне регресије, уз тачно одређен ниво значаја вредности одабраних екохемијских параметара као и утврђивања разлике у односу на природну варијабилност параметара, било је од великог значаја за одређивање промене речних параметара. Помоћу њих, покушано је одређивање судбине и понашања екохемијских параметара Дунава на територији Србије и предвиђање њихове вредности у будућности. Добијени резултати открили су константно поправљање и прихватљиве трендове промена екохемијског статуса Дунава као и приметне разлике квалитета воде између улаза у Србију и излаза Дунава из Србије.

(Примљено 2. новембра, ревидирано 8. децембра 2009)

REFERENCES

1. *ICPDR*, WFD Roof Report 2004 Document IC/084, 2005
2. N. Veljković, in *Water 2007*, Serbian Water Pollution Control Society, Belgrade, 2007, p. 49 (in Serbian)
3. N. Veljković, in *Modern Technical Procedures in Seweage*, Association for Water Technology and Sanitary Engineering, Belgrade, 2005, p. 11 (in Serbian)
4. C. Madarasz, L Horvath, *Hung. Verhandlungen - Internationale Vereinigung fuer Theoretische und Angewandte Limnologie* **27** (2001) 3954
5. A. Dumbrava, S. Birghila, I. Enache, *Analele Universitatii "Ovidius" Constanta* **19** (2008) 19 (in Romanian)
6. C. Guieu, J. M. Martin, *Estuar. Coast. Shelf Sci.***54** (2002) 501
7. A. Dumbrava, S. Birghila, *Environ. Eng. Manage J.* **8** (2009) 219
8. N. Milenkovic, M. Damjanovic, M. Ristic, *Polish J. Environ. Stud.* **14** (2005) 781
9. I. Enache, *Analele Universitatii Bucuresti Chimie* **17** (2008) 61 (in Romanian)
10. D. M. Crnkovic, N. S. Crnkovic, A. J. Filipovic, L. V. Rajakovic, A. A. Peric-Grujic, M. D. Ristic, *J. Environ. Sci. Health A* **43** (2008) 1353
11. V. Orescanin, S. Lulic, G. Medunic, L. Mikelic, *Geologia Croatica* **58** (2005) 185
12. G. J. Lair, F. Zehetner, Z. H. Khan, M. H. Gerzabek, *Geoderma* **149** (2009) 39
13. R. Kalchev, D. Ionica, M. Beshkova, I. Botev, C. Sandu, *Archiv Hydrobiologie Supplement* **166** (2008) 25

14. H. Behrendt, J. van Gils, H. Schreiber, M. Zessner, *Archiv Hydrobiologie Supplement* **158** (2005) 221
15. H. Schreiber, H. Behrendt, L. T. Constantinescu, I. Cvitanic, D. Drumea, D. Jabucar, S. Juran, B. Pataki, S. Snishko, M. Zessner, *Archiv Hydrobiologie Supplement* **158** (2005) 197
16. C. Teodoru, B. Wehrli, *Biogeochemistry* **76** (2005) 539
17. J. van Gils, H. Behrendt, A. Constantinescu, F. Laszlo, L. Popescu, *Water Sci. Technol.* **51** (2005) 205
18. M. Krmar, J. Slivka, E. Varga, I. Bikit, M. Veskovic, *J. Geochem. Explor.* **100** (2009) 20
19. N. Miljevic, D. Golobocanin, N. Ogrinc, A. Bondzic, *Isotopes Environ. Health Stud.* **44** (2008) 137
20. Z. Vukovic, V. Sipka, D. Vukovic, D. Todorovic, L. Markovic, *J. Radioanal. Nucl. Chem*. **268** (2006)
21. P. Literathy, *Water Sci. Technol.* **53** (2006) 121
22. B. Vogel, *Oesterreichische Wasser- und Abfallwirtschaft* **55** (2003) 155
23. L. V. Galatchi, A. N. Vladimir, *Analele Universitatii "Ovidius" Constanta Chimie* **17** (2006) 242
24. F. Pawellek, F. Frauenstein, J. Veizer, *Geochim. Cosmochim. Acta* **66** (2002) 3839
25. V. Kundev, I. Dombalov, Y. Pelovski, *J. Environ. Prot. Ecol.* **2** (2001) 589
26. C. H. Avis, P. H. Weller, *Eur. Water Manage.* **3** (2000) 46
27. *APHA AWWA WEF, Standard Methods for the Examination of Water and Wastewater*, 18th ed., American Public Health Association, Washington DC, 1992
28. *US EPA, Methods for Chemical Analysis of Water and Wastes EPA/600/4-79/020*, 1983
29. *13.060.30 JUS H.Z1. 160, Testing of industrial waters - Determination of suspended matters – Gravimetric method*, 1987
30. *APHA AWWA WEF, 4500-NO3 – Nitrogen (nitrate)*, 1992
31. *JUS ISO 5663, Water quality – Determination of Kjeldahl nitrogen*, 1984
32. *APHA AWWA WEF 4500-P – Phosphorus*, 1992
33. *EPA 360.2 Oxygen, Dissolved (Modified Winkler, Full-Bottle Technique)*, 1971
34. *JUS ISO 8467, Water quality – Determination of permanganate index*, 1986
35. J. N. Miller, J. C. Miller, *Statistics and chemometrics for analytical chemistry*, 5th ed., Pearson Education, Harlow, 2005, pp. 45–69, 107–158
36. P. C. Meier, R. E. Zund, *Statistical methods in analytical chemistry*, 2nd ed., Wiley, New York**,** 2000, pp. 44–65, 91–137
37. M. Onderka, P. Pekarova, *Sci. Total Environ.* **397** (2008) 238
38. P. Pekarova, M. Onderka, J. Pekar, P. Roncak, P. Miklanek, *J. Hydrol. Hydromech.* **57** (2009) 3
39. I. Zweimueller, M. Zessner, T. Hein, *Hydrolog. Processes* **22** (2008) 1022
40. K. Buzas, *Water Sci. Technol.* **40** (1999) 51
41. V. Simeonov, C. Sarbu, D. L. Massart, S. Tsakovski, *Mikrochim. Acta* **137** (2001) 243
42. A. Clement, K. Buzas, *Water Sci. Technol.* **40** (1999) 35
43. L. Laurencelle, F. A. Dupuis, *Statistical Tables, Explained and Applied*, World Scientific Publishing, Singapore, 2002, pp. 1–43, 214
44. G. K. Kanji, *100 Statistical Tests*, 3rd ed., SAGE Publications, London, 2006, pp. 7–39, 93–96
45. L. Prathumratana, S. Sthiannopkao, K. W. Kim, *Environ. Int.* **34** (2008) 860
46. S. Pajević, M. Borišev, S. Rončević, D. Vukov, R. Igić, *Central Eur. J. Biol.* **3** (2008) 285

47. D. L. Corell, *J. Environ. Qual*. **27** (1998) 261
48. G. L. Wei, Z. F. Yang, B. S. Cui, B. Li, H. Chen, J. H. Bai, S. K. Dong, *China Water Resour Manage*. **23** (2009) 17..

Journal of the Serbian Chemical Society
JSCS-info@shd.org.rs • www.shd.org.rs/JSCS
J. Serb. Chem. Soc. *75* (8) 1149–1159 (2010)
JSCS–4038
UDC *CYP1A+*MT:504.054(26):597
Original scientific paper

CYP1A and metallothionein expression in the hepatopancreas of *Merluccius merluccius* and *Mullus barbatus* from the Adriatic Sea

MIRJANA MIHAILOVIĆ[1]*, MIODRAG PETROVIĆ[1], NEVENA GRDOVIĆ[1], SVETLANA DINIĆ[1], ALEKSANDRA USKOKOVIĆ[1], MELITA VIDAKOVIĆ[1], ILIJANA GRIGOROV[1], DESANKA BOGOJEVIĆ[1], SVETLANA IVANOVIĆ-MATIĆ[1], VESNA MARTINOVIĆ[1], JELENA ARAMBAŠIĆ[1], DANIJELA JOKSIMOVIĆ[2], SVETLANA LABUS-BLAGOJEVIĆ[3] and GORAN POZNANOVIĆ[1]

[1]*Institute for Biological Research "Siniša Stanković", University of Belgrade, Belgrade, Serbia,* [2]*Institite of Marine Biology, Kotor, Montenegro and* [3]*Milan Jovanović-Batut Institute for Public Health, Belgrade, Serbia*

(Received 29 October, revised 11 December 2009)

Abstract: The enzyme CYP1A is an established biomarker of fish exposure to polycyclic aromatic hydrocarbons (PAHs) and polychlorinated biphenyls (PCBs). The metallothioneins (MT), a family of Cys-rich proteins, bind a wide range of metals and participate in their metabolism. The aim of the study was to examine the correlation between CYP1A and MT expression in commercially important fish species *Mullus barbatus* and *Merluccius merluccius* and contaminants (PAHs, PCBs, toxic metals) in seawater and sediment from three localities with different level of contamination in the Adriatic Sea in winter, *i.e.*, Platamuni, Valdanos and the port of Bar. The relative concentration of CYP1A was the highest in both fish species from Bar. Increased concentrations of PCBs in the seawater were observed only in Bar. A species-specific higher increase in the protein concentration of CYP1A was observed in *Mullus barbatus* compared to *Merluccius merluccius*. The levels of MT were the highest in *Merluccius merluccius* from Bar and in *Mullus barbatus* from Valdanos. The induction of MT correlated with the elevated concentrations of Cu and Pb determined by chemical analysis of the seawater from Bar and Valdanos, respectively. According to the chemical analysis of the seawater and the biological response of the fish, the Platamuni locality exhibited the lowest level of contamination.

Keywords: CYP1A; metallothionein; polycyclic aromatic hydrocarbons; polychlorinated biphenyls; metals; fish.

* Corresponding author. E-mail: mista@ibiss.bg.ac.rs
doi: 10.2298/JSC091204099M

INTRODUCTION

Biochemical markers or biomarkers represent early warning signals that reflect on adverse biological responses to anthropogenic environmental toxins.[1] In order to assess the exposure to or the effects of environmental pollutants on aquatic ecosystems, different biomarkers are examined, *i.e*. the biotransformation enzymes (phases I and II), oxidative stress parameters, biotransformation products, stress proteins, metallothioneins, immunological, reproductive and endocrine parameters, genotoxic and physiological, histological and morphological parameters.[1]

The phase I biotransformation enzymes, notably CYP1A, belong to a group of very sensitive biomarkers in fish. They are responsible for the biotransformation of xenobiotic compounds, such as polycyclic aromatic hydrocarbons (PAHs) and polychlorinated biphenyls (PCBs).[2–4] The induction of CYP1A occurs through ligand binding of PAHs and PCBs to a cytoplasmic receptor, known as the hydrocarbon receptor. Upon heterodimerization with the aryl hydrocarbon nuclear translocator, the complex translocates to the nucleus. This is followed by its specific binding to the xenobiotic-response element on the DNA upstream from the CYP1A gene promoter and up regulation of gene transcription, which leads to elevated mRNA and protein levels, and increased CYP1A catalytic activity.[5]

Metallothioneins (MTs) are a special group of stress proteins which are inducible by both essential and toxic metals. The MTs constitute a family of low-molecular-weight, cysteine-rich proteins that regulate the essential metals Cu and Zn.[6] For nonessential metals, MT assumes a sequestering function that protects against metal toxicity.[7] Induction of MT following exposure to toxic metals can serve as a defense mechanism and a biomarker of environmental exposure to chemical stressors, such as toxic metals. Another hallmark of MTs is their induction by multiple toxic metal species at the transcriptional level. Studies of the regulation of MT gene expression revealed that the induction by metals is a direct response to increases in the intracellular metal concentrations and is mediated through the action of metal-binding regulatory factors.[8]

The aim of the present study was to examine the correlation between the expression of biomarkers (CYP1A and MT) in fish and chemical contaminants (PAHs, PCBs and toxic metals) in seawater and sediment. Relative changes of CYP1A and MT concentrations in the hepatopancreas of Red mullet *Mullus barbatus* and European hake *Merluccius merluccius* were examined. The fish were caught in three different types of localities in the Adriatic Sea in winter: Platamuni, an open sea locality; Valdanos, a locality of low urban and industrial influence, and the port of Bar, a locality of intense industrial and anthropogenic activity. Both fish species are of considerable commercial importance.

EXPERIMENTAL

Animals

Specimens of *Mullus barbatus* and *Merluccius merluccius* were collected by trawling at Platamuni, Valdanos and the port of Bar (Fig. 1). The investigations took place in winter (25th February, 2009). At least seven (and up to nine) individual fish of one species were pooled. The fish were killed immediately by spinosectomy according to standard animal care regulations. The hepatopancreas was quickly removed, washed in ice-cold 0.15 M NaCl and frozen in liquid nitrogen. Individuals of the same size were selected to ensure uniformity of samples.

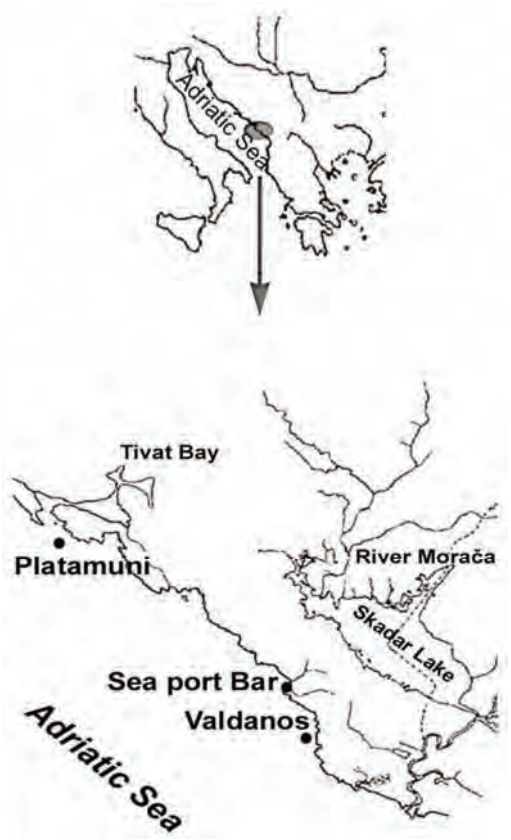

Fig. 1. A map of the Adriatic coast of Montenegro with the locations where the sea water samples were collected and the fish caught (Platamuni, Valdanos, port Bar).

Determination of PAHs and PCBs

The sampling of water and sediments was performed after trawling at the same place as where the fish were caught. PCBs from filtered seawater (1 L) were extracted using a Bakerbond spe™ C18, 6 ml, 500 mg column (JT Baker products).[9] Prior to extraction, the column was washed with ethyl acetate, dried under vacuum for 30 s and conditioned with 2×5 ml of methanol, followed by 2×5 mL of water. Samples were added to the column and drawn

through the column at 10 mL min^{-1}. After washing with water, the column was dried under vacuum for 30 min. Compounds from the column was eluted using 2×2.5 mL of ethyl acetate at a flow rate of 2 mL min^{-1}, followed by 2×2.5 mL of dichloromethane, before being concentrated to 1 mL at room temperature by evaporation under a gentle stream of nitrogen gas. PCBs from sediments were extracted using a Soxhlet apparatus employing an acetone/hexane mixture (51:49, v/v) for 8 h.[10] The dried and evaporated extract was transferred to a silica gel column (10 g, 100–200 mesh activated at 130 °C for 18 h before use), eluted using hexane and concentrated to 1 mL at room temperature by evaporation under a gentle stream of nitrogen gas.

The PCB concentrations were determined by gas chromatography (GC) with an ECD detector and linear programmable temperature vaporizer (PTV) injector.[11,12] A capillary column BPX5 30 m×0.25 mm×0.25 μm was used for all the determinations. The operating conditions were: detector temperature 310 °C, column temperature programmed to start at 80 °C for 2 min, first ramp 30 °C min^{-1} to 150 °C, second ramp 5 °C min^{-1} to 280 °C and holding for the next 5 min. The concentrations of PCBs in the samples were calculated using araclor standards. The absence of an individual peak is not reported as zero but as less than the detection limit.

The PAHs from filtered seawater (1 L) were extracted using a Bakerbond spe™ PAH Aqua, 6 mL column (JT Baker products).[13] The column was conditioned with cyclohexane and dichloromethane, dried for 15 s after each addition and again conditioned using a water/2--propanol mixture (92:8). The sample (1 L with the addition of 100 mL of 2-propanol) was applied to the column at 5 mL min^{-1} and dried using vacuum for 10 min. The PAHs were eluted using 2×3 mL and 1×2 mL of dichloromethane and then concentrated to 1 mL at room temperature by evaporation under a gentle stream of nitrogen gas.

The PAH concentrations were determined by GC with a FID detector and a linear PTV injector.[14] A capillary column DB5-MS 30 m×0.25 mm×0.25 μm was used for all the determinations. The operating conditions were: detector temperature 310 °C, column temperature programmed to start at 40 °C for 1 min, first ramp 15 °C min^{-1} to 150 °C, second ramp 5 °C min^{-1} to 290 °C and holding for the next 11 min. The concentrations of PAHs in the samples were calculated using PAH mix 13 (Supelco) standards. The absence of individual peaks is not reported as zero but as less than the detection limit.

Determination of metals

Water samples were taken in polyethylene bottles of 1.5 L volume, preserved with 5 cm^3 concentrated nitric acid during the sampling. After transport, the samples were kept at room temperature until analysis. Before analysis of the investigated toxic metals, to enable its determination, their concentration in samples were increased. For metal content determination in samples of seawater from the Montenegrin coast, the extraction method by ammonium pyrrolidine dithiocarbamate/methyl isobutyl ketone (APDC/MIBK) was used, *i.e.*, method of separation of complex metals with the organic solvent MIBK, previously examined in 1 % solution of APDC, at pH 3 and analyzed with atomic absorption spectrometry (AAS).[15,16]

Isolation of the hepatopanceas fractions

The microsomal fraction of the hepatopancreas was prepared following the procedure of Krauss *et al.*[17] The tissues were excised and homogenized (1 g liver mL^{-1}) in STM buffer: 0.25 M sucrose, 50 mM Tris-HCl, pH 7.4, 4 mM MgCl2, 1 mM PMSF) and centrifuged at 10000 x g at 4 °C for 25 min. The obtained post mitochondrial supernatant was then centrifuged at 150000 x g, 4 °C for 60 min. The obtained microsomal pellets were resuspended in STM buffer and used for analysis of CYP1A, while the supernatant was used for analysis of MT.

SDS-polyacrylamide gel electrophoresis and immunoblot analysis

For the SDS-polyacrylamide gel electrophoresis (SDS-PAGE), 20 μg of microsomal proteins were loaded onto 4 % stacking/12 % separating slab gels as described by Laemmli.[18] The gels were stained using Coomassie Brilliant Blue R-250. The proteins separated by SDS--PAGE were electroblotted onto PVDF membranes (Hybond-P, Amersham Pharmacia Biotech). Immunoblot analysis was performed according to Towbin *et al.*[19] using polyclonal antibodies to fish CYP1A and MT (CP226 and KH-1, respectively; Biosense Laboratories, Norway). The immunoreactive bands were identified by an enhanced chemiluminescence (ECL) detection system (Santa Cruz Biotechnology) according to the manufacturer's instructions. Protein concentrations were determined according to Lowry *et al.*[20] The bands were visualized and quantified with TotalLab (Phoretix) electrophoresis software (version 1.10).

RESULTS AND DISCUSSION

The effects of exposure to PAHs and PCBs on CYP1A expression

Chemical analysis of the environment and animal tissues provides information concerning the presence of specific xenobiotic compounds. However, this data on its own is not particularly indicative of the concentrations to which the animals were exposed and cannot serve as bioaccumulation markers for exposure assessment.[2] In addition, the application of biomarkers to complement traditional chemical methods of detecting pollution can reveal the presence of contaminants that were not initially suspected. CYP1A is an established biomarker of exposure to PAHs and PCBs.[2] In order to detect CYP1A, equal quantities of microsomal proteins were separated by SDS-PAGE and subjected to immunoblot analysis using polyclonal antibody to CYP1A protein (Fig. 2). CYP1A was detected in both fish species at all examined localities. The highest degree of induction was observed in both fish species that were caught in the port Bar (Fig. 2 and Table I). The results presented in Fig. 2 indicate a species-specific response of CYP1A. They show that the protein concentration of CYP1A was about 5-fold higher in the hepatopancreas of *Mullus barbatus* than in *Merluccius merluccius* (Table I).

Fig. 2. Immunoblot analysis with anti--CYP1A antibody. P – Platamuni; V – Valdanos; B – Bar. Twenty μg of proteins were subjected to 12 % SDS--PAGE, electroblotted to membranes and immunoblotting was performed with a polyclonal antibody for CYP1A. The antigen–antibody complex formation was detected using an ECL detection system.

Virgin *et al*. showed that there are large differences in CYPlA mRNA induction between species.[21] Thus, the Atlantic tomcod exhibited significant induction of CYPlA mRNA after exposure to chemicals (97-fold) and changes in the en-

vironment (34-fold), whereas in the smooth flounder, a considerably lower level of CYP1A induction was observed in response to chemical exposure (14-fold) but no change in expression after exposure to adjustments in the environment.[21] In hog chokers and striped bass, very low levels of CYP1A gene induction were detected. The degree of CYPlA mRNA inductibility above the basal level differs significantly among fish taxa, most likely as a result of differences in the regulation of gene expression. Based on their findings, the authors concluded that careful selection of sentinel species should be exercised prior to the use of CYPlA mRNA induction data in environmental monitoring programs.

TABLE I. Quantification by immunoblot analysis with anti-CYP1A antibody. Antigen–antibody complexes (changes of the relative concentrations of CYP1A), were analyzed by densitometry using Total Lab (Phoretix) electrophoresis software

Location	Fish	
	Mullus barbatus	*Merluccius merlucius*
Platamuni	446.3±15.1	88.2±2.8
Valdanos	603.7±21.5	117.1±4.2
Bar	824.1±33.4	139.2±4.9

Due to their mutagenic and carcinogenic properties, measurement of PAH concentrations are included in most monitoring programs.[22] PCBs are produced for diverse industrial applications and although their use has been banned since the 1970s, due to their resistance to breakdown and tendency for bioaccumulation, PCBs continue to cycle through the environment.[1]

Analysis of the seawater did not reveal the presence of PAHs (Table II). The limit of detection of PAHs using a GC column is 10 ng L^{-1} and the presence of PAHs at lower concentrations cannot be excluded. PCBs were observed in the seawater only in Bar, where the concentrations of PCB-28, PCB-52 and PCB-153 were 20, 15 and 15 ng L^{-1}, respectively (Table III). According to Nagpal,[23] the recommended maximal concentration of total PCB is 0.1 ng L^{-1}. Thus, the concentrations of PCBs measured in the port of Bar could be taken as representing contamination of the seawater. Since the minimal concentration of PCBs that exerts a negative impact on marine organisms, as reported in the Environmental Quality Standards for the Mediterranean Sea in Israel,[24] is 42 ng L^{-1}, the concentrations detected in Bar are at an acceptable level. The presence of PCBs in seawater is in correlation with the highest level of CYP1A induction in the hepatopancreas from *Mullus barbatus* and *Merluccius merluccius* in Bar. As the limit of detection of PCBs using a GC column is 10 ng l^{-1} (which is above the recommended maximum concentration described by Nagpa[l23]), the presence of other PCBs at other localities cannot be ruled out. The concentrations of PCBs in sediments are presented in Table III. The results revealed the presence of pcb101 in Valdanos (2.31 ng g^{-1}) and in samples PCB-101, PCB-138, PCB-153 and PCB-180

at Bar at concentrations 2.85, 3.05, 3.55 and 3.65 ng g^{-1}, respectively. Considering that the recommended maximum concentration of total PCBs is 2 μg per 100 g in sediments (Nagpal[23]), the detected PCBs in the sediment are under the recommended maximum. However, the presence of PCBs in sediment could induce the sensitive biomarker CYP1A in the hepatopancreas.

TABLE II. Concentrations of PAHs (ng L^{-1}) in seawater collected from Platamuni, Valdanos and the port of Bar

Compound	Platamuni	Valdanos	Bar
Acenaphthylene	<10	<10	<10
Fluorene	<10	<10	<10
Phenantrene	<10	<10	<10
Anthracene	<10	<10	<10
Pyrene	<10	<10	<10
Benz(A)anthracene	<10	<10	<10
Chrysene	<10	<10	<10
Benzo(B)fluoranthene	<10	<10	<10
Benzo(K)fluoranthene	<10	<10	<10
Benzo(A)pyrene	<10	<10	<10
Benzoperylene	<10	<10	<10
Indeno(1.2.3.cd)pyrene	<10	<10	<10
Dibenzo(A)anthracene	<10	<10	<10

Table III. Concentrations of PCBs in seawater and sediment collected from Platamuni, Valdanos and the port of Bar

Compound	Location		
	Platamuni	Valdanos	Bar
PCBs in seawater, ng L^{-1}			
2,4,4'-trichlorobiphenyl (PCB-28)	<10	<10	20
2,2',5,5'-tetrachlorobiphenyl (PCB-52)	<10	<10	15
2,2',4,5,5'-pentachlorobiphenyl (PCB-101)	<10	<10	<10
2,2',3,4,4',5'-heksachlorobiphenyl (PCB-138)	<10	<10	<10
2,2',4,4',5,5'-heksachlorobiphenyl (PCB-153)	<10	<10	15
2,2',3,4,4',5,5'-heptachlorobiphenyl (PCB-180)	<10	<10	<10
PCBs in sediment, ng/g			
2,4,4'-trichlorobiphenyl (PCB-28)	<10	<10	<10
2,2',5,5'-tetrachlorobiphenyl (PCB-52)	<10	<10	<10
2,2',4,5,5'-pentachlorobiphenyl (PCB-101)	<10	2.31	2.85
2,2',3,4,4',5'-heksachlorobiphenyl (PCB-138)	<10	<10	3.05
2,2',4,4',5,5'-heksachlorobiphenyl (PCB-153)	<10	<10	3.55
2,2',3,4,4',5,5'-heptachlorobiphenyl (PCB-180)	<10	<10	3.65

The effect of exposure to toxic metals on MT expression

Considering that MTs play a role in the metabolism of essential metals, they possess basal levels of expression. The occurrence of higher doses of both essen-

tial and toxic metals provokes the induction of MTs.[6,7] The same quantity of the supernatant fractions were separated by SDS-PAGE and subjected to immunoblot analysis using polyclonal antibodies to MT (Fig. 3 and Table IV). These experiments revealed that MT was present in all samples; however, MT induction was observed in *Merluccius merluccius* from Bar (Fig. 3) and in *Mullus barbatus* from Valdanos (Fig. 3).

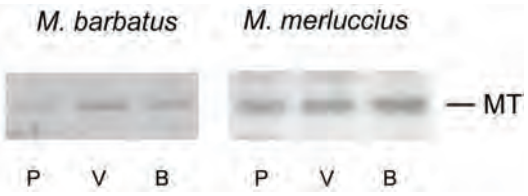

Fig. 3. Immunoblot analysis with anti-metallothionein antibody. P – Platamuni; V – Valdanos; B – Bar. Twenty μg of proteins were subjected to 12 % SDS-PAGE, electroblotted to membranes and immunoblotting was performed with a polyclonal antibody for metallothionein. The antigen–antibody complex formation was detected using an ECL detection system.

TABLE IV. Quantification of immunoblot analysis with anti-metallothionein antibody. Antigen–antibody complexes (changes of the relative concentrations of anti-metallothionein), were analyzed by densitometry using Total Lab (Phoretix) electrophoresis software

Location	Fish	
	Mullus barbatus	*Merluccius merlucius*
Platamuni	16.5±0.6	89.7±2.5
Valdanos	40.9±1.3	107.4±3.5
Bar	26.9±0.9	132.1±4.1

Analyses of metals in seawater obtained from the localities of Platamuni, Valdanos and the port in Bar during winter are shown in Table V. In view of the acceptable average concentrations according to the Environmental Quality Standards for the Mediterranean Sea in Israel[24] for the examined metals, it can be concluded that the concentration of Pb in Valdanos and of Cu in Bar were significantly increased. Namely, the recommended average concentration for both Pb and Cu is 0.005 mg L^{-1}. The measured concentrations for Pb (Valdanos) and Cu (Bar) were 0.022 and 0.009 mg L^{-1}, respectively. The minimal concentrations of Pb and Cu that have a negative impact on marine organisms are 0.005 and 0.003 mg L^{-1}, respectively.

The observed presence of Cu and Pb in seawater is in correlation with MT induction in the hepatopanceas of *Merluccius merluccius* from Bar and in *Mullus barbatus* from Valdanos. In contrast to the species-specific induction of CYP1A, 3–5-fold higher MT protein concentrations were observed in the hepatopancreas of *Merluccius merluccius* compared to *Mullus barbatus* (Fig. 3 and Table IV). Species-specific MT induction in fish was reported by Lam *et al.*[25] When carp was exposed to sub-lethal doses of Cu, Zn and Cd, MT mRNA in the gill and

liver was not induced while exposure of tilapia caused a significant induction of MT mRNA in the same tissues.[25] These results imply that the MT level in carp is not a reliable biomarker for monitoring metal pollution; the MT level in tilapia is a better biomarker. In view of these results, it can be concluded that MT induction in the hepatopancreas of *Meluccius merluccius* is a more reliable biomarker than in *Mullus barbatus*.

TABLE V. Concentrations of metals (mg L^{-1}) in seawater collected from Platamuni, Valdanos and the port of Bar

Location	Depth, m	Pb	Zn	Cd	Cu	Co	Ni
Platamuni	0	0.0	0.0	0.0	0.0	0.0	0.0
Platamuni	80 (bottom)	0.0	0.014	0.0	0.001	0.0	0.0
Valdanos	0	0.002	0.017	0.00012	0.005	0.0	0.0
Valdanos	20 (bottom)	0.022	0.009	0.0	0.0	0.0	0.0
Bar	0	0.0	0.0	0.0	0.0	0.0	0.0
Bar	10 (bottom)	0.003	0.010	0.00008	0.009	0.0	0.0

Whereas heavy pollution causes the sudden death of large numbers of fish, exposure to sub-lethal levels of pollutants has to be estimated by measurements of specific biochemical, physiological or histological responses of fish.[26] Together with chemical analysis, biomarker responses represent an additional approach in the study of the biological impact of environmental contaminants. The observed changes at the molecular level show that the pollutants had entered the organisms, been distributed between the tissues and elicited toxic effects at critical targets. This biochemical response is only the first signal of exposure to contaminants and is usually reversible, contrary to the changes manifested at higher levels of organization of an organism, the population, community and ecosystem.[1]

CONCLUSION

Increased expression of CYP1A and metallothioneins, biomarkers of fish exposure to PAHs/PCBs and toxic metals, respectively, correlated with increased levels of environmental contaminants observed by chemical analysis in Valdanos and Bar in winter. Fish from the Platamuni locality, an open sea area with very low anthropogenic and industrial influences, exhibited the lowest level of contamination and displayed significantly lower levels of biomarker responses.

Acknowledgements. This work was funded by the Federal Government of Serbia and Montenegro, grant entitled: *Bioindicators of contamination of the Montenegrin coastline*, and by the Ministry for Science and Technological Development of the Republic of Serbia, Project No. 143002. The paper was originally presented at the 2nd REP LECOTOX Workshop "Trends in Ecological Risk Assessment", 21–23 September, 2009, Novi Sad, Serbia (EC FP 6 funded project INCO-CT-2006-043559-REP-LECOTOX).

ИЗВОД

ЕКСПРЕСИЈА CYP1A И МЕТАЛОТИОНЕИНА У ХЕПАТОПАНКРЕАСУ ОСЛИЋА И ТРЉЕ ИЗ ЈАДРАНСКОГ МОРА

МИРЈАНА МИХАИЛОВИЋ[1], МИОДРАГ ПЕТРОВИЋ[1], НЕВЕНА ГРДОВИЋ[1], СВЕТЛАНА ДИНИЋ[1], АЛЕКСАНДРА УСКОКОВИЋ[1], МЕЛИТА ВИДАКОВИЋ[1], ИЛИЈАНА ГРИГОРОВ[1], ДЕСАНКА БОГОЈЕВИЋ[1], СВЕТЛАНА ИВАНОВИЋ-МАТИЋ[1], ВЕСНА МАРТИНОВИЋ[1], ЈЕЛЕНА АРАМБАШИЋ[1], ДАНИЈЕЛА ЈОКСИМОВИЋ[2], СВЕТЛАНА ЛАБУС-БЛАГОЈЕВИЋ[3] и ГОРАН ПОЗНАНОВИЋ[1]

[1]Институт за биолошка истраживања "Синиша Станковић", Универзитет у Београду, Београд, [2]Институт за биологију мора, Котор, Црна Гора и [3]Институт за јавно здравље "Милан Јовановић-Батут", Београд

CYP1A представља добро окарактерисан биомаркер код риба при излагању полицикличним ароматичним угљоводоницима (ПАХ) и полицикличним бифехолима (ПЦБ). Металотионеини (МТ) претстављају фамилију протеина који везују метале и учествују у њиховој метаболизму, транспорту и регулацији. Циљ овог рада је био да се испитају корелације између промена у нивоу CYP1A и МТ у хепатопанкреасу две комерцијално важне рибе: *Mullus barbatus* (трља) и *Merluccius merluccius* (ослић) и контаминанатата: ПАХ, ПЦБ и токсичних метала) на три локалитета у Јадрнском мору (Платамуни, Валданос и лука Бар) у зиму. CYP1A је у највећем степену индукован на локалитету Бар у обе испитиване врсте, што је у корелацији са присуством повећане количине ПЦБ у морској води у Бару. Ниво МТ је највећи код ослића изловљеног у Бару, а код трље у Валданосу. То је у корелацији са измереним повећаним концентрацијама бакра у Бару, а олова у Валданосу. На основу изучаваних параметара, Платамуни су локалитет са најмањим степеном контаминације.

(Примљено 29. октобра, ревидирано 11. децембра 2009)

REFERENCES

1. R. Van der Oost, J. Beyer, N. P. E. Vermeuulen, *Environ. Toxicol. Pharmacol*. **13** (2003) 57
2. R. Van der Oost, E. Vindimian, P. J. V. D. Brink, K. Stumalay, M. Heida, N. P. E. Vermeulen, *Aquat. Toxicol*. **39** (1997) 453
3. M. Mihailović, J. Arambašić, D. Bogojević, S. Dinić, N. Grdović, I. Grigorov, S. Ivanović-Matić, S. Labus-Blagojević, V. Martinović, M. Petrović, A. Uskoković, M. Vidaković, G. Poznanović, *Arch. Biol. Sci*. **58** (2006) 165
4. M. Mihailović, D. Bogojević, S. Dinić, N. Grdović, I. Grigorov, S. Ivanović-Matić, S. Labus-Blagojević, V. Martinović, M. Petrović, A. Uskoković, M. Vidaković, G. Poznanović, *Bull. Environ. Contam. Toxicol.* **77** (2006) 559
5. T. D. Bucheli, K. Fent, *Crit. Rev. Environ. Sci. Technol.* **25** (1995) 201
6. G. A. Bonwick, P. R. Fielden, D. H. Davies, *Comp. Biochem. Physiol*. **99C** (1991) 119
7. N. Muto, H. W. Ren, G. S. Hwang, S. Tominaga, N. Itoh, K. Tanaka, *Comp. Biochem. Physiol*. **122** (1999) 75
8. G. M. Dethloff, H. C. Bailey, K. J. Maier, *Arch. Environ. Contam. Toxicol*. **40** (2001) 371
9. J. Dachs, J. M. Bayona, *Chemosphere* **35** (1997) 1669
10. *EPA Method 3540C: Soxhlet extraction*, 1996, http://www.epa.gov/osw/hazard/testmethods/sw846/pdfs/3540c.pdf (last accessed: August, 2010)
11. N. Kannan, G. Petrick, R. Bruhn, D. E. Schulz-Bull, *Chemosphere* **37** (1998) 2385
12. *EPA Method 8082: Polychlorinated biphenyls (PCBs) by gas chromatography*, 1996, http://www.epa.gov/osw/hazard/testmethods/sw846/pdfs/8082a.pdf (last accessed: August, 2010)
13. P. W. Crozier, J. B. PlomLey, L. Matchuk, *Analyst* **126** (2001) 1974

14. H. B. Lee, G. Dookhran, A. S. Y. Chau, *Analyst* **112** (1987) 31
15. L. Rasmussen, *Anal. Chim. Acta* **125** (1981) 117
16. R. E. Sturgeon, S. S. Berman, J. A. H. Desaulniers, A. P. Mykytluk, J. W. McLaren, D. S. Rusel, *Anal. Chem.* **52** (1980) 15
17. G. J. Krauss, K. Grancharov, D. Genchev, R. Walther, N. Spassovska, G. Karamanov, H. Reinbothe, E. Golovinsky, *Biomed. Biochim. Acta* **42** (1983) 1045
18. U. K. Laemmli, *Nature* **227** (1970) 680
19. H. Towbin, T. Staehelin, J. Gordon, *Proc. Natl. Acad. Sci. USA* **76** (1979) 4350
20. O. H. Lowry, W. J. Rosebrough, A. L. Farr, R. J. Randall, *J. Biol. Chem.* **193** (1951) 265
21. I. Virgin, B. Konkle, M. Pedersen, C. Grumwald, J. Williams, S. C. Courtenay, *Estuaries* **19** (1996) 216
22. J. P. Meador, J. E. Stein, W. L. Reichert, U. Varanasi, *Rev. Environ. Contam. Toxicol.* **143** (1995) 79
23. N. K. Nagpal, *Water Quality Criteria for Polychlorinated Biphenyls*, Water Quality Branch, Water Management Division, Ministry of Environment, Lands, and Parks, Victoria, BC, 1992, http://www.env.gov.bc.ca/wat/wq/BCguidelines/approv_wq_guide/ /approved.html#toc (last accessed: August, 2010)
24. *Environmental Quality Standards for the Mediterranean Sea in Israel*, Marine and Coastal Environment Division, Ministry of the Environment, 2002, http:// //www.sviva.gov.il/ Enviroment/Static/Binaries/index_pirsumim/p0124_eng_1.pdf (last accessed: August, 2010)
25. K. L. Lam, P. W. Ko, J. K.-Y. Wong, K. M. Ghan, *Marine Environ. Res.* **46** (1998) 563
26. J. A. Mondon, S. Duda, B. F. Nowak, *Aquat. Toxicol.* **54** (2001) 231.

Journal of the Serbian Chemical Society
JSCS-info@shd.org.rs • www.shd.org.rs/JSCS
J. Serb. Chem. Soc. 75 (8) 1161–1165 (2010)
JSCS–4039
UDC 541.121+536.247+544.35:504.75
Extended abstract

EXTENDED ABSTRACT

Liquid–liquid equilibria in solutions with potential ecological importance

ZORAN P. VIŠAK

Centro Química Estrutural, Instituto Superior Técnico, Avenida Rovisco Pais 1, 1049-001, Lisboa, Portugal

(Received 23 February, revised 18 March 2010)

Abstract: In the last three years, our research follows two main issues, defined by the slogans: “green meets toxic” and “green meets green”. The first issue considers the potential use of ambient friendly solvents for toxic organic compounds of industrial and practical importance. The other is related to liquid phase behavior in solutions of ecologically sustainable substances. The “green” solvents studied are: ionic liquids, liquid poly(ethylene glycol), glycerol and 1,2- and 1,3-propanediol.

Keywords: sustainable solvents; phase equilibria, poly(ethylene glycol); glycerol; propanediols; ionic liquids.

In the past ten years, Portugal has rapidly advanced in scientific research and development, showing a consistent state strategy in this respect. Statistics and facts obviously speak in favor to this claim:[1] *i*) in 2008, Portugal invested over 2,513,000,000 Euro for this purpose, *i.e.*, 1.51 % of the gross national product (GNP), which is the highest level ever, surpassing those of Ireland and Spain; *ii*) within the aforementioned funds, nearly a half came from the private sector and this increase is enormous – almost three times more compared to 2005; *iii*) the number of researchers per thousand active members of the population reached 7.2, being now over the average in the European Union; *iv*) Portugal probably has one of the best stimulation politics for private investments in research – companies could have tax reductions of up to 82.5 % of their scientific input; *v*) in the period 2004–2008, Portugal had one of the best increase rates of scientific production – the number of publication per million inhabitants in journals acknowledged by the Information Sciences Institute (ISI) list, increased from 373 to 626 (nearly 70 %).

zoran.visak@ist.uti.pt
doi: 10.2298/JSC100223100V

This favorable scientific environment enabled us, and still does, the realization of good and productive scientific investigations. In the last three years, two main research topics – or slogans – emerged: "green meets toxic" and "green meets green". The first considers ambient friendly solvents for toxic organic compounds (generally solvents as well) of industrial and practical importance. However, the other topic is related to liquid phase behavior in solutions of "green" – ecologically sustainable – substances.

Ambient friendly solvents of our interest are ionic liquids, liquid poly(ethylene glycol), glycerol, 1,2- and 1,3-propandiol.

Ionic liquids constitute a class of compounds the number of which – already enormous (over 1,000,000 known class members)[2] – is constantly rising. The present definition is that they are ionic compounds (salts) that possess glass transition and/or melting points below 100 °C.[3] The complex but diverse structure and versatile solvent properties of ionic liquids offer wide possibilities for both fundamental studies and practical applications.[2,4] Their high asymmetry, robust (ugly) cations (and sometimes anions as well) contribute to their low melting points. Some of the "green" aspects of ionic liquids – toxicity and biodegradebility – are still under discussion,[3] while achieving good purity remains a challenging task.[5,6] However, their favorable properties, extremely low volatility,[7–9] in principle zero flammability[10] and relative thermal stability[11] yet makes them good candidates for alternative solvents. Due to their dual nature – they consist of polar and non-polar domains – they have versatile solvent–solute properties and exhibit a rich phase behavior.[12]

Liquid poly(ethylene glycol) (PEG) (average molar weight 200 and 400 g mol^{-1}) is a good polar solvent which acts both as a proton donor and proton acceptor.[13] It is ambient friendly since it has a rather high boiling point but has a very low toxicity as well and is biodegradable to a large extent.[14] Another interesting aspect of PEG is that it may change its polarity depending on the polarity of the other component in a solution[15] – this aspect obviously contributes to its diversity as a solvent.

1,2- and 1,3-Propandiol and glycerol have high boiling points as well and thus present ecologically sustainable substances. Generally, their toxicity is low, particularly that of glycerol which is practically edible. All these polyalcohols are quite polar and good hydrogen bonding solvents.

Within the aforementioned slogan "green meets toxic", the first issue that was considered is solutions of a highly toxic compound – nicotine – and ionic liquids. In this respect, ionic liquids, 1-alkyl-3-methyl-imidazolium bis(trifluoromethyl sulfonyl) amide ($[C_n mim][NTf_2]$, n = 2–10)) and 1-ethyl-3-methyl-imidazolium ethyl sulfate ($[C_2 mim][EtSO_4]$ – ECOENG212) were initially studied. It was found that ionic liquids of the first series were all completely miscible with nicotine over a wide range of temperatures. However, the solubility tests in the

case of ECOENG212 showed a very limited miscibility – a "wall-like" phase diagram was obtained.[16] The latter presents an extremely narrow one-phase region on the nicotine-rich side and a much higher miscibility on the ionic liquid-rich side. Thus, it was decided to combine the two ionic liquids with the same cation [C_2mim][NTf_2] and [C_2mim][$EtSO_4$] (these are completely miscible) to form a combined solvent. For distinct molar ratios of these two ionic liquids (actually ratios of two different anions), it was possible to fine-tune the temperature-composition phase diagram for the system (nicotine + combined solvent) – the solvent compositions that provide complete miscibility at ambient temperatures were determined.[16]

The same strategy was applied when the ionic liquids 1-alkyl-3-methyl-imidazolium chloride ([$C_n$mim][Cl], n = 6–10) were applied.[16] When the number of the carbon atoms in the cation (n) is 10, the ionic liquid is a very good solvent for nicotine – the upper critical solution temperature (UCST) is below 298.15 K. However, as the carbon number n decreases, the mutual miscibility in the system is reduced. Therefore, in these cases, the combined solvents for tuning the nicotine phase diagrams were practically distinct mixtures of imidazolium cations and a commonly – chlorides.

Following the other slogan "green meets green", ionic liquids and aqueous (high average molecular mass) polyethylene glycol solutions were combined.[17] The main issue was to use ionic liquids as salts to eventually provoke a salting--out effect – low critical solution temperature (LCST) decreases – in PEG solutions with water, following the long-known pattern with inorganic salts that is applied in extraction and separation processes, mainly in biochemistry.[18–20] In this respect, 1-alkyl-3-methyl-imidazolium chloride ([$C_n$mim][Cl], n = 2–10) and ECOENG212 were studied. However, although ionic liquids are salts (molten salts), their behavior towards aqueous PEG solutions was shown to be much more complex than that of inorganic salts. While ionic liquids with short alkyl chains provoked a salting-out effect, those with long ones realized the opposite, the so-called salting-in phenomenon – PEG solubility in water, and thus the LCST of the solution, increased. To be more precise ECOENG212 provoked both effects – the initial salting-in effect was followed by the salting out. The results revealed the possibility of combining ionic liquids and inorganic salts to adjust liquid phase demixing (salting-in or salting-out) effects in aqueous PEG solutions.

Another study that is related to the "green" issue is connected to solutions of imidazolium ionic liquids with polyalcohols. In this work,[21] liquid–liquid equilibria (LLE) of solutions of imidazolium-based ionic liquids with either bistriflamide ([$C_n$mim][NTf_2], n = 2 and 10) or triflate anions ([C_2mim][OTf]), with 1--propanol, 1,2-propanediol, 1,3-propanediol and glycerol (1,2,3-propanetriol) were studied. The obtained phase diagrams showed a remarkable difference in solva-

tion properties between the ionic liquids with NTf_2 or OTf anions towards the aforementioned alcohols; thus, while [C_2mim][NTf_2] constantly exhibited partial miscibility, [C_2mim][OTf] was always completely miscible. This divergence is likely to be related to the distinct abilities of NTf_2 and OTf anions towards hydrogen bonding. There are more than a few evidences and/or facts – based on distinct liquid phase behavior, anion basicity or spectroscopic studies – that speak in favor of this claim (in this respect see ref. 21 and references cited therein). The results of this work enabled speculation on the possibility of using a combined solvent – a mixture of [C_2mim][NTf_2] and [C_2mim][OTf] ionic liquids (or, again, actually a mixture of two anions and a common cation) for a practical purpose – to separate 1,3-propanediol from glycerol and water. Namely, 1,3-propanediol is an important substance in the production of some polymers (polyesters, polyethers and polyurethanes).[22] One of the methods for its production is fermentation from glycerol and the most costly part of this process is the separation of the diol from the fermentation broth. This presents quite a technological challenge, since 1,3-propanediol and glycerol both have high boiling points – the hitherto applied separation methods all have questionable efficiency and/or high energy consumption.[22] Therefore, in this work, a phase diagram was presented that clearly indicates the possibility to realize the aforementioned separation by a sustainable process under ambient conditions.

Our near-future research is also attempting to combine ecologically favorable compounds, ionic liquids, liquid polymers and glycerol – this time in an attempt to obtain hybrid sustainable materials. These studies are to be pursued within our project “green meets green” – “Sustainable hybrid solvents or materials based on ionic liquids, glycerol and liquid polymers”, that has been approved by the Foundation for Science and Technology (FCT) of the Portuguese Ministry of Science, Technology and High Education (MCTES).[23]

ИЗВОД

РАВНОТЕЖА ТЕЧНОСТ–ТЕЧНОСТ У РАСТВОРИМА ОД ПОТЕНЦИЈАЛНОГ ЕКОЛОШКОГ ЗНАЧАЈА

ЗОРАН П. ВИШАК

Centro Química Estrutural, Instituto Superior Técnico, Avenida Rovisco Pais 1, 1049-001, Lisboa, Portugal

Наша истраживања у последње три године иду у два правца: а) повезивања еколошких растварача и токсичних једињења и б) повезивања еколошких растварача и нетоксичних, подношљивих компоненти. Прва линија истраживања подразумева потенцијално коришћење “зелених” растварача за органске, токсичне супстанце од индустријског и лабораторијског значаја. Друга се односи на понашање течних, еколошких, раствора. Проучавани еколошки растварачи су: јонске течности, течни поли(етилен-гликол), глицерол, 1,2- и 1,3-пропандиол.

(Примљено 23. фебруара, ревидирано 18. марта 2010)

REFERENCES

1. *Inquiry of the National Scientific and Technological Potentials (IPCTN)*, Portuguese Ministry of Science, Technology and High Education (MCTES), 2008
2. N. V. Plechkova, K. R. Seddon, *Chem. Soc. Rev*. **37** (2008) 123
3. D. R. MacFarlane, K. R., Seddon, *Aust. J. Chem*. **60** (2007) 3
4. H. Zhao, S. Xia, P. Ma, *J. Chem. Technol. Biotechnol*. **80** (2005) 1089
5. P. J. Scammells, J. L. Scott, R. D. Singer, *Aust. J. Chem*. **58** (2005) 155
6. A. Stark, P. Behrend, O. Braun, A. Müller, J. Ranke, B. Ondruschka, B. Jastorff, *Green Chem*. **10** (2008) 1152
7. M. J. Earle, J. M. S. S. Esperança, M. A. Gilea, J. N. Canongia Lopes, L. P. N. Rebelo, J. W. Magee, K. R. Seddon, J. A. Widegren, *Nature* **439** (2006) 831
8. Y. U. Paulechka, G. J. Kabo, A. V. Blokhin, O. A. Vydrov, J. W. Magee, M. Frenkel, *J. Chem. Eng. Data* **48** (2003) 457
9. L. P. N. Rebelo, J. N. Canongia Lopes, J. M. S. S. Esperança, E. Filipe, *J. Phys. Chem. B* **109** (2005) 6040
10. M. Smiglak, W. M. Reichert, J. D. Holbrey, J. S. Wilkes, L. Y. Sun, J. S. Thrasher, K. Kirichenko, S. Singh, A. R. Katritzky, R. D. Rogers, *Chem. Commun*. **24** (2006) 2554
11. K. J. Baranyai, G. B. Deacon, D. R. MacFarlane, J. M. Pringle, J. L. Scott, *Aust. J. Chem*. **57** (2004) 145
12. L. P. N. Rebelo, J. N. Canongia Lopes, J. M. S. S. Esperanca, H. J. R. Guedes, J. Lachwa, V. Najdanovic-Visak, Z. P. Visak, *Acc. Chem. Res*. **40** (2007) 1114
13. I.-W. Kim, M. D. Jang, Y. K., Ryu, E. H. Cho, Y. K. Lee, J. H. Park, *Anal. Sci*. **18** (2002) 1357
14. D. J. Heldebrant, H. N. Witt, S. M. Walsh, T. Ellis, J. Rauscher, P. G. Jessop, *Green Chem*. **8** (2006) 807
15. C. Chen, M. A. Even, J. Wang, Z. Chen, *Macromolecules* **35** (2002), 9130
16. Z. P. Visak, S. L. Yague, J. N. Canongia Lopes, L. P. N. Rebelo, *J. Phys. Chem. B* **111** (2007) 7934
17. Z. P. Visak, J. N. Canongia Lopes, L. P. N. Rebelo, *Monatsh. Chem*. **138** (2007) 1153
18. P. Albertson, *A Partitioning of Cell Particles and Macromolecules*, 3rd ed., Wiley, New York, 1986
19. B. Y. Zaslawsky, *Aqueous Two-phase Partitioning – Physical Chemistry and Biological Applications*, Marcel Dekker, New York, 1995
20. N. J. Bridges, K. E. Gutowski, R. D. Rogers, *Green Chem*. **9** (2007) 177
21. C. A .S. Trindade, Z. P. Visak, R. Bogel-Lukasik, E. Bogel-Lukasik, M. Nunes da Ponte, *Ind. Eng. Chem. Res*. **49** (2010) 4850
22. Z.-L. Xiu, A.-P. Zeng, *Appl. Microbiol. Biotechnol*. **78** (2008) 917
23. *Project PTDC/QUE-EPR/103505/2008*, Foundation for Science and Technology (FCT), Portuguese Ministry of Science, Technology and High Education (MCTES), 2008.